INVESTIGATING THE REGULATION OF THE ENDOCYTOSIS OF TYROSINE KINASE RECEPTOR TIE2

By

Marta Giralt Pujol

A thesis submitted for the Degree of Doctor of Philosophy at the Biomedical Science Department, University of Sheffield

May 2017

Dedication

Als meus pares, per tot el que m´han donat; tant material com immaterial.

Al meu marit, que és un model a seguir i del qual no podria estar més orgullosa.

A la meva filla, per a qui m'esforço cada dia a deixar un món millor.

To my parents, for all they have given me, material and immaterial.

To my husband, who is a model to follow and from whom I could not be prouder.

To my daughter, for whom every day I strive to leave a better world.

Abstract

Tie2 receptor is a cell surface tyrosine kinase receptor expressed almost exclusively in endothelial cells, where it is mainly studied for its role in angiogenesis. Indeed, Tie2 has been related to various pathologies with vascular implication such as pulmonary hypertension, diabetes retinopathy and tumour growth. The regulation of Tie2 activation and function is complex, involving multiple factors that are still being investigated. For instance, after activation by the agonistic ligand Angiopoietin-1 (Ang1), Tie2 is internalized in cells by an endocytic mechanism that has yet to be fully characterised. As it has been shown that endocytosis of molecules can play a regulatory role in intracellular signalling in various ways I believe that the endocytosis of Tie2 may also be important in the regulation of its activity and cellular output. Therefore, I decided to characterise the endocytic mechanisms involved in the internalization of Tie2 to determine whether endocytosis can be a regulator of Tie2 signalling.

To facilitate the study of Tie2 I created a HeLa cell line with inducible expression of a $Tie2^{FLAG}$ receptor that emulates both expression levels and characteristics of endogenous Tie2 in Human Umbilical Vein Endothelial Cells. To study the endocytosis of Tie2 receptor I developed an immunofluorescence-based assay to quantify the amount of internalized agonistic ligand Ang1 in a high throughput Screening format. I also performed complementary immunofluorescence and western blot analysis to investigate the characteristics of Tie2 internalization.

Overall, components of both clathrin-dependent and -independent endocytosis (CME and CIE) were highlighted as potential regulators of the membrane trafficking of Tie2. I believe our results indicate that internalization of Tie2 can occur via CME yet that Tie2 can also be internalized by at least one alternative endocytic mechanism. I have provided a selection of hits that will need to be further validated and their role in Tie2 endocytosis investigated. Nonetheless, it was especially relevant to find Rac1 as a robust potential modulator of the internalization of Tie2, as Rac1 is activated by the signalling cascade triggered by Tie2 phosphorylation and it is implicated in physiological and cancer angiogenesis by promoting cellular migration. This results highlight a potential cross-talk between the endocytosis and signalling of Tie2 that I believe needs to be further investigated.

Table of contents

Table of Figures

List of Tables

List of Abbreviations

Ang1	Angiopoietin ligand 1
AP-2	Adaptor Protein complex 2
BSA	bovine serum albumin
CCP	Clathrin-coated pit
CCV	Clathrin-coated vesicle
GEEC	GPI-enriched early endosomal compartments
CHC	Clathrin Heavy Chain
CIE	Clathrin-independent endocytosis
CLIC	Clathrin-independent carrier
CME	Clathrin-mediated endocytosis
CTxB	Cholera toxin subunit B
DAPI	4',6-diamidino-2-phenylindole
DMSO	dimethyl sulphoxide
DNA	deoxyribonucleic acid
EC	endothelial cell
EDTA	ethylenediaminetetraacetic acid
EEA1	Early Endosome Antigen
EGF	Epithelial Growth Factor
EIPA	5- N-ethyl-N-isopropyl amiloride
ELISA	Enzyme-linked Immunosorbent assay
EM	Electron microscopy
FEME	Fast endophilin-mediated endocytosis
FITC	Fluorescein isothiocyanate
GPCR	G-protein coupled receptors
GPI	Glycosylphosphatidylinositol
GRAF-1	GTPase regulator associated with focal adhesion kinase-1
Grb	Growth factor receptor bound
GTP	Guanosine-5'-triphosphate
GTPase	guanosine triphosphatase
HEPES	4-(2-hydroxyethyl)-l-piperazineethanesulfonic acid
hrAng1^{His}	Human recombinant Ang1 His tagged
HRP	Horseradish peroxidase
HUVEC	Human umbilical vein endothelial cell
Ig	Immunoglobulin
IPTG	Isopropyl-β-D-thiogalactopyranoside
kDa	Dalton
KDR	Kinase insert domain receptor or VEGFR-2
LDL	Low density lipoprotein
mβCD	Methyl-beta-cyclodextrin
Pak	P21-activated kinase
PBS	Phosphate-buffered saline
PCC	Pearson correlation coefficient
PI3K	Phosphatidylinositol-3-OH kinase
PIC	Protease Inhibitor Cocktail
PMA	Phorbol myristate acetate
Rac1	ras-related C3 botulinum toxin substrate 1
RhoA	Ras homolog gene family member A
RNA	ribonucleic acid
çAP2-GFP	sigma-AP2-eGFP subunit

SDS	sodium dodecyl sulphate
SDS-PAGE	SDS-polyacrylamide gel electrophoresis
SEM	standard error of the mean
ShcA	Src homology 2 domain-containing-transforming protein C1
siRNA	small interference RNA
SRSF	Sheffield siRNA Screening Facility
SV40	Simian Vacuolating virus 40
TBS	Tris-buffered saline
TEK	Tie2 gene
TEMED	1,2-bis (dimethylamino)-ethane
Tfn	transferrin
TBS	Tris-buffered saline
Tie	Transmembrane receptor with immunoglobulin and EGF domains
$Tie2^{FLAG}$	Tie-2 FLAG tagged
$Tie2^{K855R}$	Tie-2 Kinase dead mutant, lysine 855 to arginine
VEGF	Vascular Endothelial Growth Factor
VEGFR	VEGF Receptor

Acknowledgements

I am most grateful to British Heart Foundation for their financial support during my PhD and for making it possible.

I am indebted to Liz for allowing me to enrol in this project and for all her guidance and patience.

I thank my advisors, Dr. Kai Erdmann and Prof. Steve Winder for their critical questions and valuable suggestions.

I thank as well all of the Smythe lab members, past and present, for their scientific help and for all the nice chit-chat in between incubations. Where would I be without Filipe´s and Dave´s help and patience?

I would also like to thank the SRSF lab for their technical support and advice as well as for the friendly environment, and the Cardiovascular Department of the Faculty of Medicine for allowing me to isolate HUVECs.

CHAPTER 1

Introduction

1.1 Tie receptors are key regulators of vascular functions

Organisms with closed blood circuits are characterised by a cardiovascular system that transports cells, nutrients and oxygen as well as other components around the body for the adequate function of tissues (Marieb & Hoehn 2013). The correct transportation of blood is achieved thanks to the structure of blood vessels, which are lined with a specialized epithelium called endothelium. The endothelium, which can also be found in lymphatic vessels, is composed of endothelial cells (ECs) and it is involved in the regulation of important vascular functions. For instance, the permeability between ECs to solutes allows for the maintenance of tissue fluid homeostasis, while the extravasation of leukocytes into tissues is increased in response to inflammation (Bazzoni & Dejana 2004). Furthermore, ECs are also involved in the maintenance of vessels integrity and in the formation of new blood and lymphatic vessels (processes called angiogenesis and lymphangiogenesis respectively) in normal and pathological conditions, which occurs by regulation of their migratory and differentiation state. For instance, maintenance of vessels is achieved by maintaining a stable population of differentiated endothelial cells in quiescent state. On the other hand, the generation of new vessels is achieved by the spreading of sprouting vessels, which are characterized by different forms of differentiated endothelial cells: in sprouting vessels an endothelial tip cell, which is a highly migratory EC rich in filopodia, leads to the formation of new vascular vessels by stalk cells, which are proliferative ECs that ultimately differentiate to quiescent ECs conforming the new vessels (Augustin et al. 2009) (***Figure 1***). Vascular homeostasis and development are processes directed and regulated by multiple growth factors and signals provided by the environment that ultimately affect the behaviour of ECs (McCarron et al. 2017).

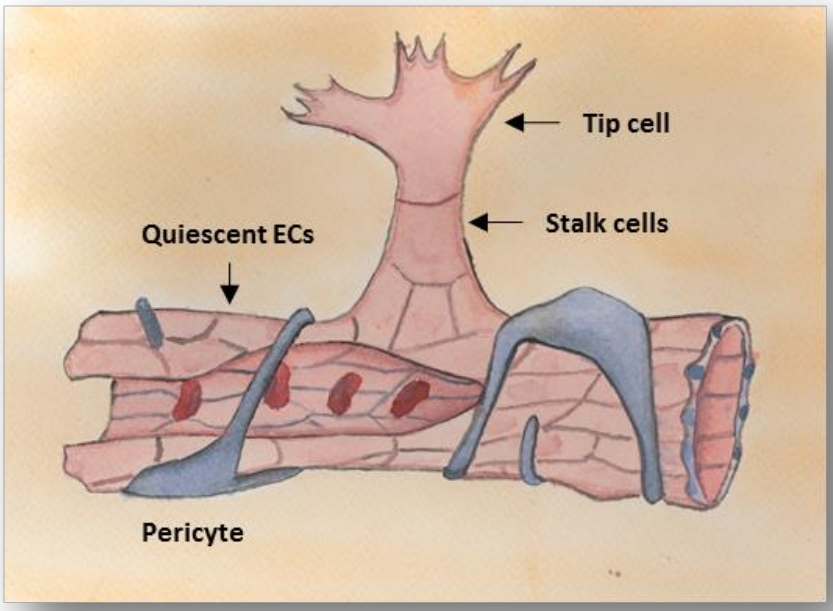

Figure 1. Representation of the development of a new blood vessel. A stalk cell with its multiple filopodia leads the direction of the new vessel. Following stalk cells will proliferate causing the enlargement of the new vessel. Ultimately proliferating endothelial cells will become quiescent and conform a "pebble" like pattern delimiting the vessel lumen. Mature vessels are supported by specialised cells known as pericytes. Scheme is an artistic representation and it is not made to scale.

The molecular mechanisms directing ECs behaviour are highly complex and not yet completely unveiled. Indeed, multiple molecular pathways and factors are known to be implicated (Ferrara & Kerbel 2005; Adams & Alitalo 2007). The Vascular Endothelial Growth Factor Receptor (VEGFR) and the angiopoietin (Ang)/Tie receptor systems are considered two of the most important systems implicated in development and regulation of homeostatic ECs functions (Augustin et al. 2009; Eklund et al. 2016). The expression of both families of receptors is almost exclusive to endothelial cells, suggesting the specific functional relevance that the receptors have in vascular physiology (Keating & Williams 1987).

Up to date, the Vascular Endothelial Growth Factors and their receptors (VEGF and VEGFRs) are the most studied pathways in relation to regulation of ECs function. Also, the family of VEGFRs appear to be the most critical and decisive on determining ECs function (Jeltsch et al. 2013). The family of VEGFRs is formed by three different

transmembrane growth factor receptors with tyrosine kinase activity that bind to 5 VEGFs with different affinity (Jeltsch et al. 2013). As tyrosine kinase molecules, VEGFRs possess the ability to bind Adenosine Triphosphate (ATP) nucleotides and to catalyse the transfer of the phosphate group in ATP to tyrosine amino acid residues of their own intracellular domain (auto-phosphorylation) or other proteins, which activates a cascade of signalling events within cells (Ferrara 2004). The activation of transmembrane receptor tyrosine kinases such as VEGFRs is regulated by the binding of ligands that are known as growth factors (Ferrara 2004). Most VEGFRs are expressed in the cell surface of ECs although a significant population of VEGFR-2 (or Kinase insert domain receptor, KDR) was found to reside in intracellular compartments of cells (Gampel et al. 2006). Study of VEGFRs has revealed that in the case of blood vessels, they act by promoting vasculogenesis (formation of embryonic primary blood vessels) during embryonic stage and angiogenesis (remodelling or dispersing of blood vessels originating from other blood vessels) during embryonic and adult life (Ferrara 2004). Furthermore, VEGFRs were also found to be involved in the inflammatory response by enhancing vascular permeability to allow the extravasation of leukocytes (Vestweber 2012).

Nonetheless, despite the relevance of the VEGF/VEGFR pathway, the family of Tie receptors is also widely studied for its role in the regulation of ECs behaviour and vascular physiology (Jeltsch et al. 2013). The family of receptors is composed of Tie1, which still remains an orphan receptor, and Tie2, which has been found to bind the ligands angiopoietin 1, 2 and the human and mouse orthologues Ang3 and Ang4 (Davis et al. 1996; Maisonpierre et al. 1997; Valenzuela et al. 1999). Tie receptors are also transmembrane receptors with tyrosine kinase activity and have been implicated in embryonal and adult angiogenesis as well as vascular cell stability (Schnürch & Risau 1993). Indeed, the knock-out of Tie2 receptor in mice caused general vascular abnormalities and early embryonic lethality at E9.5-10.5, mainly because embryos failed to develop vascular branching (Dumont et al. 1994; Sato et al. 1995). Also, knock-out of the agonistic Ang1 ligand and overexpression of the context-dependent agonist Ang2 ligand caused similar parameters as seen for the downregulation of Tie2 receptor suggesting their role as agonist and antagonist of the receptor (Suri et al. 1996;

Maisonpierre et al. 1997). In humans, missense mutations in the cytoplasmic tail of Tie2 that lead to an increase in the auto-phosphorylation levels of the receptor were reported to be the cause of Multiple Cutaneous and Mucosal Venous Malformations (VMCM), a hereditary or spontaneous vascular condition that is characterised by the presence of multiple vascular lesions composed of disorganised venules with variable thickness of the vascular wall (Boon & Vikkula 1993).

Vascular physiology as therapeutic target

Given the multiple and important roles of the vascular endothelium, it is not surprising that regulation of ECs function is being studied in order to find solutions for multiple pathological processes with vascular implication such as sepsis, ischemia or cancer. In the case of sepsis, potential therapies aim to inhibit the vascular permeability that leads to toxic shock (Aman et al. 2016). In a different approach, multiple pro-angiogenic factors have been tried for improving the prognosis on patients affected by episodes of ischemia (Ko & Bandyk 2014). Nonetheless, the main aim of anti-angiogenic therapy is finding a way to inhibit tumour expansion and development by disrupting the tumour-induced angiogenesis that allows tumour survival and enlargement (Ye 2016). Therefore, understanding the molecular mechanisms implicated in normal and pathogenic vascular function is important to develop and improve therapies with a full understanding of their effects (Ferrara & Kerbel 2005; Radeva & Waschke 2017).

Since the expression of Tie receptors, as well as VEGFRs, is almost restricted to ECs both systems are good candidate targets for multiple therapies. For instance, the first anti-angiogenic drug that was used to treat tumours was bevacizumab, a soluble monoclonal antibody that inhibits VEGFA action (Tarallo & De Falco 2015). Indeed, multiple anti-angiogenic drugs targeting VEGF pathway are being used to complement chemotherapy in the treatment for cancer. Nonetheless, the clinical prognosis obtained has not been as good as anticipated and research has expanded towards targeting other angiogenic pathways in order to implement VEGF targeted anti-angiogenic therapies. Indeed, soluble Tie2 was long ago seen to inhibit angiogenesis by inhibiting the action of Ang1 on the receptor (Lin et al. 1997). High serum levels of Ang2 are considered to be biomarkers of poor prognosis for multiple cancers and many studies have focused on

Ang2 blockers as potential anti-therapeutic targets (Thurston & Daly 2012). Also, Ang1 mimetics such as Vasculotide have been used in pre-clinical trials to reduce endothelial permeability and therefore inhibit extravasation of metastatic cells (Wu et al. 2015).

However, before applying complementary anti-angiogenic therapies multiple factors need to be considered such as the potential secondary effects of combined therapies (Ye 2016). Furthermore, multiple potential anti-angiogenic drugs targeting the Ang/Tie system have failed to provide positive results in clinical trials (Moore et al. 2015; Chiu et al. 2016; Thurston & Daly 2012). Moreover, controversial results obtained when targeting the Ang/Tie pathway have highlighted the importance of fully understanding the complex regulation of the system, which not only appears to be context dependent yet also affected by other vascular factors (Thurston 2003; Thurston & Daly 2012).

1.2 Multiple factors regulate the Ang/Tie function in endothelial cells in a cell- and context-dependent manner

Since the Tie receptor was first described and studied, 25 years ago, the Ang/Tie system has been revealed as a complex pathway the regulation of which depends on the interaction of multiple factors and the function of which is cell- and context-dependent (Eklund & Saharinen 2013).

Although presenting many similarities to the other RTKs, Tie receptors are known to have multiple structural particularities. As RTKs, Tie receptors are structurally characterized by an extracellular ligand-binding domain, a single transmembrane domain and an intracellular core with intrinsic Tyrosine Kinase (TK) activity (Lemmon & Schlessinger 2010). Tie receptors possess a complex and unique extracellular domain composed of various homology domains. Tie1 and Tie2 were first identified as orphan receptors and owe their name to the immunoglobulin (Ig) and Epidermal Growth Factor (EGF) homology domains of their extracellular portion (Tyrosine kinase with Ig and EGF homology domains, Tie) (Partanen et al. 1992; Schnürch & Risau 1993; Dumont et al. 1993). As well as the 3 Ig and 3 EGF repeats, the Tie receptors are also characterised by having 3 Fibronectin-like III (FNIII) repeats in their unique and complex extracellular domain (***Figure 2***). In contrast to the other RTKs, crystallography studies of the ectodomain of Tie2 interacting with the Ang-2 ligand revealed that the conformation of the receptor is not changed upon binding to the ligand and that the interaction rather resembles the one between immunoglobulins and their antigens (Barton et al. 2006). The tyrosine kinase domain of Tie2 was crystalized by Shewchuk et al (2000) and the crystal structure revealed that, again in contrast to most of the kinase domains found in RTKs, the nucleotide binding loop is positioned in an inhibitory conformation whereas the activation loop is in an “active-like” conformation in the absence of phosphorylation (Shewchuk et al. 2000). By analogy to other RTKs, the crystallization of the kinase domain of Tie2 also revealed the importance of the K855 and E872 amino acid residues in the correct positioning for the catalysis of ATP molecules (Shewchuk et al. 2000). Indeed, the $Tie2^{K855R}$ mutant was shown to be a dead kinase mutant in later works

(Cascone et al. 2005; Fukuhara et al. 2008). Similarly to other growth factor receptors, the activation of Tie2 is achieved by a ligand-induced oligomerization on the plasma membrane that leads to the auto- and trans-phosphorylation of tyrosine residues along the cytoplasmic tail (Procopio et al. 1999; Kim et al. 2005; Bogdanovic et al. 2009) (***Figure 2***).

As mentioned above, Tie2 has been observed to bind the 4 members of the family of Angiopoietins, Ang1, Ang2 and the human and mouse orthologues Ang4 and 3 (Davis et al. 1996; Maisonpierre et al. 1997; Valenzuela et al. 1999). Angiopoietins are secreted glycoproteins containing a specific amino-terminal domain followed by a coiled-coil domain and a carboxy-terminal fibrinogen-like region. The fibrinogen-like region regulates the interaction with Tie2 and the coiled-coil and specific amino-terminal domains mediate ligand-dimerization and multimerization (Thomas & Augustin 2009; Davis et al. 2003) (***Figure 2***).

The ligands of the Tie2 receptor are secreted by different cell types and can have multiple effects on vascular physiology through their context-dependent activation of Tie2 (Eklund & Olsen 2006). Of the 4 angiopoietin ligands described to bind the Tie2 receptor, Ang1 and Ang2 still remain the best characterized. Ang-1 is secreted by vascular supportive non-endothelial cells such as pericytes and has been identified as the main agonist and mediator of Tie2 cellular functionality based on studies with transgenic mice and cells in culture. By enhancing ECs cell-cell and cell-matrix adhesion Ang1 is considered to be a vascular stabilizer regulating endothelial cell permeability. Nonetheless, the Ang1-induced cell migratory response is key in the induction of angiogenesis (Thomas & Augustin 2009). On the other hand, Ang-2 is stored in Weibel-Palade Bodies by endothelial cells before being secreted and it is described as a vascular activator that appears to counteract Ang-1 by destabilizing the vasculature integrity through different mechanisms (Thurston & Daly 2012): for instance, since Ang1 elicits a stronger phosphorylation of Tie2 than Ang2, Ang2 was proposed to act by attenuating effect of Ang1 on endothelial cells (Maisonpierre et al. 1997). Furthermore, the oligomerization states of angiopoietins were seen to influence the cell-

compartmentalisation of Tie2 as native dimerized Ang2 promoted the mobilization of the receptor towards cell-matrix contact areas, while oligomerised Ang1 and Ang2 caused the translocation of Tie2 complexes to the retractile and lateral sides of sub-confluent cells (Pietilä et al. 2012). Therefore, different cell responses can be activated upon activation of Tie2 by the angiopoietin ligands that are ultimately determined by the cell state and environment (***Figure 3***). The two ligands were found to bind in a very similar way to the ectodomain of the receptor and the differential effect on the receptor was shown to change by mutating three amino acids of the ligands interaction interface (N468G, S417I and S480P) (Barton et al. 2006; Pietilä et al. 2012; Yu et al. 2013).

The different cellular responses triggered by the angiopoietin ligands are mediated by multiple downstream signalling pathways that can be activated following the phosphorylation of the Tie2 receptor (***Figure 2***). After receptor oligomerization, tyrosine 992 is auto-phosphorylated and it is followed by the receptor cross-phosphorylation of other tyrosine residues located within the kinase domain and intracellular C-terminus, namely Y814, Y1101, Y1108 and Y1112 (Huang et al. 1995; Sturk et al. 2010). It appears that the particular tyrosine residues phosphorylated along the C-terminal tail of Tie2 are involved in defining the specificity of the downstream signalling pathway of the activated receptor by specifically recruiting different docking proteins, which will determine the cellular response to the activation of the receptor (Eklund & Olsen 2006). For instance, Tie2 regulation of cell survival is thought to be mediated through the activation of the Phosphatidylinositol-3-OH Kinase (PI3K)/Akt signalling pathway after the recruitment of the subunit p85 of PI3K to the phospho-tyrosine Y1101 of Tie2 (Kontos et al. 1998; Kim, Kim, So, et al. 2000). Although later PI3K was also described to mediate cell migration by activation of Focal Adhesion Kinase (FAK) (Kim, Kim, Moon, et al. 2000) and Rho GTPases Ras homolog gene family member A (RhoA) and Ras-related C3 botulinum toxin substrate 1 (Rac1) (Cascone et al. 2003). Activation of PI3K was also seen to be necessary for the inhibition of endothelial cell death by A20 binding inhibitor of NF-κB activation-2 (ABIN-2) (Tadros et al. 2003), although the direct interaction between Tie2 and ABIN-2 was necessary for the Ang-1 induced inhibition of nuclear factor-kappa B (NF-κB), which mediates the potent anti-inflammatory response induced

in vascular endothelium by Ang1 (Hughes et al. 2003). Nonetheless, the phosphorylated Y1101 in Tie2 was also reported to recruit the p52 isoform of the Src homology 2 domain-containing-transforming protein C1 (ShcA) via its SH2 domain. ShcA was revealed to be important in the regulation of ECs motility but not survival (Audero et al. 2004). Dok-R, which was found to associate with the phosphorylated Y1108, mediated the interaction with Nck and Rac1/p21-activated kinase (Pak) to regulate Ang1-induced cell migration, proliferation and cytoskeletal reorganization (Eklund & Olsen 2006; Jones & Dumont 1998; Master et al. 2001). Other signalling adaptors described to bind different phospho-tyrosines of Tie2 are the growth factor receptor bound (Grb) 2, 7 and 14 and the tyrosine phosphatase Shp2, which interact with Tie2 through their SH2 domain to mediate cell survival and migratory responses (Jones et al. 1999; Sturk & Dumont 2010; Ahmed et al. 2013). On the other hand, Y1112 residue in the C-terminal tail of Tie2 was seen to have a negative regulatory role on the activation of the receptor and to also influence the activation of downstream signalling substrates like Dok-R, p85 or Shp2 (Sturk et al. 2010).

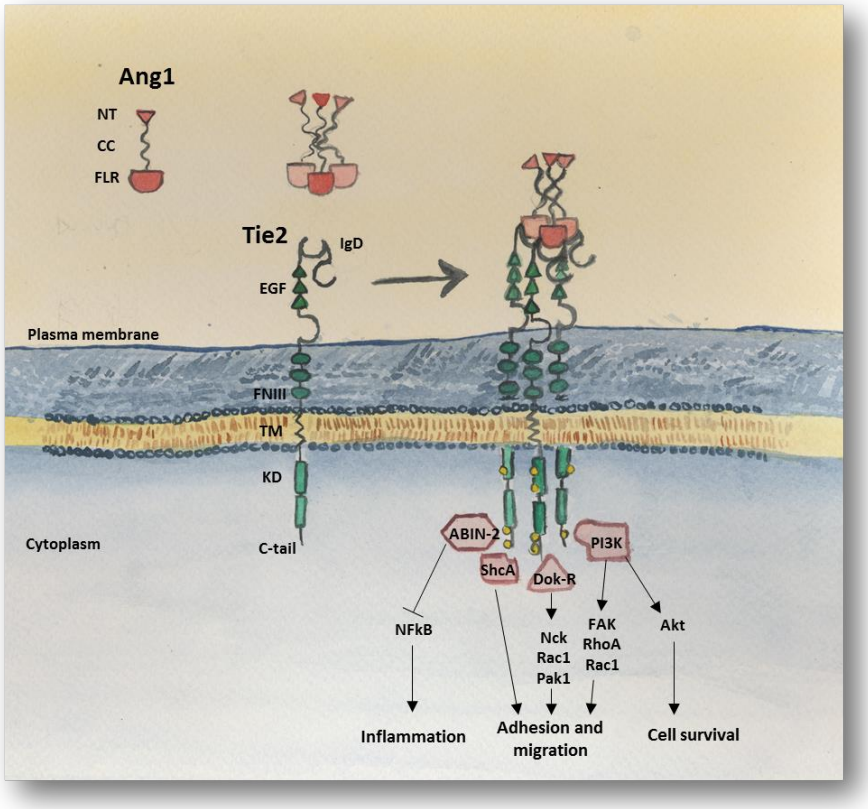

Figure 2. Activation of Tie2 receptor by Angiopoietin 1 ligand (Ang1). Angiopoietins are composed by a N-terminal domain (**NT**), a coiled-coil domain (**CC**) and a fibrinogen-like region (**FLR**). Tie2 ectodomain is composed by 3 Immunoglobulin domains (**IgD**) intercalated with 3 epithelial growth factor homology domains (**EGF**) and 3 Fibronectin-like III repeats (**FNIII**). Tie2 has a single trans-membrane domain (**TN**) and one kinase domain (**KD**) which has the C-terminus and N-terminus domains separated by a linking region. Various molecules of Ang1 are associated through the coiled coil domain, which promotes the oligomerisation and activation of multiple Tie2 on the plasma membrane. Oligomerisation of the receptor leads to the auto- and trans-phosphorylation of tyrosine residues along the kinase domain and the C-terminal cytoplasmic tail (**C-tail**). Activated Tie2 can recruit different adaptors and initiate intracellular signalling cascades that inhibit inflammatory responses, promote cell survival and proliferation or induce cell adhesion and migration.

Although remaining an orphan receptor, Tie1 also appears to regulate the activity of the Ang/Tie pathway in different ways. Different studies indicate that Tie1 oligomerises with Tie2 on the cell surface and that this might be regulating the angiopoietin-induced activation and signalling of Tie2 (Hansen et al. 2010; Song et al. 2012; Seegar et al. 2010). For instance, it was shown that Ang1 was able to phosphorylate Tie1 in a Tie2-dependent manner to modulate the cell survival response to the activation of Tie2 (Yuan et al. 2007); and different recombinant ligands were shown to be able to activate Tie1 and promote its interaction with Tie2 (Saharinen et al. 2005). Song et al. (2012)

described how the relative proportion of available Tie1 and Tie2 in lymphatic or venous endothelial cells would determine the agonistic or antagonistic role of Ang2 depending on the cell type. Actually, it was reported that a non-conserved 3 amino acid peptide in Ang2 determines the stability of the association of Tie1 with Tie2 in the cell surface (Yu et al. 2013). Furthermore, in accordance with the described role of Tie1, the regulated intramembrane proteolysis of Tie1 induced by phorbol myristate acetate (PMA) was seen to influence the Ang1 activation of Tie2 by increasing the interaction between the ligand and the receptor (Marron et al. 2007).

The function of the Tie2 receptor in endothelial cells is also dependent on cell confluency (***Figure 3***). Recent work revealed that the interaction between Tie2-expressing cells determine the sub-cellular location of Tie2 in domains of the plasma membrane as well as the specificity of downstream signalling pathways. When confluent cultures of HUVECs were incubated with Ang1, the PI3K/Akt signalling pathway inducing cell survival process was activated, while migration-inducing signalling pathways were triggered in non-confluent cultures of cells (Fukuhara et al. 2008; Saharinen et al. 2008).

Moreover, the Ang/Tie pathway is also influenced by other molecules such as integrins, phosphatases and activated VEGFRs, which also appear to have an important role in determining the cellular behaviour induced by the Ang1/Tie system (Thomas & Augustin 2009). In the case of integrins, it was early seen that Ang1 could mediate cell adhesion independently of the expression of Tie2 yet dependent on integrins (Carlson et al. 2001), while Ang2 was seen to mediate endothelial cell destabilization via activation of integrin β1 (Hakanpaa et al. 2015). In a different example, the activation of Tie2 by Ang1 in cell-cell contacts was shown to counteract the endothelial destabilizing effect induced by VEGFR by interfering in the VEGF-induced signalling pathway (Gavard & Gutkind 2006; Gavard et al. 2008).

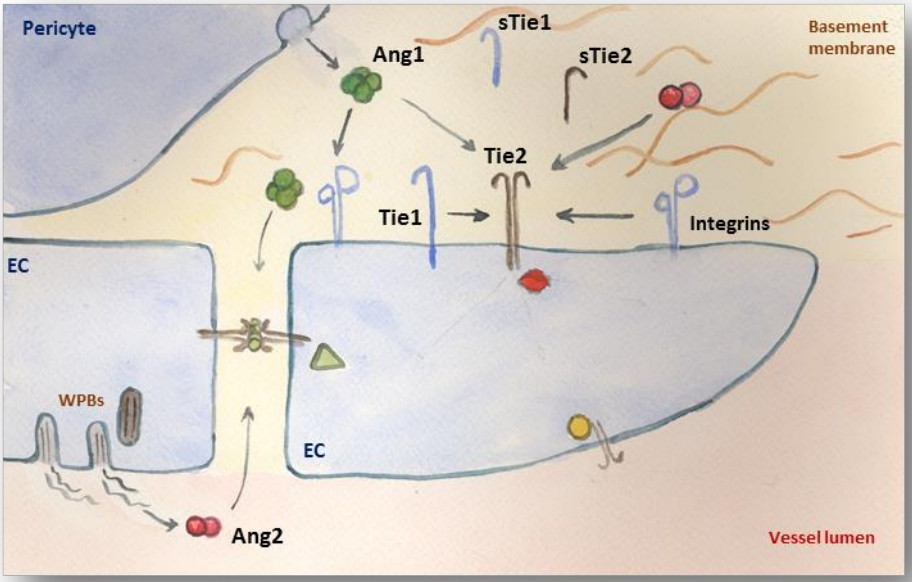

Figure 3. The Ang/Tie pathway is complexly regulated by its environment and cell context. Representation of various factors described to regulate the function of Tie2 receptor in endothelial cells. The main agonistic ligand Ang1 is secreted by pericytes, while the context-dependent agonist Ang2 is produced by endothelial cells and contained within the Weibel paladel bodies. Ang2 only induces a weak activation of Tie2 and competes with Ang1. The orphan receptor Tie1 can oligomerise with Tie2 and regulate its activation, furthermore, Tie1 oligomerised with Tie2 can also be activated by Ang1. Both receptors can be cleaved and soluble Tie1 and Tie2 are believed to sequester the ligands. Interaction with other proteins such integrins can also modulate the ligand-induced activation of the receptor. Furthermore, localization of the receptor within the cell surface can also influence the final cellular behaviour to activation of Tie2 by Ang1. **EC**, endothelial cell; **WPBs**, Weibel-Paladel bodies; **sTie**, soluble receptor. Scheme is an artistic representation and it is not made to scale.

1.3 The functionality of the Ang1/Tie2 system could also be modulated by its endocytic mechanisms

Although in recent years endocytosis of multiple membrane receptors has been shown to be part of their regulating mechanism, little is known about the endocytosis of Tie2 and its role in modulating the Ang/Tie pathway.

Endocytosis is the process by which cells form specific plasma membrane structures or invaginations to internalize cell surface and extracellular material. Different mechanisms have been described for the internalization of molecules into cells that can be determined by the cargo itself and other factors (Conner & Schmid 2003). Endocytosis begins with the selection of cargoes at the plasma membrane, which can be done using protein-based recognition cues or also lipid-based recognition cues. Recognition patterns for a specific cargo determine the recruitment of specific molecular adaptors and mediators that are responsible for the formation of membrane deformation and formation of vesicles. Ultimately, vesicle trafficking to intracellular compartments is achieved by a different set of molecular regulators and tethers (Mayor & Pagano 2007). The different endocytic mechanisms involved in the endocytosis of a cargo can determine a variety of factors such as the rate of internalization, intracellular or transcellular destination or modulation of cell behaviour and physiology so it is important to unveil and understand the different endocytic pathways and their mechanisms of internalization (Conner & Schmid 2003).

Up to date, different endocytic pathways have been described, of which Clathrin-Mediated Endocytosis (CME) is the most well-known of those. Still, multiple Clathrin-Independent Endocytosis (CIE) pathways are also being studied (***Figure 4***).

Clathrin mediated endocytosis

CME is characterised by the formation of small pits (approximately 120 nm) that are formed due to the assembly of clathrin molecules on the cytosolic side of the plasma membrane (Conner & Schmid 2003). The Adaptor Protein complex 2 (AP-2) is considered the main adaptor protein that functions as an intermediate between clathrin and the transmembrane cargoes internalized via CME, although alternate clathrin

adaptors have been described more recently that could function as a way to modulate some kind of CME plasticity. These include arrestins, ARH, disabled-2 (Dab-2) and Numb and the Epsin superfamily (Traub 2003). Indeed, it has been shown that different clathrin-coated pits can lead to differential dynamics of endocytosis driven by the intracellular domains of the internalized cargos so that membrane proteins internalized by CME may be internalized in segregated CCVs (Tsao & Von Zastrow 2000; Puthenveedu & von Zastrow 2006; Mundell et al. 2006).

After formation of clathrin-coated pits (CCPs) by the assembly of AP-2 and clathrin in the plasma membrane, clathrin coated vesicles (CCVs) are pinched off from the plasma membrane and trafficked to intracellular compartments (Doherty & McMahon 2009). Scission of CCVs from the plasma membrane is achieved by the action of the GTPase dynamin, which is currently believed form a constrictive "collar" around the neck of the forming CCPs. The role of actin in the formation of CCVs is thought to depend on the location of the CCP within the cell and on the cell type: in mammalian cells, situations where a high membrane tension is opposing the formation of CCPs, actin polymerisation would be necessary to generate a pulling inward force for the successful generation of CCVs yet actin may not be necessary in other situations (Boulant et al. 2011; Yao et al. 2013). On the other hand, actin polymerisation is always required for the formation of CCVs in yeast, where the cell needs to overcome a constant membrane tension (Kaksonen et al. 2006; Aghamohammadzadeh & Ayscough 2009).

Clathrin independent endocytosis

CIE pathways are classified depending on different characteristics as not all can be identified with a single endocytic mediator. Indeed, identification of CIE pathways is complicated because multiple requirements can be shared between them and identification can be sometimes based on negative results or morphological characteristics. In terms of molecular mechanisms, as Mayor and Pagano proposed, CIE can be classified based on its dependence of dynamin and whether functional ADP-ribosylation factors (Arf) and Rho GTPases are required for the successful internalization of endocytic mechanisms (Mayor & Pagano 2007). Nonetheless, given the involvement

of Arfs and Rho GTPases in multiple cellular functions it is difficult to isolate their direct involvement in each endocytic mechanism.

Phagocytosis

Phagocytosis consists in the engulfment of opsonized bacteria or large cell particles originated from apoptotic cells (***Figure 4***a). Phagocytosis is generally restricted to specialized cells from the immune system such as macrophages, although a limited number of other cells such as fibroblasts can also perform phagocytosis (Pauwels et al. 2017). Phagocytosis is induced by the detection of opsonins or markers of apoptotic cells by specific cell membrane receptors expressed on phagocytic cells. Activation of the receptors leads to the initiation of signalling cascades that trigger the remodelling of actin cytoskeleton for the formation of plasma membrane extensions around the phagocytosed particle. The phagocyted particle is engulfed in a compartment know as phagosome, which matures by transient fissions with early and late endosomes to ultimately fuse with lysosomes (Pauwels et al. 2017). Phagocytosis is independent of dynamin yet dependent on actin cytoskeleton remodelling triggered by RhoA, Rac1 or Cdc42 depending on the phagocytic receptors activated (Jae-Bong Park 2003; Doherty & McMahon 2009).

Macropinocytosis

Macropinocytosis is an endocytic process that consists in the formation of cell surface ruffles that collapse onto plasma membrane to trap and internalise large volumes extracellular fluid within structures known as macropinosomes, which usually have diameters above 500 nm (Doherty & McMahon 2009). Macropinocytosis can be performed by a multitude of cell types and, although it is not considered a selective endocytic process, can be induced by a strong activation of receptors. Multiple growth factor receptors have been seen to be internalized via macropinocytosis in some circumstances and it has been proposed as a mechanism for the cell to respond to stimulation by growth factors by engulfing large areas of plasma membrane (Watanabe & Boucrot 2017). For instance, recently it was shown that while unstimulated VEGFR is internalized via CME, stimulated VEGFR is internalized by ECs through macropinocytosis (Basagiannis et al. 2016). Macropinosomes are usually uncoated and have a diameter

larger than 500 nm. Forming macropinosomes can be readily identified by their size and the visualization of the actin-rich membrane ruffles at the cell edge (Doherty & McMahon 2009; Basagiannis et al. 2016). The remodelling of the actin cytoskeleton for the formation of membrane ruffles is mediated by Rac1 and its effector p21-activated Kinase-1 (Pak1) (Dharmawardhane et al. 2000). The plasma membrane Na^+/H^+ exchanger is essential for the formation of successful membrane ruffles and macropinosomes so the Na^+/H^+ exchanger inhibitor 5- N-ethyl-N-isopropyl amiloride (EIPA) inhibits the internalization of macropinocytic markers (Ivanov 2008; Koivusalo et al. 2010; Li et al. 2015).

Caveolae-mediated endocytosis

Caveolae-mediated endocytosis is characterised by the formation of small flask-shape invaginations of about 60 nm in size that are coated by caveolin proteins, which are required for the formation of the caveolae (Shvets et al. 2014). The presence of caveolae on the cell surface is variable depending on the cell type, yet in the case of endothelial cells caveolae can represent as much as 10-20% of the total cell surface (Conner & Schmid 2003). Caveolae in ECs can be found as single caveolae budding from the plasma membrane or also linked in invaginations of the plasma membrane in rosette or tree-like shapes. Furthermore, caveolae have also been seen to connect the apical and basal membrane surface of ECs, the reason why they are believed to have an important role in the endothelial vascular physiology promoting transcytosis through the endothelium (Parton & Simons 2007). Indeed, besides internalizing cargo, caveolae are also believed to have other functional roles such as acting as supports for activated receptors initiating signalling cascades or for conferring endothelial cells with shear stress resistance (Parton & Simons 2007; Doherty & McMahon 2009; Cheng & Nichols 2016). Caveolae are formed associated to detergent-resistant subdomains of the plasma membrane and are dependent on membrane components such as glycosylphosphatidylinositol (GPI) and cholesterol. Indeed, the cholesterol interfering compounds Filipin and methyl-beta-cyclodextrin (mβCD) are known to disrupt the formation and internalization of caveolae (Parton & Simons 2007; Doherty & McMahon 2009). Although caveolae are rather stable structures on the plasma membrane, phosphorylation of caveolin-1 causes caveolae to

bud from the plasma membrane in a process that is dependent on dynamin and on the active remodelling of the actin cytoskeleton (Sverdlov et al. 2007; Shvets et al. 2014). Known endocytic markers of caveolae are bovine serum albumin, insulin receptor, Low Density Lipoprotein, the GPI-linked protein cholera toxin subunit B (CtxB) and the Simian Vacuolating virus 40 (SV40), although the last ones have been also reported to be internalized via other mechanisms (Nabi & Le 2003; Doherty & McMahon 2009). So far the most common identification method of caveolae-mediated internalization is its sensitivity to disruption of caveolin-1 function, although due to the multiple roles of caveolin-1 in cell this is not a completely direct identification instrument (Nabi & Le 2003; Doherty & McMahon 2009; Shvets et al. 2014).

CLIC/GEEC

Another internalization pathway being characterised is the Clathrin-independent carrier (CLIC) internalization, which delivers cargoes to GPI-enriched early endosomal compartments (GEEC), therefore known as CLIC/GEEC internalization pathway (Doherty & McMahon 2009). CLIC/GEEC is characterised by the formation of long tubular ring structures that can have lengths of up to several micrometres. CLIC/GEEC internalization is also dependent on the integrity of the actin cytoskeleton yet it appears that in this case that actin reorganisation is dependent on the activity of Rho GTPase Cdc42 also known for be involved in the formation of filopodium (Doherty & McMahon 2009). Also, the characteristic tubulo-vesicular structures where cargoes are internalized seem to be maintained by the action of the GTPase Regulator Associated with Focal Adhesion kinase-1 (GRAF-1), which is also used to identify the pathway (Doherty & Lundmark 2009). As well as caveolae-mediated endocytosis, the CLIC/GEEC internalization relies on particular membrane domains enriched in cholesterol and GPI, although it does not depend on dynamin (Doherty & McMahon 2009). In this case, also CtxB and GPI-associated proteins are also described cargoes for this internalization pathway (Mayor & Pagano 2007; Doherty & McMahon 2009). Cargoes within the GEECs are rapidly recycled to the plasma membrane and are considered a mechanism by which cells controls membrane dynamics and tension (Gauthier et al. 2012).

FEME

More recently, a fast endophilin mediated endocytosis (FEME) has been described that was shown to be dependent on endophilin A2 for the clathrin-independent internalization of several receptors from the edges (Renard et al. 2014; Boucrot et al. 2015). FEME has been shown to be activated upon stimulation of specific receptors at the leading edge of spreading cells. It is considered a mechanism used by cells to quickly internalize plasma membrane and receptors to avoid over-stimulation (Watanabe & Boucrot 2017). Although it has been recently described, several membrane receptors have been shown to be internalized by FEME upon stimulation by their ligands, such as G-protein coupled receptors (GPCR), Interleukin Receptor-2 and several tyrosine kinase receptors like EGFR and VEGFR (Boucrot et al. 2015). Endophilin A2 was identified to mediate the interaction with endocytic mediators such as dynamin 2 through its SH3 domain and to also regulate membrane curvature with its BAR domain (Renard et al. 2014; Boucrot et al. 2015). FEME was described to occur only in lamellipodia, where Endophilin A2 is recruited by lamellipodin. Due to its association with migratory processes remodelling of the actin cytoskeleton is also critical for the successful recruitment of Endophilin A2 and FEME, in that sense, activation of Rac1 and Cdc42 was also seen to be essential for the internalization of FEME endocytic carriers (Boucrot et al. 2015; Watanabe & Boucrot 2017)

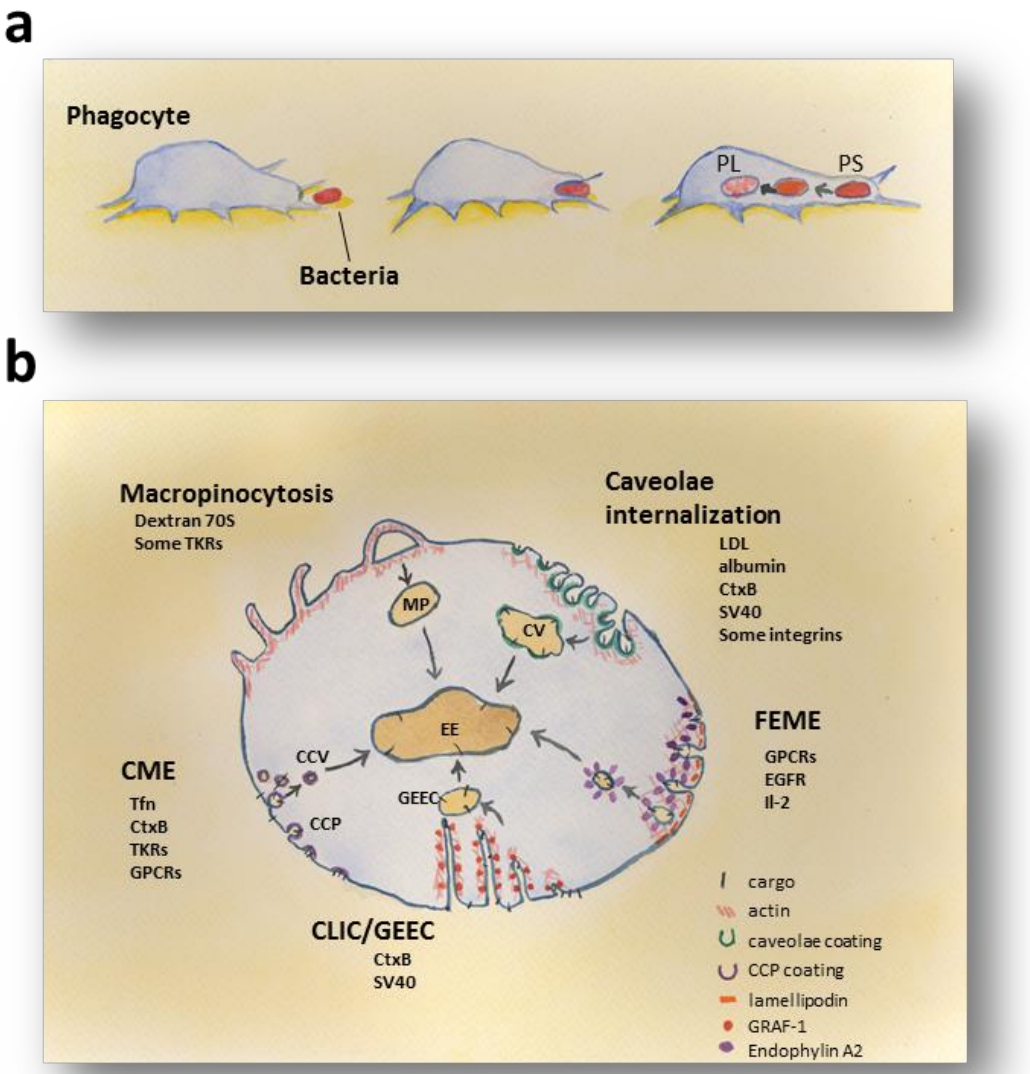

Figure 4. Schematic representation of different endocytic mechanisms. (a) A phagocytic cell engulfs a bacteria by extending projections of plasma membrane around it. The bacteria is internalized into a phagosome (**PS**), which by fusion with different compartments matures to a phagolysosome (**PL**), where the phagocytosed particle is degraded. **(b)** The endocytic mechanisms best characterised to date are clathrin mediated endocytosis (**CME**), macropinocytosis, caveolae-mediated internalization (CI), fast Endophilin-mediated endocytosis (**FEME**) and the clathrin-independent carrier internalization (**CLIC**). This endocytic process regulate the internalization of extracellular fluid, plasma membrane and cargos into early endosomes, from where cargos are either directed for being recycled back to the plasma membrane or trafficked to other intracellular compartments for degradation (not depicted). Macropinosomes (**MPs**), caveosomes (**CVs**) and GPI-enriched early endosomal compartments (**GEECs**) constitute preliminary endosomal compartments for cargos internalized via macropinocytosis, CI and CLIC correspondently. The different endocytic mechanisms are characterised by morphological particularities and/or essential proteins determining the successful internalization of cargos (depicted and indicated in the figure key). Also, different cargos are internalized by different endocytic mechanisms, as indicated by some examples. **Tfn**, transferrin; **Dex70**, Dextran 70S; **RTKs**, Receptor tyrosine kinases; **CTxB**, Cholera Toxin B subunit; **SV40**; Simian Vacuolating virus 40 **BSA**, Bovine Serum Albumin; SV40, Simian Vacuolating virus 40; **IL-2**, Interleukin receptor 2; **EGFR**, Epithelial growth factor receptor; **GPCRs**, G-protein coupled receptors. Schemes are an artistic representation and it is not made to scale.

Endosomal trafficking

The correct transition of events for the effective trafficking and delivery of cargoes between endosomal compartments is regulated by monomeric G-protein Ras-like small GTPases, Rab GTPases (Stenmark 2009). Rab proteins act as molecular switches that cycle between their active GTP-bound form and their inactive GDP- bound. Rab GTPases in their inactive state are found in the cytosol but their active GTP form drives them to integrate in lipid membranes. The specific intracellular localization of their effectors and the molecular functions of those determine the functions of the Rab GTPases in membrane trafficking. Hence Rab proteins can be used to identify different endosomal compartments (Stenmark 2009). For instance, early endosomes can be identified by Rab5 and its effector, Early Endosome Antigen-1 (EEA1) or adaptor protein containing pleckstrin homology domain, phosphotyrosine binding domain and leucine zipper motif (APPL1), which can actually identify different sub-populations of early endosomes (Kalaidzidis et al. 2015). In contrast to initial beliefs, it is now known that all sort of endocytic pathways can deliver cargoes into early endosomes, from where cargos can be sorted for recycling or degradation (Doherty & McMahon 2009). Other Rab proteins are Rab4, which is required for endocytic recycling (Sönnichsen et al. 2000) or Rab7, which regulates the maturation to late endosomes and fusion with lysosomes (Jordens et al. 2001).

The correct intracellular trafficking of vesicles is also achieved due to the involvement of the Soluble N-ethylmaleimide-sensitive factor Attachment Proteins (SNARE) which mediate vesicle fusion. SNARE proteins have been traditionally functionally classified between target-SNARE (t-SNARE) residing at the target membrane, and vesicle-SNARE (v-SNARE) localized in a trafficking vesicles. SNAREs contained in vesicles are recruited by cargo adaptors and determine the final destination and fission of the vesicles by interacting with specific t-SNARE proteins and by forming the fission SNARE complex (Hong 2005). For instance, the t-SNAREs syntaxin 6 and syntaxin 16, which are mainly localized in the Golgi apparatus and in some endosomes, regulate protein trafficking to and from the trans Golgi network by interacting with the v-SNARE VAMP3 or VAMP4 (Mallard et al. 2002; Hong 2005).

Endocytosis and signalling

Although the endocytosis of activated receptors was for a long time considered only as a way to down-regulate receptor signalling, multiple lines of evidence support the emerging paradigm that endocytosis is also a mechanism to influence cell signalling and behaviour (Sorkin & Von Zastrow 2009; Miaczynska et al. 2004; Di Fiore & De Camilli 2001). Different mechanisms have been reported with which endocytosis and trafficking influence cellular responses to multitude of stimuli. For instance, Goh *et al*. (2010) demonstrated that the time course of activation of signalling molecules differed when the internalization of the Epidermal Growth Factor Receptor (EGF-R) was specifically inhibited (Goh et al. 2010). By mutating a series of internalisation motifs within the cytoplasmic tail of EGF-R, Goh *et al*. (2010) obtained an EGF-R mutant that was still phosphorylated yet not internalized. Since the internalisation-defective mutant still had the kinase activity intact it was able to trigger the activation of downstream signalling pathways. Nevertheless, when the internalisation-defective mutant was activated the kinetics of pERK and pAkt where clearly altered for the first 120 min. In a different way, interaction of Placental Growth Factor with VEGFR1 was found to influence the formation of vessel branches in co-cultures of HUVECs and human dermal fibroblasts through promoting the Rab4 dependent recycling of $\alpha_5\beta_3$ integrin to focal adhesions in the plasma membrane (Jones et al. 2009). In another example, Schenck et al (2008) shown that localization of the Akt effector GSK-3 in Appl1 containing endosomes was determining for eliciting cell survival response and avoiding apoptosis in cells of zebrafish embryos, hence providing an in vivo example of how endosomal sorting can provide signalling specificity (Schenck et al. 2008).

Tie2 endocytosis and signalling

Even though no one has established a direct relationship between the endocytosis of Tie receptors and modulation of the Ang/Tie signalling, different results point out that the cellular response to the activation of the Ang1/Tie2 system could also be modulated by endocytic mechanisms. Similar to other RTKs, Tie2 is internalized after activation by its main agonist Ang1, as seen in different works and previous experiments from our lab

(Bogdanovic et al. 2009; Marron et al. 2000; Wehrle et al. 2009). In the case of Tie2, the hypothesis of a bi-linked regulation between endocytosis and signalling is suggested by different results. First, as Bogdanovic *et al*. highlight, the temporal dynamics of Tie2 internalisation and phosphorylation show that Tie2 clearly remains phosphorylated long after being endocytosed and before degradation (Bogdanovic et al. 2009). Similarly, unpublished data from our laboratory indicates that intracellular mediators of Tie2 signalling remain phosphorylated long after the internalisation peak time of the receptor (Unpublished; Maxwell, Ferreira and Smythe). Also, when the dominant negative mutant of dynamin was overexpressed in Human Umbilical Vein Endothelial Cells (HUVECs) the downstream signalling of Akt after ligand-induced activation of Tie2 was no longer observed (Unpublished, Maxwell and Smythe). Furthermore, the overexpression in HUVECs of a HA tagged Rme-6 construct, which is a regulator of the small GTPase Rab5 involved in the intracellular membrane trafficking of internalized proteins (Sato et al. 2005), inhibited the Ang1-dependent production of pAkt while increasing the phosphorylation of p38.

However, although data from different works suggest that Ang1 activation of intracellular signalling pathways might be influenced by the internalization of Tie2 and its sub-cellular localisation, none of the approaches used was known to specifically inhibit the internalization of Tie2 receptor after activation by Ang1. Actually, still little is known to date about the endocytosis of Tie2. In reference to that, it was established in HUVECs that the incubation with Ang1 triggers the internalization of Tie2 in a phosphorylation dependent manner (Bogdanovic et al. 2006). In agreement with this the kinase dead mutant $Tie2^{K855R}$ is not internalized even though that the mutant is also oligomerized in the cell surface after interaction with the ligands (Fukuhara et al. 2008). Moreover, the Tie2 ligand Ang2, which induces a weaker phosphorylation of the receptor, lead to a much slower internalization rate than the agonist ligand Ang1 (Bogdanovic et al. 2006). Nonetheless, the phosphorylation of neither Y1100 nor Y1106 was seen to be relevant for the internalization of the receptor in HUVECs, as Bogdanovic (2009) mentioned in her thesis that the mutation of these tyrosines did not inhibit the internalization of the receptor. It was also described that the Ang1-dependent

ubiquitination of Tie2 by the ubiquitin ligase Casitas B-lineage Lymphoma (Cbl) was required for the internalization and degradation of the receptor, as is the case for other receptors (Yokouchi et al. 1999; Kobayashi et al. 2004; Takayama et al. 2005; Wehrle et al. 2009; Bulut et al. 2013). Even so, the particular lysines that are ubiquitinated in an Ang1-dependent way were not identified and hence an ubiquitin-defective Tie2 mutant that would aid in the study of its internalization has not been reported yet. For instance, in the case of EGFR, multiple mutants defective in ubiquitination and other structural molecular motives were used to determine the determinants in the cytoplasmic tail of EGFR that collectively regulated the internalisation of EGFR (Goh et al. 2010). Although no other internalization motifs have been described for Tie2, I identified up to 4 AP-2 binding consensus sequences in the endodomain of the receptor (YxxΦ, WLSL or WxF) (Boll et al. 1996; Wernick et al. 2005)

Moreover, the specific internalization pathway of Tie2 receptor has not been clearly elucidated. Although Tie2 was seen to co-localize with Clathrin Heavy Chain (CHC) at the cell surface and intracellular compartments of HUVECs by Transmission Electron Microscopy, the knock down of CHC by a 70-90% did not inhibit the internalization of Tie2 (Bogdanovic et al. 2009). Inhibition of the internalization of Tie2 was only achieved by the depletion of K^+ and de-acidification of lysosomes by NH_4Cl, which are methods that have been later shown to have pleiotropic effects on the actin cytoskeleton and hence are not considered to be completely selective for CME (Ivanov 2008; Boucrot et al. 2015). Nonetheless, whether Tie2 could also be internalized in a clathrin-independent way remains controversial since although it was shown that Tie2 localization in caveolae of endothelial cells was required for the Ang1 induced activation of MEK/ERK (Yoon et al. 2003), Tie2 was not found in HUVEC caveolae using electron microscopy after incubation with Ang1 (Bogdanovic et al. 2009).

Therefore, although some results indicate that, as for the case of other RTKS, the internalization of Tie2 could be playing a role in the regulation of the downstream signalling of the activated receptor, the partial knowledge about the endocytosis of the receptor limits the possibility to further investigate this.

1.4 Project aims and outline

Understanding how endocytosis may be modulating the Ang1/Tie2 pathway and endothelial cell behaviour would enlarge our knowledge on the system and could become relevant in the design of new therapies against relevant diseases with vascular implication such as sepsis, ischemia or cancer. Therefore, in this project I aimed to characterise the internalisation mechanism of the Ang1-activated Tie2 receptor in order to determine the necessary approaches to investigate the role of endocytosis in regulating the Ang1/Tie2 system.

CHAPTER 2

Materials and Methods

2.1 Materials

Molecular biology and bacterial culture

EcoRV restriction enzyme and buffers (New England Biolabs)
HyperLadder I (BioLine Ltd)
LB agar dehydratated (Miller)
Lysozyme from hen egg white (Sigma-Aldrich)
NEB 5-alpha competent E. coli (New England Biolabs)
NZY broth (Fisher chemicals, Fisher scientific)
Pfu ultra DNA polymerase and buffers (Agilent Technologies UK)
Phusion High-Fidelity DNA polymerase and buffers (New England Biolabs)
QuikChange mutagenesis kit (Agilent Technologies UK)
QIAquick Gel extraction Kit (QIAGEN)
QIAprep spin Miniprep Kit (QIAGEN)
T4 ligase (Biolabs)
XhoI restriction enzyme and buffers (New England Biolabs)
XL-10 Gold ultra competent cells (Agilent technologies)

Cell culture and transfections

Cell culture general plasticware (Greinger)(Cellstar)
Cell culture microplates 96 wells with, Lid with condensation rings (Greiner)
Cell culture 384-well ViewPlate (PerkinElmer)
Collagenase, type IV (lyophilized; 150 to 200 U/mg; Invitrogen)
Dharmafect (Dharmacon)
DMEM High glucose with phenol red (Sigma)
Dulbecco's Modified Eagle Medium (DMEM)
Endothelial cell growth supplement (Millipore)
Flp-In T-REx Core Kit (Invitrogen, life technologies)
Gelatin from porcine skin powder (Sigma)
Heparin (Gibco)
Penicillin/streptomycin solution (Sigma-Aldrich)
Phosphate Buffered Saline (Dulbecco A) EDTA free sterile PBS (Sigma-Aldrich)
Neon transfection system (Neon)

siGLO RISC-free control siRNA from Dharmacon (# D-001600-01) was obtained from the Sheffield siRNA Screening Facility (SRSF)
siGENOME siRNA (Dharmacon)
Polyfect Transfection reagent (QIAGEN)
ON-Target plus siRNA (Dharmacon)
Sodium bicarbonate, 7.5 % solution (w/v) (Gibco)
Tissue culture plasticware (Greiner)
Trypsin solution, 10x (0.5%), without phenol red (Gibco)

Chemical Inhibitors

5-(N-ethyl-N-isopropyl)amiloride (EIPA) (Sigma Aldrich)
Cytochalasin B (Sigma-Aldrich)
Cytochalasin D (Sigma-Aldrich)
Filipin III (Sigma Aldrich)
Filipin complex (Sigma Aldrich)

Endocytic ligands and cell staining reagents

Cholera toxin subunit B Alexa Fluor 555, 488 or 647 conjugates (Molecular probes)
DAPI (Cell signalling)
Dextran 70S FITC conjugate (Molecular probes)
Human recombinant Ang1-His tagged (923-AN, R&D systems)

Cell-based protocols

3X FLAG peptide (Sigma-Aldrich)
Ammonium Chloride (BDH AnalaR)
Bio-Rad protein (Bradford) Assay regent (Bio-Rad)
Complete protease inhibitor cocktail, EDTA free (Roche)
Color protein standard, broad range (11-245 kDa)(New England Biolabs)
Color prestained protein standard, broad range (11-245 kDa)(New England Biolabs)
Ultra pure protogel 30% (w/v) acrylamide stock solution. Protein and sequencing electrophoresis grade (GeneFlow)
EDTA 2Na (EDTA) (Sigma-Aldrich)
ELISA plates (Costar)
Enhanced Chemiluminescence (ECL), ECL Plus and ECL Advance (GE Healthcare, Life sciences)
FLAG M2 affinity Gel (Sigma Aldrich)
Gold anti-fade reagent (Molecular probes)
Other general laboratory chemicals (Sigma-Aldrich)
Milk, dried skimmed milk (Marvel)

Mini-Protean II protein gel electrophoresis and gel drying equipment (Bio-Rad Laboratories limited)
Nitrocellulose transfer membrane (Amersham)
N,N,N,N Tetramethylethylenediamine (TEMED) (Sigma Aldrich)
Paraformaldehyde (PFA)(Sigma-Aldrich)
Phalloidin-TRITC (Sigma-Aldrich)
Phenylmethylsulfonyl Fluoride (PMSF) (Sigma-Aldrich)
Phosphate Buffered Saline (Dulbecco A) tablets (Oxoid)
N-Lauroylsarcosine sodium salt (Sigma-Aldrich)
Sodium-2-mercaptoethanesulphonate (Sigma-Aldrich)
Sodium actate anhydrous (BDH laboratory supplies)
Sodium dodecyl sulphate (Melford laboratories Ltb)
Streptavidin-peroxidase conjugate (Polysciences, Inc.)
Whatman paper (GE healthcare)

Antibodies

α-adaptin (AP-2) monoclonal antibody produced in-house from hybridoma clone AP.6
Actin monoclonal antibody (AC-40, Sigma-Aldrich)
Ang1 antibody (MAB9231, R&D systems)
Ang1 biotynilated antibody (BAF923, R&D systems)
APPL1 rabbit monoclonal antibody (D83H4, Cell signalling)
His mouse antibody (MAB050, R&D systems)
Nucleolin mouse monoclonal antibody (C-23, Santa Cruz Biotechnology, Inc)
Secondary Goat anti-mouse IgG – HRP conjugated (Santa Cruz Biotechnology, Inc)
Secondary Goat anti-rabbit IgG – HRP conjugated (Santa Cruz Biotechnology, Inc)
Phospho-Tie2 (Y992) rabbit polyclonal antibody (AF2720, R&D systems)
Tie2 ectodomain goat polyclonal antibody (AF313, R&D systems)
Tie2 endodomain rabbit polyclonal antibody (C-20, Santa Cruz Biotechnology, Inc)
Ubiquitin monoclonal antibody (P4G7, Covance)

2.2 Methods

Cloning of Tie2^{FLAG}

The FLAG tag sequence was added to the Human Tie2 construct by PCR amplification with specifically designed primers (***Table 1***). The primers were designed to add the FLAG tag at the carboxy-terminus before the codon stop. Also, the recognition sequences of EcoRV and XhoI were introduced at each end of the cDNA of Tie2 in order to insert the Tie2^{FLAG} cDNA in the pcDNA5$^{FRT/TO}$ plasmid, required for the generation of the HeLa T-REx cell lines. The conditions for the PCR were optimized by a previous member of our lab working on the project (Kelly Radford). PCR was run with 10 ng of Tie2 cDNA, 125 ng of each primer, 1.5 nM Mg^{2+}, 0.02 U/µL of Phusion Polymerase and 200 µM dNTPs in Phusion High-Fidelity (HF) buffer. The PCR consisted of an initial denaturation step (98˚C, 30 s) followed by 30 consecutive cycles of denaturation (98˚C, 10 s), annealing (70˚C, 30 s) and extension (72˚C, 4 min). PCR was finished with a final extension cycle of 5 min at 72˚C. A 1 % (w/v) agarose gel in TAE with 0.1 % EtBr was used for analysing the PCR results (**Figure *5***a).

Table 1. Nucleotide sequence of the PCR primers for the addition of a FLAG tag at carboxy-terminus and EcoRV and XhoI target sequences. From 5' to 3':

NAME	SEQUENCE
FW_TIE2NTERFLAG	GTAGATATCGCCACCATGGACTCTTTAGCCAGCTTAGTTCTCTGTGGAG
REVERSE_TIE2_C-FLAG	GAAGCTCGAGCGGCTACTTATCGTCGTCATCCTTGTAATCGGCCGCTTCTTCAG CAGAACAGTCAATTCCTGCATAAGTAAACTTCTCATAAAG

PCR products were purified using the Quiagen PCR purification kit following manufacturer's instructions. PCR products and pcDNA5$^{FRT/TO}$ were double restricted for 1h at 37˚C with 400 U/ml of EcoRV and XhoI in NEB buffer 3 with Bovine Serum Albumin (BSA) (1x). The products of the digestion were separated in a 1 % agarose gel with SYBR Green safe DNA stain and purified using a QIA quick gel extraction kit following manufacturer's instructions. DNA content of the digested PCR products and vector were quantitated by comparing the band density with the Hyperladder I bands in a 1 % agarose gel (**Figure *5***b).

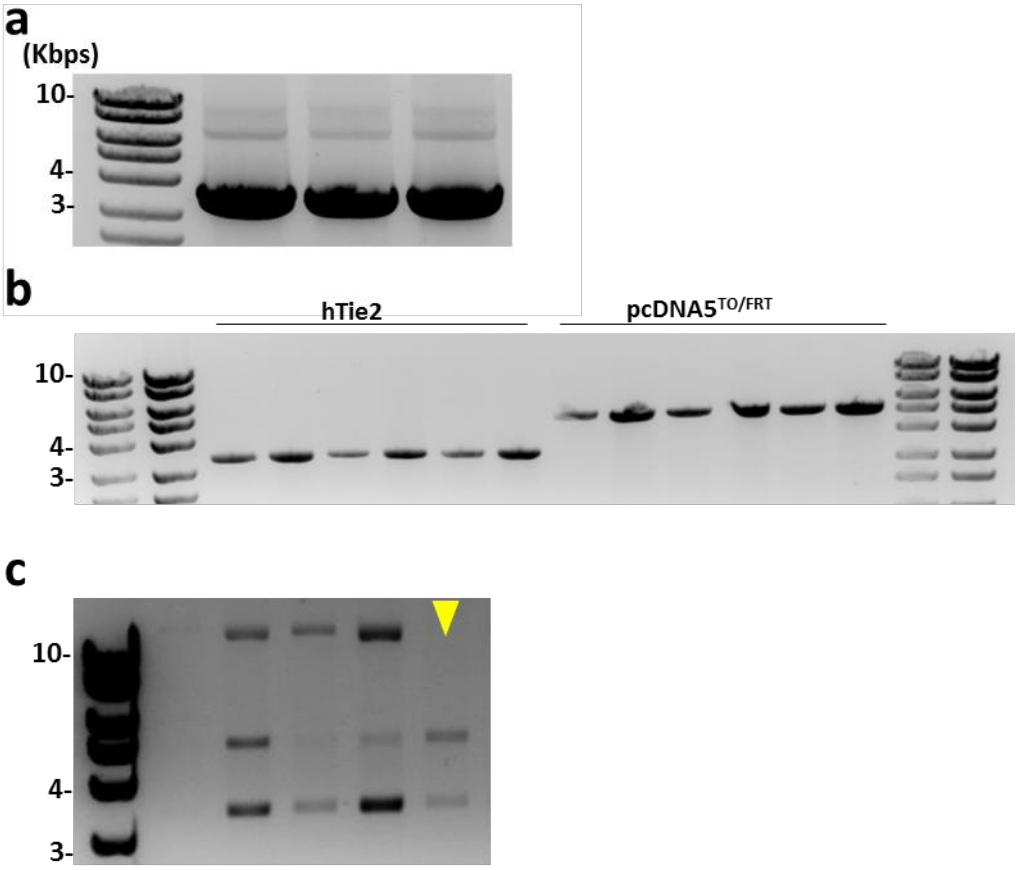

Figure 5. Cloning of Tie2FLAG in the vector for the Flp-In T-REx system, pcDNA5FRT/TO. (a) Product of the PCR run with Tie2 cDNA (3.3 kbp) and the primers containing the FLAG tag, EcoRV and XhoI target sequences. The product was run in a 1% agarose gel with 10% EtBr. (b) EcoRV and XhoI digested PCR products and pcDNA5FRT/TO (5.1 kbp) were quantitated by comparison to HyperLadder I in preparation for the ligation in a 3 to 1 molar ratio. Ligated product was purified and transformed into xL10gold for the selection of plasmids containing the ampicillin resistance cassette. (c) Plasmid DNA was extracted from selected colonies and digested for the selection of constructs with the right size cuts, indicated with an arrow.

A ligation was then set with 3 to 1 molar ratio of insert to vector. Ligation was performed overnight at room temperature with a total of 100 ng DNA and 20 000 U/ml of T4 ligase in Ligase buffer. A control reaction without ligase was set for each digested PCR product. Ligation products were purified by cold ethanol precipitation. Briefly, NaAc was added to ligation product for a final 0.3 M together with 100% cold ethanol equivalent to 2 volumes of ligation product before spinning DNA samples at 14 000 rpm for 20 s, 4˚C. After discarding the supernatant, 250 µL of cold 70 % ethanol was added to the pellet

and centrifuged again for 5 min. Supernatant was discarded and residual ethanol was left to evaporate. Purified DNA product was re-suspended in MQ water.

After ethanol purification of the ligation products, xL10®-gold bacteria were transformed with the products in order to generate more copies of the ligation products. Briefly, 5 µL of purified ligation product were kept on ice with 50 µL ultra-competent xL10gold cells for 30 min before being submitted to a heat shock at 42˚C for 30 s and returned to ice for 2 min. Bacteria were allowed to recover in 450 µL of warm SOC media (SOB medium, 10 mM $MgCl_2$, 20 mM glucose) for 45 min at 37˚C shaking at 200 rpm and were plated in LB-agar selection plates (0.1 µg/ml ampicillin). Resulting colonies were selected and cultured overnight in an LB broth with ampicillin (100 µg/mL). Plasmid cDNA was purified from overnight bacterial cultures using the QIAprep Spin miniprep kit following manufacturer's instructions and eluted in MQ water. Purified plasmid DNA was sent to be sequenced by the Core Genomic Facility (Medical School, University of Sheffield) to confirm the presence of the FLAG tag Tie2 construct (**Figure *5***c). Sequencing primers had been designed by Kelly Radford (**Table *2***). Sequencing of the $Tie2^{FLAG}$ in the $pcDNA5^{FRT/TO}$ revealed 2 silent mutations compared to the TEK transcript variant 1 mRNA (NCBI Reference Sequence: NM_000459.4), one at base pair (bp) 1962 and another at bp 2322 **(Sup. Table 1**, Annex A).

Table 2. hTie2 sequencing primers (by Kelly Radford).

NAME	SEQUENCE
PRIMER 1	GCCCCGGCATGAAGTACCTG
PRIMER 2	GCTAAGCTTCTGGCTGGCCG
PRIMER 3	GACTTTTATGTTGAAGTGG
PRIMER 4	GTGCAAAGGAGAATGG
PRIMER 5	GCAAAAATAGCAGATTTTGG

Site Directed Mutagenesis of hTie2^{K855R}

The QuikChange Site-Directed Mutagenesis (SDM) kit allows introducing point mutations for single amino acids mutagenesis using a plasmid with an insert of the protein of interest in a single PCR. Using the kit I created the Tie2$^{K855R/FLAG}$ dead kinase mutant. Forward and reverse primers were designed by Kelly Radford.

Table 3. Primers for the Site Directed Mutagenesis PCR to obtain the Tie2$^{FLAG/K855R}$.

NAME	SEQUENCE
TIE2_K855R_ PRIMER 1	CATATTCTTTCATTCTCCGGATGGCAGCATC
TIE2_K855R_PRIME 2	GATGCTGCCATCCGGAGAATGAAAGAATAT

Briefly, a PCR was run with 10 ng of pcDNA5$^{TO/FRT}$ plasmid containing the hTie2^{FLAG} cDNA, 125 ng of each primer, 0.02 U/µL Pfu polymerase and 200 µM dNTPs in Pfu polymerase buffer. The PCR consisted of an initial denaturation step (95˚C, 30 s) followed by 16 consecutive cycles of denaturation (95˚C, 30 s), annealing (55˚C, 1 min) and extension (68˚C, 8 min 40 s). Parent plasmids were digested with 10 U/ml DpnI restriction enzyme for 1h at 37˚C. Digested PCR plasmid products were purified by cold ethanol precipitation and transformed into xL10gold ultra-competent cells as described before, except that supplemented NZY^{+} medium was used instead of SOC medium (NZY^{+} medium with 125 mM $MgCl_2$, 125 $MgSO_2$ and 20 mM glucose). Selected colonies from LB-agar (0.1 µg/ml ampicillin) were cultured overnight in an LB broth with ampicillin (100 µg/mL). Plasmid cDNA was purified from overnight bacterial cultures using the QIAprep Spin miniprep kit following manufacturer's instructions and eluted in MQ water. Purified plasmid DNA was sent to be sequenced by the Core Genomic Facility (Medical School, University of Sheffield) to confirm the presence of the K855R mutation (**Sup. Table 2**, Annex A).

Bacterial glycerol stocks

Glycerol stocks of transformed bacteria were obtained by mixing overnight bacterial culture in the appropriate selection medium with equal volume of sterile 30 % glycerol.

Flp In T-REx system

The generation of Flp-In T-REx expression cell lines was done following the kit instructions. Briefly, host Flp-In T-REx cells were cultured with complete media supplemented with 4 µg/mL blasticidin and 50 µg/mL zeocin. Host Flp-In T-REx cells were co-transfected with the pOG44 plasmid, which constitutively expresses the Flp recombinase, and the pcDNA5$^{FRT/TO}$ containing the gene of interest in a 9:1 ratio with Polyfect (QIAGEN). Fresh medium was added 24 h after the transfection. 48 h after transfection cells were split to 25% confluency into media containing 4 µg/mL blasticidin and 200 µg/mL hygromycin B. Transfected HeLa T-REx Tie2^{FLAG} were grown until cells formed colonies distinguishable by eye. Cells from colonies were then picked with a pipette after being submitted to 3 min incubation with trypsin solution (0.05 %). Cells picked from different colonies were then grown separately.

Cell culture

HeLa Flp-In T-REx host cells were maintained in complete DMEM containing Zeocin to ensure maintenance of the clone (DMEM, 10 % FBS, 2 mM L-glutamine, 100 U/mL penicillin, 100 µg/mL streptomycin, 4 µg/ml Blasticidin, 50 µg/ml Zeocin). HeLa Flp-In T-REx expression clones were maintained in Flp-In T-REx selection media (DMEM, 10 % FBS, 2 mM L-glutamine, 100 U/mL penicillin, 100 µg/mL streptomycin, 4 µg/ml blasticidin, 200 µg/ml hygromycin) and passaged before reaching confluency. HUVECs were isolated from umbilical cords at the Cardiovascular Department in the Medical School (University of Sheffield) following an established protocol (Marin et al. 2001). Briefly, the vein of umbilical cords was cannulated and washed with complete M199 media (M199, 2 mM L-glutamine, 100 U/mL penicillin, 100 µg/mL streptomycin and 0.75 % (w/v) sodium bicarbonate). Endothelial cells from the vein were detached by a 20 min

incubation with M199 containing 0.01 % collagenase IV and recovered after centrifugation at 1000 rpm for 5 min. HUVECs were grown on tissue culture plates coated with 2 % (w/v) sterile porcine gelatin in Complete Growth Medium (complete M199, 10 % newborn calf serum, 10 % fetal bovine serum, 5 ng/ml endothelial growth supplement, 90 ng/ml heparin). HUVECs were only maintained until passage 6 and in general were preferentially used before passage 4. M199 media used in the cell assays was equilibrated with CO_2 in an incubator before addition to HUVECs.

After the optimization experiments explained in chapter 3, section 3.1, to induce the expression of $Tie2^{FLAG}$ and $Tie2^{K855R/FLAG}$ a pulse of 6h with 1 µg/mL of doxycycline followed by a 16h chase with doxycycline was used. The only exceptions being when cells were grown in 364-plates for high-throughput imaging, as removing the media using automatic aspirators and dispensers would increase the cell loss and the risk of contamination.

Transient transfections with Polyfect

Transfections were performed using Polyfect and following manufacturer's instructions. Briefly, 200 000 cells of on-going cultures were seeded in 3.5mm wells 24h before transfection. A volume containing 1.5 µg of template diluted in 100µL DMEM was incubated with 12 µL Polyfect for 5 min before adding 600 µL of supplemented DMEM (10 % FBS, 2 mM L-glutamine, 100 U/mL penicillin, 100 µg/mL streptomycin). Fresh medium was added after 24h if cells were maintained until 48h post-transfection.

Transient transfections with Neon transfection system

Cells were transfected according to manufacturer's instructions. On the day of the transfection cells were trypsinised and resuspended in Neon resuspension buffer at a final density of 2.0×10^7 cells/ml. The appropriate amount of plasmid DNA, cell number and resuspension buffer were used following Neon's Quick reference card. HeLa Flp-In T-REx and HUVECs were electroporated using two pulses of 1005mV for

35ms before being transferred to warmed antibiotic-free media plated in the appropriate cell culture support.

Ang1 stimulation assays

In indicated, cells were stimulated with oligomerised hrAng1^{His} before detection of protein levels by western blot, cell immunofluorescence or Enzyme-linked immunosorbent assay (ELISA). Human recombinant His tagged Angiopoietin 1 (hrAng1^{His}) was obtained from R&D systems. Unless stated, stock hrAng1^{His} in PBS was oligomerized by a 30 min incubation on ice with mouse poly-histidine antibody (MAB050, R&D systems) for a final concentration of 200 ng/ml and 5 µg/ml respectively. The oligomerised ligand was diluted to the final concentration of 200 ng/ml in the appropriate serum-free media, either DMEM or M199 media depending on the cells. Unless indicated, incubations with hrAng1^{His} were performed using a final concentration of 200 ng/mL of oligomerised hrAng1^{His}.

Prior to incubation with oligomerised hrAng1^{His}, cells were serum starved in the appropriate serum-free media for 2h. If indicated, the ligand was pre-incubated with cells on ice for 30 min, otherwise warm hrAng1^{His}-containing media was directly added to cells and incubated in a 37˚C, 5% CO_2 containing pre-warmed water in a recipient, were cell plates or dishes were incubated for the indicated times in each experiment. At the required time-points media was aspirated, plates were placed on ice and cells were washed three times with ice-cold PBS to stop all membrane trafficking.

Acid wash stripping of cells

If specified, cell surface hrAng1^{His} was removed by acid stripping of cells prior to solubilisation of cells for ELISA or fixation for cell immunofluorescence. Briefly, cell surface bound hrAng1^{His} was stripped by three 5 minute incubations with ice-cold acid wash buffer (50 mM glycine-HCl, pH 3.0, 2 M urea, and 100 mM NaCl). Cells were rinsed once with ice-cold PBS in between every incubation and 3 times before fixation or solubilisation (Semerdjieva et al. 2008)

Ang1 detection by Enzyme-linked immunosorbent assay (ELISA)

Unless otherwise indicated, ELISA plate wells were coated with 100 µL of 1 µg/ml or the indicated concentration of monoclonal mouse Ang1 antibody (MAB9231, R&D systems) and incubated 3h at 37°C or overnight at 4°C. ELISA plate was washed 3 times in between all steps with wash buffer (0.05 % Tween in phosphate buffer saline, PBS). Plates were blocked for 1h at room temperature or overnight at 4°C using ELISA Blocking Buffer (0.2% w/v BSA, 1% w/v Triton X-100, 0.1% w/v sodium dodecyl sulphate (SDS), 1 mM EDTA, 50 mM NaCl, 10 mM TrisCl pH 7.4). Standard curves were prepared by diluting hrAng1^{His} in BB. Standard hrAng1^{His} or cells solubilised in BB were plated in duplicates and incubated for 2h at 37˚C or overnight at 4˚C. Biotinylated Ang1 antibody (BAF923, R&D systems) was used as detection antibody at 0.4 µg/ml in PBS and incubated 2 h at 37^{o}C. Plates were then incubated with 0.2 µg/mL of Streptavidin-HRP (BB) for 1h at 37˚C. HRP developing solution was made fresh every time and consisted of 25 ml of HRP assay buffer (51 mM Na_2HPO_4 + $2H_2O$, 27 mM sodium citrate, pH 5, 0.2 µm filtered) with 10 µL of 30 % (v/v) H_2O_2 and 1 tablet of O-phenylendiamide. HRP reaction was stopped by adding 50 µL of 2M H_2SO_4 and absorbance was read within 30 min. Absorbance was measured 3 times at 492 nm and the average was corrected by deduction of each well's average reading at 550 nm wavelength. Concentrations of Ang1 from the standards were transformed to a logarithmic scale using GraphPad Prism and then the 4PL non-linear regression of the log (ng/ml) to absorbance was calculated using GraphPad Prism. The 4PL non-linear regression fit from the standard curve was used to extrapolate the concentration of Ang1 from cell samples. Then the total amount of Ang1 contained in each sample was calculated considering the volume of cell lysate in BB.

Cell lysis and immunoprecipitation

Cells were lysed in basic lysis buffer (PBS, 1 % Triton X-100, protease inhibitor cocktail (PIC) and 1 mM APMSF), complete lysis buffer I (50 mM Tris-HCl pH 7.4, 1% Triton-X, 1% NP-40, 150 mM NaCl, 1x PIC, 1 mM APSMF, 5 mM EDTA) or complete lysis buffer II (50 mM Tris-HCl pH 7.4, 1% Triton-X, 10 % glycerol, 150 mM NaCl, 1x PIC, 1 mM APSMF, 5

mM EDTA, 10 mM NEM, 50 mM NaF, 200 µM sodium pervanadate). Sodium pervanadate was prepared fresh every time as in (Huyer et al. 1997). Briefly, 62.5 µL of 0.2 M Na_3VO_4 was mixed with 1 µL of 30 % (v/v) H_2O_2 in 536.5 µL of PBS and incubated at room temperature for 5 min. Reaction was stopped by incubation for 5 min with 6 µL of 20 mg/mL of catalase in PBS. Reaction product was used assuming a concentration of 20 mM sodium pervanadate (Huyer et al. 1997). Cell lysates were centrifuged at 14 000g for 10 min at 4˚C to obtain a clarified cell lysate. To ensure equal loading in SDS-PAGE gels, MultiDsk ubiquitin-enrichment or immunoprecipitations, protein content in cell lysates was measured comparing the protein content of each sample with a BSA standard curve using the Bradford Method. Briefly, cell lysate or BSA standard were mixed with diluted Bio-Rad Protein Assay reagent and the absorbance of the mixture was measured in a spectrophotometer at 595 nm.

For immunoprecipitation of endogenous Tie2 of HUVECs, anti-Tie2/protein G beads were used. To prepare protein G beads, 20 µL of packed beads for each reaction were washed 3 times with 1 mL of complete lysis buffer and centrifuged for 30 s at 5000 rpm. Washed protein G beads were incubated with 2 µg of Goat Tie2 antibody (R&D systems) for 1h in a shaker at 4˚C. Unbound Tie2 antibody was washed 3 times with 1 mL of complete lysis buffer. Tie2 was then immunoprecipitated by overnight incubation of cell lysates with the anti-Tie2/protein G beads in 1 mL of complete lysis buffer at 4˚C. Beads were then washed 3 times in 0.5 mL of TBS incubated with gentle shaking at 4˚C with 100 µL of 150 ng/mL of 3X FLAG peptide in TBS to elute the purified Tie2.

FLAG tag immunoprecipitation was performed using the anti-FLAG affinity gel (Sigma-Aldrich) following the manufacturer's instructions. Briefly, 40 µL of 1:2 gel suspension per reaction was washed by resuspension in 0.5 mL of TBS and 30 s centrifugation at 5000 g. To remove any traces of unbound anti-FLAG antibody the resin was washed once with 0.5 mL of 0.1 M glycine HCl pH 3.5, followed by 3 washes in 0.5 mL of TBS. Volumes of cell lysate containing 40 µg of protein were incubated with 20 µL of washed packed beads in 1 mL of complete lysis buffer. Beads were then washed 3 times in 0.5 mL of TBS and mixed with SDS-PAGE sample buffer.

Preparation of the MultiDsk-affinity resin and ubiquitin enrichment of cell lysates

The MultiDsk recombinant construct was kindly donated by Dr. Rob Piggot from Prof. Steve Winder's lab in the University of Sheffield. Cells transformed with the MultiDsk pGST construct were cultured overnight at 37 ˚C in LB medium supplemented with 100 µg/mL ampicillin. 1 mL of overnight starter culture was used to inoculate 600 mL of fresh LB-Amp media and the optical density of the cultured media was monitored regularly until it reached and optical density of 0.6 (OD_{600}). IPTG was then added to the culture media to a final concentration of 1 mM and incubated for 4h at 30˚C. Harvested cells by centrifugation at 6000 g for 15 min were washed once with PBS and lysed considering the MultiDsk insolubility in normal lysing conditions (Neel & Frangioni 1993; Wilson et al. 2012). Briefly, washed pellets were resuspended in STE buffer (10 mM Tris pH 8, 1 mM EDTA, 100 mM Nacl and PIC) with 100 µg/mL of lysozyme. After pellet lysis with lysozyme Dithiothreitol (DTT) was added to a final concentration of 5 mM, followed by the addition of N-Lauroylsarcosine sodium salt (Sarkosyl) to a final concentration of 1.5 % and brief 5 s vortex. Sarkosyl stock had been prepared as a 10 % dilution in STE buffer. Re-suspended pellet was briefly sonicated in an ice bath sonicator in 1.5 mL aliquots in 4 periods of 15 s ON and 30 s OFF. Sonicated solution was clarified by 5 min centrifugation, 10 000 g at 4 ˚C. Triton was added to a final concentration of 3 % from a 10 % stock in STE buffer and sample was vortex for 5 s. Aliquots containing 60 mg of protein or other amounts as indicated were incubated with 800 µL (50 % slurry) of pre-equilibrated gluthatione agarose beads for 4h at 4˚C in STE buffer. The resulting MultiDsk-GSH beads were washed with with 10x volume of wash buffer high in salts (10mM Tris pH 8, 1mM EDTA, 500mM NaCl, 0.1% Triton, 1 x PIC) and 10x of wash buffer low in salts (10mM Tris pH 8, 1mM EDTA, 50mM NaCl, 0.1% Triton, 1 x PIC). Beads were stored in wash buffer for up to 3 months at 4˚C.

Cultures of HeLa T-REx $Tie2^{FLAG}$ or HUVECs grown to 80 % confluency in 100 mm dish were washed with PBS and lysed with JS buffer (50mM Hepes pH 7.5, 150 mM NaCl, 1.5 mM $MgCl_2$, 5 mM EDTA, 10 % (w/v) glycerol, 1 % (w/v) Triton X-100, 5 mM N-ethylmaleimide, 1 mM sodium orthovanadate, 10 mM sodium fluoride, 1 mM

dithiothreitol, 1 mM phenylmethylsulfonyl fluoride, PIC). Cells were lysed for 15 min on ice and scraped. Collected cell lysates were sonicated in an ice-cold waterbath 30s ON/30s OFF and centrifuged for 20 min at 20 000*g*. Protein content in cell lysates was measured by absorbance using the Bradford reagent and BSA as a standard. After measuring protein concentration cell lysates were diluted in JS buffer-low Triton for a final concentration of a 0.25 % Triton X-100 and incubated 4h with 40 µL 50 % slurry MultiDsk-resin at 4˚C. Beads were thoroughly washed with JS buffer-low Triton and boiled for 10 min with Laemmli sample buffer (60 mM Tris, pH 6.8, 2 % (w/v) SDS, 10 % (w/v) glycerol, 0.1 % (w/v) bromophenol blue, 5 % (v/v) β-mercaptoethanol) for resolving protein content by protein immunoblotting.

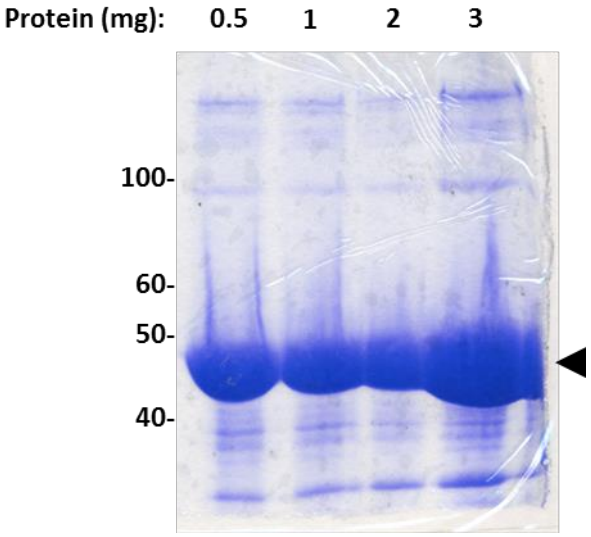

Figure 6. MultiDsk ubiquitin-affinity resin. 0.5, 1, 2 or 3 mg of protein extract from BL21 bacteria transformed with MultiDsk pGST construct was purified with GSH beads and a sample from each reaction was run in an 8 % SDS-PAGE gel. Arrowhead points at the band corresponding to the MultiDsk recombinant protein.

Protein immunoblotting

Proteins in cell lysis buffers were resolved by SDS-polyacrylamide gel electrophoresis (SDS-PAGE) on an 8% SDS-PAGE gel immersed in electrophoresis running buffer (25mM Tris, 190mM glycine, 1% (w/v) SDS) and transferred to nitrocellulose membranes in western blotting transfer buffer (25 mM Tris, 190 mM glycine, 20 % (v/v) methanol. Membranes were blocked for 1 h in Tris-buffered saline (TBS)(20mM Tris, pH 7.4, 137

mM NaCl) containing 5 % non-fat dry milk or 5 % BSA for the detection of phosphoproteins. Membranes were incubated with 1:500 anti-Tie2 rabbit antibody, 1:100 anti-phosphotyrosine 995 Tie2 rabbit antibody, 1:1000 anti-ubiquitin antibody, 1:1000 anti-actin antibody, 1:1000 anti-tubulin antibody or 1:1000 anti-nucleolin antibody. Protein bands were visualized with secondary antibodies conjugated to HRP (incubated at 1:5000 dilution in 5% Milk or BSA) and revealed by enhanced chemiluminescence. Images were acquired with an UVIprochemi or a BioRad camera system. If required, membranes were striped by 2 incubations of 10 min with stripping buffer (1% SDS, 200 mM glycine pH 2.5) followed by 2 incubations of 10 min with PBS and two incubations of 5 min with TBS (0.02% Tween).

Triton wash of live cell membranes

Cells grown in glass cover-slips were incubated 30 min on ice with 200 ng/ml hrAng1^{His} and 5 µg/ml transferrin (Tfn) conjugated to Alexa Fluor 567 or 1 µg/ml CTxB conjugated to Alexa Fluor 555. Cells were then incubated for 1 min in ice-cold 0.5 % Triton (1x PBS) before fixation or after fixation with 4 % paraformaldehyde (PFA) in case of the control cells. Fixation of samples was performed as explained below.

Cell immunofluorescence

For immunofluorescence assays cells were grown on glass cover-slips. Cells were washed three times with PBS before fixation with 4 % PFA for 20 min. PFA was neutralized with two 5 min washes with 50 mM NH_4Cl. After a PBS wash cells were permeabilized with 0.2% Triton X-100 for 3 min. Non-specific binding was blocked using a 30 min incubation with blocking buffer (PBS, 0.2% fish skin gelatin). Primary and secondary antibodies, at the appropriate dilution in blocking buffer, were incubated for 1h and 30 min respectively. If indicated, Tetramethylrhodamine (TRITC) – phalloidin was added at a 1:200 dilution with the secondary antibodies. Nuclei were stained using the DNA intercalator 4',6-diamidino-2-phenylindole (DAPI) at 0.2 µg/µL. Glass cover-slips

with immunostained cells were mounted in glass slides with Gold anti fade reagent (Molecular Probes) and allowed to dry for 24h.

Images were acquired with an Olympus BX61 epifluorescence microscope, widefield Deltavision or a Nikon laser Dual-camera system microscopes available in the Wolfson Light Microscopy Facility (Biomedical Science Department, University of Sheffield).

High throughput internalization assay and siRNA screening

Transfection of siRNA into HeLa was performed in 384-well plates and transfection of HUVECs was performed in 96-well plates pre-coated with 2% gelatin. Loading and aspiration of liquid in sterile or non-sterile conditions as required was performed using the MultiDrop automatic dispensers and BioTek multi-well aspirator robots in the siRNA Sheffield Screening Facility (SRSF), Biomedical Sciences Department, University of Sheffield) in the case of using HeLa T-REx tie2^{FLAG} cells. While in the case of using HUVECs experiments were performed manually in our quarantine tissue culture section or laboratory facilities with the aid of multichannel pipettes.

Transfection complex was prepared by incubating equal volumes of siRNA in sterile water and Dharmafect 1 in serum and antibiotic-free medium for 30 min at room temperature. siRNA was used at a final concentration of 30 nM for transfection of HeLa T-Rex Tie2^{FLAG} cells or 62.5 nM for transfection of HUVECs. Whereas Dharmafect 1 was used at a final 0.24 % for HeLa T-REx Tie2^{FLAG} cells or 0.005 % for HUVECs. Transfection complexes of siRNA and Dharmafect 1 were prepared directly in the wells of 386-well plates when transfecting HeLa T-Rex Tie2^{FLAG} cells or separately in the case of transfecting HUVECs to avoid any interference from the gelatin used to pre-coat the 96-well plates. Cells were trypsinised and re-suspended to the appropriate concentration in media without antibiotics for a final cell seeding of 3000 cells/well in the primary screen and 2000 cells/well or 4000 cells/well in the secondary screen with HeLa T-REx Tie2^{FLAG} cells. For the transfection of HUVECs 10 000 cells were used for each well in a 96-well plate. In the case of transfecting HUVECs, fresh media was added to transfected cells 24h post-transfection to supplement culture media with Penicillin/Streptomycin.

The hrAng1^{His} stimulation assay and cell immunofluorescence staining protocols were adapted to a high throughput assay format in 386-well plates by proportionally reducing liquid volumes and increasing components concentrations assuming that the BioTek Aspirator robot was leaving an average residual volume of 10 µL/well. When screening HeLa T-REx Tie2^{FLAG} cells, expression of the Tie2^{FLAG} receptor was induced by the addition of media containing doxyxycline for a final well concentration of 1 µg/ml as usual, yet I decided not to pulse cells with doxyxycline in the case of using 386-well plate to avoid any disturbance of cells by the automatic well aspirator and dispenser. After serum starvation of cells for 2h, plates were cooled on ice for 5 min and ice-cold media containing Ang1 was added. HeLa Tie2^{FLAG} cells were incubated with a final concentration of 200 ng/mL hrAng1^{His}, considering the average 10 µL of residual washout left by the BioTEK aspirator. HUVECs were incubated with 300 ng/mL of hrAng1^{His} as incubation with lower levels of hrAng1^{His} did not lead to detectable signal by the High Content microscope (data not shown). To allow for homogenous distribution of the ligand, plates were pre-bound on ice with the ligand for 30 min and then transferred to a 37˚C waterbath or an incubator for 45 min. Membrane trafficking was stopped with washes of cold PBS and cell surface ligand was removed with 3 series of acid-stripping washes. After fixation and immunostaining of cells, multiple images were acquired from each well depending on cell confluency. Image acquisition was automated using the ImageXpress Microscope available at the SRSF facility.

Inhibition of endocytosis with chemical compounds

For analysing the effect of different compounds on the endocytosis of internalization markers the above internalization assay was used. Additionally, serum starved cells were pre-incubated for 30 min at 37˚C with cell culture media containing the appropriate concentration of chemical inhibitor. HeLa Tie2^{FLAG} were incubated with 0.1 % DMSO, 25 µM of 5'-(N-ethyl-N-isopropyl) amiloride (EIPA), 25 µM Cytochalasin B or 5 µM of Filipin III from Streptomyces filipensis. HUVECs were incubated with 2 % DMSO, 834 nM EIPA, 20 µM Cytochalasin D, 2 µg/mL Filipin complex or 10 µM EHT1864. Endocytic markers pre-diluted in culture media at 50x of the desired final concentration were then added

in order to reduce alteration of the concentration of chemical compounds. To determine the effect of the inhibitors of endocytosis HeLa Tie2^{FLAG} cells were incubated with 20 µg/mL Fluorescein isothiocyanate (FITC)-dextran 70kDa (Dextran 70S) and 200 ng/mL of hrAng1^{His} or with 5 µg/mL Alexa Fluor 555-conjugated Cholera Toxin B subunit (CTxB^{555}) and 200 ng/mL hrAng1^{His}. Dextran 70S was incubated for a total of 40 min, hrAng1^{His} and CtxB^{555} were incubated for a total of 30 min. HUVECs were incubated for 30 min with 300 ng/mL hrAng1^{His}, 100 µg/mL FITC-Dextran 70S or 10 µg/mL Alexa Fluor 568-conjugated transferrin.

Stock dilutions of Cytochalasin B, Cytochalasin D, 5'-(N-ethyl-N-isopropyl) amiloride (EIPA) and EHT1864 were prepared with DMSO and stored at -20˚C. Filipin stock dilutions were freshly prepared with DMSO and protected for light. A 100x working solutions were prepared freshly from the stock dilutions using cell culture media.

Data handling and analysis

Raw data obtained in experiments was organised using Microsoft Excel and then analysed using Microsoft Excel using specifically designed spreadsheets or GraphPad Prism. The indicated statistical analysis was performed in GraphPad Prism.

Images acquired with the Deltavision or Nikon microscopes were deconvolved using the deconvolution softwares available for each microscope. Co-localization analysis was performed using the Volocity software also available in the Wolfson Light Microscopy Facility. Images acquired with the ImageXpress microscope were visualised and automatically analysed using the MetaXpress image analysis software also available in the SRSF (***Table 4***). Normalization of data within each independent experiment was performed to neutralise systematic errors generated during the screening so that data from different plates and experiments could be compared (Birmingham et al. 2009). As explained in each relevant section, data from primary screen was normalized by calculating the Robust Z. Score using each plate median (**Equation *2*** and **Figure *35***); while data from the secondary screen and the pilot screen on HUVECs was normalized as the

% of those non-targeting mRNA that appeared to not have any effect on the parameters analysed.

Any other image analysis and preparations were performed using ImageJ.

Table 4. Different algorithms were designed using the Custom Edit Module in the MetaXpress High Content image analysis software. Unless specified, the intensity above local background was determined specifically for each experiment.

ALGORITHM	DESCRIPTION
CME1	**Segmentation** 1. Set DAPI and GFP as channels to analyse 2. Find blobs in DAPI (30.02 – 5000 µm maximum size) 3. Find Round objects in DAPI (6.4 – 30 µm maximum size) 4. Remove marked objects in 2 from 4. 5. Grow objects from 4 without touching (30 pixels) 6. Remove border objects from 5 7. Find Blobs in GFP (5- 3000 µm) 8. Find Round objects in GFP (0.2 – 2 µm) 9. Remove marked objects in 8 from 10. **Measure** Use objects from 6 as a mask. Measure DAPI, report counts Within each object apply 9 as a mask and measure GFP, report counts
CME1_HUVECS	**Segmentation** 1. Set DAPI and GFP as channels to analyse 2. Find blobs in DAPI (30.02 – 5000 µm) 3. Find Round objects in DAPI (4 – 6 µm, 1500 intensity above local background) 4. Find Round objects in DAPI (6.4 – 50 µm) 5. Remove marked objects in 2 from DAPI 6. Remove marked objects in 3 from 5. 7. Grow objects from 6 without touching (100 pixels) 8. Remove border objects from 7 9. Find Blobs in GFP (5- 3000 µm) 10. Find Round objects in GFP (0.2 – 2 µm) 11. Remove marked objects in 8 from 10. **Measure** Use objects from 8 as a mask. Measure DAPI, report counts Within each object apply 11 as a mask and measure GFP, report counts

CHAPTER 3

Generation and characterisation of HeLa Flp in cells expressing Tie2^{FLAG} and Tie2$^{K855R/FLAG}$

In order to study the internalization of Tie2 receptor I decided to generate HeLa cell clones with inducible expression of Tie2 using the Flp-In T-REx system (Invitrogen). The Flip-In system allows the insertion of a particular cDNA into the genome of mammalian cell lines under the regulation of a TET repressor (O'Gorman et al. 1991). This particular system permits the selection of Flp-In T-REx cells depending on the levels of protein expression, so it can be used to avoid the effects of overexpression of transfected proteins. It was observed previously in our laboratory that an overexpression of Tie2 in HEK293 cells can lead to a ligand-independent phosphorylation of the receptor (Maxwell and Smythe, Unpublished). Hence, by using the Flp-In cell line with a single Tie2 insert I expected to avoid this ligand-independent activation of the receptors at the cell surface. The Flp-In cell line is thus a more convenient tool, as it allows the controlled expression of the gene of interest for a desired time. Finally, since HeLa cells do not express Tie2 it would be possible to analyse Tie2 expression in a null endogenous background.

With the aim to facilitate the detection and purification of Tie2 from the HeLa T-REx cells in future experiments I decided to incorporate a FLAG tag to the CDS of Tie2. The FLAG tag was cloned in the carboxy-terminus of the cDNA of Tie2 after I established that the amino-terminus of the translated cDNA is a signal peptide that is cleaved after post-translational processing in the endoplasmic reticulum as predicted (Zhang & Henzel 2004; Wasmuth & Lima 2016)(**Figure *7***).

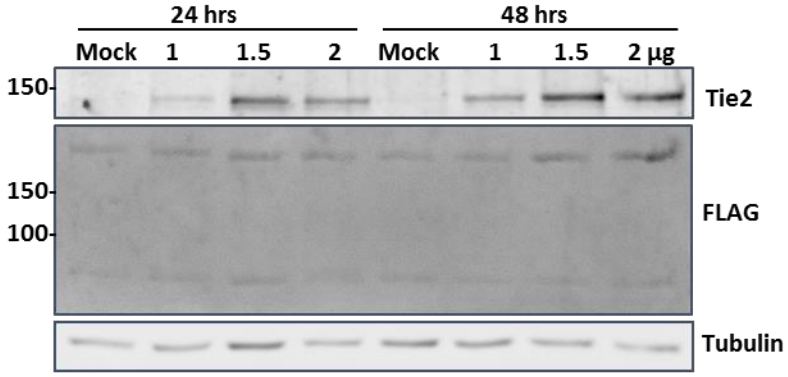

Figure 7. The absence of a FLAG-tagged Tie2 band indicates that the FLAG tag is cleaved from the N-terminus of Tie2, yet un-specific staining by the FLAG antibody is observed. HeLa cells were transiently transfected with different amounts of N-terminal tagged ^{FLAG}Tie2 cloned in pcDNA5 plasmid as indicated. Protein expression was analysed by western blot at 24 or 48h post-transfection.

Furthermore, I used the Tie2^{FLAG} inserted in the pcDNA5$^{FRT/TO}$ as a template to obtain a Tie2$^{K855R/FLAG}$ mutant using the QuickChange Site Directed Mutagenesis kit, which allows for the generation of point mutations by PCR using specifically designed primers in a quick and efficient way. As explained before, Tie2^{K855R} has been previously predicted and described to be a dead kinase receptor that is not internalized in HUVEC cells (Shewchuk et al. 2000; Fukuhara et al. 2008). I wanted to generate HeLa T-REx Tie2$^{K855R/FLAG}$ cells with inducible expression of the mutant receptor to be used as a control of the blockage of the internalization. The ability of Tie2^{K855R} to bind the agonistic ligand Ang1 is not affected by the mutation and the ligand also drives the oligomerisation of the mutant receptor, as this is dependent on the extracellular domain of Tie2 (Fukuhara et al. 2008; Saharinen et al. 2008).

The details of the cloning and mutation of the Tie2^{FLAG} and Tie2$^{K855R/FLAG}$ mutants are described in the Materials and Methods chapter. Before generating the HeLa T-REx Tie2^{FLAG} cells I transiently transfected HeLa cells to evaluate by western blot that the Tie2 was being expressed in cells (**Figure *7*** and **Figure *8***).

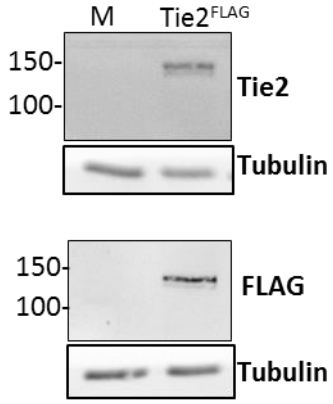

Figure 8. The expression of the Tie2^{FLAG} construct transiently transfected in HeLa cells is detected by immunoblotting for either Tie2 or FLAG presence. HeLa cells were transiently transfected with Tie2^{FLAG} containing-plasmid or empty plasmid (M). Protein expression was analysed by western blot using Rabbit Tie2 antibody and Mouse FLAG antibody.

After I confirmed that Tie2^{FLAG} was being expressed in HeLa cells, HeLa T-REx Tie2^{FLAG} and Tie2$^{K855R/FLAG}$ were generated from our own HeLa Flp-In Host cells following the standard procedure for the Flp-In T-REx system, as detailed in the Materials and Methods chapter. Furthermore, a control HeLa cell line T-REx pcDNA5$^{FRT/TO}$ was generated by stably transfecting the HeLa Flp-In host cells with an empty pcDNA5$^{FRT/TO}$ plasmid.

3.1 Expression of Tie2^{FLAG} and Tie2$^{K855R/FLAG}$ in HeLa T-REx cells

The recombination of genes in the genome of T-REx host cells is an aleatory process that creates random different clones after the transfections. To ensure that the levels of Tie2 were homogenous within the cells and not overexpressed in relation to HUVECs, individual clones of each cell line were isolated and the expression of the receptor was evaluated.

To optimize the expression of the receptor in the HeLa Tie2^{FLAG} cells, cells were exposed to different concentrations of doxyxycline in complete culture media for 24 and 48h and then the expression and phosphorylation state of Tie2^{FLAG} was evaluated by western blot. HeLa T-REx carrying the empty vector pcDNA5$^{FRT/TO}$ were used as a control to show that the expression of Tie2 in HeLa cells was null. As seen in **Figure 9**a, only the HeLa Tie2^{FLAG} cells expressed Tie2 and only after induction by doxyxycline. Furthermore, I compared the expression of Tie2^{FLAG} in HeLa T-REx cells to the expression of endogenous Tie2 in HUVECs. The lysates of HUVECs were obtained from a former member in the lab and had been exposed to Ang1 for 5 min. None of the concentrations of doxycycline used caused the over-expression nor ligand-independent activation of the Tie2^{FLAG} as compared to the endogenous expression of Tie2 in HUVECs (**Figure 9**a). Most of the different concentrations and times of the exposure of cells to doxycycline that I tested gave similar results, as it is shown by the quantitation of the bands in the western blots (**Figure 9**Error! Reference source not found.**b**). This is due to the nature of the T-REx system, where the presence of Tetracycline or a derivative simply triggers the transcription of the gene as an On/Off system, rather than in a dose/response manner. I decided to expose cells with 1 µg/ml of doxyxycline for a maximum of 24h, which is also what previous members of the lab had been using with other HeLa T-REx cell lines.

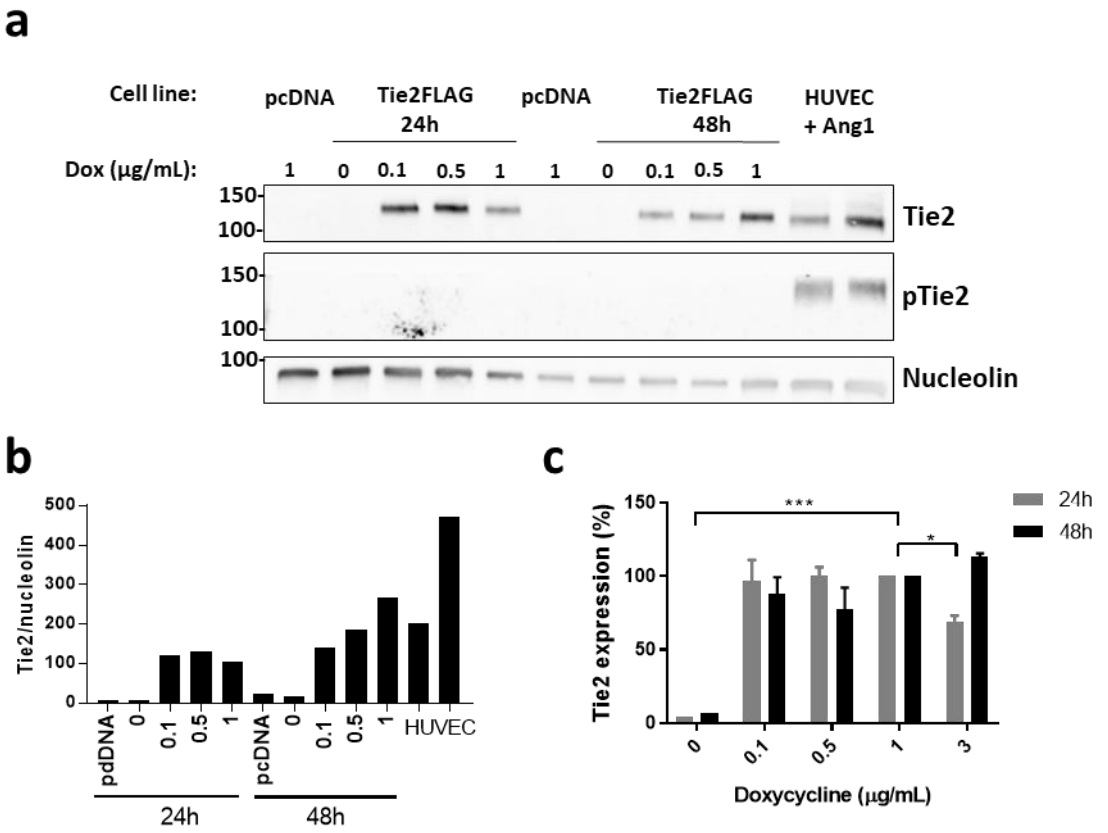

Figure 9. Expression of Tie2^{FLAG} in HeLa T-REx is induced by exposure to doxycycline at similar levels of endogenous Tie2 in HUVECs. (a) and **(b)** HeLa T-REx cells stably transfected with Tie2^{FLAG} or empty plasmid (pcDNA) using the Flp-In system were exposed to different concentrations of doxycycline for 24 or 48h as indicated. Lysates of HUVECs exposed to Ang1 were donated by a former member of our lab. Cell lysates were processed for western blot to analyse the expression levels of Tie2, pTie2 and nucleolin as indicated. Bands were quantitated and the normalized intensity of Tie2 is shown in **(b)**. **(c)** Quantitation of the Tie2 expression measured by western blot. The intensity of each band was normalized using the loading control for each lane and the 1 µg/ml condition of each experiment. Bars showing Mean ± SEM, n=3 in all except for 3 µg/mL, where n=2 independent experiments. Statistically significant differences to the 1 µg/ml doxyxycline were inferred with Dunnett's multiple comparisons test and *one-way* ANOVA. (α = 0.05; * indicates $p < 0.05$; *** indicates $p < 0.0002$).

However, when I analysed the expression of Tie2 by immunofluorescence I observed that the expression of Tie2^{FLAG} was not homogenous amongst the HeLa T-REx Tie2^{FLAG} cells and that a few cells appeared to express much higher amounts of Tie2^{FLAG} than the rest (**Figure *10***a). Since I had already selected a single HeLa T-REx Tie2^{FLAG} clone I tried to optimize the expression of the receptor by exposing cells to a pulse of doxycycline rather than a continuous exposure. Indeed, when I incubated cells for 4, 6 or 24h with 1 µg/ml

doxycycline followed by a 16h culture in normal complete media the expression of Tie2^{FLAG} appeared more homogenous among cells (**Figure *10***b). The 16h chase after the pulse with doxycycline ensured a better expression (**Figure *10***c). Therefore, I stablished that, if possible, I would ideally pulse cells for a period of 6h with 1 µg/ml doxyxycline the day before of an experiment.

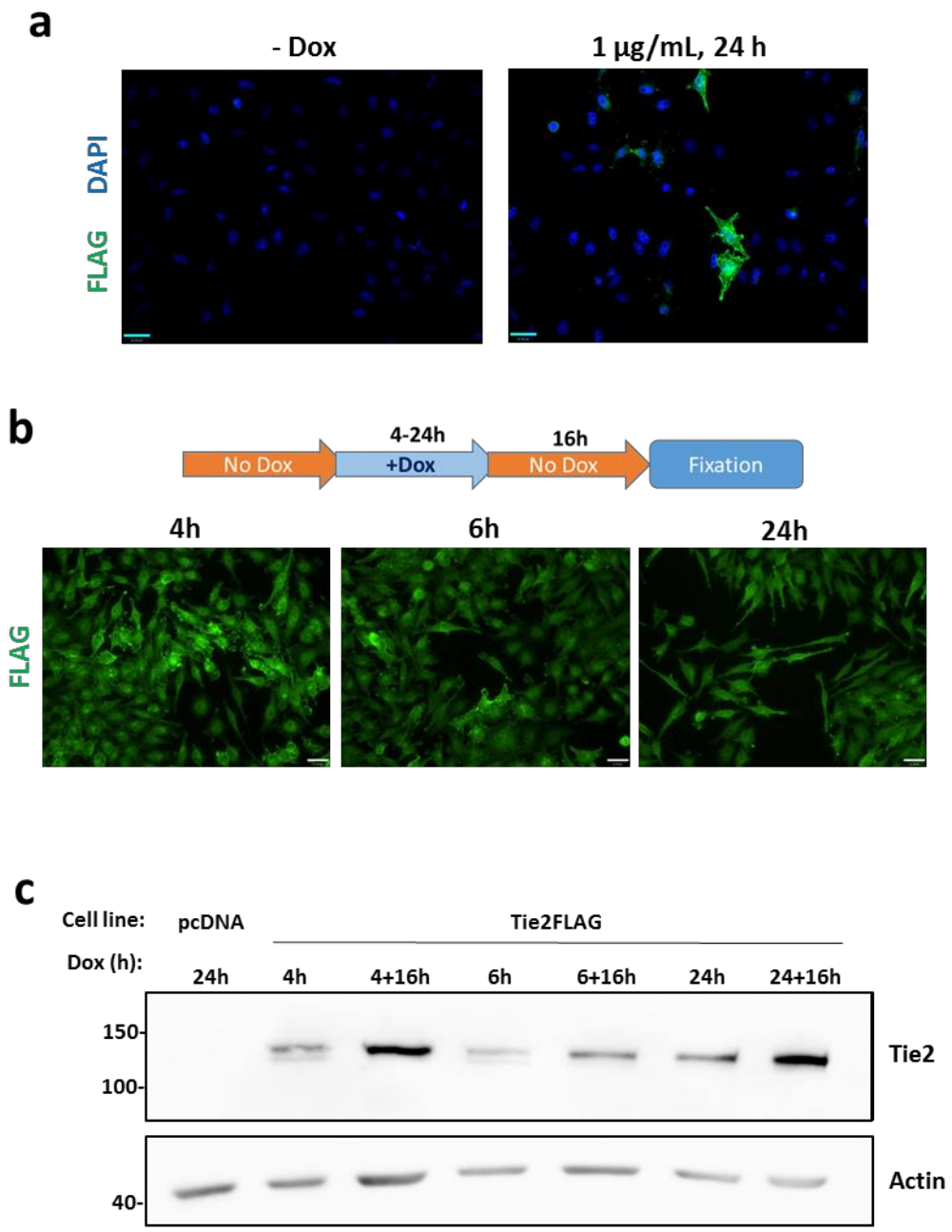

Figure 10. The expression of Tie2^{FLAG} was more homogenous after a 24h chase without doxycycline. **(a)** The expression of Tie2^{FLAG} is not homogenous amongst HeLa T-REx Tie2^{FLAG}. HeLa T-REx Tie2^{FLAG} cells grown on glass cover-slips were cultured in complete media containing 1 µg/ml of doxycycline for 24h or left untreated before being fixed for immunofluorescence staining of FLAG and stained with the nuclear dye DAPI. Some cells with higher levels of Tie2^{FLAG} expression appeared, masking the expression of Tie2^{FLAG} from the remaining cells. **(b,c)** HeLa cells stably transfected with the empty plasmid pcDNA5$^{FRT/TO}$ (**pcDNA**) or with Tie2^{FLAG} (**Tie2^{FLAG}**) were incubated with media containing 1 µg/ml of doxycycline for 4h, 6h or 24h. Cells were then either analysed directly or incubated 16h without doxycycline, as represented by the scheme in top of **(b)**. Samples were then either analysed by immunofluorescence **(b)** or by Western Blot **(c)**. Immunofluorescence images were acquired using the Olympus BX61 Epifluorescence microscope. Scale bars indicate 6.00 µm

Since the HeLa T-REx Tie2$^{K855R/FLAG}$ clones did not have to necessarily respond as the HeLa T-REx Tie2^{FLAG} to doxyxycline, I also analysed the expression of Tie2$^{K855R/FLAG}$ in response to different pulsed times and concentrations of doxyxycline. As seen in **Figure *11***, the expression of the mutant receptor in the HeLa T-REx Tie2$^{K855R/FLAG}$ clone A exposed to 1 µg/ml of doxyxycline for a 6h pulse and followed by 16h chase without doxyxycline was slightly higher than the expression of Tie2^{FLAG} in the HeLa T-REx clone and the endogenous Tie2 in HUVECs. However, to ease the experimental protocols I decided to use the same conditions for both stably transfected HeLa T-REx cell lines. Therefore, a pulse of 6h with 1 µg/mL doxycycline followed by 16h chase in doxyxycline-free media was used thereafter to induce the expression of Tie2^{FLAG} and Tie2$^{K855R/FLAG}$ in the HeLa T-REx cell lines and are to be considered the conditions in the following experiments unless stated.

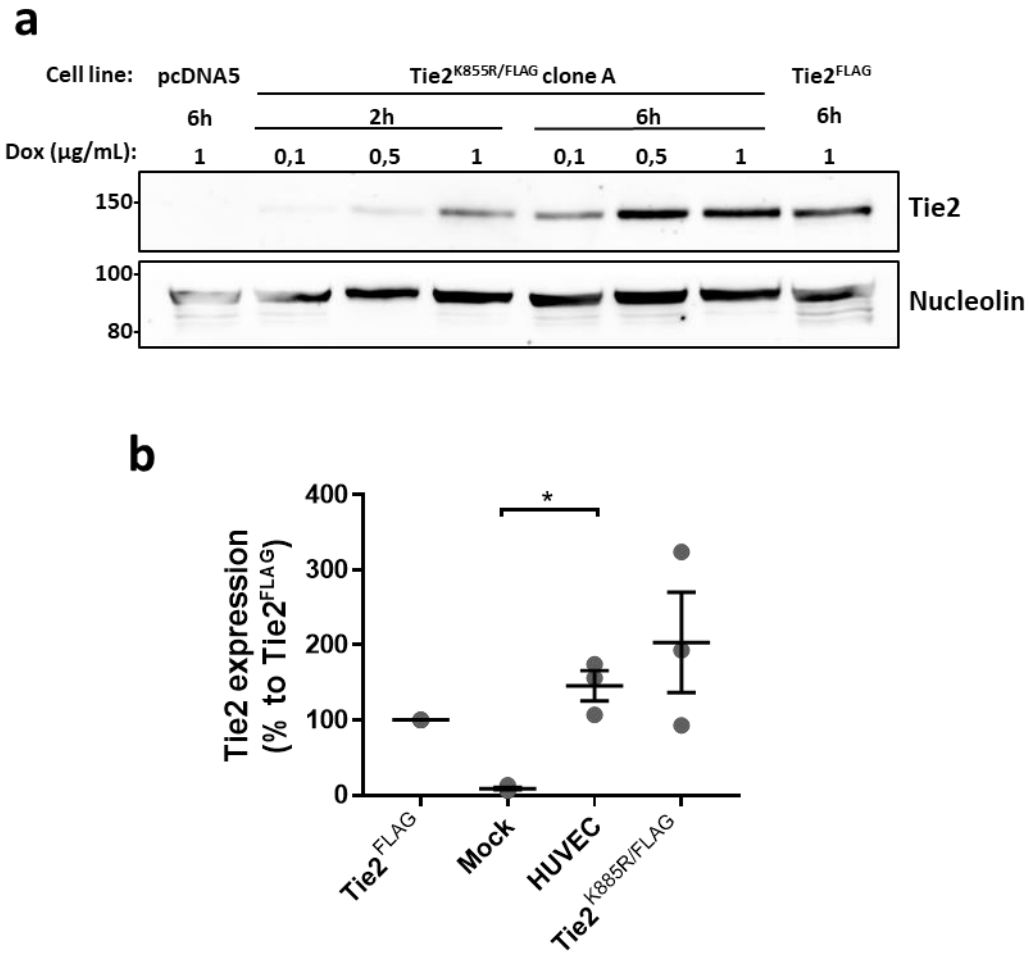

Figure 11. HeLa T-REx cell lines express Tie2$^{K855R/FLAG}$ after induction by doxycycline at similar levels than HUVECs and HeLa T-Rex Tie2^{FLAG} cells. (a) Expression of Tie2$^{K885R/FLAG}$ in stably transfected HeLa T-REx cells is also induced by exposure to doxyxycline. HeLa T-REx Tie2$^{K855R/FLAG}$ cells were pulsed for the indicated time with doxyxycline-containing media at the concentrations indicated and left 16h in media without doxyxycline. Cells were lysed and the expression of Tie2 was analysed by western blot.**(b)** Expression of Tie2$^{K885R/FLAG}$ in stably transfected HeLa T-REx cells is slightly higher than expression of Tie2^{FLAG} in HeLa T-REx cells and endogenous Tie2 in HUVECs. Expression of Tie2 in the HeLa T-Rex inducible cell lines was induced by a 6h pulse and 16h chase of 1 µg/mL of doxyxycline. The levels of expression of Tie2^{FLAG} in HeLa Tie2^{FLAG} cells was compared to the expression of Tie2^{FLAG} in cells transfected with an empty pcDNA5 plasmid (Mock), endogenous Tie2 in HUVECs or Tie2$^{K855R/FLAG}$ in HeLa Tie2$^{K855R/FLAG}$. To do so, expression of Tie2 analysed by western blot was normalized using the loading control for each lane and to the Tie2^{FLAG} expression in each separate blot. HUVECs from 3 different donors were used. Bars represent Mean ± SEM of at least three independent experiments for each cell type ($n \geq 3$). Statistically significant differences were inferred with *one-way* ANOVA and Dunnett's multiple comparisons test to HUVECs. ($p < 0.05$; * indicates $p < 0.05$).

3.2 Analysing the functionality of the Tie2^{FLAG} receptor expressed in HeLa Flp-In cells

Endogenous Tie2 receptor is localized to the plasma membrane of endothelial cells. To ensure that the Tie2^{FLAG} expressed in HeLa T-REx cells was also localised in the plasma membrane of cells I analysed the location of Tie2^{FLAG} by immunofluorescence staining. HeLa T-REx Tie2^{FLAG} expressing the receptor were stained for FLAG and CHC, which is localized at the plasma membrane and in intracellular vesicles, or β-dystroglycan, which can be found in the plasma membrane. The HeLa T-REx pcDNA5$^{FRT/TO}$ were used as a control for the null detection of receptor. As seen in **Figure *12***, the expression of Tie2^{FLAG} was mainly found delimiting the cell cytoplasm, as contrasted by the intracellular CHC staining, and co-localizing with β-dystroglycan at the plasma membrane. Interestingly, I was also able to observe that Tie2^{FLAG} was enriched at intercellular contacts as it has been described to occur with the endogenous Tie2 in HUVECs (Fukuhara et al. 2008; Saharinen et al. 2005). I noted that the control HeLa T-REx pcDNA5$^{FRT/TO}$ cells presented a substantial background FLAG staining mainly localized in the nuclei. Since I had not detected any expression of Tie2^{FLAG} by western blot in the control HeLa T-REx pcDNA5$^{FRT/TO}$ cells (**Figure *9***), I assumed that this effect was due to a non-specific binding of the FLAG antibody. Indeed, I had also detected in the past non-specific affinity of the antibody by WB, as it can be seen in **Figure *7***.

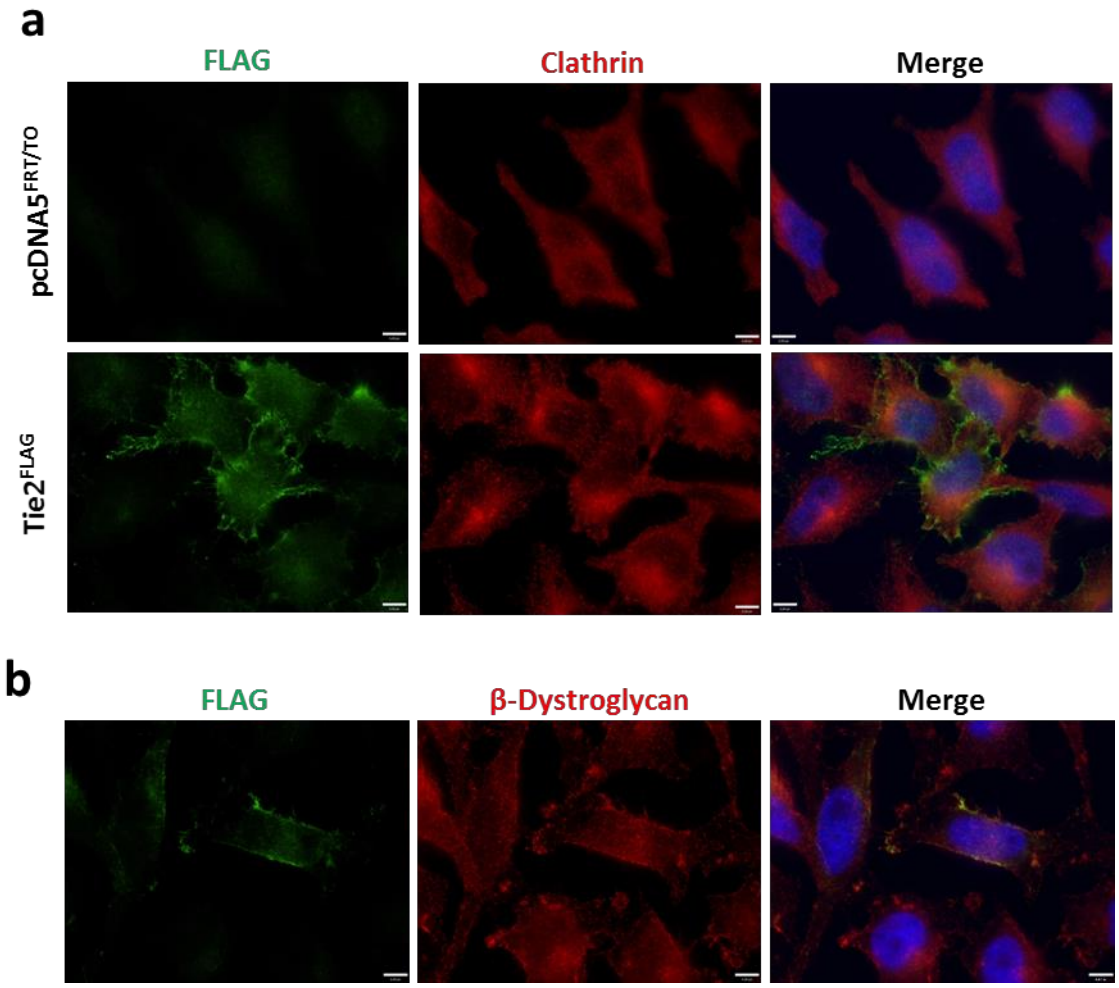

Figure 12. Tie2^{FLAG} is expressed on the plasma membrane of HeLa T-REx cells. HeLa cells stably transfected with Tie2^{FLAG} were pulsed for 6h with 1 µg/ml of doxycycline. Cells were fixed and prepared for immunofluorescence analysis using anti-FLAG antibodies and **(a)** anti-Clathrin Heavy Chain (CHC) antibodies, which is distributed in the cytosol and vesicles, or **(b)** β-dystroglycan, which is located on the plasma membrane of cells and in the cytoplasm. Cell nuclei were stained with DAPI. Images were acquired using Olympus BX61 Epifluorescence microscope. Scale bars indicate 6.00 µm.

After ensuring that the Tie2^{FLAG} expressed in HeLa T-REx cells was localized in the plasma membrane I proceeded to evaluate the functionality of the receptor. It was shown for HUVECs that in the presence of serum in the culture media, which contains angiopoietins, Tie2 would localize in cell-cell contacts of confluent cultures of HUVECs; while after a long period of serum starvation Tie2 would be homogeneously distributed over the plasma membrane (Fukuhara et al. 2008). As seen in **Figure *13***, this effect was also observed for the Tie2^{FLAG} expressed in HeLa T-REx cells. This indicated that the

ectodomain of the Tie2^{FLAG} was able to bind to the angiopoietin ligands, as previously published for endogenous Tie2 in HUVEC (Fukuhara et al. 2008; Saharinen et al. 2008).

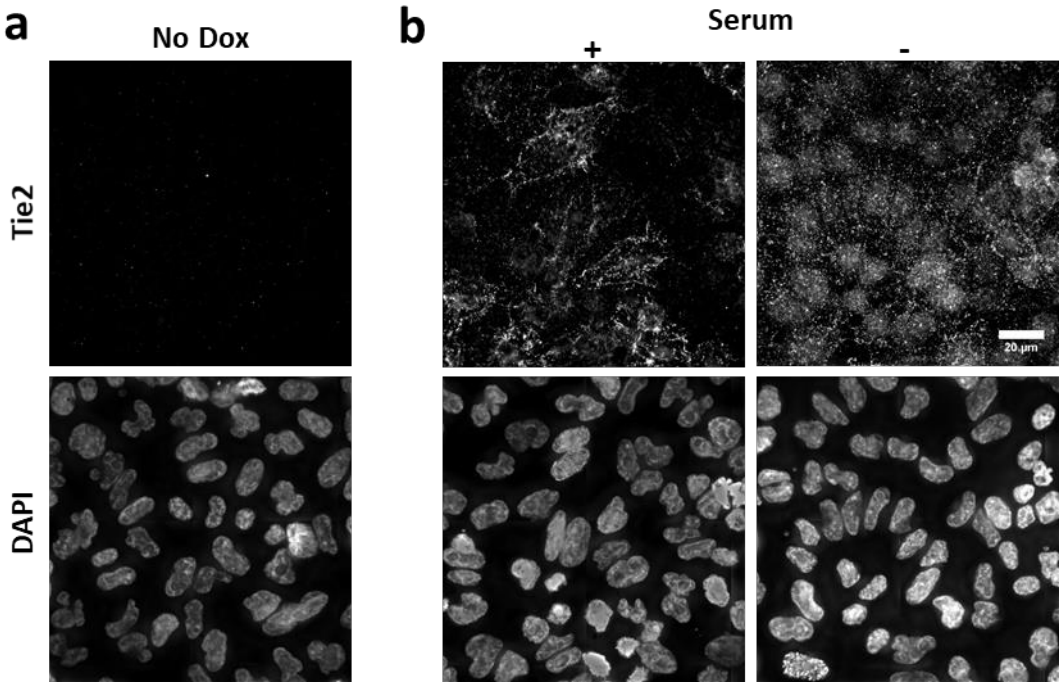

Figure 13. Tie2 localizes at cell-cell contacts in the presence of serum. HeLa T-REx Tie2^{FLAG} cells grown on glass cover-slips were left untreated (-Dox) **(a)** or were pulsed with 1µg/ml doxycycline for 6h (+Dox) in the presence (+) or absence (-) of serum **(b)**. Cells were fixed and prepared for immunofluorescence analysis using rabbit anti-Tie2 antibody and DAPI. Sub-figure **(a)** indicates that the Rabbit Tie2 antibody effectively and specifically stains Tie2. Images from several Z-sections were acquired using the Nikon dual camera system. Images were also deconvolved using the Nikon software and Z-sections were projected using ImageJ. Scale bars indicate 20.00 µm

Nonetheless, this was not an indication of the functionality of the Tie2^{FLAG} kinase domain, as the ability of the receptor to oligomerise upon incubation with Ang1 was described to be independent of the endodomain of Tie2 receptor (Fukuhara et al. 2008; Saharinen et al. 2008). To analyse whether the receptor was phosphorylated by the agonistic ligand Ang1 I incubated serum starved cells with 200 ng/ml of oligomerized human recombinant Ang1^{His} (hrAng1^{His}) for 20 min and I analysed the presence of phospho-Tie2 by western blot using the pY992-Tie2 antibody, which is the first tyrosine to be phosphorylated after Tie2 activation (Murray et al. 2001). Recombinant angiopoietins are broadly used to study the Ang1/Tie pathway since the oligomerisation

state of His tagged recombinant angiopoietins can be adjusted using different proportions of ligand and anti-His antibody (Saharinen et al. 2005; Bogdanovic et al. 2006; Wehrle et al. 2009). The pY992-Tie2 had previously given weak bands of signal as observed in **Figure *14*** (3rd box, 8, 9 and 11th row), yet the experience from our lab was that the phosphorylation of Tie2 with the pY992-Tie2 antibody could only be detected specifically upon exposure of cells to Ang1. Furthermore, I later managed to improve the conditions for the western blot staining using the pY992-Tie2 (**Figure *22*** and **Figure *23***). Nonetheless, although the pY992-Tie2 bands were not optimal, it was possible to see that only Tie2 in HeLa T-REx $Tie2^{FLAG}$ and HUVEC cells exposed to $hrAng1^{His}$ were phosphorylated (**Figure *14***).

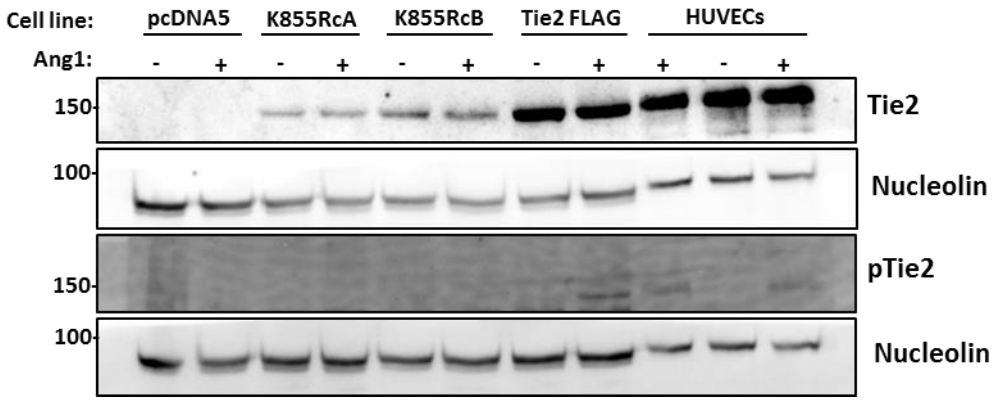

Figure 14. $Tie2^{FLAG}$ expressed in HeLa T-Rex cells is phosphorylated by the agonistic ligand Ang1, whereas $Tie2^{K855R/FLAG}$ is not. HeLa $pcDNA5^{FRT/TO}$, clones A and B of HeLa T-REx $Tie2^{K855R/FLAG}$ and HeLa T-REx pulsed for 6h with 1 µg/ml of doxycycline were serum starved for 24h and incubated with 200 ng/mL of $hrAng1^{His}$ for 20 min. Cells were lysed and the presence of Tie2, p(Y995) Tie2 and nucleolin was analysed by western blotting. Cell lysates of HUVECs serum starved or incubated with 200 ng/mL Ang1 for 5 minutes donated from a former member of the lab were used as a positive control of the phosphorylation of Tie2.

Since the receptor is not internalized in a ligand-dependent manner unless it is phosphorylated (Bogdanovic et al. 2006), to further evaluate the functionality of $Tie2^{FLAG}$ I confirmed by cell immunofluorescence that the $Tie2^{FLAG}$ was co-localizing with the $hrAng1^{His}$ and that the receptor was being internalized.

I first evaluated whether Ang1 was being bound to the HeLa T-REx clones by cell immunofluorescence. To do so, I incubated the control HeLa T-REx cells, HeLa T-REx $Tie2^{FLAG}$ or HeLa T-REx $Tie2^{K855R/FLAG}$ that had been exposed to doxycycline with

oligomerized hrAng1^{His} for 10 min at 37°C. Cells were fixed and prepared for the immunofluorescence staining of hrAng1^{His} and stained with DAPI. It was observable from the samples that the control HeLa T-REx pcDNA5$^{FRT/TO}$ had a small amount of hrAng1^{His} associated to cells but it was clear that HeLa T-REx Tie2^{FLAG} and HeLa T-REx Tie2$^{K855R/FLAG}$ cells had higher amounts of hrAng1^{His} bound to cells (**Figure *15***). Actually, in accordance with the higher levels of expression of Tie2$^{K855R/FLAG}$ receptor reported by western blot, the HeLa T-REx Tie2$^{K855R/FLAG}$ also appeared to bind higher amounts of ligand than the HeLa T-REx Tie2^{FLAG} cells. These results suggested that the agonistic ligand Ang1 was binding the Tie2 receptor with high specificity.

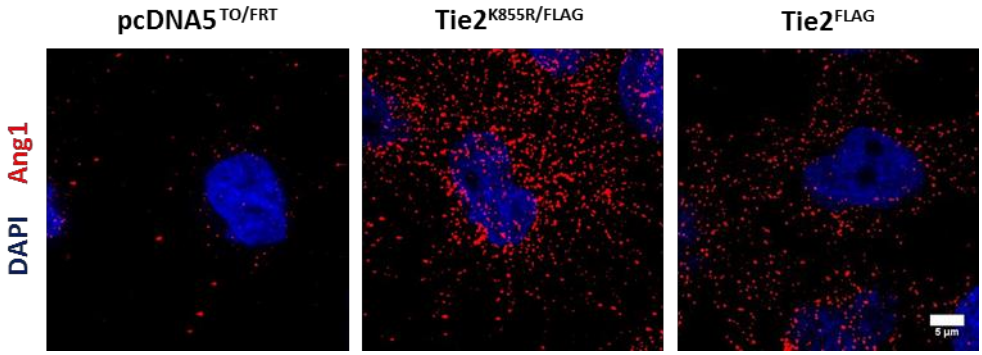

Figure 15. HeLa T-Rex cells expressing Tie2^{FLAG} or Tie2$^{K855R/FLAG}$ bind more agonistic ligand hrAng1^{His} than the control HeLa T-REx cells. HeLa T-REx stably transfected with Tie2^{FLAG}, Tie2$^{K855R/FLAG}$ or control vector pcDNA5$^{FRT/TO}$ grown in glass cover-slips were pulsed for 6h with 1 µg/ml of doxycycline and serum starved for 2h. Cells were then incubated with 200 ng/ml of oligomerized hrAng1^{His} at 37˚C for 10 min. The ligand was oligomerized using 5 µg/ml of Mouse His antibody. Cells were fixed with 4% PFA and prepared for the immunofluorescence staining of the ligand with anti-Mouse antibody conjugated to Alexa Fluor 488. Cell nuclei were stained with DAPI. Several Z-stacks of cells were acquired using a Deltavision microscope and deconvoluted with the Deltavision software. Z-stacks were projected into a single image using ImageJ. Scale bar indicates 5 µm.

To further confirm that the Tie2^{FLAG} receptor was able to bind the oligomerized ligand Ang1 I incubated serum starved HeLa T-REx Tie2^{FLAG} cells with hrAng1^{His} for 5 and 30 minutes or left them untreated to evaluate the co-localization of the receptor with the ligand at different time-points of incubation. In this experiment I used the rabbit Tie2 antibody for the immunofluorescence staining of the receptor. After deconvolution of images the Tie2 staining appeared as a punctate pattern along the periphery of cells and indicating the limits between contacting cells as described previously in the literature

(Zhang et al. 2011; Saharinen et al. 2008) (**Figure *16***). This pattern was more evident with serum starved cells than with cells incubated with hrAng1 indicating that the ligand was mobilizing the receptor. After 5 min of incubation with hrAng1^{His}, co-localization of hrAng1^{His} and Tie2^{FLAG} fluorescent signal was rather appreciable at apical and middle Z-sections of cells than at the extreme basolateral Z-sections of cells, whereas at 30 min of incubation the co-localization of hrAng1^{His} and Tie2^{FLAG} was clearly appreciable at all Z-sections were Tie2 signal was visualised. Furthermore, at 30 min of incubation Tie2^{FLAG} and hrAng1^{His} appeared to be co-localizing in some kind of perinuclear structures that appeared to be of bigger size than the co-localization dots of earlier incubations time-points; although it was not possible to determine with confidence whereas those were inside the cell without any cellular marker other than DAPI. The evident co-localization between Tie2^{FLAG} and hrAng1^{His} confirm that the ligand is mostly binding to the receptor in the HeLa T-REx Tie2^{FLAG} cells. Images showed that while most of the Ang1 was co-localizing with the receptor, it was not the case for the receptor, meaning that I were not working with saturating concentrations of the ligand. Furthermore, the results also indicated that Tie2^{FLAG} was being mobilized by hrAng1^{His} and suggested that the receptor was being internalized upon the interaction with the ligand (**Figure *16***).

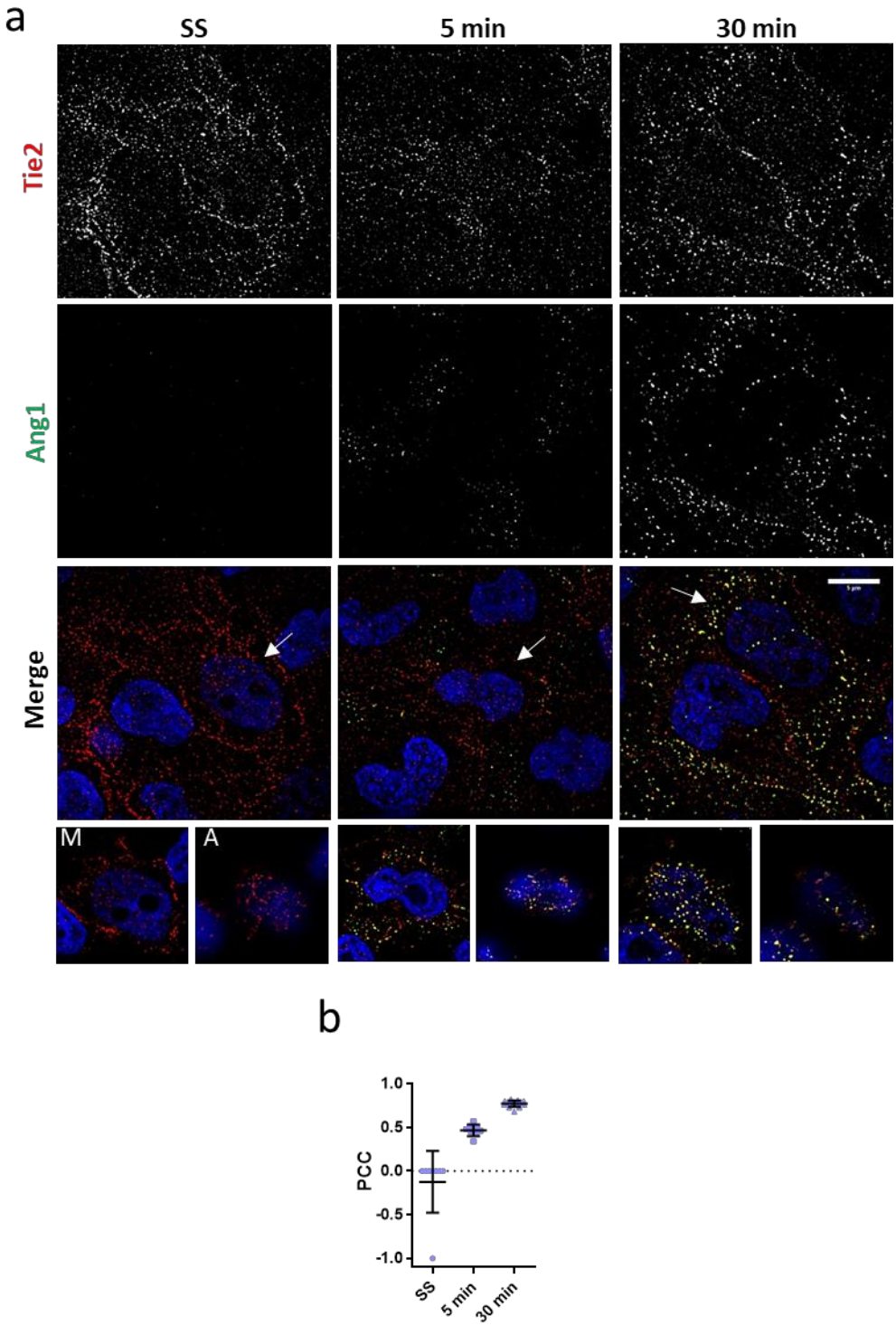

Figure 16. Tie2^{FLAG} expressed by HeLa T-REx cells binds the agonistic ligand hrAng1^{His}. HeLa T-REx Tie2^{FLAG} cells grown in a glass cover-slip were pulsed pulsed for 6h with 1 µg/ml of doxycycline and serum starved for 2h. Cells were then incubated for 5 and 30 min (**5 min, 30 min**) or left untreated (**SS**) before being fixed for immunofluorescence analysis of Tie2^{FLAG} and Ang1 distribution. Cells nuclei were stained with DAPI. Several Z-sections of cells were acquired using a Deltavision microscope and deconvoluted with the Deltavision software. **(a)** shows representative images of the basolateral extreme of cells (B, top bigger panels) for the different conditions and regions from more medial and apical sections (M and A, bottom

panels) of cells indicated with an arrow. **(b)** Pearson's Correlation Coefficient (**PCC**) were calculated with Volocity image analysis software. Images show Mean ± SD of at least 8 measured cells from a single experiment.

To finally confirm whether the receptor/ligand complex was being internalized by cells I investigated whether hrAng1^{His} localized with the EEA1^{+} endosomes. I incubated serum starved cells with oligomerised hrAng1^{His} for 5, 15 or 30 min at 37˚C or for 30 min on ice. Cells were fixed for immunofluorescence analysis of the ligand and EEA1^{+}. As seen in the previous experiment, hrAng1^{His} appeared to be mobilizing the Tie2 receptor from the peripheral localization towards the nuclei (**Figure *17***). Furthermore, after 30 min of incubation at 37˚C I was able to visualize some degree of co-localization of hrAng1 with EEA1^{+}, which was also reflected by the Pearson's correlation coefficient (PCC). Therefore, I was able to confirm that hrAng1^{His} was being internalized with the receptor into intracellular compartments and I learned that at least a fraction of the internalized hrAng1^{His} was being delivered to Early Endosomes in HeLa T-REx Tie2^{FLAG} cells.

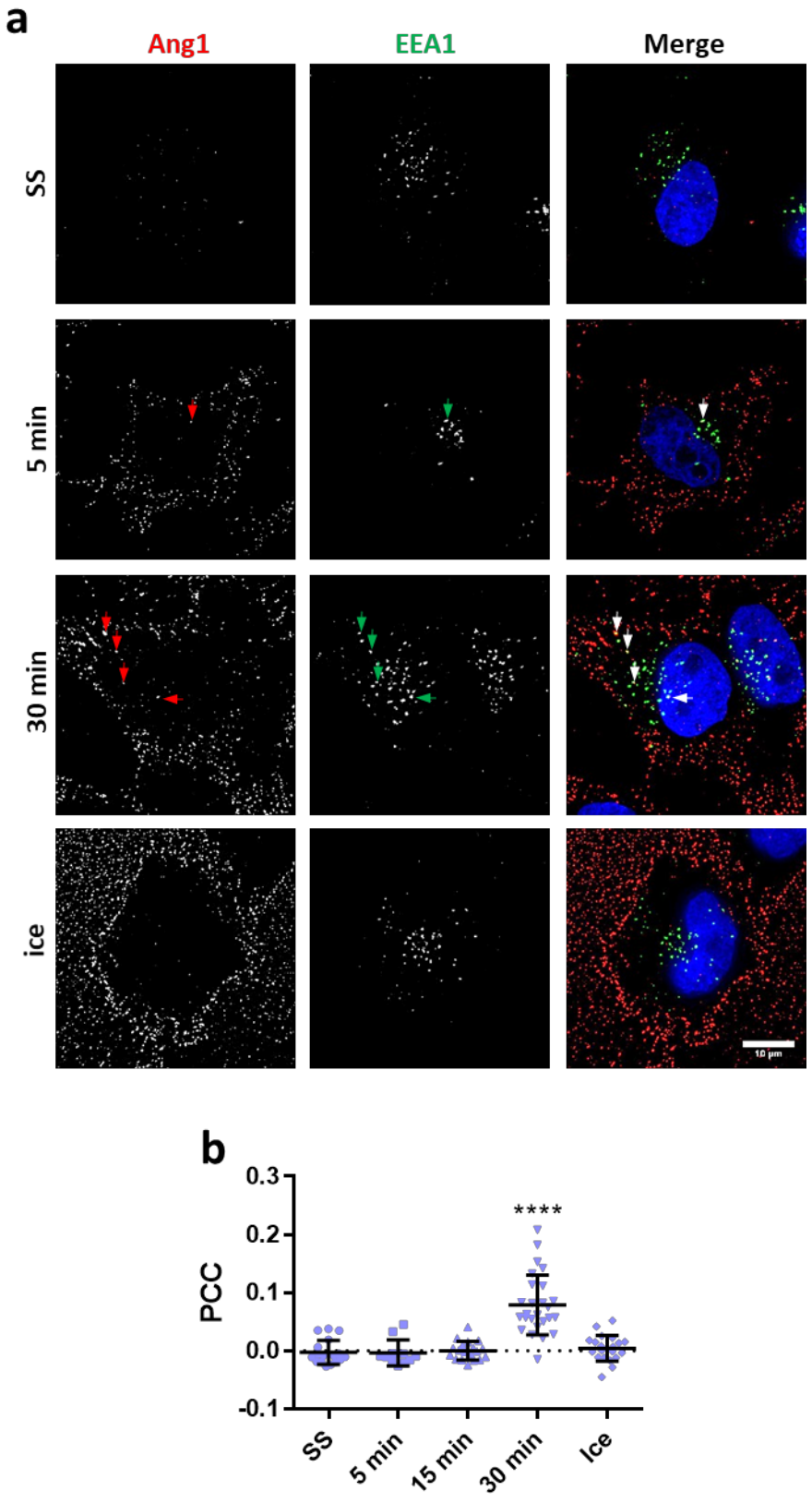

Figure 17. hrAng1^{His} is internalized to early endosomal compartments by HeLa T-REx Tie2^{FLAG} cells. HeLa T-REx Tie2^{FLAG} cells grown in cover-slips and pulsed pulsed for 6h with 1 µg/ml of doxycycline were serum

starved for 2h before incubation with 200 ng/mL of oligomerised hrAng1^{His} at 37˚C for 5 or 30 min (**5 min**, **30 min**) on ice for 30 min (**Ice**) or left untreated (**SS**). Cells were fixed for immunofluorescence analysis of oligomerised hrAng1^{His} and Early Endosomal Antigen (EEA1). Cells nuclei were stained with DAPI. **(a)** Deconvoluted images of medial Z-sections of cells acquired using a Deltavision microscope are shown. Arrow heads highlight co-localization of Ang1 with EEA1. **(b)** The Pearson's correlation coefficient from regions of interest (ROIs) including a single cell each were calculated using Volocity image analysis software. Mean ± SD of at least 15 cells for each condition, measured in a single experiment. Dunnett's multiple comparisions test for *one-way* ANOVA, $p < 0.05$ (**** if $p < 0.0001$).

Furthermore, I repeated the incubation at 37˚C for 30 min using the HeLa T-REx expressing the Tie2$^{K855R/FLAG}$ mutant and I was not able to see any co-localization of hrAng1^{His} with EEA1^{+} endosomes neither any apparent internalization of the ligand. Interestingly, in contrast to the HeLa T-REx Tie2$^{K855R/FLAG}$ incubated for 10 min with hrAng1^{His} from **Figure *15***, after 30 min of incubation with the ligand I was not able to see as much hrAng1^{His} associated with the cells. This suggested that, although the Tie2$^{K855R/FLAG}$ was also capable of oligomerising and binding to the ligand, hrAng1^{His} was released from the kinase-dead receptor due to the absence of auto-phosphorylation or internalization. In the case of the Tie2^{FLAG}, the ligand was found co-localizing again with EEA1. Actually, the co-localization index was higher this time as more internalized Ang1 was found within early endosomes. This difference may reflect some kind of experimental variability during the incubation or small epigenetic differences between the different lots of HeLa T-REx Tie2^{FLAG} clone.

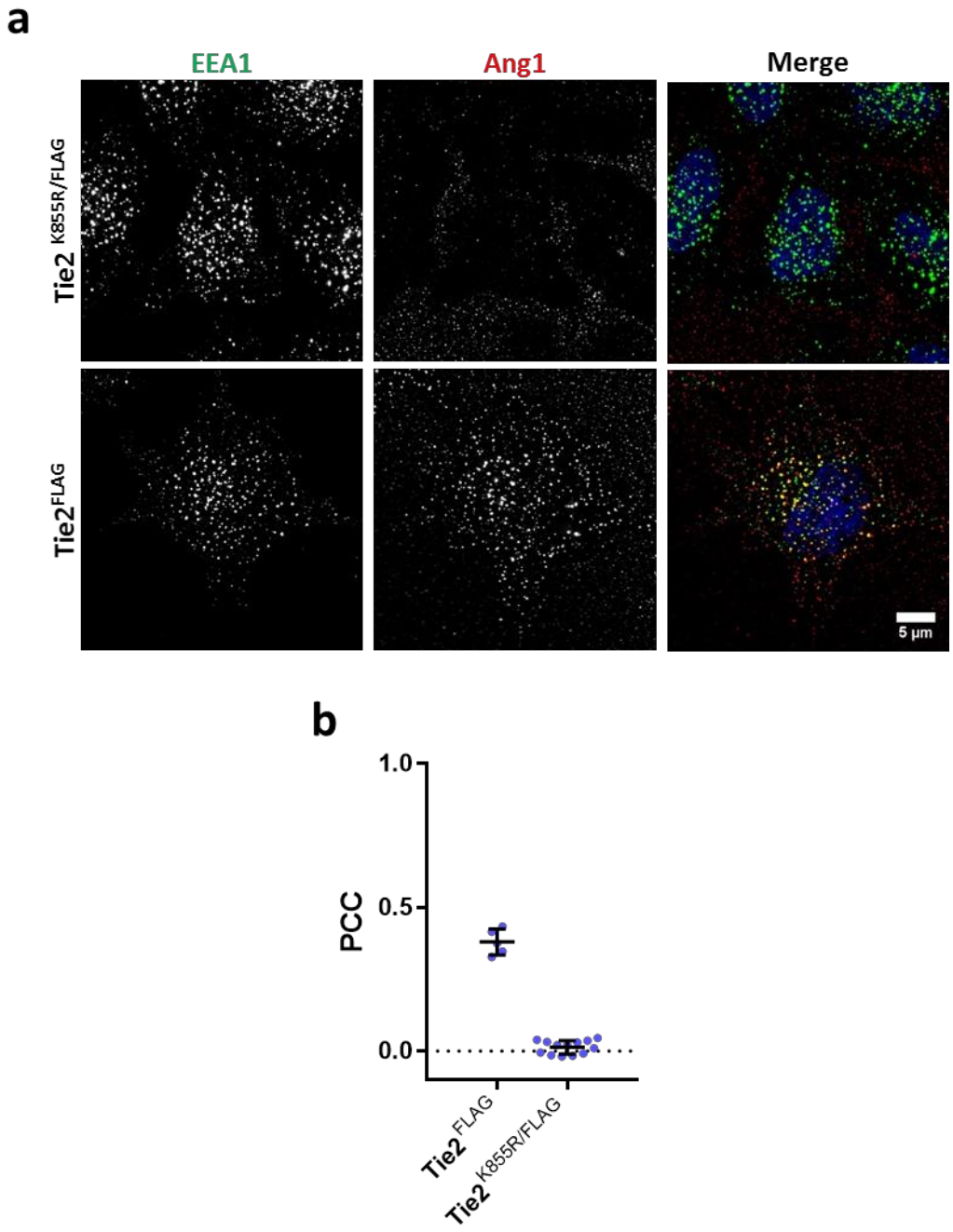

Figure 18. The agonistic ligand hrAng1^{His} is internalized by the HeLa T-REx Tie2^{FLAG} cells but not by the HeLa T-REx Tie2$^{K855R/FLAG}$ cells. HeLa T-REx cells expressing the Tie2^{FLAG} receptor or the dead kinase mutant receptor T-REx Tie2$^{K855R/FLAG}$ grown in cover-slips were pulsed for 6h with 1 µg/ml of doxycycline serum starved for 2h and incubated with oligomerized hAng1His ligand for 30 min at 37˚C. Cells were fixed for immunofluorescence analysis of hrAng1^{His} and EEA1. Cells nuclei were stained with DAPI. Several Z-stacks of cells were acquired using a Deltavision microscope and deconvoluted with the Deltavision software. **(a)** Representative extended images composed of several cell's Z-sections are shown for each cell type. **(b)** The Pearson's correlation coefficient from ROIs including a single cell each were calculated using Volocity image analysis software. Mean ± SD of 5 representative cells from cells expressing Tie2^{FLAG} and 13 cells in the case of cells expressing Tie2$^{K855R/FLAG}$.

As well as being delivered into early endosomes containing EEA1, internalized cargos in cells can also be transported to other sub-populations of endosomes that are characterised by the presence of different Rab proteins and effectors. The adaptor protein APPL1 identifies a subset of early endosomes that were shown to be sorting endosomes from where cargoes can be distributed to other compartments, including $EEA1^{+}$ endosomes (Kalaidzidis et al. 2015). APPL1 containing endosomes are also known as signalling endosomes since APPL1 has been found to interact with components of signalling pathways of various receptors and because evidence suggests that APPL1 containing endosomes are involved in the regulation of multiple cellular functions derived from activation of different molecules (Liu et al. 2017). Since I saw that activated Tie2 receptor was internalized into $EEA1^{+}$ endosomes (**Figure *17***, **Figure *18***), I decided to investigate whether Tie2 was also being delivered to APPL1-containig endosomes after activation by Ang1. After incubating cells for 30 min with oligomerised $hAng1^{His\ I}$ found that a small proportion of ligand would co-localize with APPL1 in intracellular compartments with endosomal-like shape in the HeLa T-REx $Tie2^{FLAG}$ but not in the HeLa T-REx $Tie2^{K855R/FLAG}$ cells (**Figure *19***).

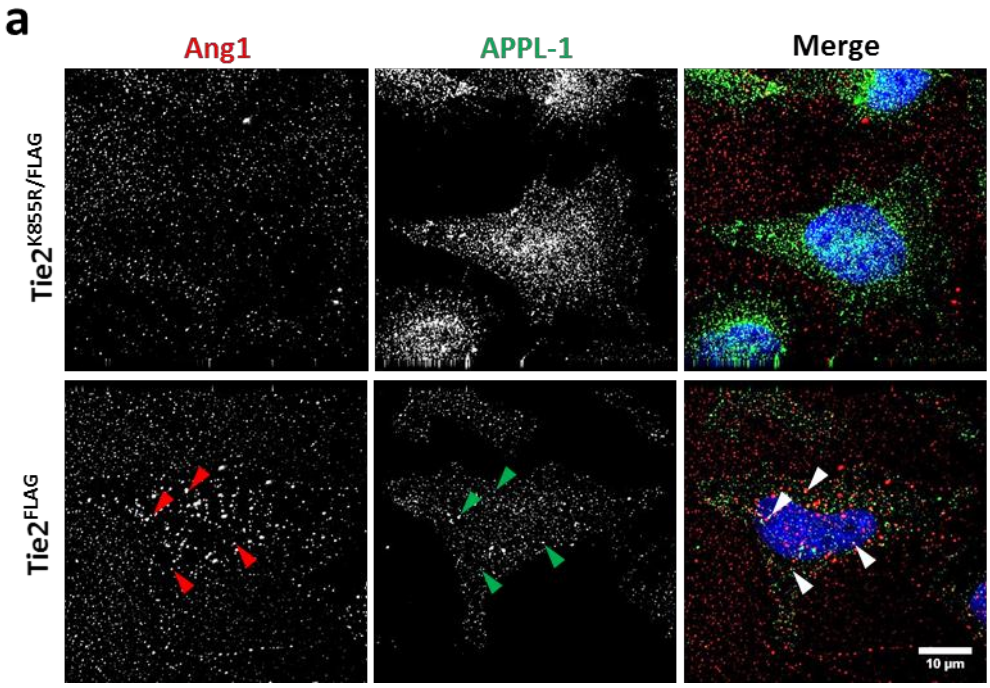

Figure 19. A fraction of the internalized hrAng1^{His} is internalized into APPL1 containing endosomes. HeLa T-REx expressing Tie2$^{K855R/FLAG}$ or Tie2^{FLAG} (pulsed for 6h with 1 µg/ml of doxycycline) were serum starved for 2h and incubated with hrAng1^{His} at 37°C for 30 minutes. Cells were then fixed and analysed by immunofluorescence staining of hrAng1^{His} and APPL1. Nuclei were stained with DAPI. Some of the internalised hrAng1^{His}, contained in perinuclear endosomal-like structures, co-localised with APPL1 in the Tie2^{FLAG} expressing cells but not in cells expressing the dead kinase mutant (Arrowheads). Scale bar shows 10µm.

Overall, it was clear that I had been able to demonstrate that hrAng1^{His} is internalized upon binding to the Tie2^{FLAG} receptor in the cell surface, as former members of the lab had described for the Tie2 receptor in HUVECs. The internalization of the Tie2^{FLAG} was dependent on the auto phosphorylation ability of the receptor, as has been described previously for HUVECs (Fukuhara et al. 2008). In contrast, although it has been repeatedly mentioned in the literature that Ang1 is not internalized with the receptor (Bogdanovic et al. 2006; Wehrle et al. 2009; Fukuhara et al. 2008), I had observed the contrary. Therefore, the HeLa T-REx Tie2^{FLAG} were validated as a useful model for the study of Tie2 internalization and I proceeded to investigate the regulatory mechanisms of the endocytosis of Tie2 in HeLa T-REx Tie2^{FLAG}. Nonetheless, conclusive results with the HeLa T-Rex Tie2^{FLAG} would later need to be confirmed using endothelial cells such as HUVECs.

3.3 Ubiquitination of Tie2 could not be detected after Ang1-induced activation

Ubiquitination of some cell surface receptors has been described to have an important role in determining their internalization. As explained before, Tie2 has been reported to be ubiquitinated in an Ang1 dependent manner in HUVECs and it was shown that the interaction with the ubiquitin ligase c-Cbl was essential for the internalization and degradation of the receptor in 293F–Tie2-expressing cell lines (Wehrle et al. 2009). I attempted to purify ubiquitinated Tie2 from both HeLa T-REx Tie2^{FLAG} and HUVECs so that any Ang1-dependent ubiquitinated sites in Tie2 could be identified by mass spectrometry. In the case of being able to purify ubiquitinated Tie2 and identify specific ubiquitination sites of the activated receptor I wanted to create different ubiquitin-deficient Tie2 mutants to generate new HeLa T-REx cell clones and evaluate the effect of the mutations in the internalization and signalling of Tie2.

To determine the ubiquitinated levels of Tie2 in HUVECs I initially used the recombinant protein MultiDsk, which contains 5 ubiquitin binding domains of the yeast protein Dsk2 together with a GST domain and 12 His tag (**Figure *20***). The MultiDsk recombinant protein was designed for the enrichment or purification of ubiquitinated proteins from cell lysates (Wilson et al. 2012). Since it binds directly to the ubiquitins in proteins, the MultiDsk recombinant protein also protects ubiquitin chains from the activity of de-ubiquitinase enzymes (Wilson et al. 2012). The MultiDsk recombinant protein is produced by transformed BL21(DE3) bacteria and then purified using GSH-beads as described in the methods chapter. The MultiDsk-associated beads can then be directly used to isolate ubiquitinated proteins form cell lysates.

Figure 20. Representation of the multiple domains composing the recombinant protein MultiDsk that can be used to enrich mammalian cell-lysates with ubiquitin-containing proteins. The protein contains 5 Dsk2 ubiquitin binding domains from yeast separated by flexible linkers. MultiDsk also contains multiple His tags and a GST tag that can be used for the purification, immobilisation and identification of the protein (Wilson et al. 2012).

Therefore, to determine whether I was able to purify ubiquitinated Tie2 using the MultiDsk recombinant protein I initially used a pool of frozen HUVECs lysates exposed to Ang1 for different amounts of time (provided by Dr. Filipe Ferreira. It is necessary to mention that lysates were not prepared for this particular protocol and the lysis buffer lacked inhibitors of de-ubiquitinase enzymes. After incubating the lysates with MultiDsk beads I then investigated by western blot whether Tie2 was being pulled down in the ubiquitin enrichment of lysates. As seen in **Figure *21*** (top panel), after the incubation of lysates with the MultiDsk-associated beads I was able to select a large amount of ubiquitinated proteins from the original lysate. Furthermore, although some ubiquitinated material was lost in the incubation supernatant, there wasn't any appreciable signal in the successive washes. When I then blotted the membrane for Tie2 I was able to detect a main band of ubiquitinated Tie2 together with some weaker bands of smaller size (**Figure *21***). The Ponceau staining of the western blot membranes can be used to evaluate the presence of the MultiDsk protein in the beads lane (**Figure *21***, bottom panel), the band in the Ponceau staining of the membrane corresponds with the gap in the lane for the MultiDsk-beads stained for ubiquitin, as the MultiDsk protein is not ubiquitinated. The Ponceau staining of the MultiDsk protein can be used to ensure that similar volumes of beads were loaded for the enrichment. This result indicated that the MultiDsk containing beads were able to enrich HUVECs lysates with ubiquitinated proteins and that Tie2 was being pull down with the ubiquitinated proteins.

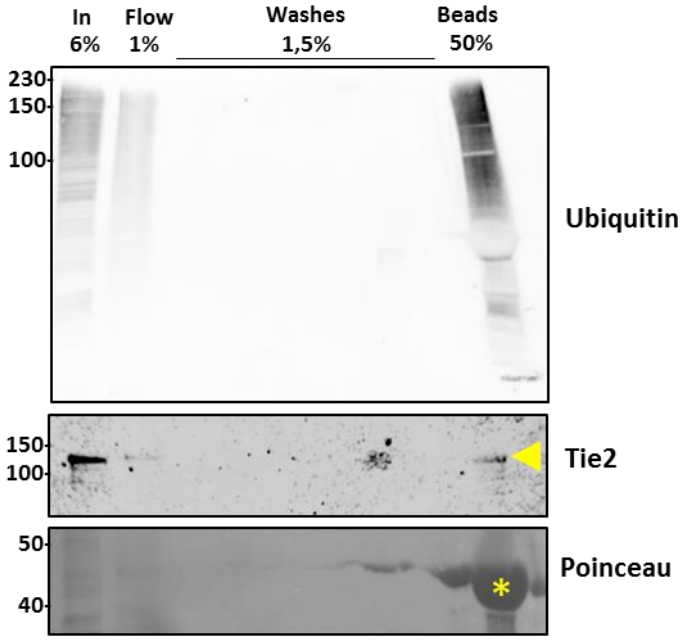

Figure 21. Tie2 was identified from an ubiquitin enriched lysate of HUVECs obtained using MultiDsk. Lysates of HUVECs incubated with Ang1 for 5, 10, 15, 20 and 30 min were pooled together and incubated with MultiDsk/GST beads for 4h at 4°C. The indicated percentages of whole cell lysate (Input, **In**), flow through from the beads (**Flow**), washes and ubiquitin-enriched beads were run in an SDS-PAGE gel and transfered to a nitrocellulose membrane for a western blot analysis. Membranes were then stained for the presence of Tie2 and ubiquitin with Rabbit anti-Tie2 and Mouse anit-Ubiquitin antibodies. The yellow arrowhead indicates a Tie2 positive band in the ubiquitin enriched lysate. Ponceau staining was used to evaluate the presence of MultiDsk protein between 40 and 50kDa (*****).

To determine whether the pull down of Tie2 by MultiDsk beads was induced after the Ang1-activation of the receptor I purified ubiquitinated Tie2 from cell lysates of HUVECs incubated with Ang1 for 5 min or left untreated. In order to increase the yield of Tie2 pull-down I used fresh lysates prepared with lysis buffer containing inhibitors of de-ubiquitinating enzymes. As before, I was able to visualize Tie2 in the lane of ubiquitin-enriched lysate. Several bands were appreciable for Tie2 and some presented a weight shift upwards, which indicated that more post-translation modifications had been added to Tie2. Nevertheless, taking into account the loading of MultiDsk-beads in each lane (**Figure *22***, bottom panel), the ubiquitination of Tie2 did not appear to be Ang1-dependent. Whereas when I blotted the membranes for phosphorylated Tie2 I was able to perceive a weak albeit sharp band of activated Tie2 in an Ang1-dependent manner. Although I attempted to improve the pull down of Tie2 using the MultiDsk-beads in

various ways, as well as testing different incubation times with Ang1, I never managed to visualize any dependence on the activation by Ang1 (data not shown).

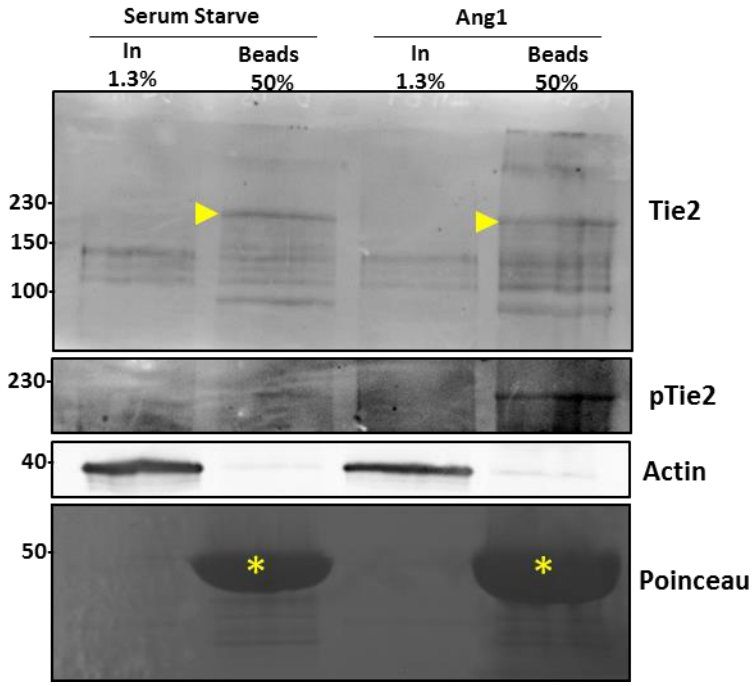

Figure 22. Ubiquitination of Tie2 was not found dependent on the incubation with hrAng1^{His} in HUVECs. Serum starved HUVECs were left untreated or incubated with hrAng1^{His} for 5 min. Ubiquitin-enriched cell lysates were then obtained after incubation with MultiDsk containing beads and analysed by western blot. The indicated percentages of Whole cell lysate (Input, **In**) and ubiquitin-enriched beads (**beads**) were analysed for the presence of Tie2 and pTie2 by western blot. Arrowheads point at a Tie2 band with higher weight than the Tie2 found in serum starved cells. Asterisks indicate the Ponceau staining of the MultiDsk protein.

In order to determine whether Tie2 itself was ubiquitinated rather than being pulled down in complex with a ubiquitinated protein I used the HeLa T-REx Tie2^{FLAG} cells to immunoprecipitate Tie2^{FLAG} with the anti-FLAG M2 resin (Sigma-Aldrich). As seen in **Figure *23***, using the anti-FLAG M2 resin I obtained a good yield of purified Tie2^{FLAG} as little was found remaining in the supernatant of the incubation. Nonetheless, although the Tie2^{FLAG} was clearly activated by Ang1, there wasn't any ubiquitination of the receptor appreciable in the blots (**Figure *23***) As well as for the MultiDsk pull-down of ubiquitinated proteins in HUVECs lysates, I attempted to improve the protocol but it repeatedly seemed that TieFLAG was not being ubiquitinated in HeLa T-REx Tie2^{FLAG}. Actually, I used the MultiDsk-beads to enrich lysates of HeLa T-REx Tie2^{FLAG} cells with ubiquitinated

proteins and I was only able to note a weak smear of pulled-down Tie2^{FLAG} in the blots (**Figure *23***). Therefore, since I did not visualize any enrichment of Tie2 by the MultiDsk in an Ang1 dependent manner I could not conclude that incubation of HUVECs with the ligand triggered ligand-dependent ubiquitination of Tie2 was necessary for the internalization of the receptor in our experimental conditions. Similarly, our results indicated that Tie2^{FLAG} was not being ubiquitinated in HeLa T-REx Tie2 cells.

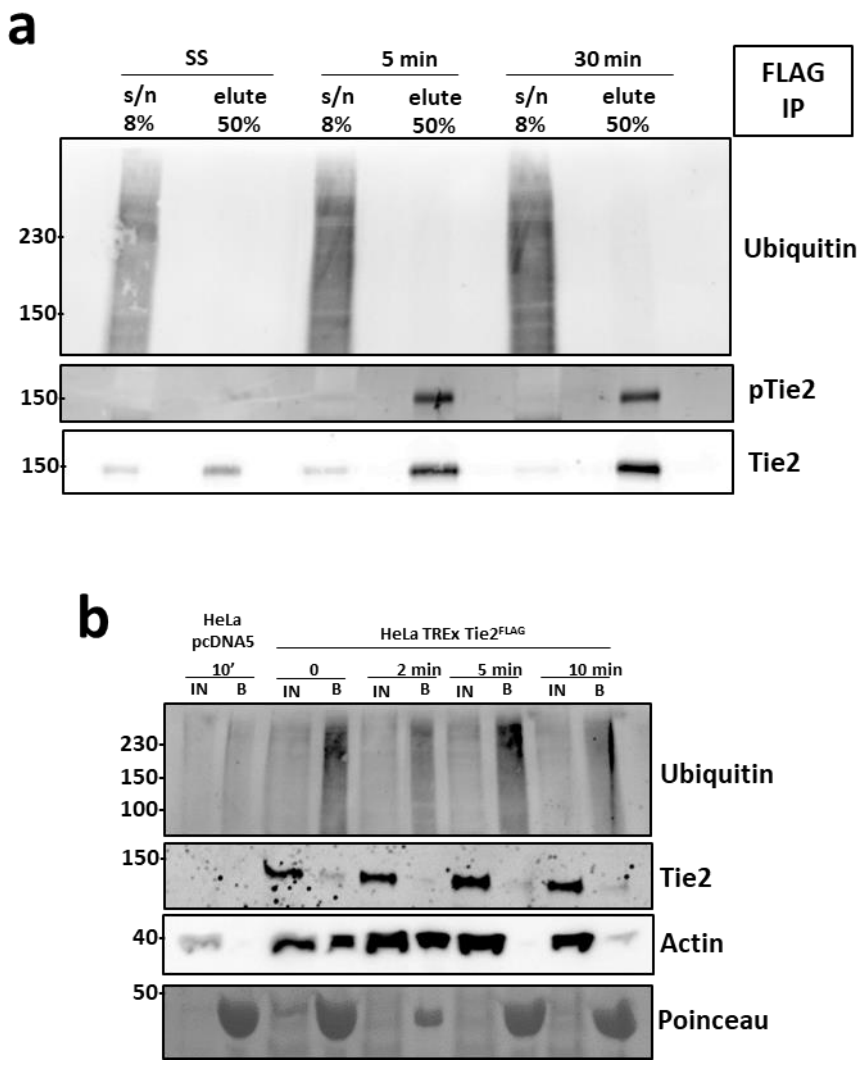

Figure 23. Tie2^{FLAG} expressed in HeLa T-REx cells was not found to be ubiquitinated after the activation by hrAng1^{His}. (a) Tie2^{FLAG} expressed in HeLa T-REx cells pulsed for 6h with 1 µg/ml of doxycycline was immunoprecipitated with Mouse FLAG resin from lysates of cells incubated with Ang1 for 5 and 30 minutes or left untreated (**SS**). The indicated amount of resulting supernatant (**s/n**) and elute from the beads (**elute**) were analysed by western blot for the presence of ubiquitin, Tie2 and pTie2. **(b)** Lysates from control HeLa T-REx cells (pcDNA5) or HeLa T-REx expressing Tie2^{FLAG} incubated with hrAng1^{His} for the indicated amounts of time were incubated with MultiDsk beads to obtain ubiquitin-enriched lysates. The

presence of ubiquitin and Tie2 in the whole cell lysate (**IN**, 1% sample loaded) and beads (**B**, 50% of sample loaded) was analysed by western blot.

CHAPTER 4

Developing a quantitative assay of Tie2 internalization

As explained before, the mechanisms of endocytosis of Tie2 are currently unknown. In order to study how the ligand-induced internalization of Tie2 regulates the activity and cellular functionality of the activated receptor I need to uncover which endocytic mechanisms are responsible for the internalization of the activated Tie2. To begin with, I decided to optimize an assay that would allow us to quantitate the internalization of the receptor.

4.1 Optimization of a sandwich ELISA based assay to quantitate the internalization of Ang1

In order to quantitate the amount of internalized Tie2 by cells I decided to optimize a sandwich ELISA based assay. ELISA stands for Enzyme-Linked Immunosorbent Assay and it is based in the immunoreactivity of antibodies for the detection of an analyte. In a sandwich ELISA assay in particular, a capture antibody non-specifically adsorbed in a multi-well plate is used to specifically select an analyte from a sample matrix. A different antibody is then used as a detection antibody. The detection antibody is conjugated to an enzyme that will generate a colorimetric reaction when in contact with the enzyme substrate in the appropriate conditions. The colour generated the antibody conjugated enzyme is proportional to the presence of analyte and can be measured to extrapolate the amount of analyte in each sample by using a standard curve of known concentrations of analyte.

In our case, since I had found that significant amounts of Ang1 were being internalized with Tie2 receptor in both HeLa T-REx cells and HUVECs, I decided to quantify the amount of Ang1 in cells as an indirect measure of internalized Tie2 receptor. An ELISA kit for the quantitation of human Angiopoietin-1 is available commercially although I preferred to prepare our own plates for reasons of cost (Quantikine ELISA/hrAng1 Immunoassay, R&D systems).

Optimization of the sandwich ELISA for the detection of Ang1

For the detection of Ang1 in a sandwich ELISA I decided to use a mouse monoclonal Ang1 antibody as a capture antibody and a mouse monoclonal biotinylated Ang1 antibody as a detection antibody (both from R&D systems). I then used horseradish peroxidase conjugated to streptavidin as a detection agent and measured the change of absorbance due to the activity of horseradish peroxidase to quantify the amount of Ang1 internalised into cells.

I first wanted to determine a concentration of the detection antibody that would give a proportional and unsaturated absorbance in response to different concentrations of Ang1. ELISA plates were coated with 2 µg/ml of monoclonal Ang1 antibody and wells

were incubated in duplicates with different concentrations of Ang1 in blocking buffer or with blocking buffer alone. The amount of Ang1 internalized by cells is not known so the antibody concentrations in the ELISA would have to be tested later using cell samples. The manufacturer recommended the use of the human Ang1 biotinylated polyclonal at 0.1 - 4 µg/ml in a sandwich ELISA so I decided to test antibody concentrations of 0.05, 0.1, 0.3 and 0.4 µg/mL. As seen in **Figure *24***a, using 0.4 µg/ml of polyclonal antibody allowed for a sensitive detection of all of the different concentrations of Ang1 tested and therefore I decided to use 0.4 µg/ml of polyclonal Ang1 detection antibody in the following optimisation experiments.

In the case of the capture monoclonal antibody, the manufacturer recommendations were to use a concentration between 2 - 8 µg/ml of monoclonal Ang1 antibody in the application of a sandwich ELISA so I decided to test the effect of 0.4, 1 and 2 µg/ml in the detection of a standard curve of Ang1 (R&D systems). As seen in **Figure *24***b, the different concentrations of capture antibody lead to similar standard curves of Ang1 so I decided to use 1 µg/ml of monoclonal Ang1 antibody in the following experiments as this would reduce the amount of antibody used.

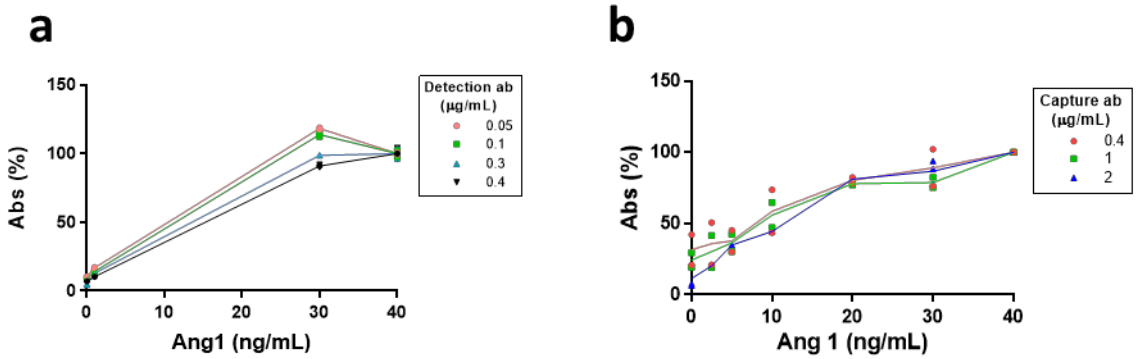

Figure 24. Optimization of the concentration of detection and capture antibodies for the quantitation of Ang1 with a sandwich ELISA. (a) A 96-well plate was coated with 2 µg/mL of monoclonal Ang1 antibody and wells were incubated with different concentrations of non-oligomerised hrAng1^{His} as indicated in the axis (0, 1, 30 or 40 µg/mL of hrAng1^{his}). Different concentrations of polyclonal Ang1 biotinylated antibody were used in duplicates, as indicated in the key, to evaluate the effect of the concentration of polyclonal Ang1 antibody on the detection of a standard curve of hrAng1^{His}. Wells were then incubated with Streptavidin-HRP conjugate and HRP buffer were used to generate a quantifiable colorimetric reaction. Absorbance was read at 492 nm in plate reader photometer and normalized as the % to the 40 ng/ml of standard hrAng1^{His}. Conditions were tested in duplicates. Mean ± Range is shown of two independent experiments (n=2). **(b)** In this case, different concentrations of monoclonal Ang1 coating antibody were

used, as indicated in the key, to evaluate the effect on the absorbance read from a standard curve of non-oligomerised hrAng1^{His}. Wells were incubated with 0.4 µg/ml of polyclonal Ang1 detection antibody. Streptavidin-HRP conjugate and HRP buffer were used to generate a quantifiable colorimetric reaction and absorbance at 492 nm was read using a plate reader photometer and normalized as the % of the 40 ng/mL of standard hrAng1^{His}. Conditions were tested in duplicates in three independent experiments (n=3) except for the 20 ng/mL point of hrAng1^{His}, for which n=1. Mean ± Range is shown.

The reading of the absorbance for the reaction of the HRP product is best acquired at 492nm light wavelength, as it represents the peak of the HRP product visible light spectra (**Figure *25***). As illustrated in **Figure *25***, it is also recommended to correct the measure of absorbance from the product of the HRP reaction using the reading at 550 nm, which is then used as a baseline that corrects for individual differences between wells. Therefore I decided to use the corrected absorbance in future experiments (R&D systems 2016).

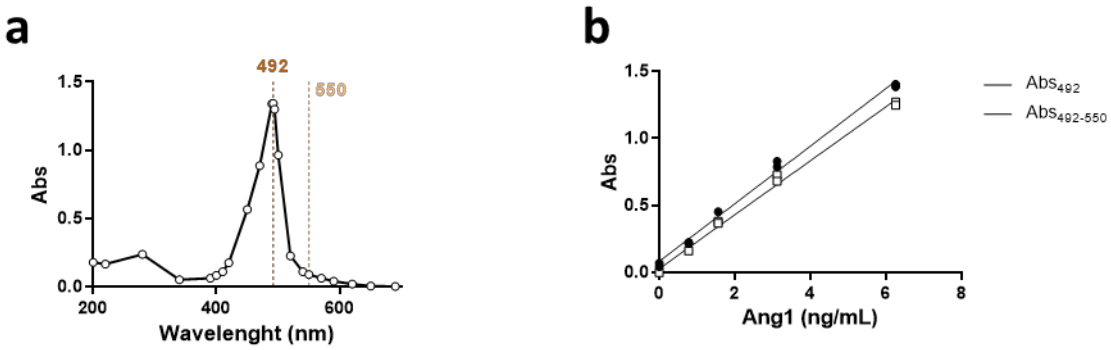

Figure 25. The standard curve of hrAng1^{His} is best represented correcting the reading of absorbance by the 550 nm reading. (a) The colorimetric products from one of the repeats from **Figure 24** were mixed in a 1 mL plastic cuvette and the absorbance spectra of the Horse Radish Peroxidase reaction product was acquired by measuring the absorbance at different wavelengths in a spectrophotometer. The spectrophotometer was calibrated with a blank measure consisting of HRP buffer at every change of wavelength. The coloured dashed lines at 492 nm and 550 nm in the X axis indicate the peak of the absorbance and the wavelength determined as the baseline correction absorbance respectively. **(b)** Example of a standard curve for hrAng1^{His} represented using the un-corrected measure of Absorbance at 492 nm or corrected with the Absorbance lecture at 550 nm. To obtain the standard curve an ELISA plate was coated using 1 µg/mL of monoclonal Ang1 antibody and different amounts of non-oligomerised hrAng1^{His}, as indicated in the X axis, were detected using 0.4 µg/mL of biotinylated polyclonal Ang1 antibody and Streptavidin-HRP conjugate. Absorbance readings at 492 nm and 550 nm were acquired for each well and the corrected Absorbance was obtained by subtracting the 550 nm read from the 492 nm read for each well. Points represent duplicates in a single experiment (n=1).

Furthermore, I realised that the Tie2 cell internalization assays were to be done using hAng1^{His} oligomerised with Mouse His antibody so I decided to test whether the use of

un-oligomerised or oligomerised hAng1^{His} would have an effect on the Ang1 standard curve for the ELISA, which would ultimately affect the accuracy of the quantitation of internalized Ang1 by cells. This is significant as the ELISA assay does not involve any de-naturing step so I would expect the Ang1 to remain oligomerized in the samples. Therefore, I used un-oligomerised and oligomerised Ang1 for the evaluation of their standard curves in the same ELISA plate. As shown in **Figure *26***, the standard curve was obviously different depending on the oligomerisation state of the Ang1. Using the oligomerised Ang1 for the standard curve caused the measure of much lower absorbances for every standard concentration, indicating that the presence of the mouse His antibody reduces the availability of Ang1 to the capture or detection antibody. Therefore, I decided to use oligomerised Ang1 as a standard analyte for the quantitation of cellular Ang1 in the following experiments.

The reading of absorbance of a colorimetric standard curve can be adjusted to both a linear regression and a non-linear 4 parameter logistic (4-PL) regression but I found that it was suggested to use the 4-PL regression as a better fit (R&D systems 2016). Hence I decided to use the non-linear 4-PL regression fit of the standards when interpolating the amount of Ang1 in cell samples. The 4-PL regression is calculated using the logarithmic values of concentration, concentration of samples are then interpolated from the regression curve and then transformed to linear scale again. **Figure *26*** shows a representative 4PL regression of the absorbance reading to the logarithmic concentration of Ang1 of the standards.

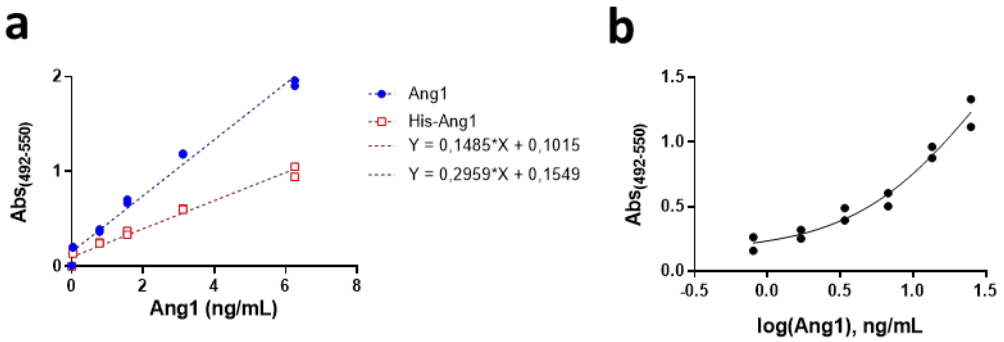

Figure 26. The standard curve of hrAng1^{His} is affected by the oligomerization state of the ligand. (a) The standard curve of Ang1 was obtained using un-oligomerised hrAng1^{His} or hrAng1^{His} oligomerised with

mouse anti-His antibody as in the cell assays. Average and range of two repeated measurements are shown. Linear regression for each condition is represented with dotted lines, difference between regression slopes was statistically significant (ANCOVA, $p < 0.05$). **(b)** Representative 4PL regression of the standard curve of Absorbance to concentration of hrAng1^{His} applying all the correction factors established. Dots in each graph represent duplicates in a single experiment (n=1)

Optimization of the cell internalization assay for the quantitation of internalized Ang1

Since I wanted to specifically quantificate the internalized Ang1 by cells I decided to implement the Ang1 internalization assay by introducing a step to remove the Ang1 remaining in the cell surface. Former members of our lab had successfully used an acidic wash buffer to strip transferrin from the cell surface of cells (Semerdjieva et al. 2008) so I tested whether I could strip Ang1 from the cell surface with the same protocol. To do so, I incubated HeLa T-REx cell clones expressing Tie2^{FLAG} cells with or without Ang1 on ice for 30 min. Cells incubated with Ang1 were then acid washed or left untreated on ice before being solubilized. As seen with the results, HeLa T-REx Tie2^{FLAG} cells bound an average of 16 ng of Ang1 (± 2.1 SEM, n=3) when the expression of Tie2^{FLAG} was induced for 8 h with 1 µg/ml of doxyxycline. Treating cells with the acid wash buffer reduced the amount of detected Ang1 in the cell samples to an average of 1.8 ng (± 0.41 SEM, n=3). Taking into the account the background signal shown by the serum starved control cells which were not incubated with oligomerised Ang1, the acid wash treatment removed an average of 91% of all the Ang1 bound to cells after 30 min incubation on ice (**Figure *27***). It is important to subtract the background signal measured in serum starved cells as the fetal bovine serum used in the cell culture media is rich in Ang1, which is not completely removed with cells with 2 hour of serum starvation.

Having ensured that the introduction of the acid wash would allow us to quantify mainly the internalized Ang1 by cells, I proceeded to evaluate the internalization of Ang1 in cells using the optimized conditions for the ELISA internalization assay. To do so, I initially performed a pilot experiment using HeLa T-REx Tie2^{FLAG} cells only. In this experiment I initially incubated serum starved cells on ice during 30 min with or without Ang1, what is called a pre-binding of ligand that ensures that the ligand is homogenously distributed on cells. For the 15, 30 and 40 min point incubation samples, Ang1-containing media was then exchanged for pre-warmed serum free media and cells were subsequently

incubated in a 37°C water bath for different lengths of time. After stopping the internalization with ice-cold PBS the remaining cell surface Ang1 was removed by acid stripping. As seen in **Figure *27***, although Ang1 was being bound to the cells, the amount of quantitated Ang1 from the different incubation time-points was similar to the 0 min control, suggesting that Ang1 had not been internalized.

In order to corroborate these results I repeated the internalization assay using the HeLa T-REx Tie2^{FLAG} cells and the HeLa T-REx Tie2$^{K855R/FLAG}$ cells. As explained before, the kinase dead mutant Tie2^{K855R} is neither phosphorylated nor internalized after oligomerization with the ligand Ang1 (Kontos et al. 1998; Cascone et al. 2005; Fukuhara et al. 2008; Saharinen et al. 2008), so I wanted to use it as a positive control of the non-internalization of Ang1. Furthermore, this time I did not perform the pre-binding on ice of Ang1 to emulate as much as possible the conditions that former members of our group had used. Therefore, serum starved cells were left untreated or directly incubated with Ang1-containing media for 3, 5, 15 and 30 min in a 37°C water bath. Again, after stopping endocytosis using ice-cold PBS/BSA, cells were acid striped of cell surface Ang1. The Total control consisted this time in cells that had been incubated with Ang1 for 30 min in the same conditions as the rest of time-points but that was supposedly not to be stripped of the cell surface Ang1. Sadly, the Total control samples were accidentally washed once with acid buffer. Nonetheless, I used the Total controls to normalize the amounts of quantitated Ang1 for each cell type and compare the internalization rates between the two cell types. As seen in **Figure *27***, the percentages of internalization in the different time-points were very similar between the two cell types, suggesting again that Ang1 was not being internalized by the HeLa T-REx Tie2^{FLAG} cells.

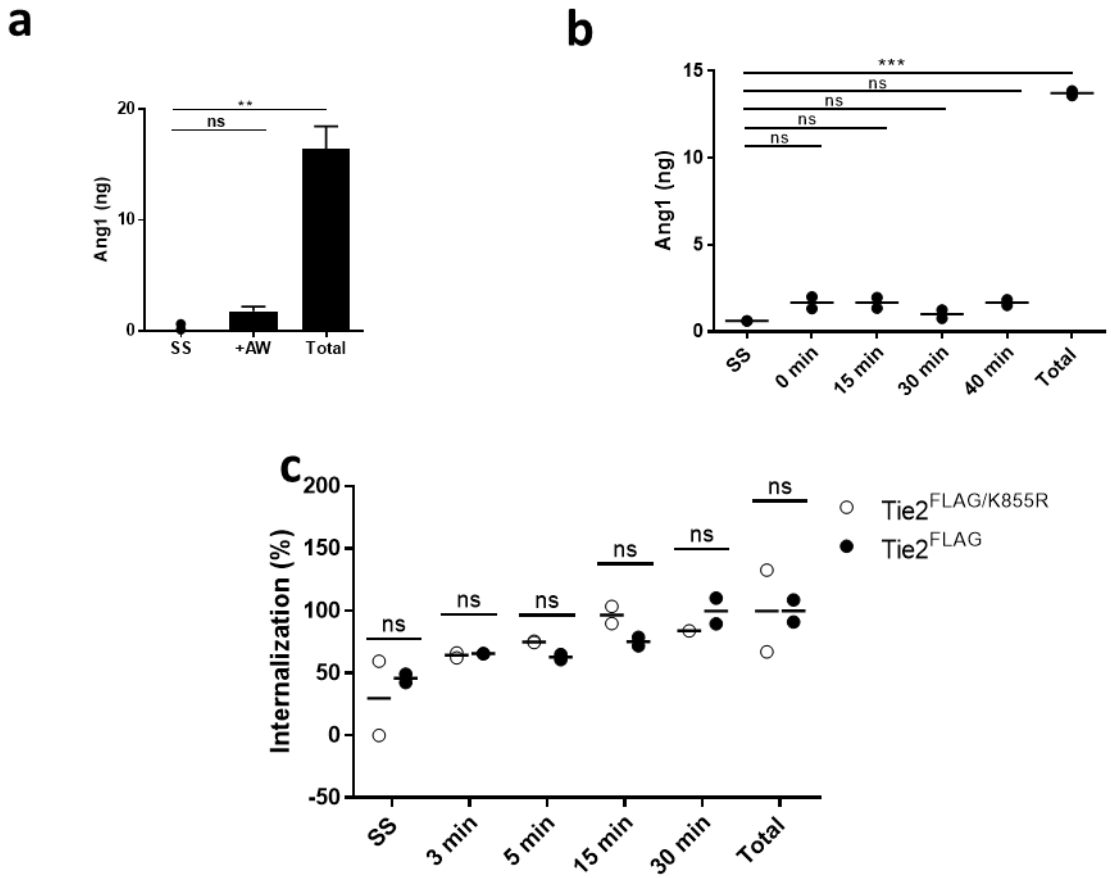

Figure 27. hrAng1^{His} is not internalized by HeLa T-REx Tie2^{FLAG} cells according to the optimized Ang1 sandwich ELISA. (a) The acid washes used in the protocol effectively remove most of the cell-associated hrAng1^{His}. HeLa T-REx Tie2^{FLAG} cells pulsed for 8 h with 1 µg/ml of doxycycline were serum starved for 2h and incubated with hrAng1^{His} at 4°C for 30 min. Then cells were then acid stripped (**+AW**) or left untreated (**Total**) on ice for the same amount of time. The amount of Ang1 was quantitated using a standard 4PL regression and is expressed as total ng per sample. Mean ± SEM, n=2 independent experiments in case of SS cells and n=3 for AW and Total conditions. Only the "Total" condition was found statistically different than the control condition "SS" (Dunnett's multiple comparision for ANOVA, α = 0.05) **(b)** HeLa T-REx Tie2^{FLAG} cells pulsed for 6h with 1 µg/ml of doxycycline were serum starved for 2 h and pre-incubated for 30 min on ice with hrAng1^{His}. Media in the 15, 30 and 40 min time-point samples was exchanged by Serum-free media without Ang1 and incubated at 37°C for the indicated times (**15, 30, 40**) or left on ice (**0 min**). Cell surface ligand was acid stripped in cold conditions from all samples except from the **Total** control. Graph shows results from a single pilot experiment, duplicates and mean in a single experiment are shown. Dunnett's multiple comparisions test for *one-way* ANOVA, α = 0.05 **(c)** HeLa T-REx Tie2^{FLAG} and Tie2$^{K855R/FLAG}$ pulsed for 6h with 1 µg/ml of doxycycline were serum starved for 2 h and incubated with hrAng1^{His} at 37°C for the indicated times. Cell surface Ang1 was acid stripped in cold conditions from all samples except from the **Total** control, which nonetheless was accidentally washed once with acidic buffer. The amount of Ang1 detected is represented as the % of the Total controls. Graph shows results from a single pilot experiment, duplicates and mean in a single experiment are shown. Differences between cell lines were not found statistically significant (*two-way* ANOVA, Dunnett's multiple comparision, α = 0.05) **(a-c) SS** refers to serum starved cells unexposed to hrAng1^{His}. The amount of Ang1 in each sample was calculated using the 4PL non-linear regression fit of a hrAng1 standard curve independent for each experiment.

Former members of our lab had demonstrated that Ang1 is internalized by HUVEC cells in the conditions used (data not shown). Furthermore, I had also seen that HeLa T-REx Tie2^{FLAG} cells internalize Ang1 in the same conditions (**Figure *17*** and **Figure *18***, section 0). Therefore, I believed that most probably the apparent non-internalization of Ang1 by cells was an artefactual product of the ELISA assay.

Evaluation of the quality of the ELISA assay

The quality of an assay depends on errors of measuring that can have an accidental or a systematic origin. Systematic errors affect the accuracy of a system so the quality of an ELISA needs to be determined to ensure that the system is producing reliable data (R&D Systems 2017). Two possible ways of evaluating the accuracy of an ELISA are calculating the linearity of a dilution and performing a spike and recovery test.

The linearity of an ELISA assay is defined as the ability of the assay to precisely interpolate the value of an analyte in a sample using a dilution of the sample. For instance, if I diluted a sample by a 1:4 factor I would expect to obtain a concentration of analyte similar to the one in the neat sample once the dilution factor is corrected. The percentage of recovery for the linearity of an assay is calculated as the % of the observed value from the expected valued divided by the dilution factor. Optimally, the recovery of linearity should be around 90-110% and values outside the 80-120% are considered bad recovery values for an ELISA assay (R&D Systems 2017). I had routinely evaluated the linearity of the experiments by diluting in EBB the lysates of the Total controls and then quantitating the amount of Ang1 in the same plate as the rest of samples. As seen in **Figure *28***, the average recoveries of the dilutions were outside the acceptance range for an ELISA. On a couple of occasions the linearity of the experiments were within an acceptable range of recovery but I could not point to any clear cause for it.

When the dilution of a sample leads to the quantitation of higher values of those found for the neat samples it is considered an indication that there is a factor in the sample matrix that is interfering with the readings of the target molecule. Since I had been able

to fit the standard curve into both a linear or non-linear 4PL regressions I suspected that some component of the biological sample rather than in the sample diluent was interfering with the measure of Ang1. In order to confirm that the biological sample contained an interferent of the assay I performed a Spike and Recovery assay, which consists in diluting a "spike" or known amount of standard analyte in a biological sample or sample diluent to see if it yields similar changes in the quantitation of analyte or not. The Recovery of a Spike assay is calculated as the percentage of the observed difference in the spiked sample from the expected value observed in the sample diluent. As seen in **Figure *28***, the standard diluted in biological sample resulted in much lower levels of quantitated Ang1 and the average recovery of the spike was 39%. I also tested in two occasions whether diluting the cell sample in blocking buffer would improve the recovery and, consistently with the recovery of the linearity, I found that the recovery of the spike was higher with higher dilutions. Still, the average recovery in a 1:6 dilution of the cell matrix was only a 75%. Overall, the recovery values obtained from either diluting or spiking the sample matrix indicated us that a component of the solubilised cells was interfering with the detection of the Ang1. Hence the amount of Ang1 in cell samples was being underestimated when being quantitated with the ELISA.

One way of decreasing the interference caused by a component of biological sample is diluting samples and estimating the content of analyte from the dilutions. However, since the recoveries were low even when the biological sample was diluted by a 1:6 factor (**Figure *28***) I decided that it would be a waste of resources to try and quantitate the amount of internalized Ang1 using this particular ELISA assay.

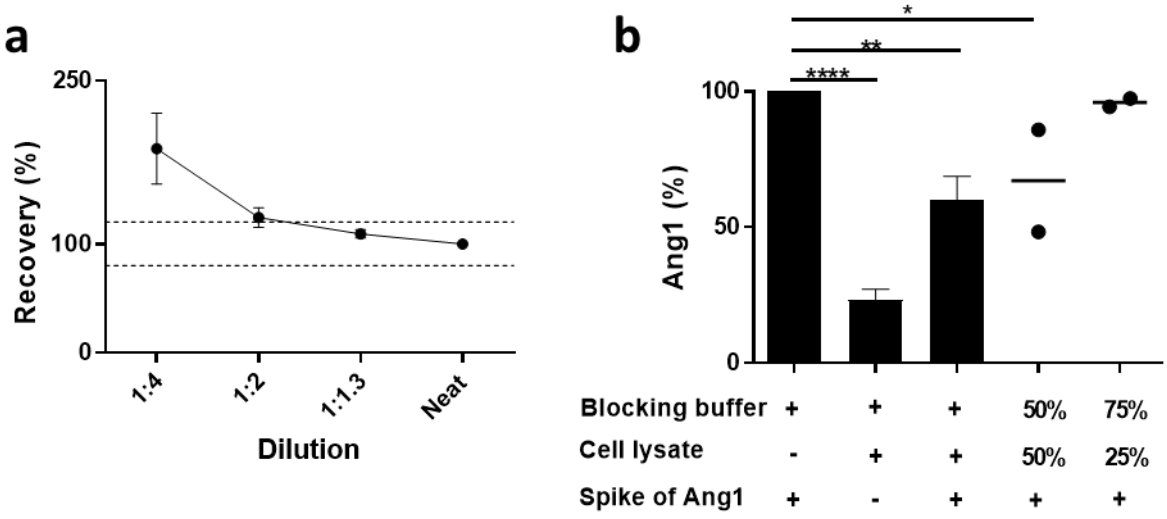

Figure 28. Quantitation of hrAng1^{His} using the optimized sandwich ELISA is interfered by a component of cell lysates (a) Linearity of the ELISA assay showed that there was an interferent in the sample matrix. In different experiments lysates of cells exposed to hrAng1^{His} were diluted in blocking buffer at the indicated dilution factors and the amount of hrAng1^{His} in each was quantitated using the optimized sandwich ELISA for Ang1. The recovery of hrAng1^{His} was calculated as the percentage of measured Ang1 in each dilution to the measured Ang1 in the Neat sample divided by each dilution factor (Mean ± SEM, n=7). Dotted lines indicate the limits for recovery values to be considered acceptable for an ELISA assay, according to manufacturers. **(b)** Spike and recovery assay showed that the sample matrix contained an interferent of biological origin. Blocking buffer or cell lysate were "spiked" with the same amount of standard hrAng1^{His} (total of 12 ng) or left untreated and then the levels of hrAng1^{His} were determined using the optimized ELISA. Also, in two occasions the cell lysate was diluted 1:2 and 1:4 with BB before adding the spike of Ang1, which improved the recovery. Bars represent the percentage of quantitated hrAng1^{His} to the standard hrAng1^{His} in Blocking buffer (Mean ± SEM, n=5 for bars and n=2 for dots. Statistically significant differences were inferred with *one-way* ANOVA and Dunnett's multiple comparisons were done between each condition and the blocking buffer with spiked Ang1 (First column, 100% reference) (α = 0.05; * if $p < 0.05$; ** if $p < 0.01$; **** if $p < 0.0001$)

4.2 Optimization of a High Throughput Screen for measuring the internalization of Ang1 by cell immunofluorescence

Since I could observe that Ang1 was internalized in the HeLa T-REx cells expressing Tie2^{FLAG} but not in the HeLa T-REx Tie2$^{K855R/FLAG}$ by cell immunofluorescence staining, I decided to develop a quantitative assay based on cell imaging for measuring the internalization of Tie2. I planned to then use the assay to identify which proteins and pathways are involved in the endocytosis of Tie2 by knocking down specific proteins with small interference RNAs.

Developing a cell immunofluorescence assay for measuring the internalization of Ang1

I adapted the Ang1 immunofluorescence feeding assay to a 384-well plate format and using the facilities in the SRSF I tested whether it was possible to measure the Ang1 internalized by cells in a high throughput format.

HeLa T-REx Tie2^{wt} and Tie2^{K855R} were seeded in 384-well plates. Cells were exposed to doxycycline for different amounts of time and fed with Ang1 at different concentrations for 30 min at 37°C. Images were automatically acquired by the ImageXpress Microscope and analysed by the MetaXpress software using the pre-configured algorithm *Transfluor*, which is designed for the detection of Pits and Vesicles within cells. As seen in **Figure *29***c, Ang1 spots were only visible if cells had been exposed to doxycycline and this was also reflected in the quantification of the images (**Figure *29***d), indicating that the detection of Ang1 signal was dependent on the presence of Tie2. Feeding the cells with 100 ng/ml of Ang1 was insufficient to obtain a good immunofluorescent signal but 200 ng/ml gave a good and quantifiable signal (**Figure *29***e,f), hence the quantitation of Ang1 was also sensitive to the presence of Ang1. However, although it was appreciable in the images that Ang1 was not being internalized by the HeLa T-REx Tie2$^{K855R/FLAG}$ cells this was not reflected in the automated quantification (**Figure *29***a,b). Because Ang1 causes the oligomerization of Tie2 on the cell surface, and because the images are acquired from a single Z-section of cells, the immunofluorescence staining of non-internalized Ang1 appears as clusters of fluorescent signal around the nuclei or over the nuclei depending on weather the image is focused at a basal or apical plane of cells

respectively. At the same time, internalized Ang1 contained in intracellular endosomes presents a very similar parameter only distinguishable from the non-internalized Ang1 for being in peri-nuclear endosomal-like structures at the basal planes of cells. Hence, the similarity between the parameters of internalized and non-internalized Ang1 makes it really difficult to automatically and effectively distinguish between non-internalized and internalized Ang1. The fact that the Tie2$^{K855R/FLAG}$ expressing cells seemed to have more Ang1 could be explained by its higher levels of expression of Tie2 (**Figure *11*** and **Figure *15***) or/and because of an effect due to the non-internalized Ang1 being stuck at the plasma membrane of the cell. Overall, these results indicated that it was feasible to adapt the Ang1 feeding and immunofluorescence protocol to a high throughput format. Furthermore, the automated quantitation of Ang1 signal was sensitive to the presence of both Tie2 and Ang1 in the cells, although it was obvious that the protocol required improvements in order to distinguish between internalized and non-internalized Ang1.

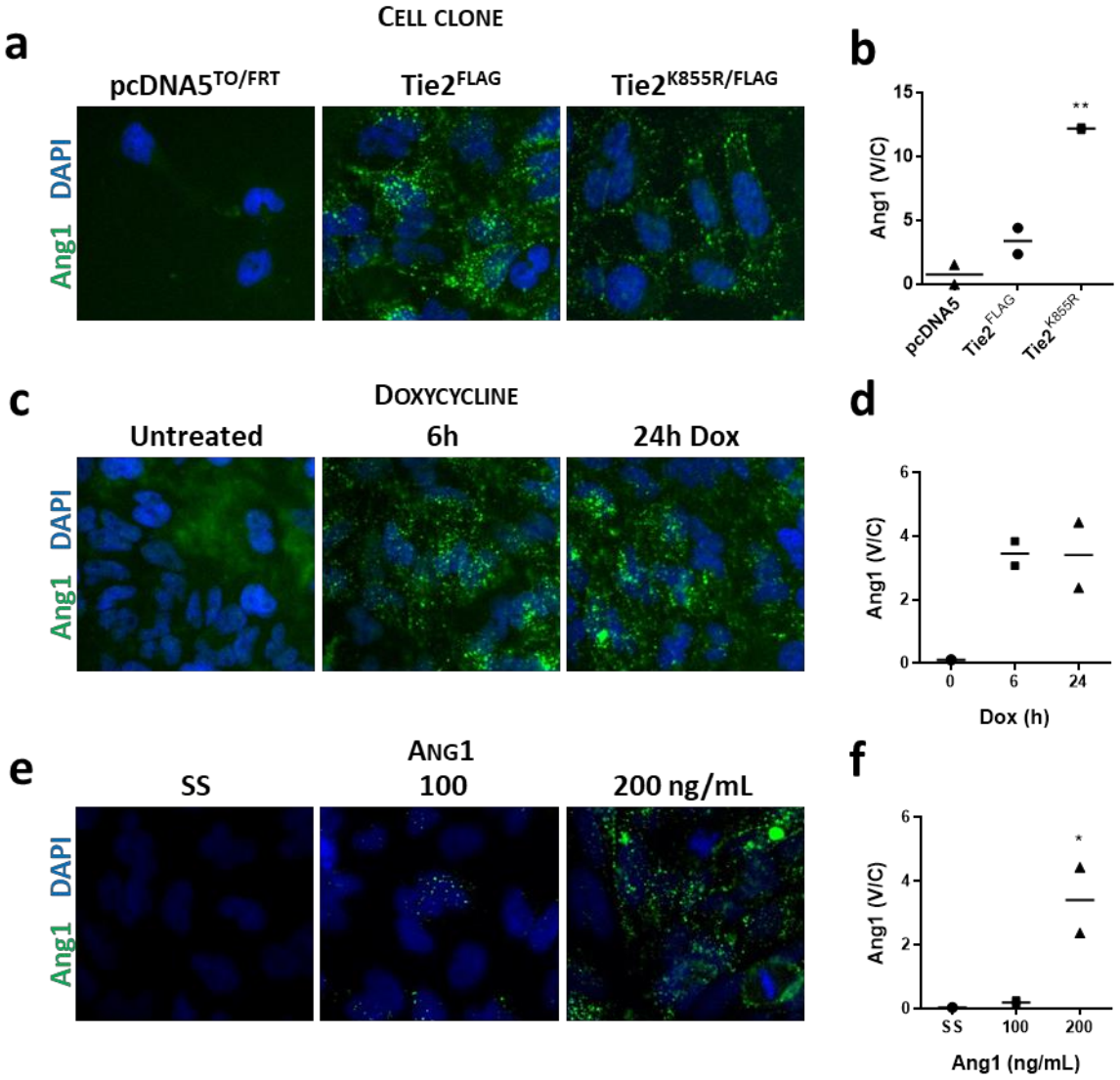

Figure 29. The amount of hrAng1^{His} associated to cells can be automatically quantified by immunofluorescence in a high throughput format yet cannot distinguish between internalized and non-internalized ligand. Control HeLa T-REx (pcDNA5), HeLa T-REx Tie2^{FLAG} and Tie2$^{K855R/FLAG}$ cells **(a,b)** seeded in a 384 well plate were exposed for 0, 6 or 24h to doxycycline **(c,d)**, incubated with 0, 100 or 200 ng/ml of hrAng1^{His} for 30 min at 37˚C **(e,f)** and stained for hrAng1^{His} and nuclei. Images were acquired using the ImageXpress microscope **(a, c, e)** and the amount of cells and vesicles of Ang1 quantified using the Transfluor algorithm of the MetaXpress image analysis software. Quantifications are represented in **(b, d, f)** where each point represents the average vesicles of a well from a single experiment (n=1). Averages calculated for each well were obtained from 6 images of each well. Dunnet's multiple comparisions for *one-way* ANOVA, $\alpha = 0.05$; * if $p < 0.05$; ** if $p < 0.01$).

To ensure that only the internalized Ang1 was quantified, a series of washes with acidic buffer were introduced in the protocol. Briefly, after the incubation with Ang1 at 37°C cells are quickly washed with ice-cold PBS and then incubated 3 times with acid wash

buffer (pH3) on ice for 5 minutes before fixation (Semerdjieva et al. 2008).The volume of acidic buffer used in the washes was 45µL, which was enough to change the pH in the wells of a 384-well plate filled with 10µL of PBS, representing the average residual volume left on the wells after an aspiration (**Figure *30***a). To test for the effectiveness of the acid wash of cell surface Ang1 I incubated cells with ice-cold media containing Ang1 for 30 min and then cells were either acid washed 3 times or left untreated before fixation. The application of the acid wash step on cells held on ice lead to the complete removal of ligand from the surface of cells, as compared to the cells that were not stripped of Ang1 (**Figure *30***b), indicating that the acid stripping was highly effective. Therefore, in this way I ensured that by acid stripping cells incubated with Ang1 in warm conditions only the internalized Ang1 would remain (**Figure *30***c). Interestingly, the application of the acid wash also reduced the amount of Ang1 background signal (**Figure *30***c). Different members of our group had previously and repeatedly observed this intense fluorescent signal on the cell support when performing cell immunofluorescence staining of Ang1 regardless of using blocking agents before the incubation of Ang1. Hence, that the acid wash reduces this background signal indicates that it is not non-specific staining of the surface but Ang1 that is somehow bound to the extracellular matrix deposited on cell culture surfaces. Overall, this results confirm that the introduction of the acid wash step would allow the automatic quantitation of the internalized Ang1 in HeLa T-REx Tie2^{FLAG} cells.

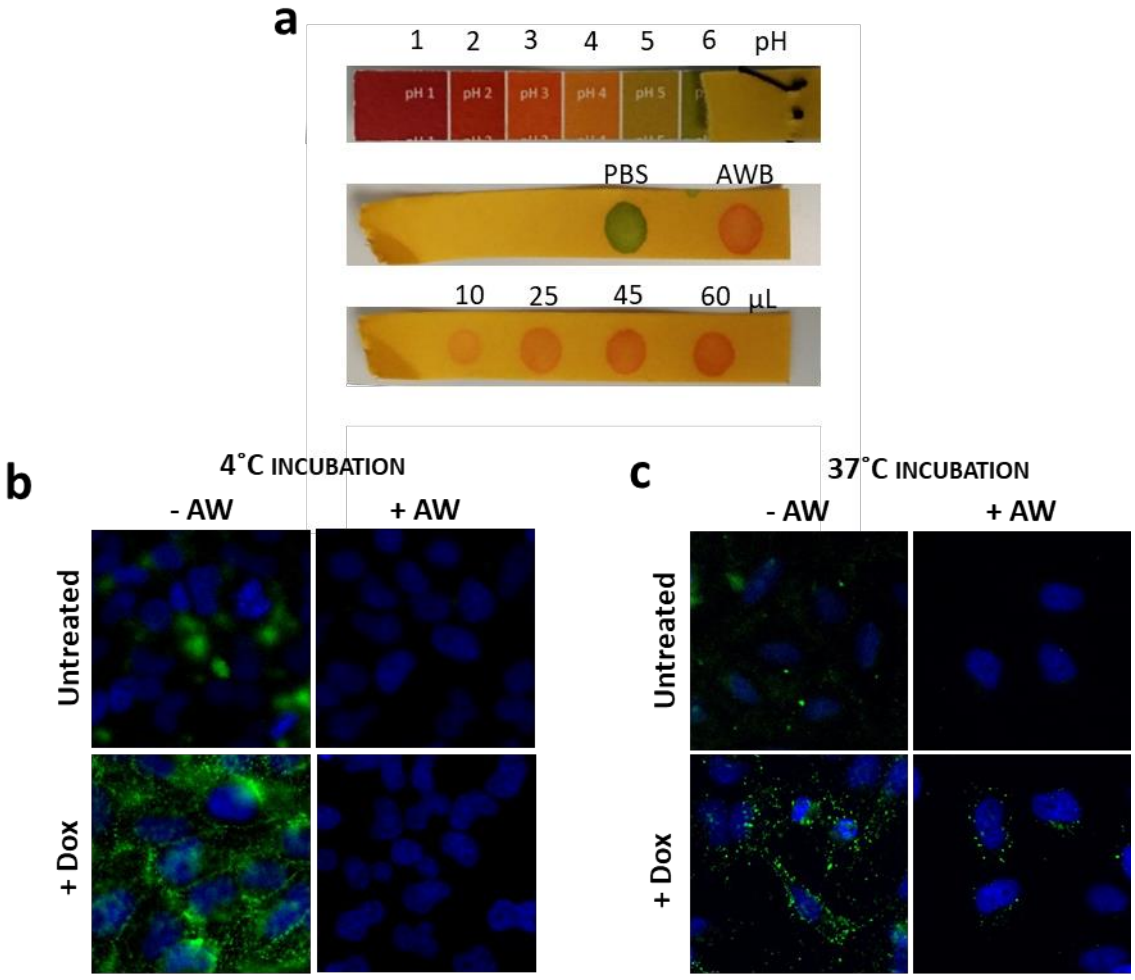

Figure 30. Acid stripping of cell surface ligand allows for the immunofluorescence analysis of the internalized hrAng1^{His}. (a) Different volumes of acid washed (AW) buffer were tested to ensure that the pH was being reduced in the wells of the 384-well plates when using automatic liquid handling devices, which leave a residual liquid volume of approximate 10µL on average. Therefore, 10 µL or PBS were mixed with 10, 25, 45 or 60 µL of Acid wash buffer and the resulting pH was measured using a pH measuring strip. Image shows the model pH colour scale of the pH testing strips (top), pH measured for PBS and AW buffer (middle) and resulting pH when adding the indicated volumes of AW buffer to 10 µL of PBS (bottom). In the final protocol, 45 µL of acid wash buffer were loaded to wells for each 5 min incubation time **(b)** HeLa Tie2^{FLAG} cells cultured in 384-well plate and pulsed or not for 6h with 1 µg/ml of doxycycline (**+Dox** or **–Dox**) were with 200 ng/mL hrAng1^{His} on ice for 30 min and left untreated (**-AW**) or acid stripped with AW buffer (**+AW**) for the same time before being fixed for immunofluorescence analysis of hrAng1^{His}. **(c)** As in **(b)** yet cells were incubated with 200 ng/mL hrAng1^{His} at 37 ˚C to allow internalization of hrAng1^{His}. Images were acquired using the ImageXpress microscope and are representative of at least 6 images from duplicate wells of a single experiment (n=1)

Automatically quantifying internalized Ang1

As well as optimizing the internalization assay, I had to develop an image analysis protocol for the quantification of the Ang1 signal in the images. Optimizing a HTS is a

complex task due to the amount of images obtained in each experiment and due to the high amount of data generated. Comparing different conditions or analysis settings for an HT assay can be difficult and overwhelming so various mathematical indexes have been developed that ultimately determine the quality of an assay and that can be used during the development of such assay (Birmingham et al. 2009). In our case, I decided to use the Z' factor for its ease of calculation and interpretation. It is also the most widely quality factor used for screeners.

$$\boldsymbol{Z'factor = 1 - (3\sigma_{nc} + 3\sigma_{pc})/\left|\mu_{nc} - \mu_{pc}\right|}$$

Equation 1. Z' factor can be used as an indicator of the quality of an assay. Given a certain parameter and the population distribution of a negative control (**nc**) and a positive control (**pc**) of this particular parameter, the Z' factor is calculated as the difference to 1 of the sum of 3 standard deviations of each population divided by the absolute difference between the means of the pc and nc.

Given the positive and negative controls for an assay, the Z' factor is calculated using both the difference between the means of positive and negative controls and the variability of the populations of each control. It is used to determine the quality of an assay and it ultimately represents how confident I can be that a real hit could be distinguished from a negative control. At the same time, the Z' factor can be used during the optimization of a HTS to see the effect over an assay of variations in the protocol or in the data analysis. Given the mathematical formula of the Z' factor, its value can range from 1 to -∞. Conventionally, a Z' factor between 0.5 and 1 defines a high quality HTS, a 0 to 0.5 identifies a weak HTS and a Z' value below 0 is considered unacceptable for screening. However, I decided not to be tied by such classification since the Z' factor was originally developed for describing the quality of small molecules screens, which can achieve greater quantifiable changes. Also, repeats and replicates can be added in order to identify hits using screens with low signal-to-noise ratio (Birmingham et al. 2009). Still, since the Z' factor is easy to calculate and interpret I used it as a tool to simplify the optimization of the assay protocol and data analysis, as it would allow us to compare the effects on the signal to noise ratio of any changes applied to the protocols or analysis of the data.

Accompanying the ImageXpress Microscope in the SRSF there is the MetaXpress image analysis software that is designed for the analysis of fluorescence images obtained from high throughput format assays. The MetaXpress is easy to use and it contains different pre-designed algorithms for the segmentation of fluorescent signal in different ways. For instance, the *Transfluor* algorithm can identify fluorescently labelled nuclei and vesicles to quantify the internalization of a fluorescent compound or ligand. Furthermore, the MetaXpress software contains a user-friendly custom module editor for the creation of more complex algorithms.

In order to reduce the complexity of the HTS data analysis I decided to select a single parameter within the Transfluor segmentation output. The Transfluor image analysis algorithm from the MetaXpress software identifies the nuclei based on the DAPI staining and segments the Ang1 fluorescence in "Pits" and "Vesicles" depending on a custom non-overlapping determined size and intensity signal above background. Pits size was set to detect bright particles from 0.09 µm to 0.1 µm, so that particles were big enough to be distinguished from background; while vesicles were set at 0.1 to 5 µm. The range of the vesicles size was configured to up to 5 µm so that antibody non-specific staining in "blob" shapes would be counted as few vesicles instead of hundreds or thousands. The intensity cut-off above background was determined for every experiment by testing different settings on various images from each independent experiment. Using the conditions "+doxycycline" and "-doxyxycline" as negative and positive controls respectively I began by selecting a small group of Transfluor parameters that I found to be sensible to the presence of Tie2 in the cells. The selected parameters were pit and vesicle count per cell, area per cell and average intensity.

In order to easily compare them I calculated the Z' factor using the well-average value of the "-Dox" and "+Dox" conditions. Each experiment had at least 8 wells for each condition, including more than 300 cells from at least 9 images per well. The Z' values calculated for each Transfluor parameter and in each experiment are represented in **Figure *31***a. Although the differences between conditions were appreciable by eye in the images (**Figure *30***c), the Z' values were mostly found below 0. This can be explained

because the negative controls presented a wide variability of the values obtained for each analysis parameter and because the difference between the means of positive and negative controls was not enough to overcome this variability. The Z' value did not appear to vary greatly between most of the parameters but it seemed that determining the Ang1 internalization using parameters based on the intensity and area of the fluorescence was less robust than counting the Ang1-containing Pits and Vesicles (**Figure *31***).

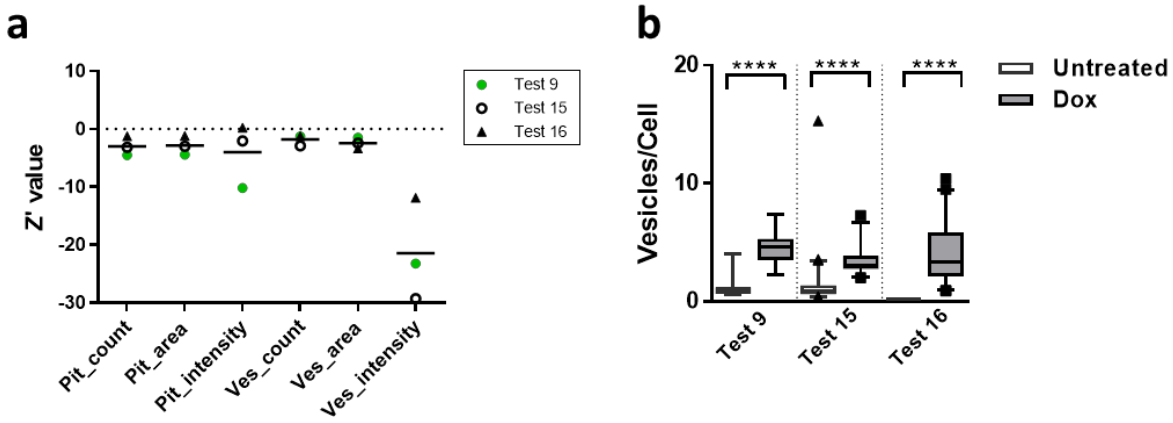

Figure 31. The automatic segmentation protocol for the analysis of immunofluorescence images acquired with the ImageXpress Microscope was optimized using the MetaXpress Image analysis software. The images of 3 different optimization experiments with HeLa T-REx Tie2^{FLAG} cells were used to study different ways to analyse the internalization of hrAng1^{His} by immunofluorescence. **(a)** The amount of internalized hrAng1^{His} in HeLa T-REx Tie2^{FLAG} cells exposed or not overnight to 1 µg/mL of doxycycline was quantitated using the Transfluor segmentation protocol from the MetaXpress microscope, which gave different quantitative parameters of the hrAng1 fluorescence, indicated in the graph. Using the results obtained from cells un-exposed to doxycycline as positive controls I calculated the Z'value of a selection of parameters, which are shown in the graph. I considered the counting of vesicles or pits per cell the best parameter to determine the differences between the controls, so I re-configured the Transfluor for the quantitation of both pits and vesicles as "Vesicles". The resulting quantitation is graphed in **(b)** for each different optimisation experiment, boxes include the 25th and 75th percentile of at least 8 replicates, whiskers indicate the 5th and 95th percentile. Mann-Whitney test, $\alpha = 0.05$ (**** indicates $p < 0.0001$).

Based on this comparison between the different parameters from the *Transfluor* algorithm I decided to quantify the internalization of Ang1 using the amount Pits and Vesicles per cell together, meaning that I would configure the image analysis algorithms to quantitate all small fluorescent events in a single category, defined as "Vesicles". The

Transfluor image algorithm was then re-configured to detect as “Vesicles” any events 0.9 to up to 5 µm size were quantitated. The means and standard deviations of the amount of vesicles per cell used to calculate the Z’value from this three experiments are represented in **Figure *31***b.

In order to further implement the image analysis I optimized a new algorithm for quantitating the amount of vesicles per cell using the custom module editor from MetaXpress. The new segmentation protocol was called CME1 and included the following implementations:

- Not accounting for any big debris stained with DAPI or Ang1 that could be accounted as multiple nuclei or vesicles.
- Not accounting for edging cells that would decrease the average vesicle/cell value of an image
- Only including those Ang1 vesicle-like fluorescent signal that is within a certain range from a nuclei so that any small cell debris stained with Ang1 are not included as vesicles.

As seen in **Figure *32***, although there was a high variation in the amount of Ang1 internalized by cells, there was a clear difference of quantified vesicles per cell depending on whether the HeLa T-REx Tie2 cells were exposed or not to doxycycline. Therefore, I decided to use the CME1 segmentation protocol for any further image analysis (Detailed in methods).

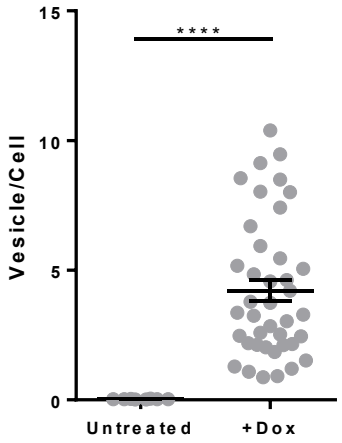

Figure 32. The CME1 segmentation protocol was designed for a more specific quantitation of the internalized hrAng1^{His} by cells. HeLa T-REx Tie2^{FLAG} cells grown in a 384-well plate were exposed to 1 µg/mL of doxycycline overnight or left untreated and then incubated with 200 ng/mL hrAng1^{His} at 37˚C for 30 min to allow the internalization of the ligand. Cell surface ligand was acid stripped on ice for the analysis of the internalized hrAng1^{His} by cell immunofluorescence. Several Images were automatically acquired for each well using the MetaXpress microscope and the amount of hrAng1^{His} fluorescence was quantitated using the developed CME1 segmentation protocol in the MetaXpress image analysis software. The CME1 was designed to quantitate only green fluorescent particles of small size that are within a certain distance from a DAPI-stained nuclei. Each replicate value of vesicles/cell was averaged from 9 images acquired within each well (or replicate). Each dot indicates one replicate within a single experiment (n=1) and bars show Mean ± SD (8 and 50 replicates for Untreated and +Dox respectively). Welch's t-test, $\alpha = 0.05$ (**** indicates $p < 0.0001$).

Inhibition of endocytosis by transfection of specific siRNAs

The knock-down of a particular protein can be achieved by transfecting small interfering RNA (siRNA) to cells that will target the mRNA of a target protein for degradation. siRNA are double-stranded RNA specifically designed to be complementary for the mRNA of a targeted protein (Elbashir et al. 2001). Transfected siRNA are processed by the ribonuclease Dicer into single stranded RNA and the sense strand is then delivered to the RNA-induced silencing complex (RISC), which will promote the degradation for the endogenous mRNA that has a complementary sequence to the siRNA. Since siRNA are ultimately degraded the effect of a transfection is temporary and can be observed for about 2 to 4 days after transfection (Scherr & Eder 2007; Aronin 2006).

For the transfection of siRNAs into the HeLa T-REx Tie2 cells I decided to use the protocol provided by the SRSF. The siRNA was introduced in the cells using a lipid based transfection reagent (Dharmafect 1) in a protocol that is known as reverse transfection.

Reverse transfection of siRNA is achieved by transfecting cells in suspension rather than adding the transfection complex of siRNA and transfection reagent on attached cells (known as forward transfection). Reverse transfection has been seen to give better results than forward transfection and knock-downs can be achieved using much lower amounts of siRNA. Using lower amounts of transfection reagent and siRNA obviously reduces the economic expenditure on assays and also decreases the occurrence of non-specific effects, also known as "off-target" effects. Off-target effects are any molecular changes in the cell that are not caused by the knock-down of the target protein on cells and two possible causes are a cell response to the lipid reagent and activation of the interferon in response to foreign siRNA (Sledz et al. 2003; Lin et al. 2005; Aronin 2006). As seen in **Figure *33***a, the common protocol used in the SRSF was successful in delivering fluorescently labelled scrambled siRNA into cells and I did not observe any dramatic effect on cell confluency (not shown).

Although it was clear that the siRNA was being transfected into the cells, I wanted to evaluate whether the transfection efficiency in these conditions was enough to affect the endocytosis of a ligand. With this in mind, I transfected HeLa T-REx Tie2^{FLAG} cells with siGENOME siRNAs targeting Clathrin Heavy Chain (CHC, CLTC gene) and then quantified the internalization of fluorescently labelled transferrin (TF) as a canonical marker of Clathrin Mediated Endocytosis (CME). At the same time, I also measured the internalization of CTxB, which is mainly internalized by CIE pathways (Mayor & Pagano 2007) (**Figure *33***b and c). Non-targeting siRNA #5 was used as expected negative control to account for any non-specific effect on the internalization induced by the transfection of siRNA itself. Polo Like Kinase 1 (PLK1) is a kinase involved in cell cycle progression that was used to account for the effectiveness of the transfection: since it causes the arrest of cell cycle those wells with PLK1 siRNA should have lower cell densities than others. As expected, the transfection of CLTC siRNA compromised the internalization of TF but not of CTxB: the counts of CTxB vesicles per cell were very similar between the non-transfected cells and the CLTC siRNA, but were reduced by 83% for TF (**Figure *33***c). The non-targeting siRNA #5 seemed to have a slight effect on TF but not on CTxB internalization. Although the control siRNAs are supposed to be non-targeting siRNA it

is common to find that they do show an effect in some assays and not in others. As expected, knock-down of PLK1 decreased the amount of cells observed in the images. Surprisingly, the PLK1 siRNA seemed to have opposite effects on the compounds: increasing the internalized TF and decreasing internalization of CTxB. Although I did not expect this effect, it was recently published that PLK1 mediates the internalization of certain proteins in a cell-cycle dependent manner so it is not completely unreasonable that it could somehow affect TF and CTxB endocytosis in the HeLa cells (Shrestha et al. 2015). However, since the results were obtained from a single 3-replicate experiment small differences are expected due to simple statistical variation. The non-transfected control including only transfected reagent appeared to have a clear effect on cell survival as seen from the images (**Figure *33***b) and cell count per image (data not shown). Nonetheless, the clear and drastic effect of the CLTC-siRNA on the internalization of TF confirmed the reliability of the assay and the quality of the siRNA transfection.

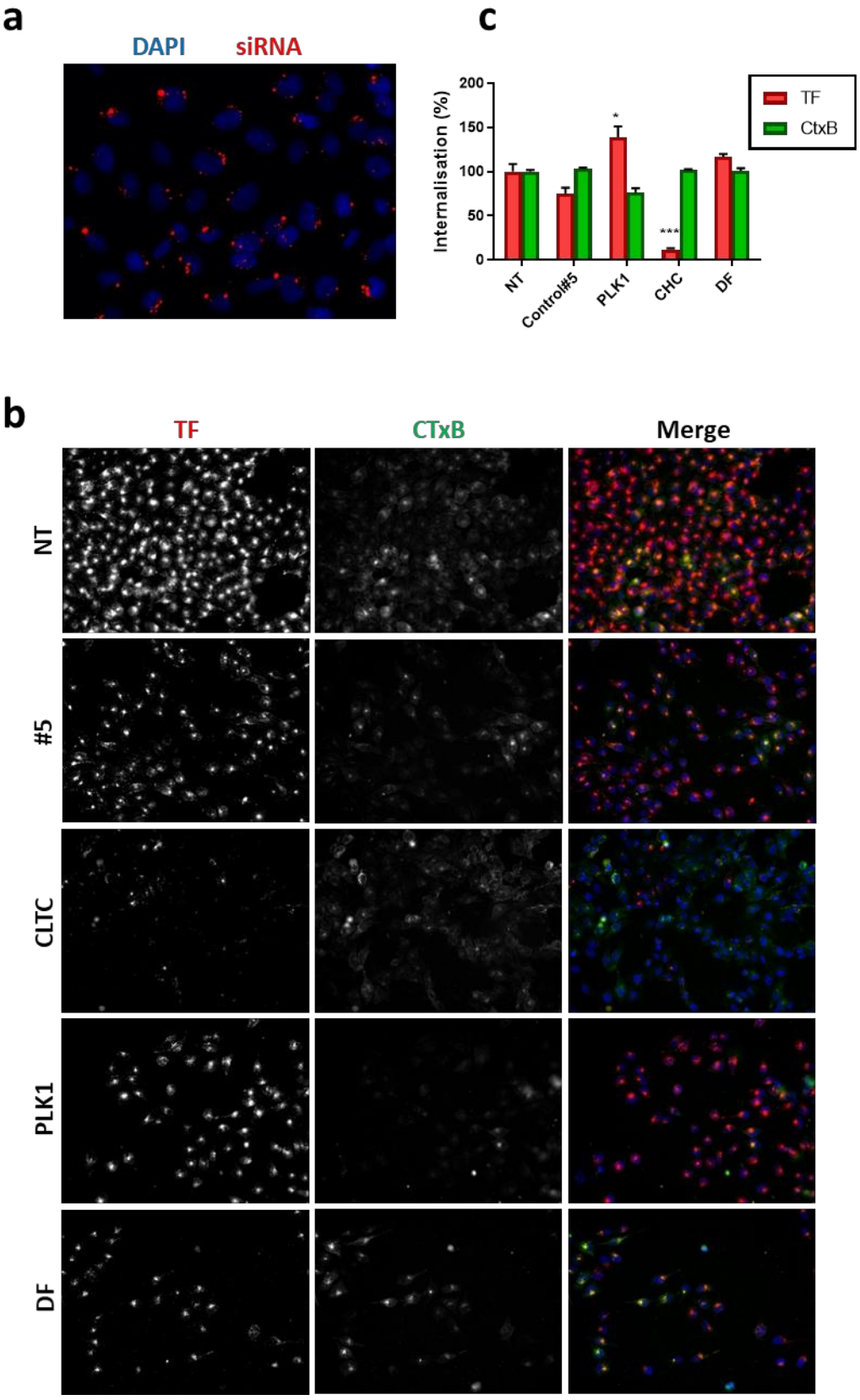
a
DAPI
siRNA
c
Internalisation (%)
200
150
100
50
0
TF
CtxB
*
***
NT
Control#5
PLK1
CHC
DF
b
TF
CTxB
Merge
NT
#5
CLTC
PLK1
DF

Figure 33. The effect of specific siRNAs on the endocytosis of TF and CTxB can be quantified using the endocytic assay. (a) Fluorescent siGLO non-targeting siRNA transfected in HeLa T-REx Tie2^{FLAG} cells unexposed to doxyxycline was visualized in peri-nuclear intracellular compartments 72h post-transfection. **(b,c)** HeLa T-REx cells unexposed to doxycycline were transfected with scrambled #5, Clathrin Heavy Chain (CLTC), Polo Like Kinase targeting siRNAs or left untrasfected in the presence of dharmafect (**DF**) or media (non-transfected, **NT**). After 72h, cells were serum starved and incubated with serum free media containing 5 µg /mL transferrin (**TF**), a canonical marker of clathrin-mediated endocytosis (CME), and 5 µg/mL of Cholera Toxin subunit B (**CTxB**), which can be used as a marker of clathrin-independent endocytosis (CIM) internalized via Clathrin independent pathways. Transfection of CLTC inhibited the internalization of TF but not CTxB, as seen in the images acquired **(b)** and in the quantitation of vesicles/cell using the CME1 segmentation algorithm **(c)**. In **(c)** bars were coloured in red for Tfn and in green for CTxB. Several images were acquired for each repeat and the averaged amount of vesicles/cell for each repeat were normalized using the values in the Non-transfected condition. Bars indicate mean ± SEM of 3 technical repeats. Statistically significant differences to the "NT" condition are indicated. Dunnett's multiple comparisions test for *two-way* ANOVA, $\alpha = 0.05$ (* if $p < 0.05$, *** if $p < 0.001$).

A further pilot screen was performed to test 5 non-targeting siRNAs (Control#1 to #5), and siRNA for Tie2 (TEK), Dynamin2 (DNM2), the subunit 2 of actin related protein complex (ARPC2) and PLK1 on the internalization of Ang1 (**Figure *34***). The scrambled siRNAs #2-4 appeared to have an effect on the endocytosis of Tie2 compared to the non-transfected control, but non-targeting controls #1 and #5 gave similar values of vesicles/cell compared to the un-transfected cells. The knockdowns of both Tie2 and ARPC2 gave a clear inhibition of the internalization of Tie2. In the case of DNM2, it was appreciable in some of the images that DNM2 siRNA was inhibiting the internalization of Ang1 (**Figure *34***b), yet the effect was variable within different images (data not shown) and the overall quantitation of vesicles per cell was not far from the non-transfected cells (**Figure *34***c), I guessed that maybe with a higher sample acquisition (more images per well) I would have got a better quantitation result. Both the PLK1 siRNA and the Dharmafect-only control seriously affected cell viability and wells only contained few cells with round bright nucleus, which indicates that cells were apoptotic cells. I believe this was due to an improvement in the transfection efficiency, as for this experiment I transfected 25% fewer cells than for the experiment in **Figure *33***. Nonetheless, this result meant that when screening siRNA I should be aware of ensuring that low internalization of Ang1 was not due to the presence of apoptotic cells induced by the transfected siRNA. The Z'-factor calculated between the positive control TEK and the negative controls are summarized in **Figure *34***c. Since Control#1 and #5 had mean vesicle per cell values close

to the non-transfected cells and also had Z' factors relatively high I decided to use them as the standard non-targeting siRNA controls in the library. Overall, these experiments indicated that the assay was capable of identifying differences in the internalization of Ang1, although the low Z'-factors indicated that higher sample acquisition and multiple repeats were necessary for clearly identifying hits.

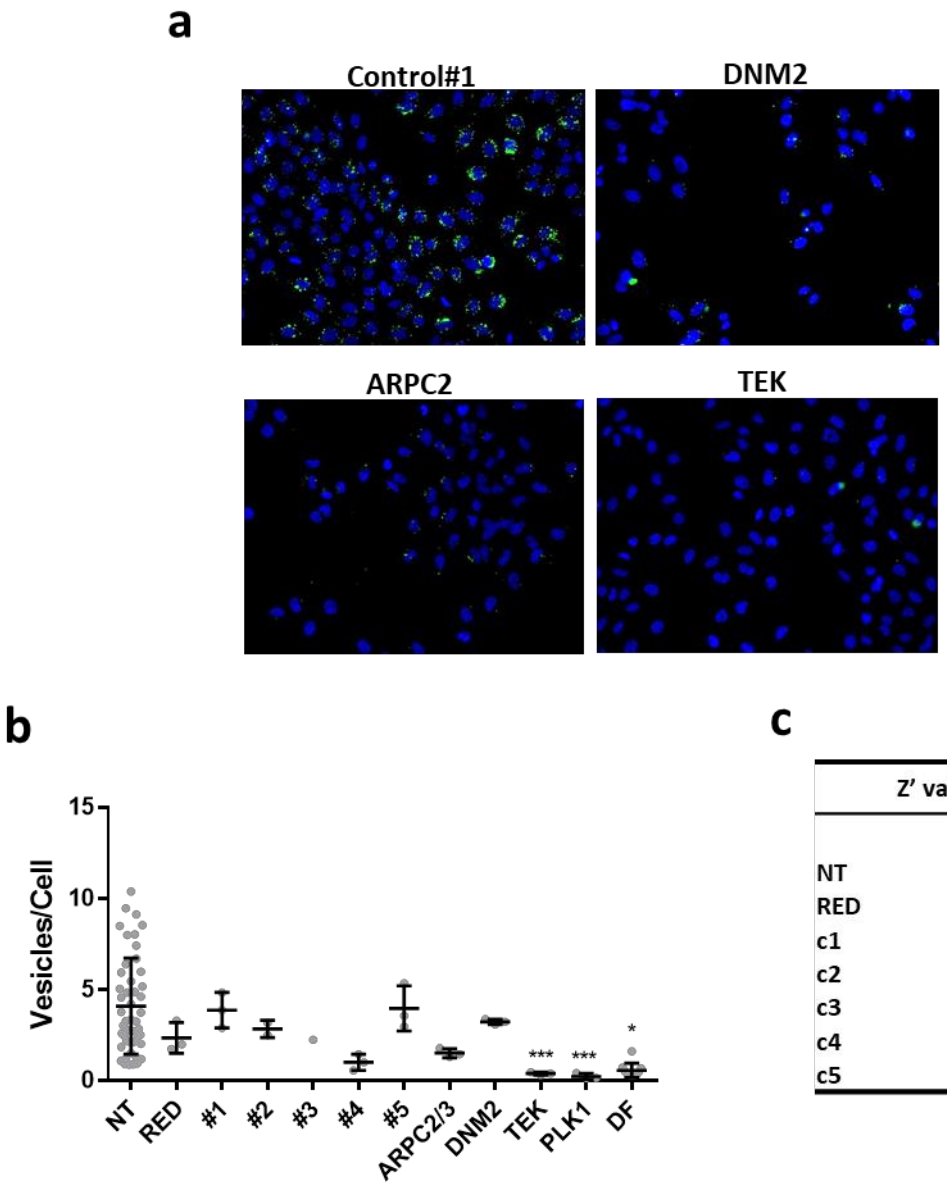

c

Z' value	
	TEK
NT	-0,54228
RED	-0,3264
c1	0,127798
c2	0,355593
c3	nr
c4	-0,21539
c5	-0,06664

Figure 34. The effect of specific siRNAs on the endocytosis of hrAng1^{His} can be quantified using the high throughput format endocytic assay. Cells were transfected with scrambled #1-5, siGLO siRNA (RED), PLK1, Actin Related Protein Complex subunit 2 (ARPC2), Dynamin2 (DNM2) or Tie2 (TEK) or left un-transfected with or without Dharmafect (NT and DF correspondently). Cells were exposed to 1 µg/mL doxyxycline overnight at 2 days post-transfection and serum starved at 3 days post-transfection. Serum starved cells

were incubated with hrAng1^{His} for 45 min. After cold acid stripping cells were fixed for immunofluorescence staining of hrAng1^{His} and nuclei stained with DAPI. Several images were automatically acquired for each repeat **(a)** and the amount of internalized hrAng1^{His} was quantitated as vesicles per cell using the CME1 fluorescence segmentation algorithm **(b)**. Graph shows Mean ± SEM of three technical repeats for each transfection. Effect of each transfection was compared to NT. Statistically significant differences are indicated. Dunnet's multiple comparisons for *one-way* ANOVA, $\alpha = 0.05$ (*** if $p < 0.001$. **(c)** Z'values were calculated between all the negative controls and TEK siRNA as a positive control. Only one well was transfected with siRNA #3 hence Z' value was not calculated (no-replicates, **nr**)

CHAPTER 5

siRNA screening on the internalization of Ang1/Tie2 complex

5.1 Primary Screen

After I had optimized a HTS assay to quantify the amount of internalized Ang1 by Tie2 expressing cells I decided to carry out a targeted siRNA screen on a small size customized library including a commercially available library from Dharmacon (Membrane trafficking) and a selection of other siRNAs targeting components required for membrane trafficking with a specific, though not exclusive, emphasis on endocytosis. The library was called 'Traffickome' and consisted of siRNAs targeting a total of 211 proteins.

Different measures were put in place in order to avoid non-specific effects caused by the transfection of siRNA, also known as off-target effects. As explained above, off-target effects can be generated by a cell response to the lipid transfectant and to the foreign siRNAs transfected. Furthermore, uncomplete degradation of the non-coding siRNA or incorrect digestion of the sense siRNA strand can generate non-targeted knock-downs. As well as partial or complete complementarity with other non-targeted proteins. In order to reduce the incidence of off-target effects I applied different approaches. As mentioned before, low amounts of siRNA and Dharmafect 1 were used in order to reduce the activation of cell defence pathways towards foreign lipids and siRNA. Also for each target protein, a pool of 4 siRNAs with different base pairs sequence was used. Furthermore, for the initial screen of the whole Traffickome library I decided to use the superior ON-Target*plus* siRNAs from Dharmacon; these are designed and chemically modified to ensure the knock-down of target proteins and to reduce the incidence of unspecific effects. Finally, the introduction of non-targeting controls in the screen was also meant to control for the presence of any off-target effects.

I screened the Traffickome library a total of 5 times with HeLa T-REx Tie2^{FLAG} passaged from different frozen vials. One of the repeats was discarded due to an abnormal high rate of cell death in most of the plate. Each repeat of the screen consisted of a single 384-well plate including 1 replicate transfection for each targeting siRNA and 10 replicates of each negative control non-targeting siRNA #1 and #5. The non-transfected control conditions (NT) consisted of cells exposed to the same concentration of

Dharmafect 1 without the presence of siRNA and including media instead. Furthermore, in some of the repeats I also included 10 replicates with siRNA targeting Cbl (CBL) and Dynamin 2 (DNM2) as positive controls (Human siGENOME library, GE Dharmacon) (***Figure 36***b, top panel). I chose to also include the ubiquitin ligase CBL as it was the only protein reported to be required for Tie2 internalization when this work started (Wehrle et al. 2009). Despite not having a positive result in the pilot screen (**Figure *34***), DNM2 is required in most membrane trafficking processes and our lab has demonstrated that DNM2 is required to elicit the Ang1-mediated activation AKT which is a downstream target of activated Tie2 (Data not shown). Hence I decided to use it as positive control.

Selection and normalization of data

For each well several images were automatically acquired by the ImageXpress Microscope. Automatically acquisition of images can only be done of a single Z-section from cells and the optimal Z-depth of focus was determined individually for every plate by sampling different control wells. I aimed to acquire images from the middle section of cells, where most of the Ang1-containing endosomes were found in the negative controls. In order to ensure the data was homogenous, only those images containing between 0 to 100 cells were included in the normalization (**Figure *35***a). Two pair of rows from one of the repeats were discarded due to the Ang1 or doxycycline not being dispensed properly, what resulted in all the wells of the two rows having very low values of vesicles per cell. Normalization of data within each independent experiment was performed to neutralise systematic errors generated during the screening so that data from different plates and experiments could be compared (Birmingham et al. 2009). Data from each screen was normalized using the plate median by calculating the Robust Z-score (**Figure *35***a). The Robust Z-score (R. Z-score) is a variation from the Z-score, which normalizes the values of results depending on their distance from the mean. In the case of the R. Z-score the normalization is done using the median in order to avoid the effect that outliers have in the mean. The Robust Z-score is calculated as in **Equation *2*** and **Figure *35*** and is recommended for the normalization of data of a primary siRNA screen and specially for assays with weak effects on parameters (Birmingham et al. 2009). Finally, I used the median Robust Z-score of each siRNA in each screen to determine hits (**Figure**

35b); those siRNAs with a median R. Z-score above 1 or below -1 were considered weak hits and those above 2 or below -2 were considered strong hits.

$$Robust\ Zscore = \frac{x_i - median}{MAD}$$

$$MAD = median\ |x_i - median|$$

Equation 2. Where x_i designates the average parameter vesicles per cell for each well in a screening plate. The median is calculated from the plate, as well as the Median Absolute Deviation (MAD). MAD is the median value of the differences to the plate median from each well value.

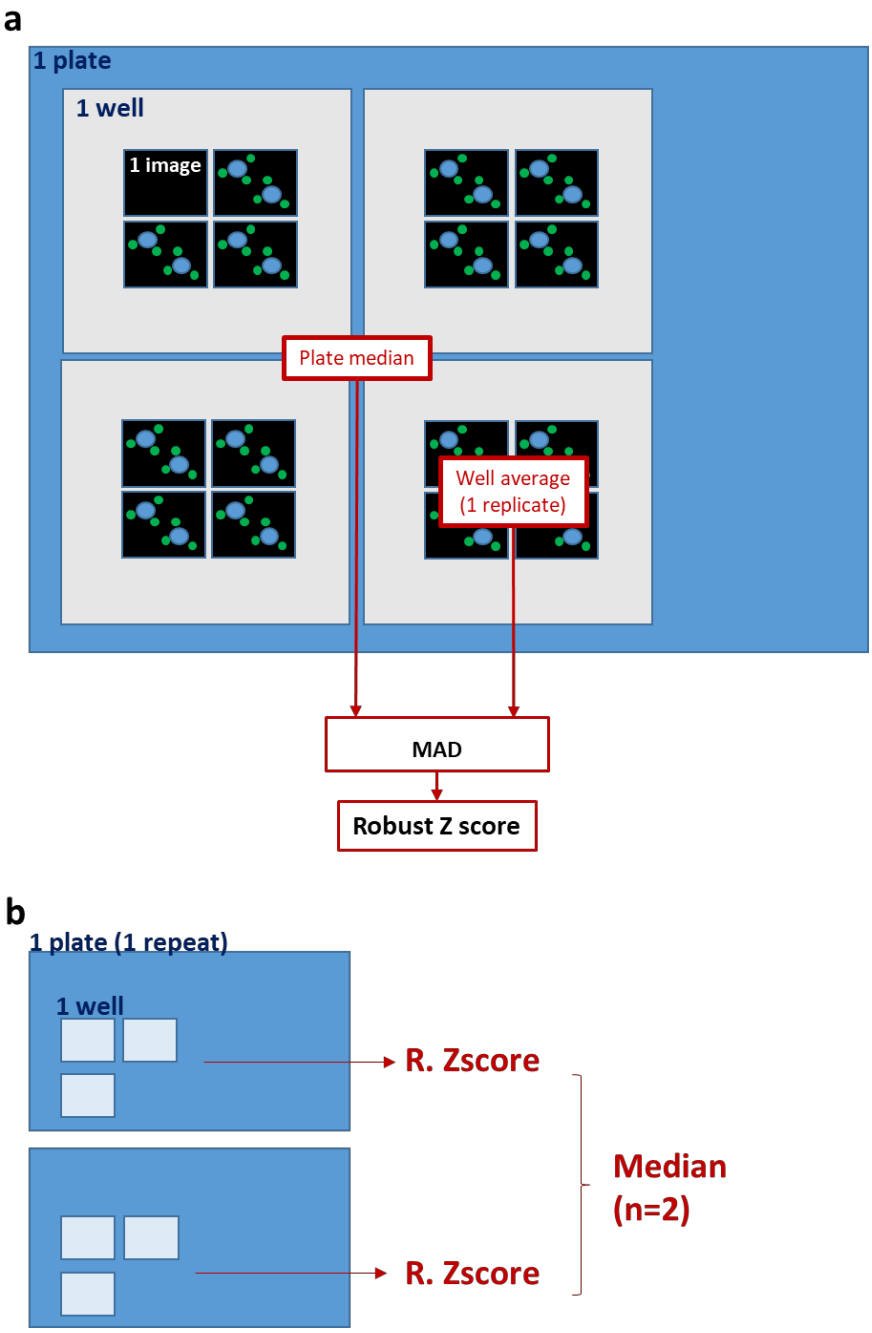

Figure 35. Flowchart representing the HT analysis. (a) Given an independent experiment, in our case consisting on a single 384-well plate; several images (a minimum of 6) were automatically acquired and analysed for each well, giving a specific value for a given parameter such as Ang1 vesicles/cell. Only those images containing certain number of cells were included in this average. The value for a parameter averaged from a single well constituted a replicate of a specific condition in any independent experiment. After discarding those wells that were suspected of being a result of a plate effect the median of all the wells within a single plate was obtained. The plate median was used to calculate the Median Absolute Deviation (**MAD**) and Robust Z-score for each individual replicate or well. **(b)** The median of replicates' Z-score values for a specific transfection or condition in an individual experiment was used to calculate the total median for that particular condition in any single experiment and a final R.Z-score value was used to compare data between independent experiments and determine those siRNA considered robust hits.

Evaluation of hits

The negative controls siRNAs #1 and #5 and the positive controls CBL and DNM2 had all robust median R. Z-Scores (**Figure *36***a). The non-targeting #1 had a median R. Z-score of -0.36 (n=4), falling within the range of non-significant siRNAs, yet the non-targeting #5 had a median R. Z-score of -1.1 (n=4), indicating that although it was considered a negative control it did have an effect on the internalization of Tie2. In accordance with previous data, both CBL and DNM2 were found to inhibit the internalization of Ang1 with median R. Z-scores of -1.7 and -2.3 respectively (n=3 and 2), hence indicating that the assay was statistically reliable.

The analysis of the plate distribution of the median R. Z-scores is shown in **Figure *36***b (bottom panel) and does not indicate the presence of any evident plate effect. The so called "Plate effects" are a common issue when performing a HTS and these are an important factor contributing to the variability of results. Plate effects are any variation of the detected parameter that occurs due to the location of a well within a plate. The causes of plate effects can be diverse and origin in multiple steps of the screening. Although careful analysis and design of a screen should overcome any mild artefactual defects it is always sensible to be aware of those when analysing the data. Plate effects can be detected by observing the distribution of values within each plate and an average of the total plates screened. The negative and positive controls are also particularly valuable for confirming the presence of plate effects.

Overall, the screen identified a total of 65 hits, 34 increased the internalization of Ang1 and were classified as "Accelerators", while 31 were inhibitory and were classified as "Inhibitors" (**Figure *36***b and **Sup. Table *5*** in Annex E).

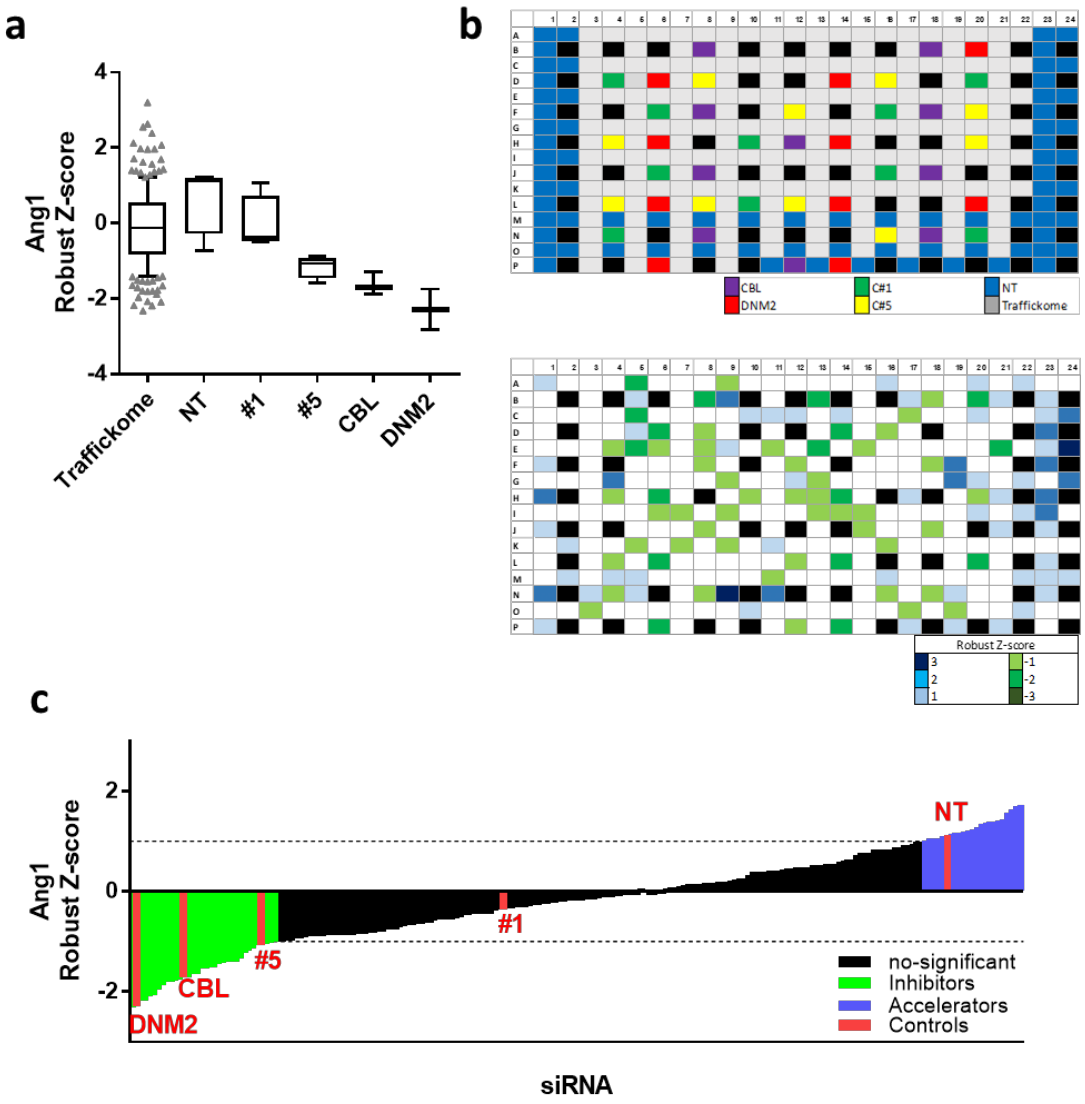

Figure 36. A primary siRNA screen revealed multiple regulators of Tie2 endocytosis. The primary screen consisted in 211 On-Targetplus siRNA targeting genes involved in membrane trafficking (Traffickome library) and was repeated 4 times. Transfected HeLa T-REx cells expressing $Tie2^{FLAG}$ after an overnight exposition to 1 µg/mL doxycycline were serum starved and pre-bound with 200 ng/mL of $hrAng1^{His}$ on ice for 30 min and then incubated with ligand for 45 min at 37˚C. Non-internalized $hrAng1^{His}$ was acid stripped on ice and cells were fixed and immunostained for $hrAng1^{His}$ and stained with DAPI. The amount of $hrAng1^{His}$ vesicles per cell were automatically quantitated and normalized with the Robust-Z score using each plate's median. **(a)** Non-targeting siRNA#1 and #5 were used as negative controls and CBL and DNM2 as positive controls. NT accounts for Non-Transfected. **(b) Top:** Plate distribution of the Traffickome library, and positive and negative controls as indicated by the colour key. **Bottom:** Plate distribution of the median Robust Z-scores. Grades of green and blue indicate the values of Robust Z-score as indicated in the key. **(c)** Graphic representation of median R.Z scores obtained for each siRNA, showing in green the inhibitors and in blue the accelerators of internalization of Ang1. The positive and negative controls are coloured in red. Each bar represents the median robust Z-score of 2 to 4 independent experiments (n=2 for DNM2, n=3 for CBL and n=4 for the negative controls and Traffickome library). The median of Ang1 internalization of all the genes targeted is detailed in **Sup. Table 5**, Annex E.

In order to aid in narrowing down the list for a second validation screen for Ang1 specific hits, I used the library to identify siRNAs affecting the internalization of transferrin and the expression of Tie2 in two separate library plates using HeLa T-REx Tie2^{FLAG} cells in both cases. I used the same non-targeting siRNAs #1 and #5 as negative controls and siGENOME siRNA for DNM2 and TEK were used as positive controls for the screen on TF and Tie2 correspondingly. In the TF screen cells were incubated with fluorescently labelled TF following the same protocol used for the assay of Ang1 internalization (**Figure *37***). In the screen on the expression of Tie2 I used the same transfection conditions and timings without exposing cells to any ligand, I then stained them for the expression of Tie2 using the endodomain Tie2 antibody (**Figure *38***). In the case of the Tie2 screen, images were acquired from the basal plasma membrane of cells. Nonetheless, images were analysed using the same segmentation protocol CME1 as it was also sensitive to the internalization of TF and the staining of Tie2.

In both cases, the corresponding positive controls DNM2 and TEK had negative R. Z-scores in contrast to the Non-targeting siRNA#1, which did not had a significant R. Z-score (**Figure *37***a and **Figure *38***a). This indicated that both screens were sensitive to its corresponding parameters, either the presence of TF or Tie2. Interestingly, Non-targeting siRNA#5 had again a negative R. Z-score when measuring the internalisation of TF, yet this was not the case for the expression of Tie2 (**Figure *37***a and **Figure *38***a). This result is in line with the suspicion that the supposedly non-targeting siRNA#5 targets some component of the internalization machinery of Tie2. It appeared from the well disposition of results that some artefactual plate effect could have affected the value of the hits, as more negative values are found around the top-left corner and more positive values around the bottom-right corner, yet the results of the positive control TEK seemed unaffected regardless of the replicates location in the plate (**Figure *38***b, bottom panel).

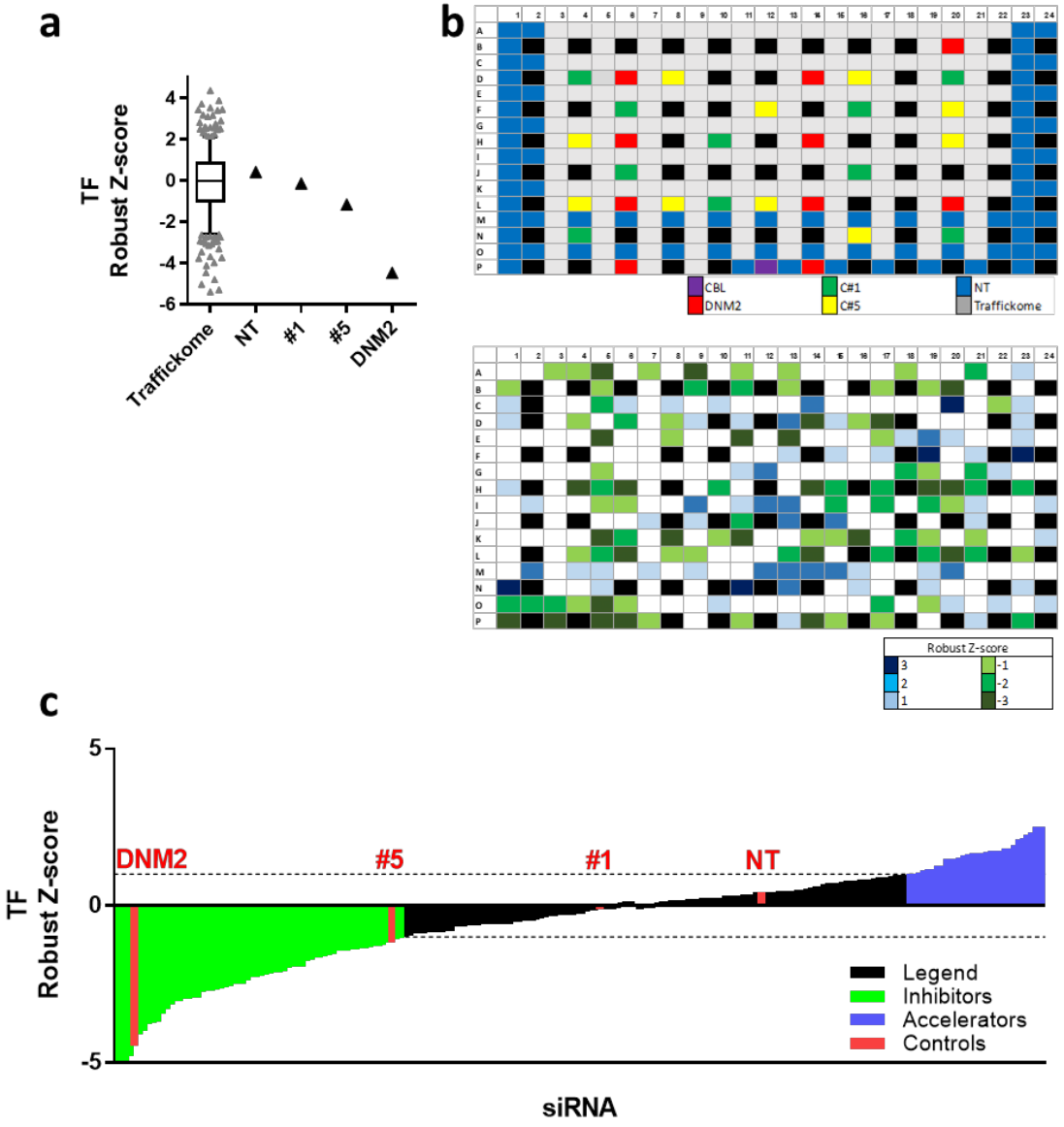

Figure 37. The Traffickome library was screened once for the siRNA effects on the internalization of transferrin. Transfected HeLa T-REx cells expressing Tie2^{FLAG} after overnight exposition to 1 µg/mL doxycycline were serum starved for 2h and pre-bound with 5 µg/mL fluorescent transferrin on ice for 30 min and then incubated for 45 min at 37˚C. Non-internalized transferrin was acid stripped on ice and cells were fixed and stained with DAPI. The amount of hrAng1^{His} vesicles per cell were automatically quantitated and normalized with the Robust-Z score using the plate's median. **(a)** Non-targeting siRNA#1 and #5 were used as negative controls and DNM2 as positive control. NT accounts for Non-Transfected. **(b) Top:** Plate distribution of the Traffickome library, and positive and negative controls as indicated by the colour key. **Bottom:** Plate distribution of the median Robust Z-scores. Grades of green and blue indicate the values of Robust Z-score as indicated in the key. **(c)** Graphic representation of median R. Z-scores obtained for each siRNA, showing in green the inhibitors and in blue the accelerators of internalization of transferrin. The positive and negative controls are indicated in red. Each bar represents the median robust Z-score of a single experiment (n=1). The median of Tfn internalization of all the genes targeted is detailed in Annex E.

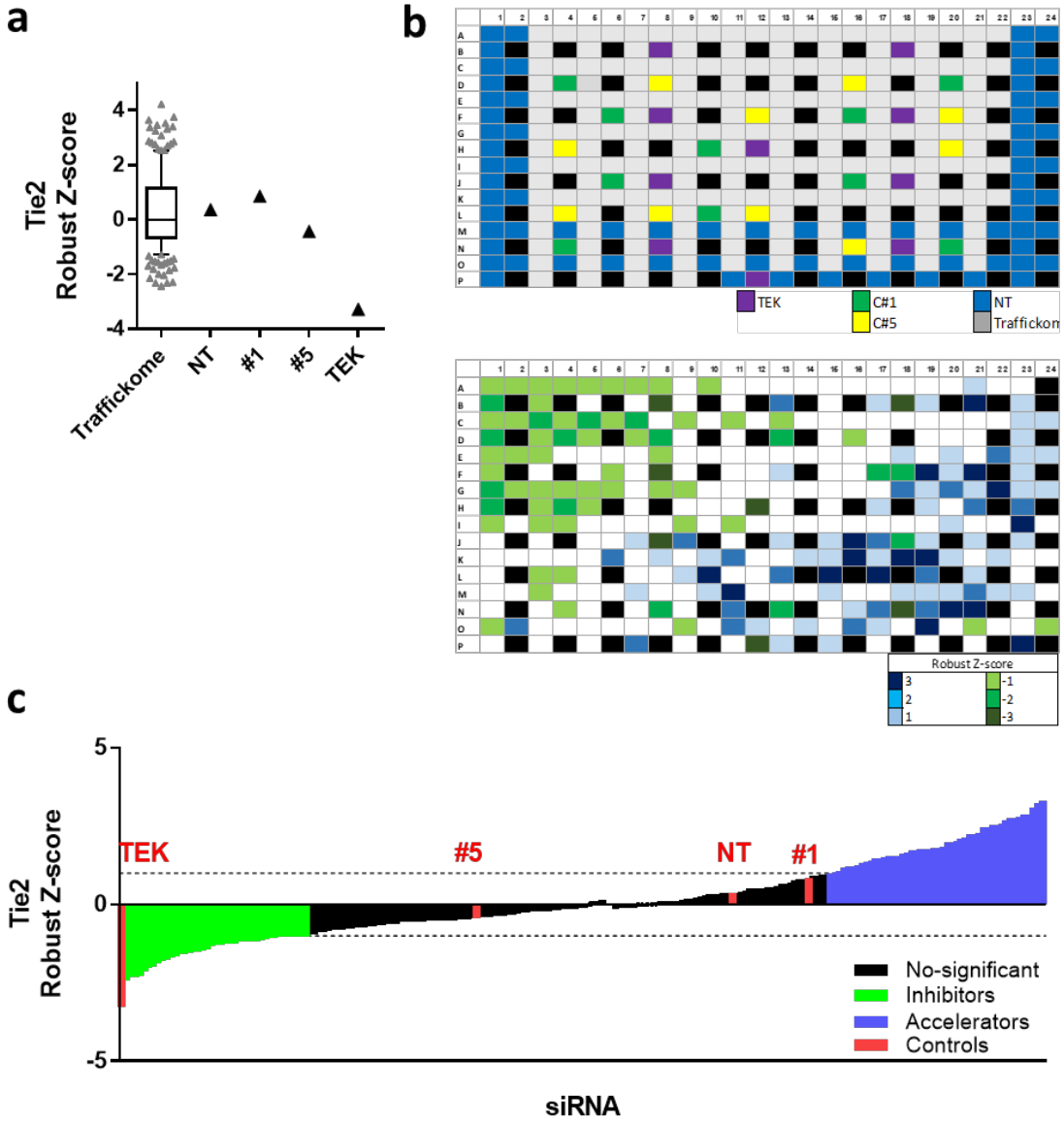

Figure 38. The Traffickome library was screened for the siRNA effects on the expression of Tie2^{FLAG}. Transfected HeLa T-REx cells expressing Tie2^{FLAG} after overnight exposition to 1 µg/mL doxycycline were fixed 3 days after transfection and immunostained for Tie2 and nuclei stained with DAPI. The amount of Tie2^{FLAG} was quantitated using the same algorithm and computed as vesicles per cell, each well's value was normalized with the Robust-Z score using the plate median. **(a)** Non-targeting siRNA#1 and #5 were used as negative controls and TEK as positive control. NT accounts for Non-Transfected. **(b) Top:** Plate distribution of the Traffickome library, and positive and negative controls as indicated by the colour key. **Bottom:** Plate distribution of the median Robust Z-scores. Grades of green and blue indicate the values of Robust Z-score as indicated in the key. **(c)** Graphic representation of median R. Z-scores obtained for each siRNA, showing in green the inhibitors and in blue the accelerators of expression of Tie2. The positive and negative controls are coloured in red and correspond to TEK, #5, NT and #1, from left to right. Each bar represents the median robust Z-score of a single experiment (n=1). The median of Tie2 detection of all the genes targeted is detailed in Annex E.

Using the same criteria for hit selection as for the internalization of Ang1 I obtained a total of 105 hits affecting the internalization of TF and 217 hits for the expression of Tie2. Since the screens consisted of a single repeat the number of hits was higher than the screening for the internalization of Ang1. Overall, the statistics from the screening on the internalization of TF and the expression of Tie2 indicated that although the assays were sensitive for each parameter I should be aware of a higher presence of false positive and false negative hits due to the lack of repeats. The median R. Z-scores of the effect of the siRNAs on the internalization of TF and the expression of Tie2 are also detailed in **Sup. Table *5*** (Annex E).

As expected, multiple siRNA targeting for components of CME were found to have an effect on the internalization of TF. Most importantly clathrin heavy chain (CLTC), subunits α1, β1, μ1 of adaptor protein complex 2 (AP2A1, AP2B1, AP2M1), phosphatidylinositol binding clathrin assembly protein (PICALM) and Epsin 1 and 2 (EPN1,EPN2). Although it appeared that only the siGENOME siRNA targeting DNM2 used as a control and not the On-Target*Plus* DNM2 affected the internalization of TF, which was surprising as TF internalisation is known to be dynamin dependent. Also, some siRNA targeting Rab proteins involved in endosomal trafficking and recycling were also found to affect the internalization of TF, such as Rab4a, Rab4b, Rab5A, Rab5B or the Rab5 effector Adaptor Protein, Phosphotyrosine interacting with PH domain and Leucine zipper 2 (Appl2). Again, this argued in favour of the reliability of the assay, especially for the screening of the internalization of Ang1, for which I had several repeats.

In reference to the Tie2 staining, I noticed that some of the inhibitors or accelerators for the internalization of Ang1 were also found to affect in the same way the presence of Tie2 in the basal membrane of cells, of which some were siRNAs targeting for proteins involved in secretory membrane traffic such as AP1 subunit β1 (AP1B1), Golgi associated PDZ and coiled-coil domain motif containing protein (GOPC), Rab2 (RAB2), Sec22B (SEC22B), Syntaxin Binding protein 2 (STXBP2) and Sec31L1 (SEC31L1). For these siRNA

most probably the increase or decrease of internalization of Tie2 is secondary to a change in the available Tie2 in the plasma membrane. However, there were siRNA targeting proteins involved in endocytosis and endosomal trafficking that unexpectedly also affected the staining of Tie2 detected in cells. Furthermore, not all of the siRNAs found to affect Tie2 expression in the basal membrane also caused a similar effect on the internalization of the receptor. Since images were acquired from a single Z-section of cells, a change in the amount of the Tie2 quantified could either be due to a siRNAs altering the amount of total Tie2 available in the cell surface or a change in the localization of the receptor. Therefore, considering as well that a single repeat was done it was difficult to obtain any robust conclusions by solely analysing this screen on the staining of Tie2.

In the case of Ang1, I also found several siRNA targeting mediators of CME to significantly affect the internalization of Ang1, such as siRNA targeting subunits α1 and μ1 of AP-2, Arrestin β2 (Arrb2), clathrin heavy chain and light chain B (CLTC, CLTB), Disabled-2 (DAB2) and Epsin 1 and 3 (EPN1, EPN3). Nonetheless, I also found several siRNAs for proteins involved in actin polymerization and organization such as different subunits of the Arp2/3 complex (ARPC2, ACTR2, ARPC5, ARPC1B), calponin and LIM domain containing 1 (MICAL1) or the Rho associated coiled-coil containing protein kinase 1 and 2 (ROCK1, ROCK2). As well as the signalling mediator RAC1 and its molecular effector Pak1 which are involved in cytoskeleton rearrangements that occur during cell motility. Interestingly, there were also several Rab proteins known for having a role in ER and Golgi transport found to be specifically affecting the internalization of Ang1 but not of TF or expression of Tie2 in the basal membrane of cells. Those were Rab1A, Rab3B, Rab8A, Rab11A and Rab31.

5.2 Secondary Screen

Small interfering RNAs are designed to specifically target the expression of a particular protein by having a sequence of base pairs that are only found in the mRNA of that particular protein (Aigner 2007). Still, as explained earlier, the transfection of siRNAs can generate what are known as off-target effects. The occurrence of off-target effects is greatly reduced by using lower amounts of Dharmafect and siRNA in the transfection, as well as by using pools of targeting siRNA or chemically modified siRNAs such as On-Target*Plus* siRNAs (Lin et al. 2005). However, off-target effects may also occur by incomplete complementarity to non-targeted mRNA (Lin et al. 2005). To ensure that the obtained effects in a screen are due to specific targeting of a protein the general practice is to re-screen a library using different siRNAs (Lin et al. 2005). These off-target effects of a siRNA could lead to either false positive or false negative hits so it would be reasonable to screen the whole library again, yet this would be costly and would also increase the complexity of hits selection. For instance, it would be complicated to decide whether a target protein is a true hit if it results in a positive effect on one screen but not in the other. Actually, off-target effects of a particular siRNA are not necessarily manifested in the parameter that is screened, hence the only way of determining whether a siRNA is truly specific would be to realize transcriptomic analysis of transfected cells (Lin et al. 2005). Again, since this is costly and unpractical in large screens, the usual approach is to select a group of positive hits to be re-screened with different siRNAs targeting the same proteins and also re-screening in different cell types. Therefore, I decided to re-screen only a small selection of the positive hits from the primary screen using siGENOME siRNA. In contrast to the On-Target*Plus* siRNAs, the siGENOME siRNAs are not as optimized to avoid inducing off-target effects so a higher presence of false negative and false positive effects is expected. Therefore siGENOME siRNAs are better to be used in a secondary screen with previously selected targets in a primary screen.

Contrasting the information from the siRNA screens of the internalization of Ang1 and TF and the expression of Tie2 I selected a total of 30 hits to be validated in a secondary

screen. To begin with, I discarded most of the hits that appeared to be strongly affecting the expression of Tie2. I then included in the selection those siRNAs that were found to be affecting the internalization of Ang1 but not TF, although I did include PAK1, RAB3B, RAB4B, STX2, STX4 and STX8 because they were functionally linked to other hits. The hits to be re-screened were distributed in triplicates in a single plate. This time the scrambled siRNAs #2, #3, and #4 were also included to cells and the siRNA for Tie2 (TEK) was also added as an extra positive control (**Figure *39***a).

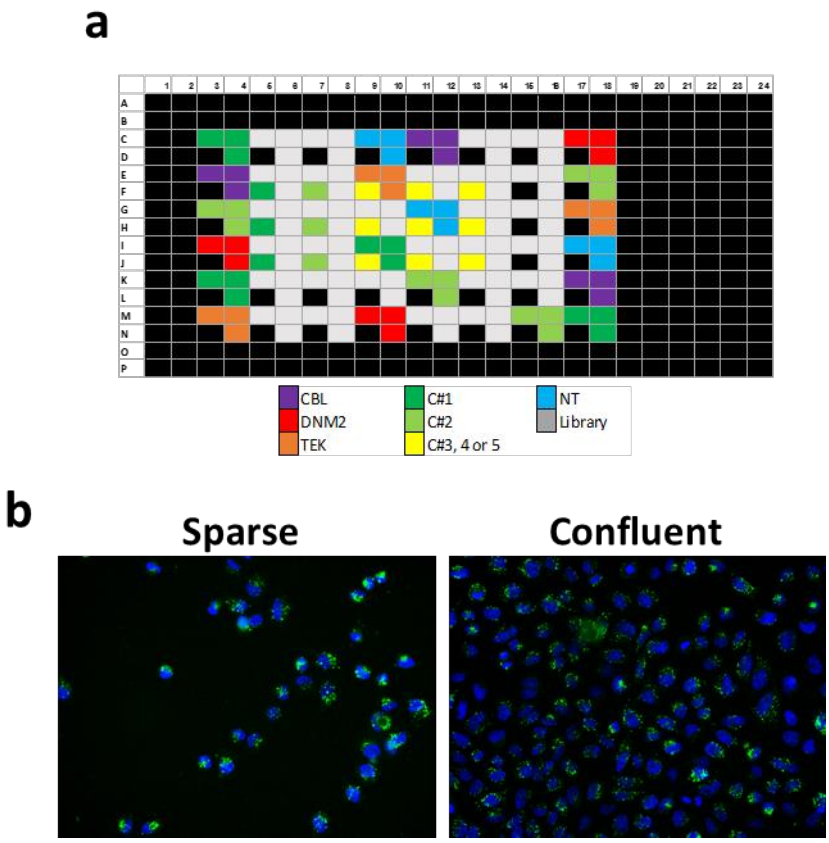

Figure 39. Plate set-up of the secondary screen with siGENOME siRNAs. The secondary screen was composed with a selection of hits from the primary screen. Non-targeting siRNAs #1 and 2 were included as the main negative controls and siRNAs for CBL, DNM2 and TEK were used as positive controls. **(a)** Schematic representation of the 384-well plate indicating the localization of each control and library siRNAs. Controls and target siRNAs were disposed in grouped triplicates as indicated by the colour key. **(b)** For the secondary screen, two sets of plates with different cell seeding number were screened in parallel, also, for each plate set images were selected to include only those images containing less than 50 nuclei per image (Sparse) or more than 200 nuclei per image (Confluent). A representative example of each is shown. Cell nuclei were stained with DAPI and internalized Ang1 is shown in green.

Selection of data

During the analysis of the primary screen I observed that, on occasion, the effect of some siRNAs on internalization seemed to be influenced by differences in cell confluency in the wells or images. Cell confluency has been previously shown to affect the localization and, importantly, signalling of Tie2 in HUVECs (Fukuhara et al. 2008; Saharinen et al. 2008). Hence, I decided to investigate if the endocytic pathway of activated Tie2 could also be affected by the density of cell culture. I set up the secondary screen to consist of two plates with sparse and confluent cell cultures. Images from sparse conditions contained up to 50 cells in the field of view while confluent cultures had between 200 and 600 cells. This criteria was set to ensure that sparse fields included as few as possible cell-cell contacts while most cells in confluent fields were in contact with other cells (**Figure *39***b). Since transferrin internalization is not known to be affected by cell confluency I also screened in parallel for the siRNAs affecting the internalization of fluorescently labelled transferrin in plates with sparse and confluent cultures of cells. Furthermore, in order to implement the selection of hits this time I co-stained cells with Ang1 and Tie2 using the anti-Goat Tie2 antibody so that I could normalize the amount of internalized Ang1 to the amount of Tie2 detected in the cells. Again, images could only be taken from a single Z-stack so interpretation on changes on the staining of Tie2 could not only be caused by changes in the expression of Tie2 but also due to changes in the localization of the receptor within the cell.

Therefore, I had three parameters with which to improve the selection of hits in the secondary screen. First, the parameters “Internalized Ang1” would note all those siRNAs having an effect in the internalization of Ang1, still changes in Tie2 availability or location in the cell surface and Tie2 total expression would indirectly also have an effect in the quantitation of Ang1. Secondly, the parameter “Tie2 staining” would be sensitive to the total expression of Tie2 within the cell, yet since I was not imaging the whole cell the parameter would also be sensitive to re-localizations of Tie2 within areas of the cell not imaged. Therefore, the ratio “Ang1/Tie2” could be considered a third parameter that would be sensitive to all the mentioned factors above as well but that could highlight hits where both Ang1 and Tie2 are affected in opposite directions and also discard hits

where both Ang1 and Tie2 are proportionally changed in same directions, such as when a decrease of internalized Ang1 would be due to a decrease in the expression of Tie2. The factors hypothesised to affect the three parameters are summarised in *Table 5*. I believed that the different parameters could be complemented in order to improve the selection of hits from the secondary screen and decided to evaluate them all individually. For instance, in the case of a siRNA with a non-significant Ang1/Tie2 yet with a decrease in Ang1 internalization and Tie2 staining would most probably be affecting the expression of the receptor, although it could not be ruled out that, alternatively, the receptor was being sequestered in intracellular compartments and hence generating the same parameters.

In the case of screening for the internalization of transferrin, the parameter "internalized TF" would be also sensitive to changes in the internalization dynamics of the ligand and changes in the transferrin receptor, as in the case for internalized Ang1 and Tie2. Though since I did not quantify the presence of transferrin receptor I would not be able to investigate which hits could be a secondary effect to a change in the receptor expressed in cells. Nonetheless, transferrin internalization has been well studied and our aim in including the screen of transferrin was to compare the results with the Ang1 internalization and see any similarities or differences.

Table 5. Summary of parameters for screening the internalization of Tie2 in cells and factors influencing the results

Parameter		Factors
Ang1		- Ang1 internalization rate - Tie2 available to ligand in the cell surface - Tie2 total expression in cells
Tie2		- Tie2 localized in the basal membrane of cells - Tie2 total expression in cells
Ang1/Tie2	**Decrease**	- Decrease in quantitated Ang1 - Increase in quantitated Tie2 - Combination of both - Disproportional increase of Tie2 to Ang1
	Non-significant	- Proportional increase or decrease in quantitated Ang1 and Tie2 - Insignificant changes in both Ang1 and Tie2 quantitations
	Increase	- Increase in quantitated Ang1 - Decrease in quantitated Tie2 - Combination of both - Disproportional decrease of Tie2 to Ang1

Normalization of data

Data for each well within a plate was normalized calculating the % of vesicles/cell to the average of Control#1 and then all replicates were averaged. The normalization of data as a % of a negative control is recommended instead of the Robust Z-score in a secondary screen, since the frequency distribution of values will be skewed when a small selection of hits is screened (Birmingham et al. 2009). Then the plate-averages for the siRNA in each repeat were averaged to determine the siRNA having a significant effect on the different parameters. Overall the secondary screen consisted in 2 repeats. The cut off for the identification of hits was set at different values of internalization for each parameter depending on the quality of the assay. As a parameter depending on the quality of the assay I used the averaged SD of the non-targeting controls #2 to 5, as I assumed that the variation within these should be representative of the ability of the assay to distinguish between non-significant and significant hits. Therefore, the cut off

points for determining which siRNAs were significantly affecting each parameter were 100 ± 10%, 100 ±20% and 100 ± 11% to Control#1 of the internalization of Ang1 and TF and staining of Tie2 correspondently. Furthermore, since the screen finally consisted on only 2 repeats for each condition I discarded any siRNA with one repeat falling within the non-significant area.

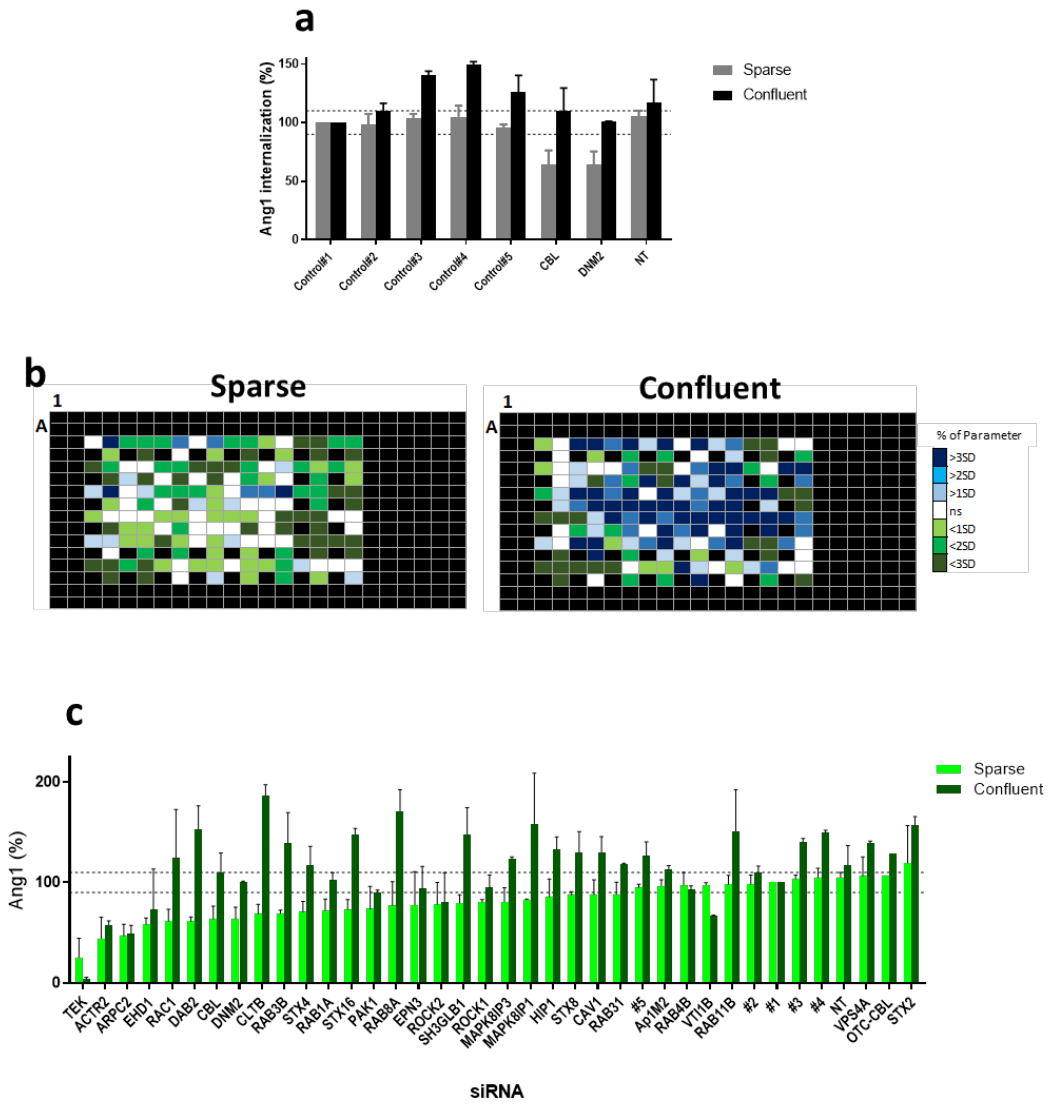

Figure 40. Secondary siRNA screen on the internalization of Tie2 using HeLa T-REx Tie2^{FLAG} cells transfected with a selection of targeting siGENOME siRNAs. Two different seeding conditions were used to yield sparse and confluent cell cultures at the end of the assay. Transfected HeLa T-REx cells expressing Tie2^{FLAG} after an overnight exposition to 1 µg/mL of doxycycline were pre-bound with hrAng1^{His} on ice for 30 min and then incubated with ligand for 45 min at 37˚C. Non-internalized hrAng1^{His} was acid stripped on ice and cells were fixed and immunostained for hrAng1^{His} and nuclei stained with DAPI. Multiple images were automatically acquired for each well using the ImageXpress Microscope. The amount of hrAng1^{His} vesicles per cell were automatically quantitated and the average of each well was normalized as the % to the average plate-value of the non-targeting siRNA #1. The range of significance was determined using the average SD of the non-targeting controls. The effect of a siRNA was considered significant if both repeats fell below or above the significant limit; indicated with dotted lines in **(a)** and **(c)**. **(a)** Graph representing the average percentage of internalized Ang1 of the negative and positive controls for Sparse (Grey) and Confluent (Black) cultures of transfected cells. **(b)** Plate distribution of the mean percentage of internalized Ang1 for each well in Sparse and Confluent conditions as indicated. Wells are coloured depending on the significance as explained. **(c)** Graph representing the average percentage of internalized Ang1 for all the siRNA transfected and Non-transfected cells (NT). Sparse and Confluent cultures are coloured in bright and dark green respectively. Bars in **(a)** and **(c)** represent mean ± range of parameter value for each siRNA, n=2.

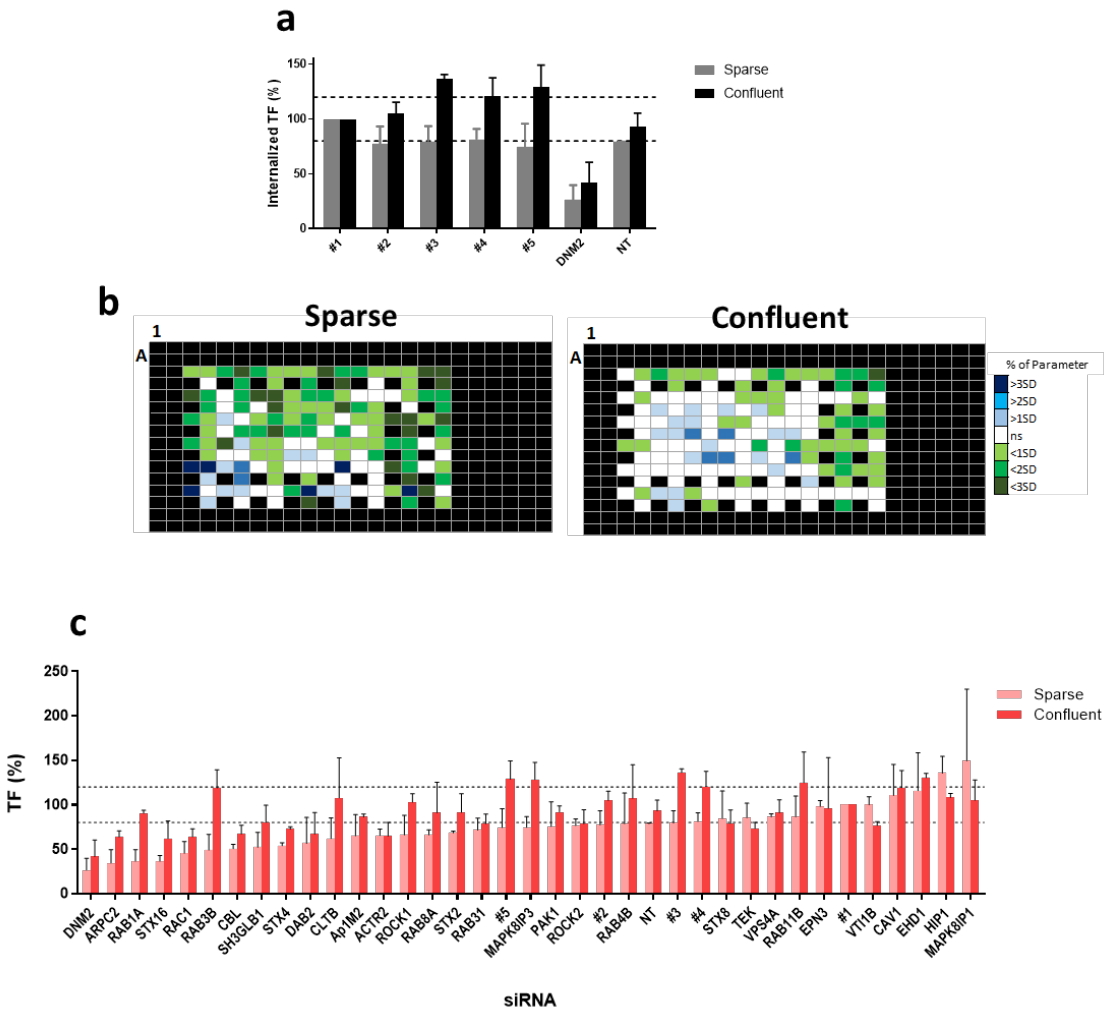

Figure 41. Secondary siRNA screen on the internalization of transferrin using HeLa T-REx Tie2^{FLAG} cells transfected with a selection of targeting siGENOME siRNAs. Two different seeding conditions were used to yield sparse and confluent cell cultures at the end of the assay. Transfected HeLa T-REx cells expressing Tie2^{FLAG} an overnight exposition to 1 µg/mL of doxycycline were pre-bound with hrAng1^{His} on ice for 30 min and then incubated with ligand for 45 min at 37˚C. Non-internalized transferrin (TF) was acid stripped on ice and cells were fixed and stained with DAPI. Multiple images were automatically acquired for each well using the ImageXpress Microscope. The amount of TF containing vesicles per cell were automatically quantitated and the average of each well was normalized as the % to the average plate-value of the non-targeting siRNA #1. The range of significance was determined using the average SD of the non-targeting controls. The effect of a siRNA was considered significant if both repeats fell below or above the significant limit; indicated with dotted lines in **(a)** and **(c). (a)** Graph representing the average percentage of internalized TF of the negative and positive controls for Sparse (Grey) and Confluent (Black) cultures of transfected cells. **(b)** Plate distribution of the mean percentage of internalized TF for each well in Sparse and Confluent conditions as indicated. Wells are coloured depending on the significance as explained. **(c)** Graph representing the average percentage of internalized TF for all the siRNA transfected and Non-transfected cells (NT). Sparse and Confluent cultures are coloured in bright and dark red respectively. Bars in **(a)** and **(c)** represent mean ± range of parameter value for each siRNA, n=2.

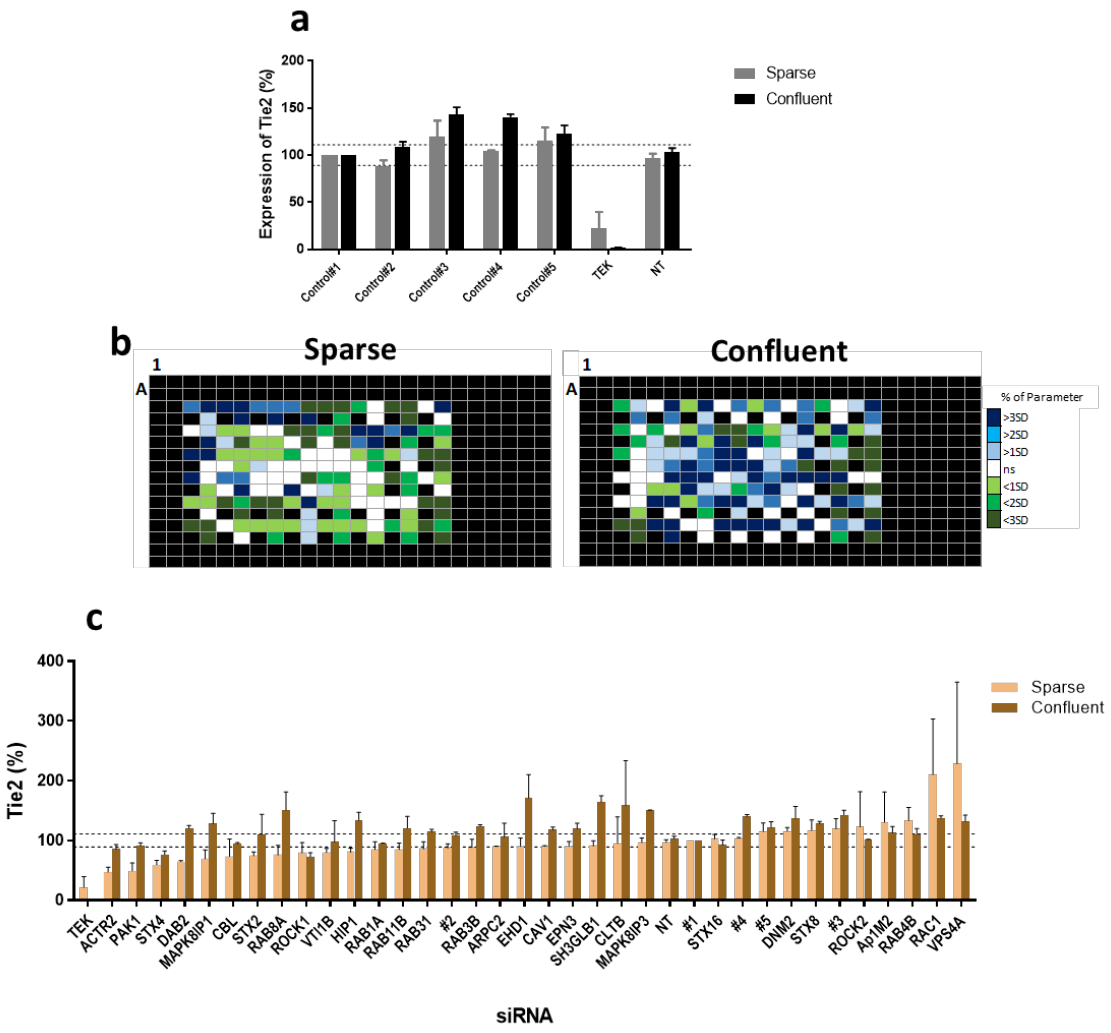

Figure 42. Secondary siRNA screen on the expression of Tie2 using HeLa T-REx Tie2^{FLAG} cells transfected with a selection of targeting siGENOME siRNAs. The same plates used to quantitate the internalization of Ang1 (**Figure 40**) were stained for Tie2 using the Goat Tie2 antibody. Multiple images were automatically acquired for each well using the ImageXpress microscope and the amount of was quantitated as vesicles per cell using the same algorithm as for the quantitation of ligand internalization. The average Tie2 per cell of each well was normalized as the % to the average plate-value of the non-targeting siRNA #1. The range of significance was determined using the average SD of the non-targeting controls. The effect of a siRNA was considered significant if both repeats fell below or above the significant limit; indicated with dotted lines in **(a)** and **(c). (a)** Graph representing the average percentage of detected Tie2 of the negative and positive controls for Sparse (Grey) and Confluent (Black) cultures of transfected cells. **(b)** Plate distribution of the mean percentage of Tie2 expression for each well in Sparse and Confluent conditions as indicated. Wells are coloured depending on the significance as explained. **(c)** Graph representing the average percentage of quantitated Tie2 for all the siRNA transfected and Non-transfected cells (NT). Sparse and Confluent cultures are coloured in bright and dark brown respectively. Bars in **(a)** and **(c)** represent mean ± range of parameter value for each siRNA, n=2.

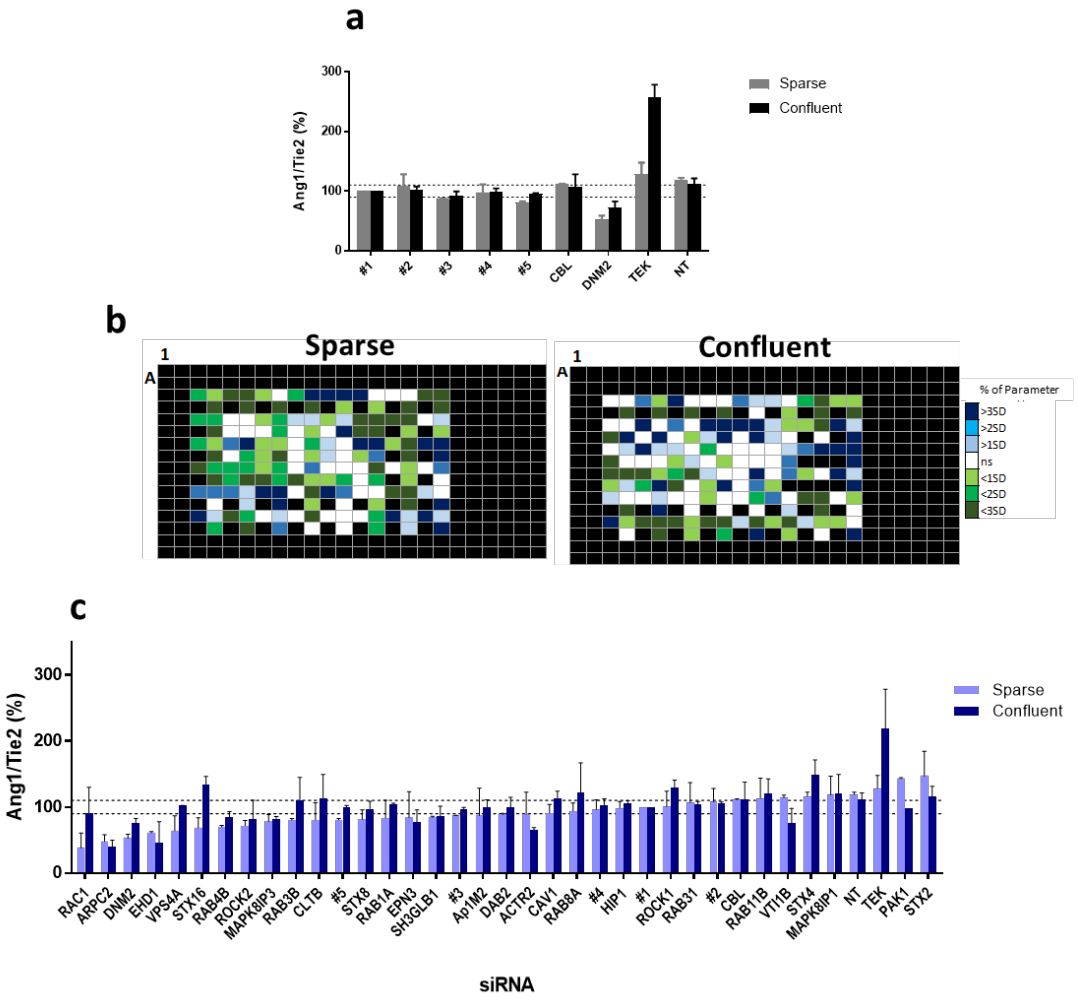

Figure 43. The normalization of the internalized Ang1 per cell using the amount of Tie2 detected per cell revealed a different siRNA hit profile. In order to evaluate whether the amount of internalized Ang1 detected was being influenced by differences in the expression of the Tie2 in cells I calculated the ratio of both parameters and analysed it as a new parameter representing the internalization of Tie2. Since images for each fluorescent signal had been acquired separately I used the average of Ang1 per cell and Tie2 per cell from each well to calculate the Ang1/Tie2 ratio. As with the other parameters, the ratio of Ang1/Tie2 for each well was normalized as the % to the plate average of the non-targeting siRNA #1 and the range of significance was determined using the average SD of the non-targeting controls. The effect of a siRNA was considered significant if both replicates fell below or above the significant limit; indicated with dotted lines in **(a)** and **(c). (a)** Graph representing the average percentage of Ang1/Tie2 of the negative and positive controls for Sparse (Grey) and Confluent (Black) cultures of transfected cells. **(b)** Plate distribution of the mean percentage of Ang1/Tie2 expression for each well in Sparse and Confluent conditions as indicated. Wells are coloured depending on the significance as explained. **(c)** Graph representing the average percentage of resulting Ang1/Tie2 for all the siRNA transfected and Non-transfected cells (NT). Sparse and Confluent cultures are coloured in bright and dark blue respectively. Bars in **(a)** and **(c)** represent mean ± range of parameter value for each siRNA, n=2.

Evaluation of Hits

From the plate distribution of the resulting values I observed a clear difference between the Ang1 Sparse and Confluent plates. As seen in **Figure *40***b, the values found within the "Sparse" plates are mostly below 90% of the average internalization for Control#1, whereas in the "Confluent" plates most of the values fall above 110%. In the case of TF, the plates of "Sparse" conditions have a higher frequency of decreased values of internalization than in the "Confluent" conditions, although the "Sparse" plates could appear to be affected by some kind of plate artefact since there was a gradation of values from the top to bottom of the plate and because some of the controls varied remarkably depending on the location of the repeats within the plates (**Figure *41***b). The distribution of the % of Tie2 staining to Control#1 showed the same tendency as for the internalization of Ang1 by showing more frequency of values above 111% in the "Confluent" plates. In the "Confluent" plates the values of percentage of Tie2 for the controls were quite robust, although for the "Sparse" plates some plate-effect seemed to have occurred (**Figure *42***b). When normalizing the amount of internalized Ang1 using the staining of Tie2 detected within each well the distribution of values was found to be then more similar between "Sparse" and "Confluent" conditions, indicating that much of the Ang1 variation was caused most probably caused by a variation in the expression of Tie2 (**Figure *43***b).

When I evaluated the validity of the controls I found that the non-targeting siRNAs #1 and #2 gave similar values to the Non-Transfected conditions for all the parameters. In contrast, the rest of non-targeting siRNAs showed to have some un-specific effects in some of the conditions. (**Figure *40***a, **Figure *41***a, **Figure *42***a and **Figure *43***a). The positive controls CBL and DNM2 resulted in a decrease below the significance limit of the internalization of Ang1 in the "Sparse" conditions (63.7 ± 12.6% and 63.9 ± 11.6%, mean ± SEM) but not in the "Confluent" conditions (**Figure *40***a). In contrast, the quantification of internalized TF was significantly decreased when targeting DNM2 in both "Sparse" and "Confluent" conditions (26.5 ± 13.3% and 41.9 ± 18.7%)(**Figure *41***a). Equally, the staining of Tie2 in the cells was significantly decreased in the positive control TEK for both "Sparse" and "Confluent" conditions (21.9 ± 17.6% and 1.9 ± 0.1%)(**Figure *42***a).

When expressing the results as the amount of Ang1 per Tie2 I did not observe anymore a clear difference between the Sparse and Confluent plating conditions for the negative controls #3 to #5 nor the positive controls CBL and DNM2, indicating that the difference was most probably due to an effect on the expression of Tie2 (**Figure *43***a). Interestingly, when applying the correction for the expression of Tie2, only the positive control DNM2 appeared to be decreasing the internalization of Ang1, but not CBL anymore. The apparent increase of internalization for the TEK transfection in the Confluent plates was due to a mathematical artefact as some of the Tie2 values in this conditions were close to 0. This effect was also observed for the cells unexposed to doxyxycline, which also had detected levels of Tie2 close to 0 (Data not Shown). From observing the plate distributions and the values of the controls I concluded that the assay was sensitive to the levels of intracellular ligands and Tie2 expression, albeit I should be aware that some of the results may include artefactual variation due to some slight plate effects.

When applying the criteria for hit selection to the results of the internalization of Ang1 I obtained a total of 16 inhibitors from the Sparse conditions, whereas 4 inhibitors and 14 accelerators were found from the Confluent conditions, including non-targeting siRNAs #3 to 5 (**Figure *40***c and **Sup. Table 6**). Only ACTR2 and ARPC2 effects seemed independent of cell confluency. Overall, 10 of the siRNA in the Sparse and 10 in the Confluent plates had the same effect on Ang1 as reported from the primary screen.

In the case of TF, 12 of the siRNA were inhibitors in the Sparse plates and 6 in the Confluent plates, while only 1 accelerator was found in the Confluent plates (**Figure *41***c and **Sup. Table 6**). I found that ACTR2, ARPC2, CBL, DNM2, RAC1, and STX4 were inhibitors of the internalization of TF independently of cell confluency, while RAB1A, RAB3B, SH3GLB1, STX16, STX2, RAB8B and EHD1 were only significant in either the sparse (first 6) or the confluent conditions (last one). Of those, only STX2 and STX4 had the same effect on the internalization of TF as in the primary screen of TF. It was interesting to see how most of the siRNAs affecting TF had the same effect on Ang1 in the Sparse conditions but not in the Confluent conditions. Namely, I found that ACTR2, ARPC2, CBL,

DNM2, RAB1A, RAB3B, RAC1, SH3GLB1, STX16 and STX4 were inhibitors of both Ang1 and TF in the sparse conditions.

When I analysed the staining of Tie2 I found that 10 siRNAs had an effect on the detected Tie2 in the Sparse plates and 15 in the confluent plates. The effect on the expression of Tie2 seemed to be dependent on the plating conditions, as only RAC1 and STX4 had similar effects in both conditions (***Figure 42***c and **Sup. Table 6**, Annex). In contrast, DAB2, HIP1 and MAPK8IP1 siRNA decreased the expression of Tie2 in low cell confluency but increased the expression of Tie2 in higher cell densities. As for the case of TEK, many of the siRNA increasing or decreasing the quantitated Ang1 also had a similar effect on the staining of Tie2, indicating that in those cases the changes in the internalization of Ang1 were most probably due a change in the availability of Tie2 in the cell surface (**Sup. Table 6**, Annex).

To compare the hits on the internalization of Ang1 between the primary and secondary screen I excluded those that appear to be a result of changes in the expression of Tie2. Comparing the remaining hits to the primary screen I found that ARPC2, CBL, DNM2, RAB1A, RAB3B, RAC1, ROCK1 and SH3GLB1 had all been reported as inhibitors of Ang1 in both the primary screen and the Sparse plates of the secondary screen. For the Confluent conditions, all of the hits apparently not affected by the expression or availability of Tie2 were found to have had the same effect as in the primary screen: ACTR2, ARPC2 and VTI1B as inhibitors and CLTB, Control#5, RAB31, STX16 and STX2 as accelerators of the internalization of Ang1. Interestingly, note that ARPC2 is the only common selected hit from the Sparse and Confluent conditions.

Although I could only compare the primary and secondary screens using the parameter of internalized Ang1, I expected that the ratio between Ang1 and Tie2 would be also a useful parameter. As explained earlier, those siRNA affecting the internalization of Ang1 as a secondary effect to changes in the expression of Tie2 would not appear anymore as hits. Although more importantly, there was the possibility that the Ang1/Tie2 ratio would highlight more hits that could complement the ones already obtained from quantitating the internalized Ang1. Indeed, although most of the hits remained the

same, some siRNAs were not considered hits anymore and some new siRNA were highlighted as significant when the expression of Tie2 was normalized. Significantly, the only reported mediator of the internalization of Tie2 besides Clathrin, CBL, did not appear as a significant hit from the normalized Ang1, implying that CBL could also be having a role in the expression of Tie2 or the available Tie2 in the cell surface in this case.

5.3 Pilot screening in HUVECs

Although the Tie2^{FLAG} receptor expressed in the HeLa Flp-In cells appeared to be as functional as the endogenous Tie2 in endothelial cells, I wanted to be able to extrapolate our results to a physiologically relevant system. Therefore, I decided to re-screen a selection of hits from the primary and secondary screens using HUVECs.

Optimization of transfection in HUVECs

Due to the characteristics of the culture of HUVECs I adapted the endocytosis assay to a 96-well plate, as it was technically very difficult to coat the wells of a 384-well plate with gelatin, which is required for a successful culture of HUVECs, and I was unaware of whether the presence of gelatin in the wells could interfere with the siRNA transfections. Since HUVECs are potential carriers of contaminants, including mycoplasma, I decided not to use the facilities in the SRSF in order to avoid contaminating the area and potentially affecting the work of other users. Hence the assays were all performed without the use of the dispensing or aspirating robots, increasing the chances of human-origin errors.

When optimizing the assay in a 96-well plate, for some reason I did not succeed in obtaining a good fluorescent signal from internalized Ang1 until I increased the hrAng1^{His} concentration to 300 ng/ml instead of 200 ng/ml so I incubated cells with 300 ng/ml of hrAng1^{His} when working with the 96-well plates.

The transfection of primary cells can be more challenging than transfections of primary cell lines. Doing a literature search I found that HUVECs have been transfected with siRNA using a wide variety of transfection reagents, including Dharmafect 1, although in some cases HUVECs were noted to be more difficult to transfect than other cells. I knew from the experience of a former member of our lab that the Neon transfection system can effectively deliver siRNAs into HUVEC cells and knock down the expression of proteins (data not shown). However, the Neon transfection system is not practical if many siRNAs have to be delivered. Hence, I wanted to see if Dharmafect 1 could be used to knock-down proteins in HUVECs. All the published protocols used a traditional forward transfection procedure, where transfection media is added to a culture of cells.

In contrast, having had a good experience transfecting HeLa cells by reverse transfection, where a suspension of cells is added to the transfection media, I decided to apply it for the transfection of HUVECs in the screen.

In a pilot experiment I compared the efficacy of the Neon system and the reverse transfection protocol with Dharmafect 1 for delivering siRNAs into HUVECs. To visually asses the internalization of the probes I used the siGLO-RISC free negative control RNA, which is labelled with DY-547. Cells were transfected with 100nM of siGLO-RISC in a final volume of 100uL per well, which is within the range of the transfections of HUVECs found in the literature. As seen in **Figure *44***, siRNA was clearly detectable in HUVECs transfected by either Neon or Dharmafect. Although the same number of cells and amount of siRNA were used, the Neon system appeared to have a higher effect on the cell number, indicating that a high cell death rate was present after the transfection procedure.

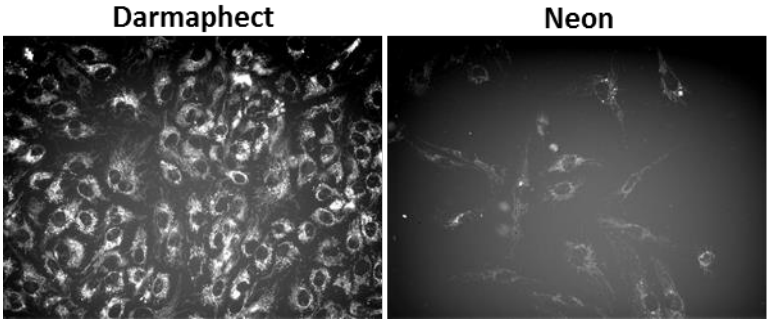

Figure 44. Reverse transfection with Dharmafect 1 effectively delivers siRNA into perinuclear areas of HUVECs. HUVECs were transfected by Neon electroporation or by reverse transfection using Dharmafect to deliver 62.5 nmol of non-targeting siRNA siGLO, which is fluorescently labelled to track the internalization of siRNA into cells. Live cells were imaged using the ImageXpress microscope 24 h after transfection.

Pilot siRNA screen in HUVECs

Having confirmed that siRNA was being internalized by cells using Dharmafect 1 in a reverse transfection protocol I proceeded to transfect HUVECs with the selected siRNAs and controls. Ideally, I would have liked to further optimize the transfection conditions for HUVECs but due to time restrictions of the project this was not possible. I selected siRNAs from the previous screens based on different factors and a detailed list can be found in **Sup. Table *7*** (Annex). Mainly, I selected hits taking into account their effects on Ang1 internalization, but I also took into account the effect of the siRNAs on Tie2 expression. I also considered the effects on the internalization of Tfn in order to decide if it was interesting to re-screen a siRNA in HUVECs (i.e. if it was Tie2 specific in HeLa cells). Furthermore, known protein interactions, either direct or indirect were also considered for the selection of hits. To do so I looked for protein interactions or common cell functions in different databases; mainly BioGrid (https://thebiogrid.org/), Gene-NCBI (https://www.ncbi.nlm.nih.gov/gene/) and Pubmed-NCBI (https://www.ncbi.nlm.nih.gov/pubmed). Finally, I also checked that certain genes were being expressed in HUVEC cells using either the Human Protein Atlas (www.proteinatlas.org) or the dataset GDS596 in GEO datasets (Su et al. 2004). In addition, this time I also included siRNA targeting ShcA (*SHC1*) and endophilin A2 (*SH3GLB1*). The ShcA is an adaptor protein containing both a PhosphoTyrosine Binding domain (PTB) and a Src Homology Domain (SH2) that is involved in the activation of signalling pathways after the activation of membrane receptors (Pelicci et al. 1992; Ravichandran 2001). ShcA has been described to bind Tie2 and to regulate Ang1-induced cell migration and sprouting (Audero et al. 2004). Furthermore, ShcA seems to be implicated in the internalization of EGFRs induced by EGF and appears to be present in early endosomes with the active receptor (Zheng et al. 2013; Oksvold et al. 2000) so I wanted to see if ShcA was involved in the endocytosis of Tie2 as well. Endophilin A2 was included for its roles in both clathrin dependent and independent internalization (Sundborger et al. 2010; Ferguson et al. 2009; Renard et al. 2014; Boucrot et al. 2015)and because I wanted to compare it to the Endophilin B1 siRNA, which had given a robust effect on Ang1 internalization in both screens with HeLa. As negative controls I included the OnTargetPlus non-targeting siRNAs #1-4 and the siGLO for the visualization of

transfected siRNA in cells. Also, one well was left as a non-transfected control by exposing cells to the same concentration of Dharmafect 1 without the presence of any siRNA. The final selection of siRNA that were screened on HUVECs is detailed in **Sup. Table *7*** (Annex). Since I had not tested the effect of the non-targeting siRNAs #1-4 in this new assay I included 4 replicates of each to ensure I could use any for the normalization of the data. However, due to technical restrictions I only included a single replicate of each siRNA to be screened and the previously used positive controls CBL, DNM2 and TEK. Two different plate configurations were used (**Figure *45***a).

Since I had previously shown that the Goat anti Tie2 antibody was specific for Tie2 in the HeLa T-REx Tie2 cells and that there was no cross-reaction of the secondary antibodies, I directly co-stained the plates for Ang1 and Tie2 so that the data acquisition could be simultaneous and the calculation of the Ang1/Tie2 ratio more accurate.

The acquired images were analysed using a modified version of the CME1 algorithm called CME1_HUVECs (**Table *4***). Because HUVECs spread in a wider area than HeLa cells I increased the area around the nuclei where the Ang1 fluorescent signal was quantitated. Furthermore, because the size of the nuclei in HUVECs is much bigger than in HeLas it was easier to create an algorithm that distinguished the smaller and brighter nuclei characteristic of dying cells. Hence I also included a module in the CME1_HUVECs algorithm that would identify and ignore nuclei with the mentioned description. In this case, Tie2 fluorescence was quantified using the CME2, which quantifies the fluorescence in the whole image instead of only a perinuclear area.

Overall, I attempted to repeat the screen 4 times although 2 of the repeats were lost due to the appearance of contamination in the wells. I previously had not had many problems due to contamination of culture in transfected HeLa cells, even though transfected HeLa cells were cultured with media without antibiotic for the 4 day long transfection experiments. However, due to the non-sterile conditions in which the umbilical cords are obtained, HUVEC cells are potential carriers of contaminants, the growth of which is unleashed after removing the antibiotics for the transfections experiments. The HUVECs used in each attempted repeat were from different donors,

and indeed, the second uncontaminated repeat was performed on an equal mix of HUVECs from two different donors, as I had seen in the literature that this was a common practice.

Selection of data

As before, I included in the normalization the data from images including a maximum of 50 cells (**Figure *45***b), after which cells started to look over confluent. This was to avoid any variation generated by differences in siRNA transfection, Tie2 internalization or cell shape affecting the segmentation of the fluorescent signal.

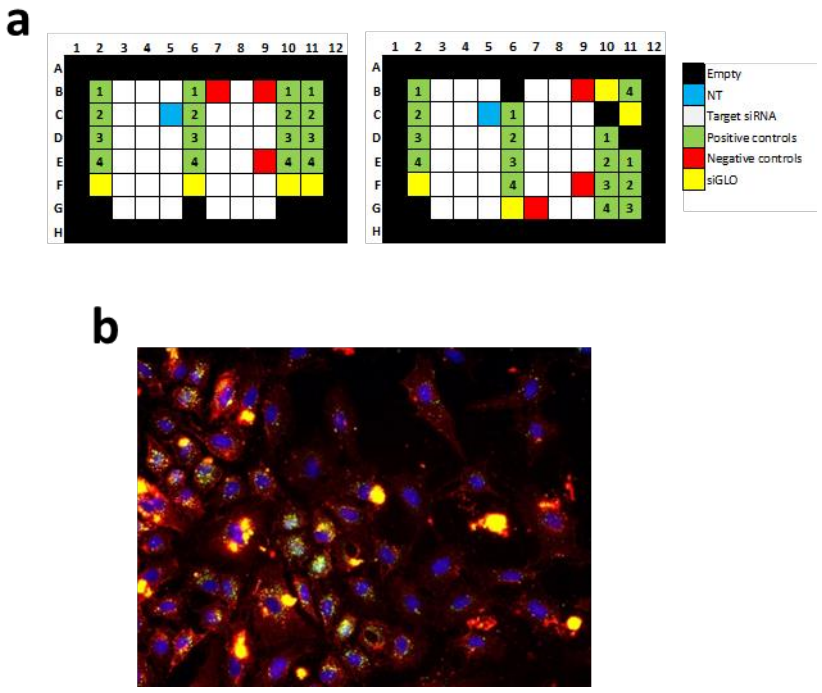

Figure 45. A selection of hits from the primary and secondary siRNA screens were re-screened on the internalization of Ang1 in HUVECs using a smaller format in 96-well plates. (a) Schematic representation of the 96-well plates and the well localization of the negative and positive controls in repeat 1 (left) and repeat 2 (right) of the pilot siRNA screen with HUVECs. The second repeat was performed on a pool of 2 HUVEC clones. Although not appreciable in the scheme, the location of many target siRNA was also changed in the second repeat. **(b)** A representative image from the screens is shown. In this case, HUVEC incubated with 300 ng/mL of hrAng1^{His} as indicated in the methods section were stained simultaneously for the internalized hrAng1^{His} and endogenous Tie2 and images were also acquired simultaneously for both. Tie2 was coloured red and hrAng1^{His} was coloured green.

I carefully looked for any technical problems or plate-effects affecting the non-targeting controls and discarded any clear outliers. In the first repeat well B2 containing non-

targeting siRNA #1 did not contain cells, wells B10 and C10 dried during an antibody incubation and presented remarkably different counts than the rest of the plate. I decided to discard as well the replicates for controls #3, #4 and siGLO in wells D6, E6, F6 as this presented unusual very high counts of Ang1/Tie2 ratio. Since I had up to 4 replicates of the negative controls in each plate, outliers were spotted with more confidence than for the candidate siRNAs. Nonetheless, in the second repeat the cells in column 5 appeared to lack any staining for Tie2 so I decided not to include those in the quantitation of Tie2 expression and Ang1/Tie2 ratio. In this case, the siRNA affected were STX8, ACTR2, ARPC2, AP2A1 and the NT control, for which I then had one repeat only. Finally, well B4 and B7 in the second repeat, containing siRNA targeting STX4 and CAV2, presented very high values of Tie2 or Ang1 and Tie2 staining and were also considered outliers.

The 96-well plates appeared to occasionally present physical defects in the base of the plate that would cause all the images of a group of adjacent wells to be out of focus. This was easily corrected by acquiring the images of the affected wells using specific focusing settings in the microscope. Nonetheless, the fluorescence in those images would be quantitated using the same exact algorithm as the wells that were initially in-focus. This was the case for row B in the first repeat, which included 2 valid repeats for C#1, and the siRNA for RAB4A, SHC1, STX8, DNM2, SH3GLB1 and TEK, and row F in the second repeat, which included the siRNA for AP2M1, ARHGAP26, CBL, RAB4B and STX6. The values for row F in the second repeat were then normalized with the rest of siRNA in the plate. The row B in the first repeat, on the other hand, also presented a problem with the antibody staining that would have led to much lower counts of Ang1 per cell and Tie2 per cell than the average of the plate. However, since the Ang1/Tie2 ratio from row B would not be affected by this problem I deduced that the whole row B in the first repeat had been exposed to a smaller volume of secondary antibodies, indicating that the proportions between the negative and positive controls in the well should be maintained. In a normal situation I would simply discard the whole row of results, but since I had no replicates and only two repeats I decided to use the negative control #1 in the same row B to normalize the values of the siRNA in row B separately from the rest

of the plate. I had previously seen when screening HeLa cells that control #1 would result in very similar results as control #2 and this was the case too for the second repeat in of the screen in (**Figure *46***). As seen in **Figure *47***, the normalized values for the positive controls DNM2 and TEK in the first repeat (both localized in row B) were extremely similar to the ones in the second repeat for internalized Ang1, Tie2 expression and Ang1/Tie2 ratio, hence indicating that the normalization of row B using the negative control #1 in the same row mathematically corrected the difference of staining. Nonetheless, I decided to be cautious when analysing the results on the rest of wells of row B in the first repeat, which contained the siRNA for RAB4A, SHC1, STX8 and, SH3GLB1.

Normalization of data

As described previously, data from each plate had to be normalized in order to be able to compare the effect of each siRNA between both repeats. Since I was screening a small selection of hits obtained from previous screens, and because I did not have the occasion to previously test which non-targeting siRNAs were optimal for screening in HUVECs using our internalization assay, I decided to normalize each plate using the averaged value for the replicates of a set of negative controls in each plate. I evaluated the means and standard deviations of each non-targeting siRNAs for each parameter: internalized Ang1, Tie2 expression and Ang1/Tie2 ratio in order to determine the negative controls to be used for each parameter. Since all the replicates for the non-targeting siRNA #1 in the first repeat where in row B, which had different fluorescent intensities to the rest of the plate, I directly excluded the previously used negative control #1 for normalizing the parameters Internalized Ang1 and Tie2 expression. Likewise, I discarded any non-targeting siRNA that appeared to be having any effect on a parameter. The spread of the replicates for each non-targeting siRNA compared to the values for CBL, DNM2, TEK and the plate results for each parameter and plate/repeat can be observed in **Figure *46***. In the end I used the non-targeting controls #2 and #4 for the normalization of internalized Ang1, controls #2 and 3 for the normalization of Tie2 expression and controls #1-4 for normalizing the proportions of Internalized Ang1 per Tie2 expression, as seen in the far right of each graph in **Figure *46***. By using more than one non-targeting siRNA I aimed to

strengthen the analysis statistics, especially after I had lost a third repeat to contamination and non-targeting control #1 in the first repeat.

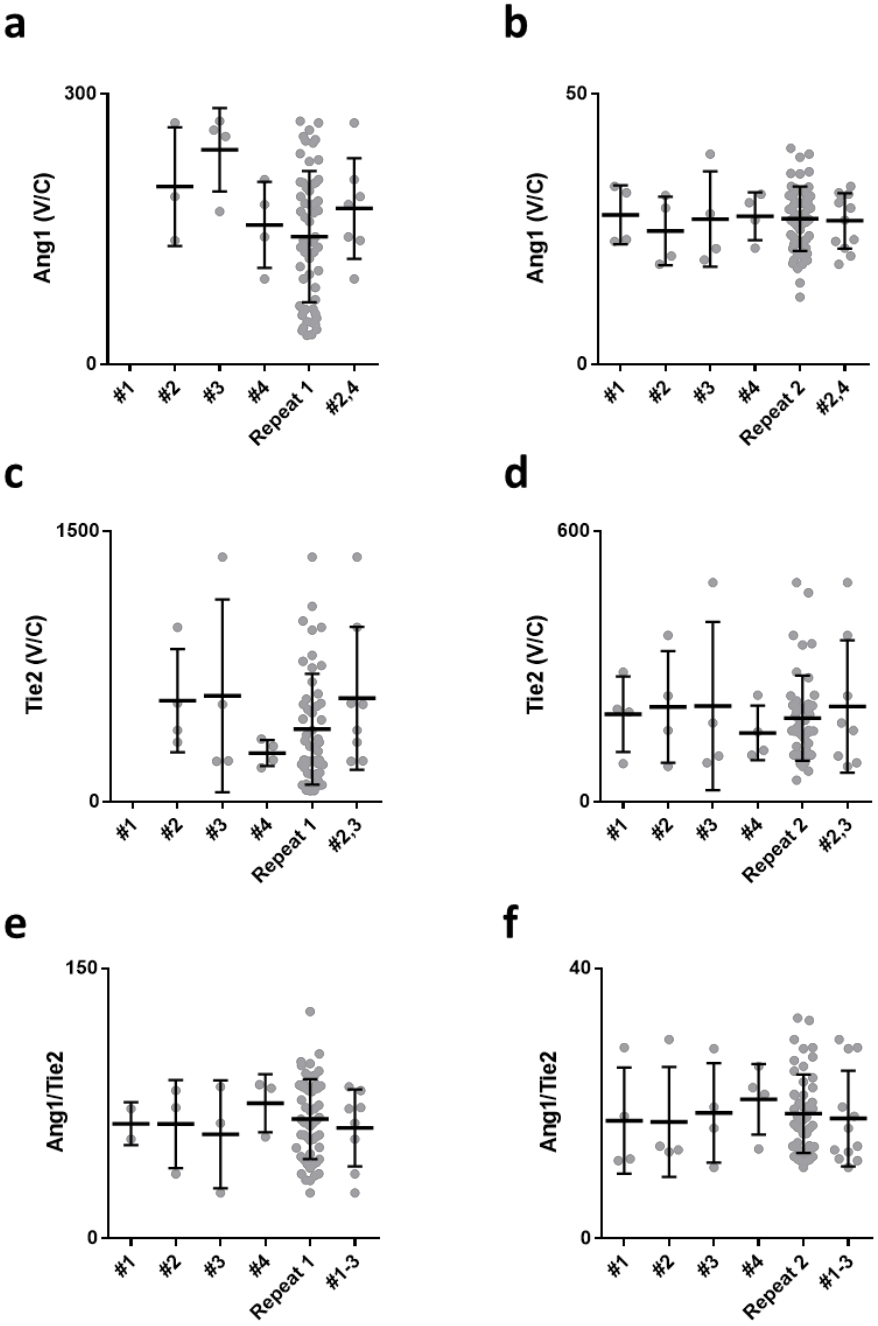

Figure 46. Results from two independent repeats of the siRNA screen in HUVECs were evaluated to determine the best negative control to be used for the normalization of each parameter. HUVECs transfected with the indicated siRNA and cultured in 96-well plates were serum starved and incubated with 300 ng/mL hrAng1^{His} for 45 min at 37˚C. Non internalized Ang1 was acid stripped on ice and cells were fixed and treated for immunofluorescence staining of hrAng1^{His} and Tie2. Several images were automatically acquired for each well in the 96-well plate and the Ang1 and Tie2 fluorescent signal was

automatically quantified and averaged for the images of each well, which represented a single replicate for each transfection within each plate. Graphs show the distribution of the replicates for the non-targeting controls **#1** to **#4** in comparison to all of the results in each repeat (**Repeat 1**, **Repeat 2**) and to the non-targeting controls used to normalize data for each parameter. The amount of quantitated Ang1-containing vesicles per cell **(a,b)**, the quantitated vesicle-like Tie2 staining per cell **(c,d)** and the percentage between last two **(e,f)** is shown for each repeat. Left hand panels **(a,c,e)** are for the first repeat and right hand panels **(b,d,f)** for the second repeat. The values for control#1 in **(a)** and **(c)** are not shown due to a plate effect affecting the intensity of all of the repeats. Mean ± SD is shown for all. Values of at least 4 replicate transfections are represented with dots for each repeat.

Evaluation of hits

The normalized values of internalized Ang1, Tie2 expression and Ang1/Tie2 ratio for the positive and negative controls in both repeats are shown in **Figure *47***. As explained for the secondary screen in HeLa cells I used the average of the standard deviations of the negative controls to determine the limit from which the effect of a siRNA would be considered significant. Furthermore, in order to consider that a siRNA was significantly affecting a parameter I determined that the values in both repeats had to be above or below the significance limit that I had defined. The limits for determining if an siRNA had a significant effect on the parameters were 100 ± 13%, 100 ± 7% and 100 ± 5% for the internalization of Ang1, Tie2 expression and the Ang1/Tie2 ratio respectively. The limits are indicated with dotted lines in the graphs of **Figure *47*** and **Figure *48***. As seen before, the negative controls 1 and 2 had similar results in this screen, whereas the effect of the non-targeting siRNA #3 and #4 was rather more variable depending on the parameter (**Figure *47***). In contrast, the transfection of siRNA targeting the positive control CBL did not yield a significant difference on the internalization of Ang1 as seen in the previous screens, but it did lead to a clear decrease in the levels of Tie2 detected, indicating that the mild significant effect observed in the Ang1/Tie2 proportion would be mainly due to the decrease in the expression of Tie2 in this case (**Figure *47***). I did observe a clear decrease in internalized Ang1 when transfecting siRNA for DNM2 as seen previously, yet since the siRNA for DNM2 decreased in a higher proportion the amount of Tie2 detected in the cells the Ang1/Tie2 ration resulted in a value that was above the significant limit in normalized data. As explained before, it could either be that the siRNA of DNM2 was causing a decrease in the expression of Tie2 or that it was causing a re-localization of the Tie2 to areas of cell that were not imaged. The reason why the internalization of

Ang1 was not decreased in the same proportion as Tie2 detection after transfection of DNM2 siRNA is uncertain, yet a plausible explanation could be that the DNM2 siRNA is causing both a decrease and a re-localization of the Tie2 receptor hence only partially affecting the internalization of Ang1; or that somehow the decrease in the internalization of Ang1 is somehow compensated. The transfection of siRNA targeting TEK did not appear to have any significant effect on the expression of Tie2, what may indicate that the transfection did not work. Still it did appear to actually increase the amount of internalized Ang1 and to decrease the proportion of Ang1/Tie2. Due to the apparent non-significant change of the expression of Tie2 I cannot explain this result, because for the proportion Ang1/Tie2 to decrease at the same time that the internalization of Ang1 is increased I would expect a proportionally much higher increase in the expression of Tie2. I believe that maybe with more repeats I would have a more logical result, as in the first repeat the levels of Tie2 detected were indeed much higher than the levels of Ang1 in proportion to the negative controls Nonetheless, I still could not explain how the transfection of siRNA targeting Tie2 receptor would be increasing the levels of internalized Ang1 and Tie2 when I would expect the contrary. I cannot rule out the implication of off-target effects. Overall, although I are confident that the siRNA were transfected into the cells, I believe that these results highlight that most probably the efficiency of the knock-down of proteins was low. Nonetheless, the fact that most of the controls had similar results in both repeats is a reassurance that at least some effect from the transfection was being observed. As mentioned before, the positive controls DNM2 and TEK had to be normalized using the negative control #1 in the first repeat due to a physical plate defect. Still, the resulting percentages were very similar between the two repeats so I decided to consider the other siRNA affected from plate defects in repeat 1 and 2 in the analysis of significant hits. Nevertheless, because all of this and because I ended with a maximum of 2 repeats per each siRNA I decided that I should be cautious in taking any conclusions from this screen and that I could rather consider it a pilot screen to maybe be implemented in the future.

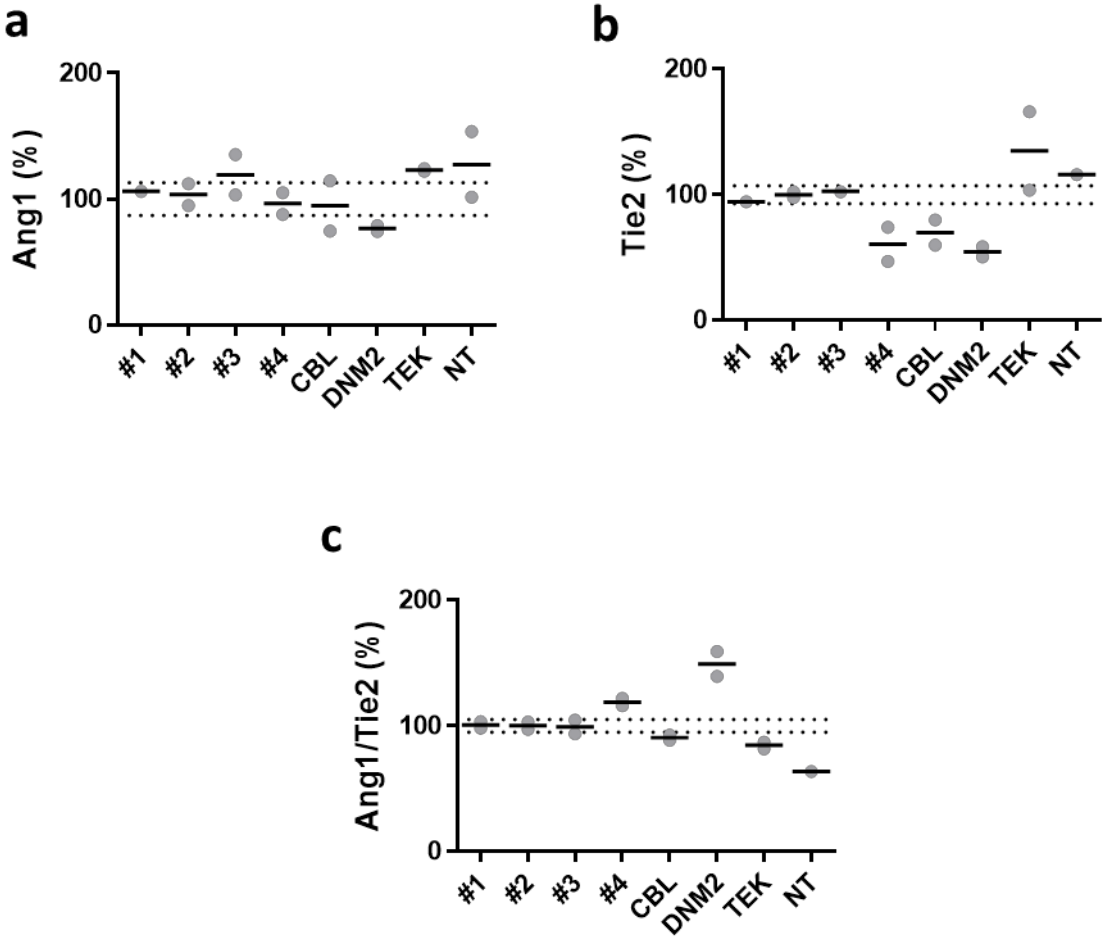

Figure 47. Efficiency of the knock-down was very low in HUVECs, yielding weak effects on the parameters. HUVECs transfected with the indicated siRNA and cultured in 96-well plates were serum starved and incubated with 300 ng/mL hrAng1^{His} for 45 min at 37˚C. Non internalized Ang1 was acid stripped on ice and cells were fixed and treated for immunofluorescence staining of hrAng1^{His} and Tie2. Several images were automatically acquired for each well and the Ang1 and Tie2 fluorescent signal was automatically quantified and averaged for the images of each well, which represented a single replicate for each transfection within each plate (represented with dots). For each parameter analysed, the normalized values of the positive controls CBL, DNM2 and TEK and of the negative controls non-targeting siRNAs #1-4 and Non-Transfected (NT) are shown. The limits for considering significant a siRNA are shown with doted lines for each parameter and those were set at 100 ± 13% for the internalization of Ang1 (a), 100 ± 7% for the detection of Tie2 (b) and 100 ± 5% for the proportion Ang1/Tie2 (c). Each dot represents the % value from an independent experiment (n=2).

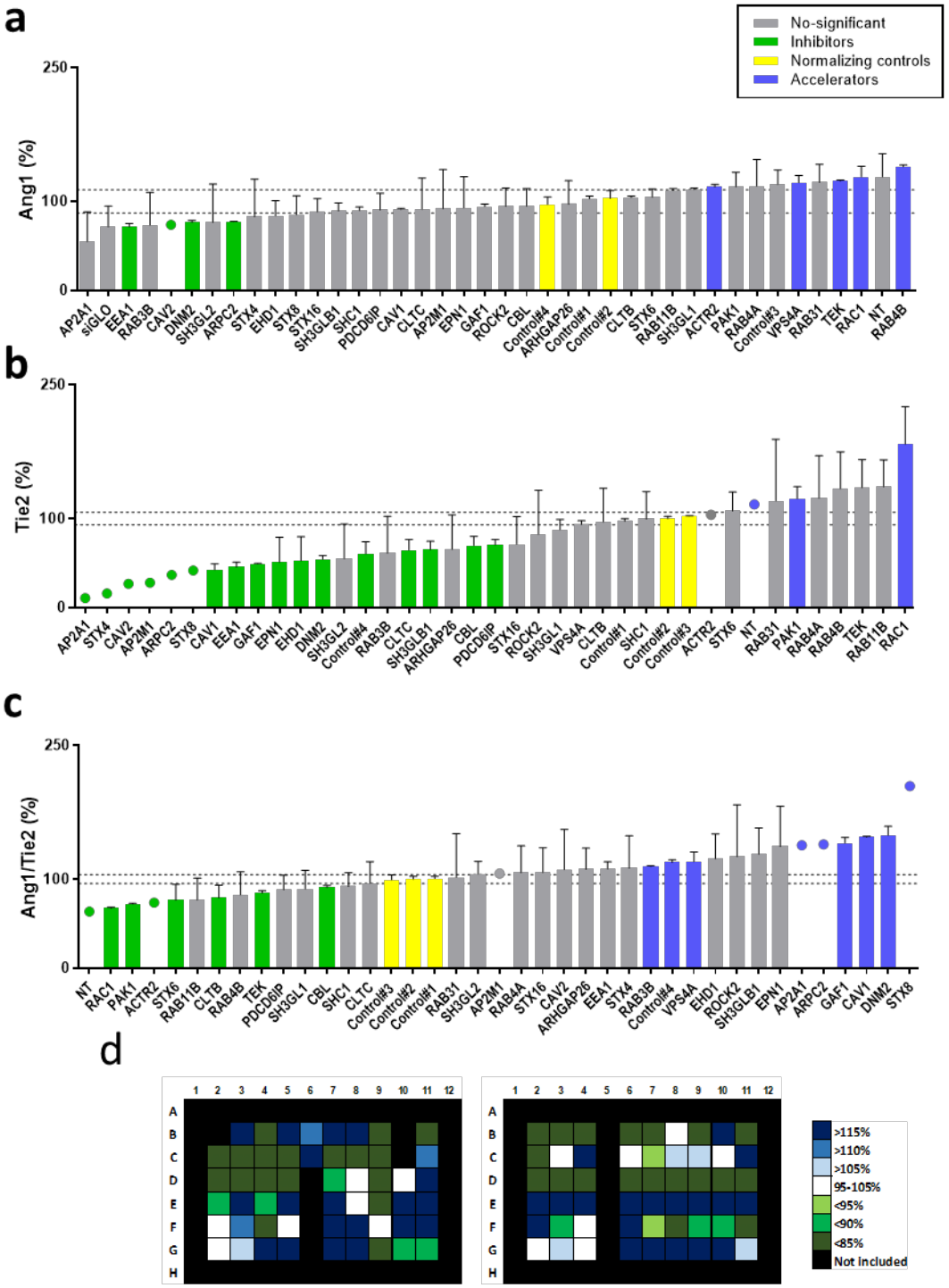

Figure 48. Although the siRNA screen in HUVEC gave much weaker effects than for the HeLa T-REx Tie2^{FLAG} cells the effect of some siRNA appeared to be robust between the two plates. HUVECs grown in 96-well plate were serum starved and incubated with 300 ng/mL hrAng1^{His} for 45 min at 37˚C. Non-internalized Ang1 was acid stripped and cells were fixed and treated for immunofluorescence staining of hrAng1^{His} and Tie2. Several images were automatically acquired for each well and the Ang1 and Tie2 fluorescent signal was automatically quantified and averaged for the images of each well. Graphs show the normalized values for each parameter analysed in HUVEC cells: **(a)** Internalized Ang1, **(b)** Tie2 expression and **(c)** Ang1/Tie2 ratio. The limits for considering that a siRNA significantly affects each

parameter are indicated by dotted lines. In order to consider the effect of a siRNA significant the value of both repeats had to be below or above the significant limit as explained in main text. Inhibitor and accelerator siRNAs, determined by the explained criteria, are coloured green and blue respectively and the non-targeting controls used for the normalization of data from each independent experiment are shown in yellow. Bars represent mean ± range two independent experiments (n=2). If one of the two repeats had to be discarded due to suspected plate effect the value of the remaining repeat is represented with a dot (n=1). **(d)** Plate location of normalized values for the parameter Ang1/Tie2, far left scheme represents the first valid repeat and far right the second valid repeat. Positions are coloured depending on the resulting normalized value as indicated in the legend

By applying the criteria explained above I found 9 siRNA that correlated with levels of internalized Ang1 that were below or above the set selection threshold (**Figure *48***a and **Sup. Table *7***). Interestingly, ARPC2, DNM2, EEA1, RAB4B and VPS4A had the same effect on the internalization of Ang1 as inhibitors or accelerators in the primary screen. Furthermore, ARPC2 and DNM2 had decreased the amount of internalized Ang1 in all three screens. Nonetheless, ACTR2 and RAC1, which had been classified as inhibitors in both screens in HeLa cells, were also found to significantly affect the amount of internalized Ang1, albeit in opposite sense (**Figure *49***a, **Sup. Table *5***, **Sup. Table 6** and **Sup. Table *7***).

I found 19 siRNA that correlated with levels of total Tie2 that were above or below the set selection threshold (**Figure *48***b), of which AP2A1, CAV1, CAV2 and PAK1 had also significantly affected the detection of Tie2 in the primary screens of HeLa cells. Cav2 knockdown had opposite effects in the HeLa versus the HUVEC screens. In contrast, only RAC1 was also found to increase the expression of Tie2 in the secondary screen (**Figure *49***b, **Sup. Table *5***, **Sup. Table 6** and **Sup. Table *7***).

Finally, I found 16 siRNAs that correlated to changes in the Ang1/Tie2 above or below the set selection threshold (**Figure *48***c). Of those, ARPC2, DNM2, PAK1, RAB3B, RAC1 and VPS4A had all also been selected as hits of the Ang1/Tie2 ratio in the secondary screen in HeLa cells, although only RAC1 had the same effect as had been observed in the secondary screen (**Figure *49***b, **Sup. Table *5***, **Sup. Table 6** and **Sup. Table *7***).

After considering the hits obtained from all three siRNA screens I decided that ARPC2, DNM2, PAK1, RAB3B, RAC1 and VPS4A were the strongest hits I was able to obtain from

the siRNA screens as they were found to repeatedly affect at least one of the parameters in all of the screens and all of them gave significant values of Ang1/Tie2 ratio in the secondary screen and in the screen in HUVECs (**Figure *49***).

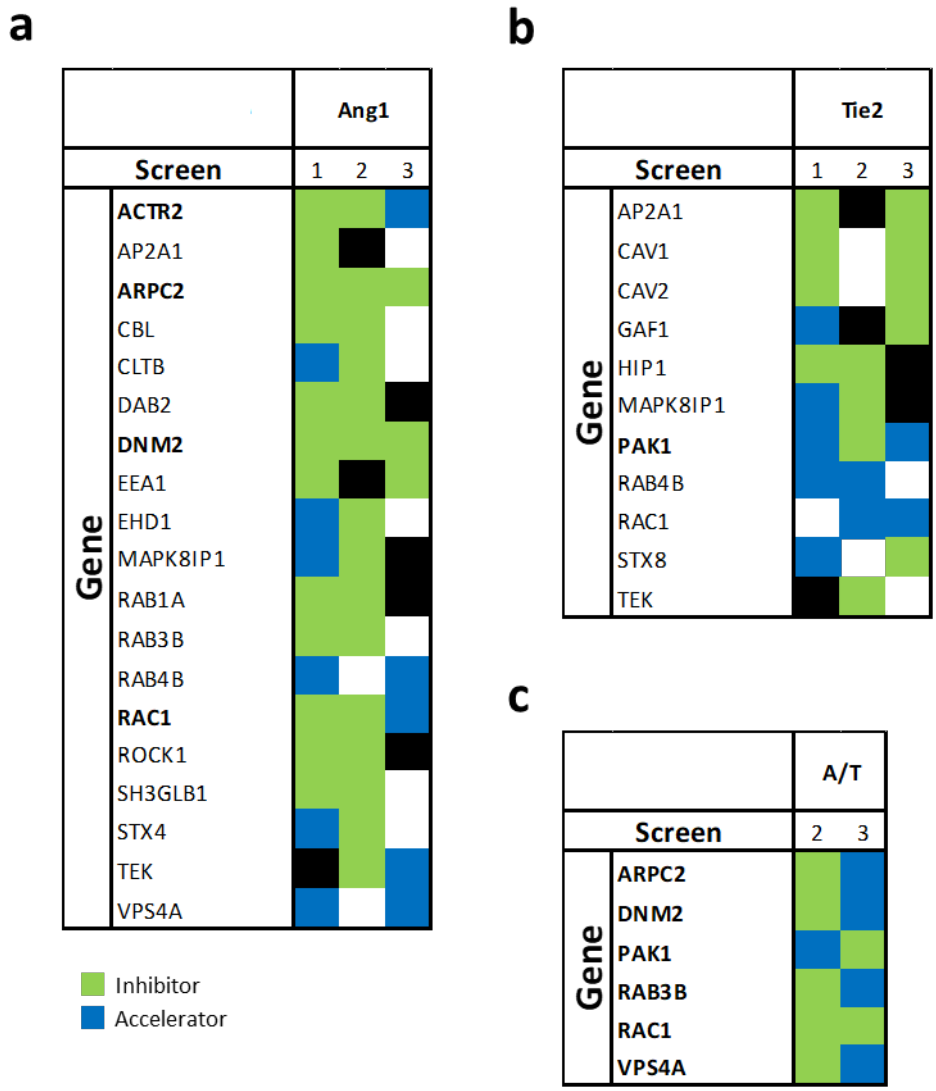

Figure 49. Selection of hits from each of the screens in HeLa and HUVECs. Genes were selected for a parameter if the siRNA transfection have caused a significant effect at least in two of the screens. The category of each gene for each screen and parameter is indicated with green or blue depending on whether it was found to decrease or increase each parameter. White colour denotes non-significance and black indicates that a gene was not screened in a particular screen. The primary and secondary screens on HeLas and the validation screen in HUVECs are named as screen 1, 2 and 3 respectively. Results are segregated depending on the parameter: **(a)** internalization of Ang1, **(b)** Tie2 staining and **(c)** Ang1/Tie2 ratio.

It is very significant that DNM2 was amongst the hits selected, as I used DNM2 as a negative control in the screens due to its known roles in membrane trafficking. The positive control CBL was not found to significantly decrease the internalization of Ang1 in HUVECs although it has been previously described to associate with Tie2 and mediate its internalization in HUVECs (Wehrle et al. 2009). Nonetheless, in the previous screens with HeLa, siRNA targeting CBL was found to have only a mild effect on the internalization of Ang1 so I believe that its absence in the last screen may be due to the weak knock-down efficiency and statistical strength.

Interestingly, the product of PAK1, the p21 (RAC) activated kinase 1 (Pak1) is activated by the ras-related C3 botulinum toxin substrate 1 or Rac1, the product of RAC1. Furthermore, Rac1 and Pak1 are known for their role in the cytoskeletal reorganisation that is required for cell motility (Edwards et al. 1999; Kumar & Vadlamudi 2002; Vadlamudi et al. 2004). In fact, Pak1 and Rac1 are both known downstream signalling mediators of Tie2 receptor for the activation of endothelial cell motility after the stimulation with Ang1 (Jones et al. 2003; Cascone et al. 2003).Furthermore, the products of ACTR2 and ARPC2 genes are known components of the Arp2/3 complex, which is implicated in the actin polymerisation associated with lamellipodia formation and cell motility (Goley & Welch 2006).

The persistence of Ras-related protein Rab3B (RAB3B) along the screens is intriguing as, along with other RAB3 isoforms, it has been implicated in secretory pathways rather than endocytosis. It has also been related to polarized transport of proteins to tight junctions in epithelial cells (Weber et al. 1994; Yamamoto et al. 2003). Although curiously RAB3B in endothelial cells localizes in the Weibel-Paladel Bodies (WPB), which contain the Tie2 ligand Ang2 among other components, but its role in WPBs is still unclear since it has repeatedly been reported not to be regulating the secretion of WPBs (de Leeuw et al. 2001; Zografou et al. 2012; Bierings et al. 2012).

Vacuolar Protein Sorting 4A, Vps4a (VPS4A) is an AAA-type ATPase that is also known for its roles in protein trafficking in yeast and mammalian cells. Interestingly, a study using overexpression of a dominant negative form of the mice paralog ($SKD1^{E235Q}$) in

mice fibrobasts demonstrated that Vps4 is necessary for normal trafficking of endosomes containing cell surface receptors and the dominant negative form induced an accumulation of receptors in late endosomes and Multi-Vesicular Bodies (Yoshimori et al. 2000; Fujita et al. 2002). Equally, human Vps4a was found to directly bind functional Ras proteins and to determine the association of Ras proteins to plasma membranes together with Vps20. Indeed, in the same study knockdown of Vps4a inhibited recycling of EGFR (Zheng et al. 2012). Consistently, I repeatedly found that transfection of VPS4A siRNA increased the amount of Ang1 detected in the primary screen, "confluent" condition in the secondary screen and in the HUVECs pilot screen. Still, results on Tie2 detection and Ang1/Tie2 ratio were not as consistent; Tie2 detection increased in the primary screen and "confluent" plating of the secondary screen but not in HUVECs; the Ang1/Tie2 ratio was decreased in the "sparse" plating of the secondary screen but increased in HUVECs.

In light of the results obtained, I think that the conditions for the transfection of siRNA in HUVECs need to be optimized and that more repeats are required in order to gain confidence in the hits obtained. Nonetheless, considering the reported relationships and results from the previous screens, I believe that it is highly feasible that Rac1, Pak1 and Arp2/3 complex are somehow involved in regulating endocytosis or trafficking of activated Tie2 receptor. The roles of Rab3B and Vps4A in Tie2 trafficking are also feasible although are less strong since no other related hits were found with them.

CHAPTER 6

Characterising the endocytic pathway of Tie2 receptor

6.1 Analysing the clathrin-mediated component of the internalization of Tie2 using immunofluorescence

As explained earlier, there is some conflicting data regarding the CME of Tie2 receptor as Tie2 was found to localise in CCPs and CCVs in HUVECs yet Tie2 internalization was not affected by knockdown of clathrin (Bogdanovic et al. 2009). Furthermore, data from a former member of our lab also showed a Tie2 internalization rate that was consistent with a CME of the receptor (Marron and Smythe, unpublished). Since the primary screen with HeLa T-REx Tie2^{FLAG} highlighted multiple hits that are involved in CME I decided to further explore whether Tie2 could be internalized by CME.

To evaluate whether Tie2^{FLAG} expressed in HeLa T-REx cells could be internalized via clathrin-mediated endocytosis I investigated the co-localisation of hrAng1^{His} with transferrin, the classical marker of clathrin-mediated endocytosis. The work of a former member of our lab showed that hrAng1^{His} did not co-localized with transferrin in HUVECs until late stages of endocytosis (Maxwell, Ferreira, data not shown). In a similar experiment, I co-incubated serum starved HeLa T-REx Tie2^{FLAG} cells with oligomerised hrAng1^{His} and fluorescent transferrin for 5, 15 and 20 min. Fixed cells were stained for the hrAng1^{His} and DAPI and I evaluated the co-localization between the ligands at the different time-points. The images showed little co-localization between transferrin and hrAng1^{His} and the co-localization coefficient was close to 0 in all the time-points (**Figure *50***). Nonetheless, I was able to spot occasional co-localization between the ligands in different areas of the cells depending on the incubation time-point. It appeared that at early stages of endocytosis (5 min) the ligands could be found partially co-localizing in the apical Z-sections of cells, whereas at later stages of endocytosis (20 min) I could observe occasional co-localization of the ligands in perinuclear endosomal-like structures. Still, as the PCC reflected, the occurrence of this events was rather small in comparison to the amount of ligand associated with cells (**Figure *50***). Overall, this results pointed out that the receptor was not internalized with transferrin in HeLa T-REx cells. Although Tie2 has been described to be only internalized in a clathrin-dependent manner, this results were in line with previous work with HUVEC from former members of our lab (Ferreira, data not shown).

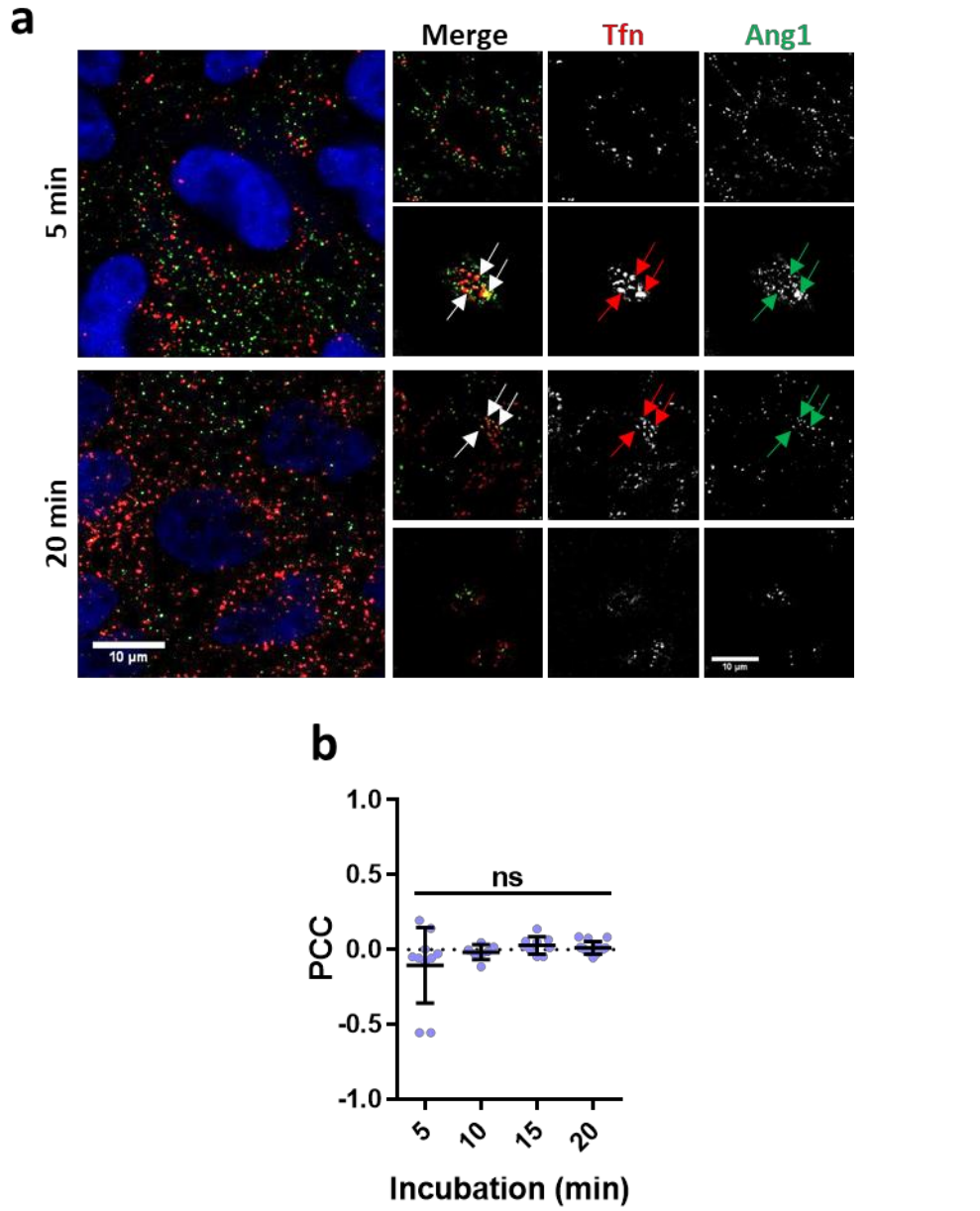

Figure 50. A small proportion of hrAng1^{His} co-localizes with Tfn in HeLa T-REx Tie2^{FLAG} cells. Serum starved HeLa T-REx cells expressing Tie2^{FLAG} were co-incubated with 5 µg/ml of fluorescent transferrin (Tfn) or 200 ng/ml of oligomerised hrAng1^{His} for 5, 10, 15 or 20 min. Ice-cold PBS was used to stop all membrane trafficking after each timep-point. Cells were then fixed and immunostained for hrAng1^{His} and stained with DAPI. Images were acquired using a Deltavision microscope and deconvolved using the Deltavision software. **(a)** Representative images of cell-basal, middle and apical sections are shown for 5 and 20 min incubation conditions. Scale bars show 10 µm. **(b)** Co-localization was measured with Volocity Image analysis software and Pearson's correlation coefficient (**PCC**) measures for single cells within a single experiment (n=1) are represented with dots. For each condition mean ± SD is shown.

Even though I did not see an apparently significant co-localization between hrAng1 and Tfn this does not rule out that the receptor could be internalized via CME, as it might only mean that the ligands were segregated in different clathrin-coated pits and delivered to a different sub population of endosomes, or internalized at different rates. To further investigate whether the receptor was internalized via CME I investigated the co-localization of the receptor with clathrin.

As seen before, cells incubated with hrAng1^{His} showed puncta that suggested that Tie2 receptor was being mobilized from the cell periphery, determined by the staining of CHC and contact with other cells, to more perinuclear locations as incubation times increased (**Figure *12***, **Figure *15***, **Figure *16*** and **Figure *17***, Chapter 3). Also, hrAng1^{His} could also be seen attached to the surface of the glass cover-slip. The staining of CHC was seen as well as punctate events distributed all over the cell cytoplasm with an enrichment of CHC in TGN as is expected (Friend & Farquhar 1967; Kirchhausen 2000) (**Figure *53***a). As seen in the figure, hrAng1^{His} showed little co-localization with endogenous CHC and this was mostly observed after late time-points of incubation. Co-localization between hrAng1^{His} and CHC could be spotted from 5 min of incubation in the apical sections and periphery of cell, but events were rare (**Figure *53***b). Co-localization events were more evident from 30 min of incubation and then hrAng1^{His} could be located with peripheral CHC puncta but also with peri-nuclear CHC staining. Nonetheless, events were still not abundant, as represented by the low correlation coefficient (PCC) (**Figure *53***c).

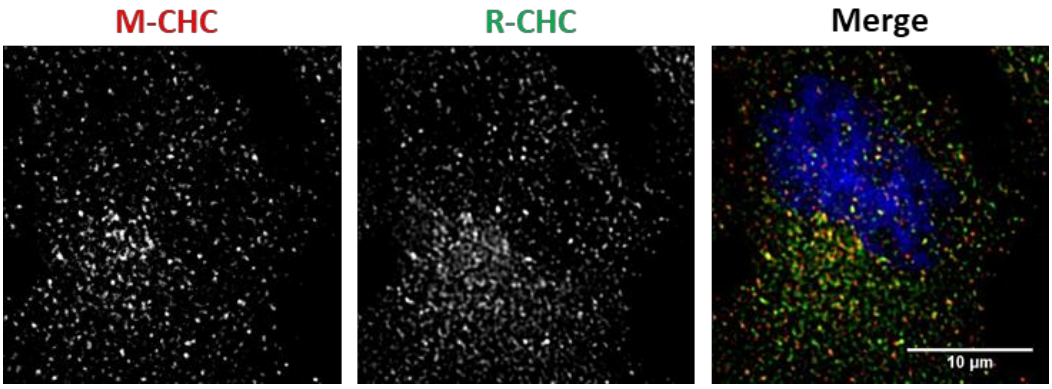

Figure 51. Mouse and Rabbit CHC antibodies present overlapping of immunofluorescence staining. HeLa T-REx Tie2^{FLAG} cells were fixed and immunostained for CHC using the mouse and the rabbit CHC antibodies available in our lab. Representative images from a single experiment are shown (n=1).

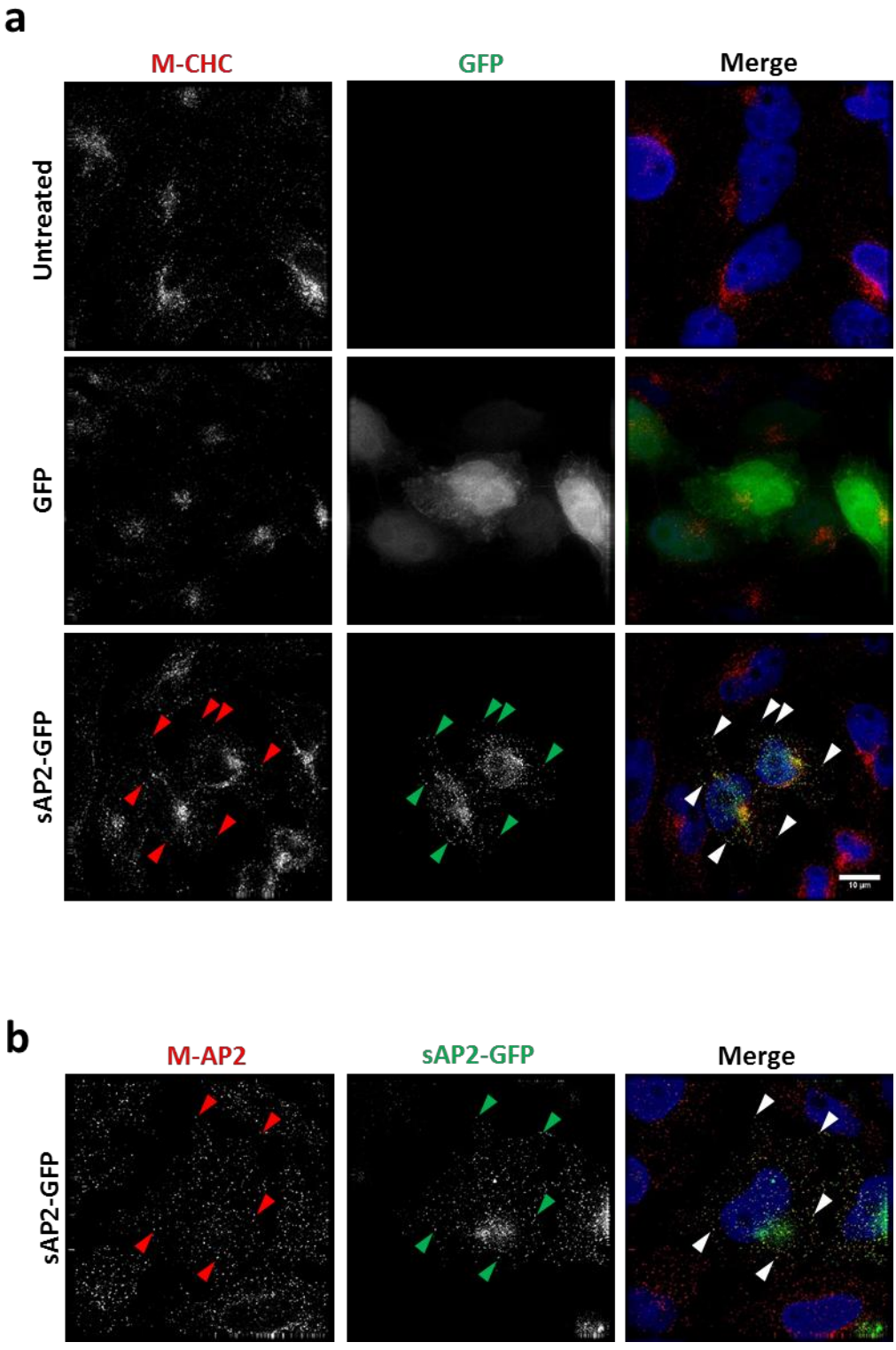

Figure 52. Control of the expression of GFP-çAP2. HeLa T-REx Tie2^{FLAG} cells were electroporated with the 5 µg of expression vector containing GFP-çAP2 and fixed for the immunostaining with **(a)** Mouse CHC and **(b)** Mouse AP-2 antibody. GFP-çAP2 expressed in cells co-localized almost completely with CHC and AP-2 antibody stainings. Representative images from single experiments are shown (n=1).

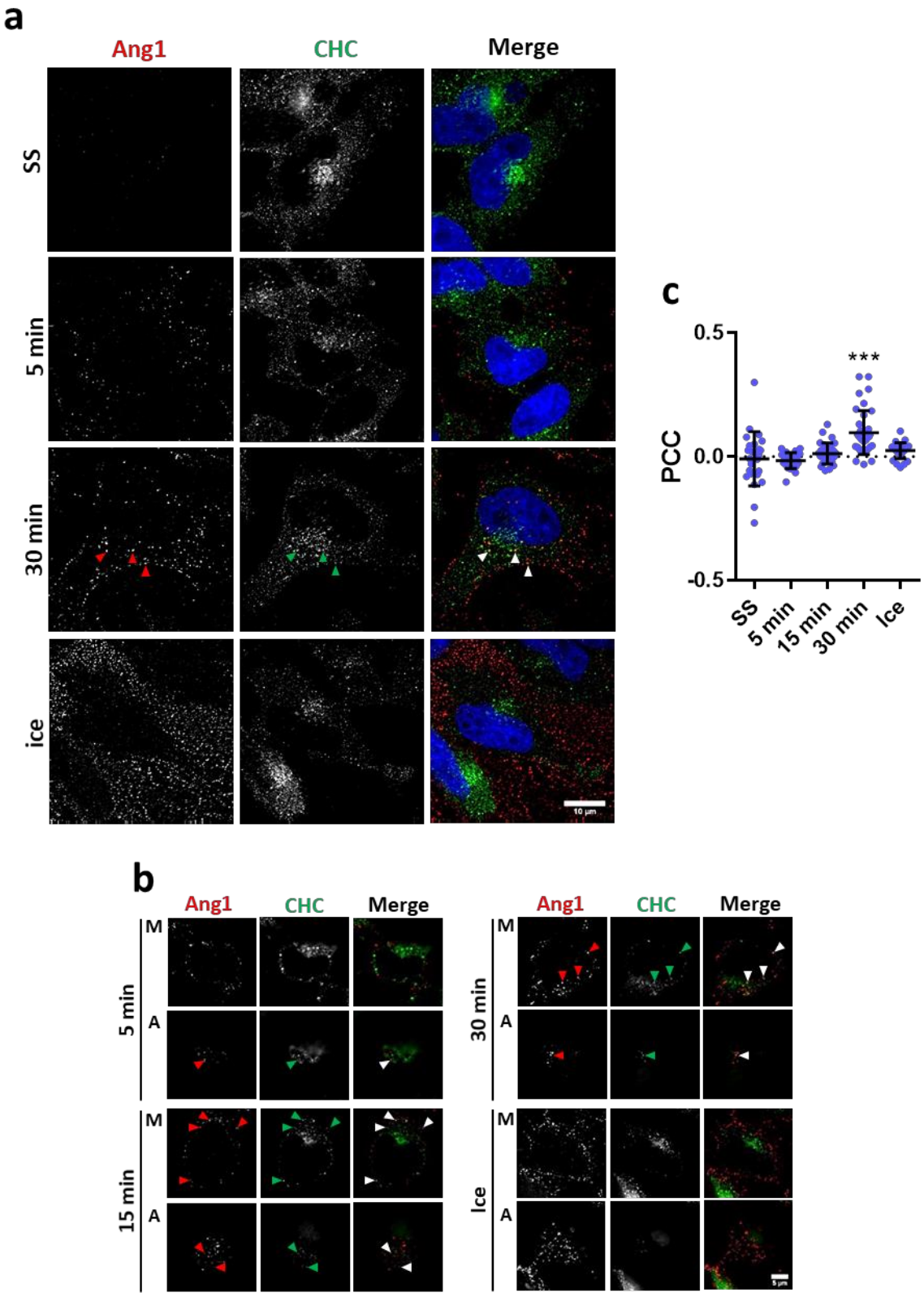

Figure 53. A small proportion of hrAng1^{His} co-localizes with Clathrin as seen by fluorescence immunostaining of Clathrin Heavy Chain. HeLa T-REx cells expressing Tie2^{FLAG} were serum starved and incubated with hrAng1^{His} for different times at 37˚C, kept on ice for 30 min or left untreated (**SS**). Ice-cold

PBS was used to stop all membrane trafficking. Cells were fixed and immunostained for hrAng1^{His} and CHC and stained with DAPI. **(a)** Representative images of basal Z-sections of cells from the different conditions. Co-localization between internalized hrAng1^{His} and CHC was appreciable only at 30 min of incubation. Images were acquired with a Deltavision microscope and deconvolved using the Deltavision software. Scale bar represents 10 µm. **(b)** Representative images of medial (M) and apical (A) Z-sections of cells. Occasional co-localization of hrAng1^{His} with CHC was spotted in apical sections of cells from 5 min of incubation and in the middle sections from 15 min of incubation with the ligand. Scale bar represents 10 µm. **(c)** Quantitation of co-localization was obtained from ROIs including a single cell each. Pearson's correlation coefficients were calculated by Volocity image analysis software and single cell measurements from a single experiment are represented with dots (n=1). Dunnett's multiple comparisions test for *one-way* ANOVA, $\alpha = 0.05$ (*** if $p < 0.001$).

To ensure that the co-localization of the hrAng1^{His} with endogenous CHC was due to the internalization of the Tie2^{FLAG} receptor in HeLa T-REx cells even if not being frequent I repeated the 30 min incubation using the HeLa T-REx cells expressing the kinase-dead mutant Tie2$^{K855R/FLAG}$ (**Figure *54***). Again, the co-localization between hrAng1^{His} and endogenous CHC in HeLa T-REx Tie2^{FLAG} cells could be visualized in both the cell periphery and perinuclear endosomal compartments. Also, as seen before, the HeLa T-REx Tie2$^{K855R/FLAG}$ cells internalised little hrAng1^{His} and this was limited to the periphery of cells, as assessed by the CHC staining. Furthermore, I could not observe any co-localization between hrAng1^{His} and CHC in the HeLa T-REx Tie2$^{K855R/FLAG}$ cells incubated with the ligand for 30 min (**Figure *54***), thus suggesting that the co-localization between hrAng1^{His} and CHC in HeLa T-REx Tie2^{FLAG} was due to the Ang1-activation and internalization of the receptor.

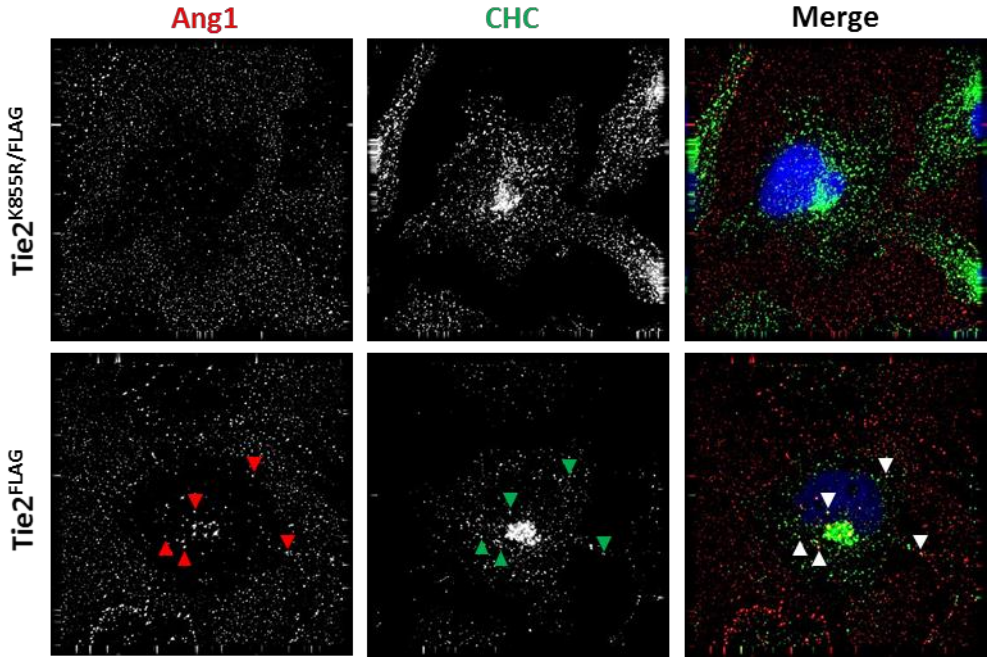

Figure 54. A fraction of hrAng1^{His} co-localized with CHC. HeLa T-REx expressing Tie2$^{K855R/FLAG}$ or Tie2^{FLAG} after 6h pulse with 1 µg/mL doxycycline were serum starved for 2h and incubated with serum free media containing 200 ng/mL hrAng1^{His} at 37°C for 30 minutes. Membrane trafficking was stopped by washing cells in ice-cold PBS. Cells were then fixed and analysed by immunofluorescence staining of hrAng1^{His} and CHC. Nuclei were stained with DAPI. Some of the Ang1 co-localised with CHC in the Tie2^{FLAG} expressing cells but not in cells expressing the dead kinase mutant (Arrowheads). Representative images from a single experiment are shown (n=1).

In order to use a different approach for the study of the co-localization of hrAng1^{His} and clathrin I transiently transfected cells with a construct encoding recombinant clathrin light chain conjugated to mCherry. In this case I used the rabbit Tie2 antibody to directly stain for the Tie2^{FLAG}. Similarly, I found that after incubating transfected HeLa T-REx Tie2^{FLAG} with hrAng1^{His} for 1, 2, 5, 15 or 30 min, occasional co-localization of the receptor was only clearly appreciable at the 30 min incubation time in the cell periphery or intracellular compartments in the medial z-sections of cells (**Figure *55***).

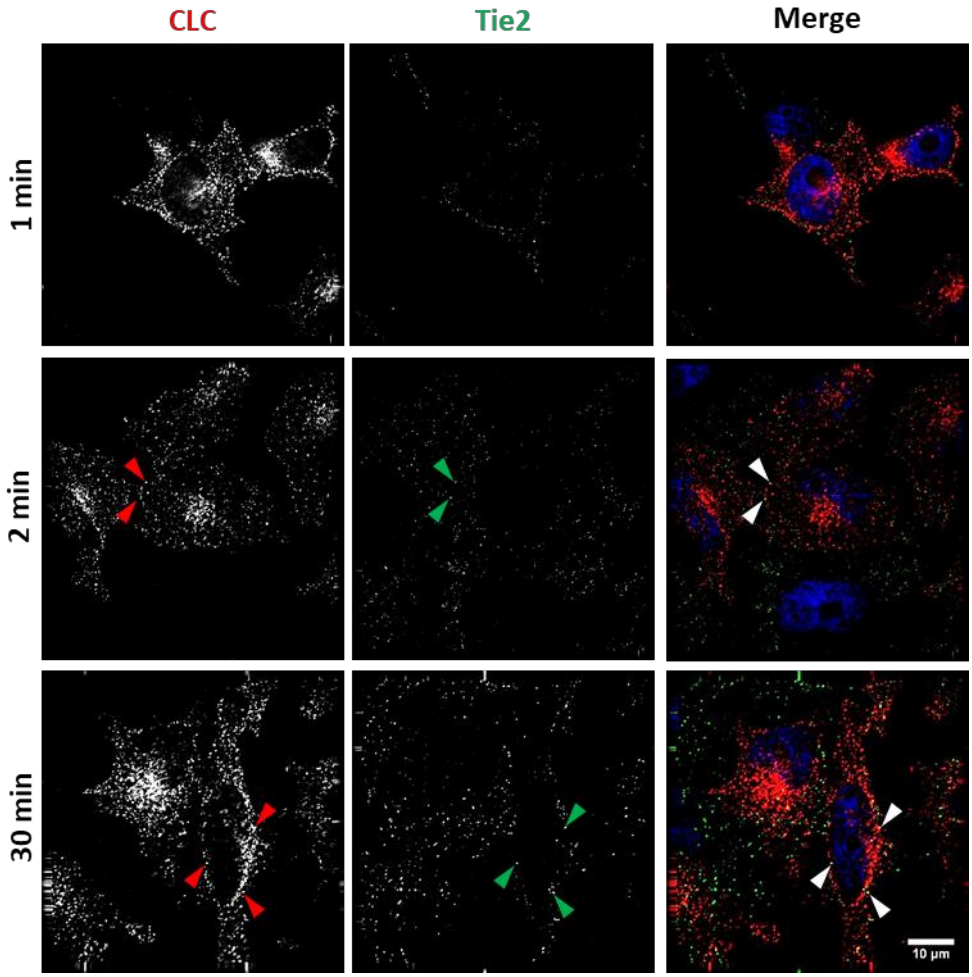

Figure 55. A small proportion of Tie2^{FLAG} co-localized with mCherry Clathrin Light Chain transfected in HeLa T-REx Tie2^{FLAG} cells after incubation with hrAng1^{His}. HeLa T-REx Tie2^{FLAG} cells electroporated with 5 µg of mCherry Clathrin Light Chain (CLC) expression construct and pulsed to 1 µg/mL doxyxycline for 6h were serum starved and incubated with serum-free media containing 200 ng/mL hrAng1^{His} for 1, 2 and 30 min at 37˚C. Ice-cold PBS was used to stop all membrane trafficking. Cells were fixed and immunostained for Tie2^{FLAG} using the rabbit Tie2 antibody. Nuclei were stained with DAPI. Images were acquired with a Deltavision microscope and deconvolved with the Deltavision software. Only basal Z-sections of cells are shown. Arrowheads point at co-localization between the ligand and mCherry CLC. Representative images from a single experiment are shown (n=1). Scale bar equals 10 µm.

Since I had found that a small portion of hrAng1/Tie2^{FLAG} co-localized with the endocytic protein clathrin, it is reasonable to think that at least a proportion of the activated receptor might be internalized via clathrin-mediated endocytosis.

CME is also very well characterized by the AP-2, which functions as a molecular adaptor between transmembrane cargoes and clathrin during the formation and transport of

clathrin coated vesicles (CCV). One of the subunits of the AP-2 complex was found to be significantly affect the internalization of Tie2 in the primary screen, therefore, I decided to investigate whether I could see a co-localization between hrAng1/Tie2^{FLAG} complex and AP-2. In this case, due to incompatibility of the antibodies available in our lab I transfected cells with a recombinant sigma-AP2-eGFP subunit (çAP2-GFP). Transfected çAP2-GFP generated a puncta pattern within cells that had a high co-localization with CHC and AP-2 antibodies staining (**Figure *52***). In line with the double-staining experiments of Ang1/Tie2 and Clathrin, I also found that çAP-2 could be occasionally spotted together with hrAng1^{His} in the cell periphery from 5 min of incubation but that co-localization was more evident only at 30 min of incubation with hrAng1^{His}. Furthermore, at 30 min of incubation the co-localization between çAP2-eGFP and hrAng1^{His} was found in small puncta close to the cell periphery or in bigger compartments closer to the nuclei (***Figure 56***). The immunofluorescence staining of CHC in the cells transfected with çAP2-eGFP and incubated with hrAng1^{His} revealed that some of the hrAng1^{His} associated with cells was again co-localizing with CHC, including few of the Ang1/çAP2-eGFP co-localizing events (**Figure *57***).

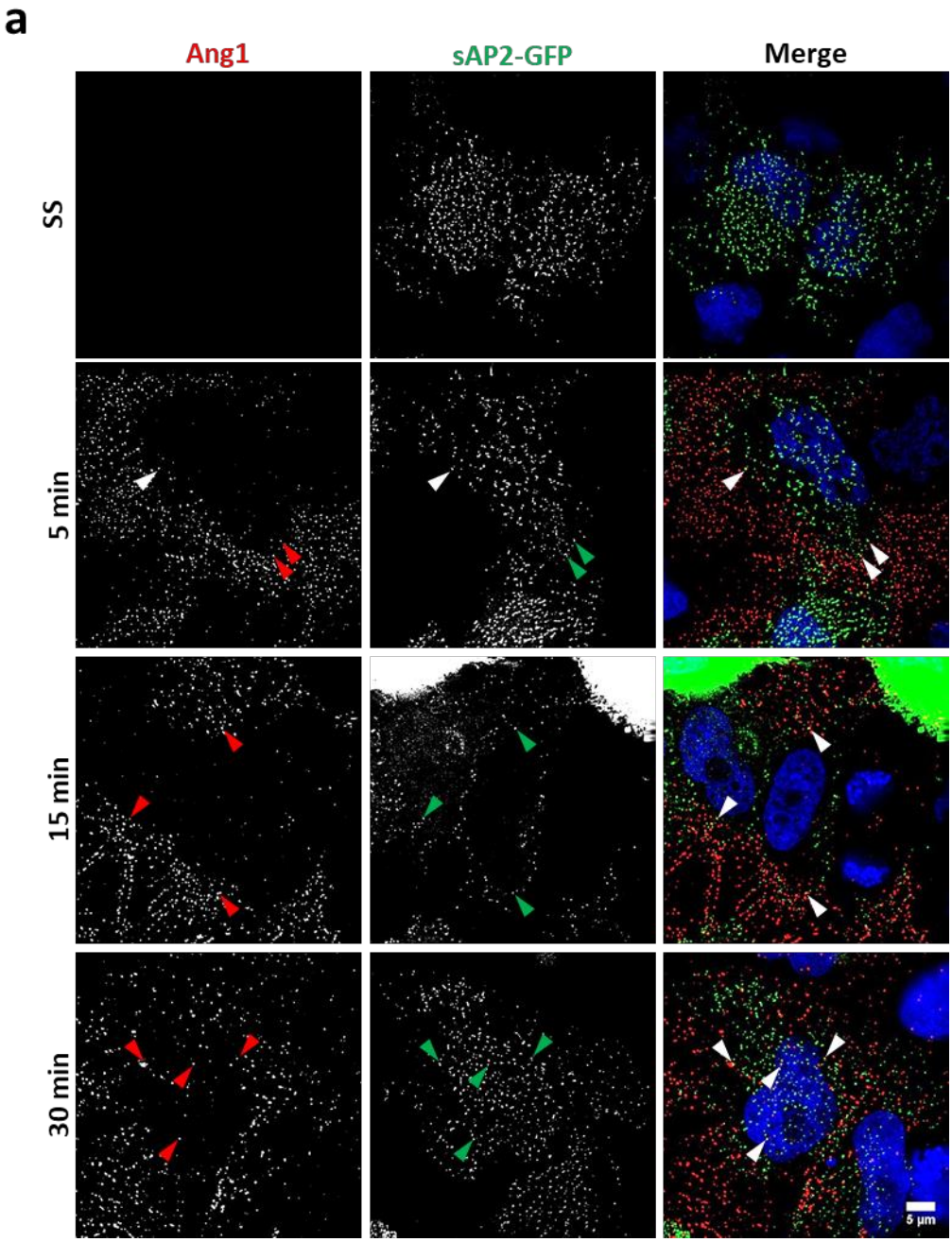

Figure 56. A small fraction of hrAng1^{His} co-localized with eGFP-ςAP2 subunit transfected in HeLa T-REx cells expressing Tie2^{FLAG} receptor. HeLa T-REx Tie2^{FLAG} cells electroporated (Neon) with 5 µg eGFP-ςAP2 expression construct and pulsed for 6h with 1 µg/mL doxyxycline were serum starved for 2h and incubated with hrAng1^{His} for 5, 15 and 30 min at 37˚C or left untreated. Cells were fixed and immunostained for hrAng1^{His} and CHC as well (Shown in Figure 57). Nuclei were stained with DAPI. Images were acquired with a Detlavision microscope and deconvolved with the Deltavision software. Only basal Z-sections of cells are shown. Arrowheads point at co-localization between the ligand and GFP-ςAP2. Representative images from a single experiment are shown (n=1). Scale bar indicates 5 µm.

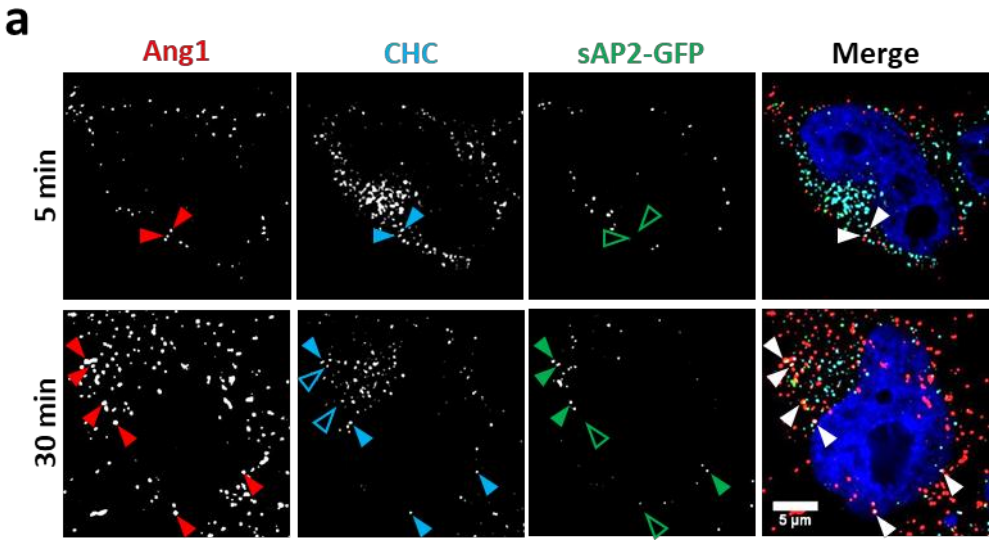

Figure 57. A small portion of hrAng1^{His} was found to co-localize with sAP2-GFP and CHC in HeLa T-REx Tie2^{FLAG} cells. Images show an enlargement of the medial sections of cells in Figure 56. Filled arrowheads highlight co-localization of fluorescent signal, while empty arrowheads highlight absence of co-localization. Representative images from a single experiment are shown (n=1). Scale bar indicates 5 µm.

6.2 Analysing the clathrin-independent component of the internalization of Tie2

Testing the sensitivity of the internalization of Tie2 to different inhibitors of internalization

In parallel to the siRNA screen I decided to test how the internalization of Tie2 was affected by pharmacological inhibitors of endocytic mechanisms. Sensitivity to certain endocytic inhibitors can be used as a broad indication of which internalization mechanisms may be involved in the endocytosis of a molecule. Nonetheless, since none of the pharmacological inhibitors known have a complete specificity for a particular endocytic pathway these were only used as a mere tool to complement the siRNA screening and immunofluorescent co-localization experiments.

In light of some preliminary results from the siRNA screening I decided to evaluate the effect of inhibitors of Clathrin-Independent Endocytosis (CIE) on the internalization of Tie2. To do so I initially decided to evaluate the effect of different inhibitors on the amount of internalized Ang1 using cell immunofluorescence in a low throughput format using HeLa T-REx Tie2 cells. Tie2 expressing HeLa T-REx $Tie2^{FLAG}$ cells were incubated with different pharmacological inhibitors and then Ang1 was added for 30 minutes. Cell surface ligand was removed by cold acid stripping and cells were fixed and prepared for cell immunofluorescence analysis. After a small literature research on pharmacological inhibitors used to inhibit different internalization mechanisms in HeLa cells I decided to use 5'-(N-ethyl-N-isopropyl) amiloride (EIPA) and Cytochalasin B at a 25µM concentration, and Filipin III from Streptomyces filipensis at a 5 µM (Ávila Olías 2014; Caì et al. 2015; Boucrot et al. 2015). EIPA is a chemical derivate of amiloride with better selectivity for inhibiting the plasma membrane Na^+/H^+ exchanger required for macropinocytosis and phagocytosis, (Ivanov 2008; Ávila Olías 2014); Cytochalasin B is a fungal metabolite that inhibits actin polymerisation (Ivanov 2008; Ávila Olías 2014), which is required for the successful completion of all CIE; and Filipin is a macrolide antibiotic and antifungal that sequesters cholesterol at the plasma membrane and hence interferes with all cholesterol dependent internalization processes such as caveolae endocytosis or macropinocytosis (Ivanov 2008; Ávila Olías 2014). Since I had

not previously tested that the inhibitors were effective at the detailed concentrations using our common protocols I co-incubated the HeLa T-REx Tie2^{FLAG} cells with Fluorescein isothiocyanate (FITC)-dextran70 kDa as a positive control of the inhibition of membrane trafficking. Dextrans are glucan compounds composed of multiple branches of glucose molecules. The average molecular weight of Dextran compounds can vary from 10 to 70kDa and, depending on the molecular weight, FITC-conjugated Dextrans can be used as markers of different internalization processes (Ivanov 2008; Li et al. 2015). For instance, FITC-Dextran70S is known to be excluded from the small pinocytic events produced during clathrin or caveolin-dependent endocytosis, so Dextran70S is used as a marker of internalization processes that involve larger volumes of membrane and fluid such as macropinocytosis or phagocytosis in cells that are rich in these events (Cole et al. 1990; Li et al. 2015). Since macropinocytosis is dependent on the plasma membrane Na^+/H^+ exchanger, actin polymerisation and cholesterol I would expect Dextran70S internalization to be affected by all three inhibitors (Mayor & Pagano 2007; Ivanov 2008; Doherty & McMahon 2009).

Using the internalization assay described above, I was able to visualize significant amounts of internalized Ang1 and small amounts of internalized Dextran70S in control cells incubated with DMSO (**Figure *58*** and **Figure *59***a). Interestingly, although in general Ang1 and Dextran70S appeared to be segregated in different intracellular compartments I did observe occasional co-localization of both molecules, suggesting that a small portion of Tie2 receptor could be internalized by macropinocytosis, although I cannot discard that smaller particles of dextran were being internalized through a different pathway (**Figure *58***).

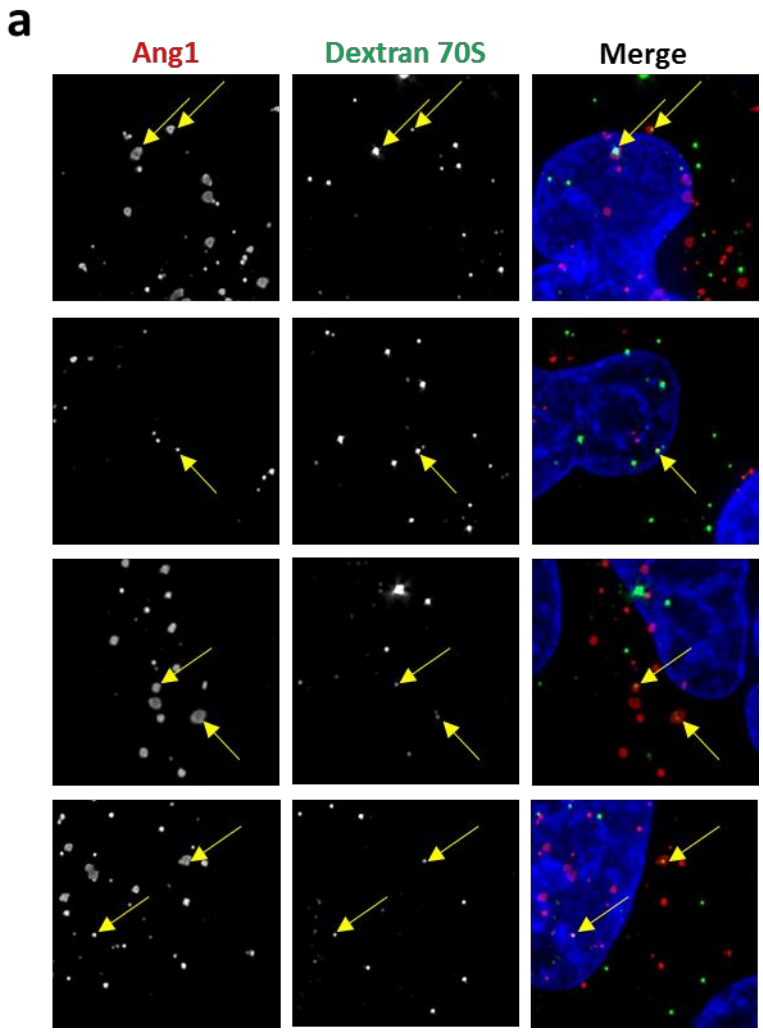

Figure 58. Some hrAng1^{His} co-localized with Dextran70S after co-incubation in HeLa T-REx Tie2^{FLAG} cells. Cells were serum starved for 2h in serum free media and then incubated at 37°C with media containing DMSO (0.1 %). After 20 min and 30 with DMSO, FITC-Dextran70S and Ang1 were added at 20 µg/ml and 200 ng/ml respectively. Ang1 was incubated for a total of 30 min before stopping all traffic with ice-cold PBS. Cell surface ligands were removed using 3 series of 5 min washes with Acid Wash Buffer. Cells were fixed with 4% PFA and stained for immunofluorescence analysis of Ang1 and nuclei using AF 568 Mouse antibody and DAPI. Several Z-stacks of cells were acquired using a Deltavision microscope and deconvoluted with the Deltavision software. Representative images from a single experiment are shown (n=1).

Despite that the amount of internalized Dextran70S was small it seemed clear that Dextran 70S containing vesicles were less frequent and smaller after incubation of cells with any of the three inhibitors (**Figure *59***). The internalization of Ang1, on the other side, appeared to be only affected by Cytochalasin B, when Ang1-containing vesicles would appear smaller and dimmer. Although EIPA and Filipin did not seem to have any drastic

effect on the internalization of Ang1 it looked like there were more Ang1-containing vesicles (**Figure *59***). Still, an image quantification method was not optimized to further confirm this observation.

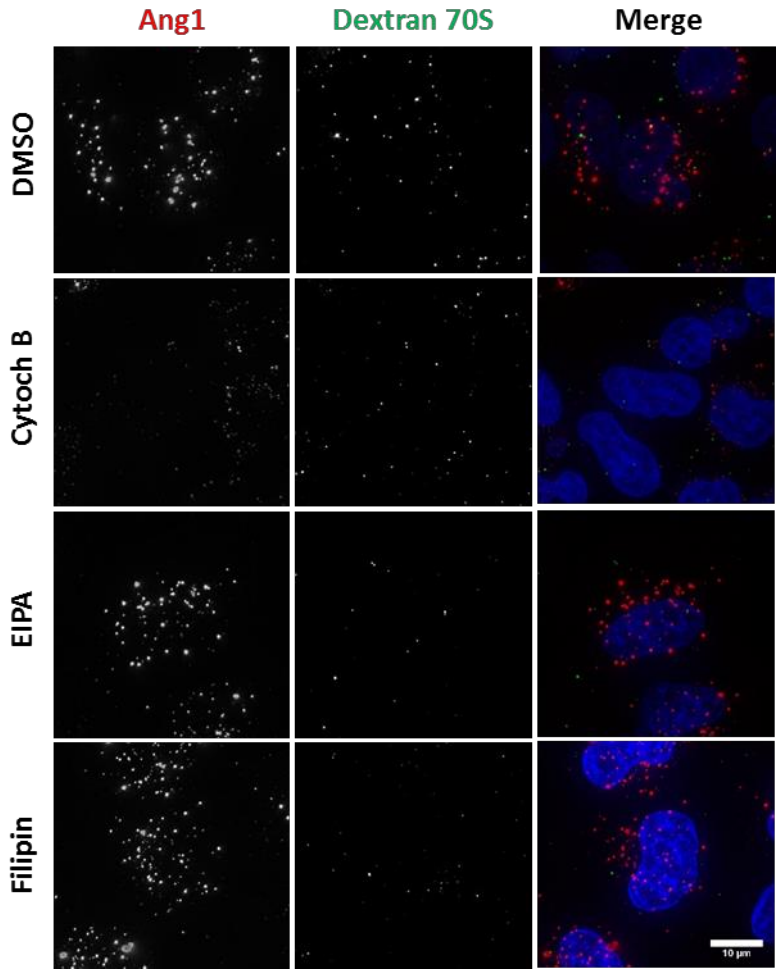

Figure 59. Internalization of hrAng1^{His} in HeLa T-REx cells was sensitive to the inhibitor of actin polymerisation Cytochalasin B. HeLa T-REx Tie2^{FLAG} cells were serum starved for 2h in serum free media and then incubated at 37°C with media containing DMSO (0.1 %), Cytochalasin B (25 µM), EIPA (25 µM) or Filipin (5 µM). After 20 min and 30 with the inhibitors FITC-Dextran70S and Ang1 were added at 20 µg/ml and 200 ng/ml respectively. Ang1 was incubated for a total of 30 min before stopping all traffic with ice-cold PBS. Cell surface ligands were removed using 3 series of 5 min washes with Acid Wash Buffer. Cells were fixed with 4% PFA and stained for immunofluorescence analysis of Ang1 and nuclei using AF 568 Mouse antibody and DAPI. Images show composition of several Z-sections from cells. Representative images from a single experiment are shown (n=1). Scale bar represents 10 µm.

In parallel to the co-incubation of Ang1 and Dextran70S I also co-incubated Ang1 with Cholera Toxin B conjugated to Alexa Fluor 555 (CtxB^{555}) in cells exposed to the same concentrations of DMSO, Cytochalasin B, Filipin or EIPA (**Figure *60***). Cholera Toxin B

subunit is known to bind GM1 gangliosides in the surface of cells and it is supposed to be internalized mainly via caveolae, although it seems that it can also be internalized via caveolin and clathrin-independent endocytosis or clathrin mediated endocytosis depending on conditions and cell type (Torgersen et al. 2001; Mayor & Pagano 2007; Blagojević & Mahmutefendić 2008). Therefore, I would expect $CtxB^{555}$ to be sensitive to Cytochalasin B and Filipin mainly but not to EIPA. Unfortunately, I found that $CtxB^{555}$ appeared to be not-uniformly distributed among the HeLa T-REx $Tie2^{FLAG}$, what made impossible to determine whether the inhibitors had an effect on the internalization of the $CtxB^{555}$. Nonetheless, I was able to observe that most of the Ang1-containing perinuclear endosomes also contained $CtxB^{555}$, while $CtxB^{555}$ was also distributed in other intracellular compartments that did not contain Ang1. Furthermore, it was clear again that exposure to Cytochalasin B generated smaller and dimmer vesicles of Ang1. Filipin and EIPA, on the other hand, did not appear to increase the amount of Ang1 containing particles (**Figure *60***). Since $CtxB^{555}$ and Ang1 were found to co-localize in some intracellular compartments it is not unreasonable to think that by co-incubating the ligands, $CtxB^{555}$ could be interfering somehow in the effect that the inhibitors have on the internalization of Ang1. For instance, in the case where $CtxB^{555}$ was competing with Ang1 for a particular internalization mechanism the effect of an inhibitor on Ang1 internalization could be seen diminished.

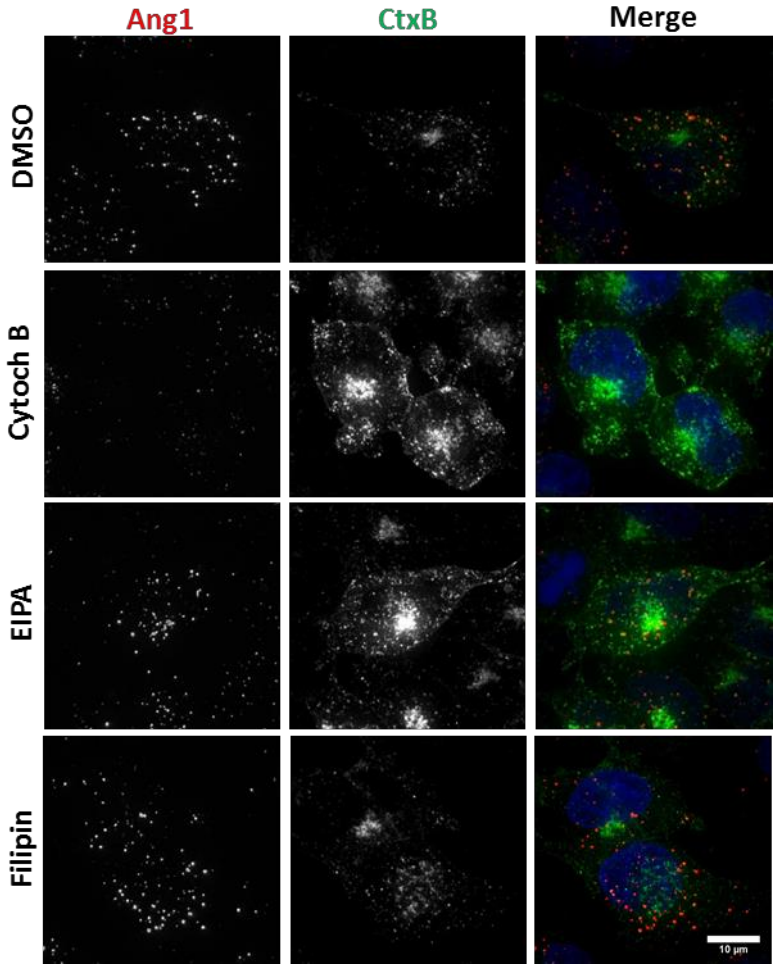

Figure 60. Internalization of hrAng1^{His} in HeLa T-REx cells was sensitive to the inhibitor of actin polymerisation Cytochalasin B. HeLa T-REx Tie2^{FLAG} cells were serum starved for 2h in serum free media and then incubated for 30 min at 37°C with serum-free media containing DMSO (0.1 %), Cytochalasin B (25 µM), EIPA (25 µM) or Filipin (5 µM). After 30 with the inhibitors AlexaFluor555-CtxB and Ang1 were added at 5 µg/ml and 200 ng/ml respectively. Ligands were incubated for a total of 45 min before stopping all traffic with ice-cold PBS. Cell surface ligands were removed using 3 series of 5 min washes with Acid Wash Buffer. Cells were fixed and stained for immunofluorescence analysis of Ang1 and nuclei using AF 568 Mouse antibody and DAPI. Images show a compilation of several Z-sections of cells. Representative images from a single experiment are shown (n=1). Scale bar represents 10 µm.

In conclusion, it appeared that the normal internalization of activated Tie2^{FLAG} in HeLa T-REx cells was sensitive to Cytochalasin B yet this effect was not quantified. A role of actin polymerisation during Ang1 internalization would not be surprising, as actin polymerisation can play a role in multiple internalization pathways. Also, this would be consistent as well with the fact that Dynamin 2 and some subunits of the Arp2/3 complex were robust hits from the siRNA screening. On the other hand, EIPA and Filipin

did not appear to have an effect on the amount of internalized Ang1 detected as changes observed were not drastic and on Ang1 internalization and were not consistent between the two conditions. As explained before, it could not be discarded that co-incubation with $CTxB^{555}$ had an effect on the internalization of Ang1 as ligands were observed to co-localize in intracellular compartments. Although it could have been interesting to develop a method to quantitate the amount of internalized ligands in order to further confirm the visual observations described, I decided not to repeat the experiment in HeLa T-REx cells as there are more specific ways than pharmacological inhibitors to elucidate the internalization pathway of Tie2 receptor.

I did, however, repeat the test using HUVECs, as they are a more physiologically relevant system than the HeLa T-REx cells. To increase the confidence in the results I performed the experiment in a high throughput format to have the images automatically acquired and analysed. After a second literature search about drug sensitivity of HUVECs I decided to use EIPA at 834nM, Filipin complex at 2 µg/mL, EHT1864 at 10 µM (Désiré et al. 2005; Shutes et al. 2007) and Cytochalasin D at 20µM (Muro et al. 2003; Huth et al. 2006; Raghu et al. 2009). Filipin complex is composed of Filipin I, II and III although Filipin III is supposed to be the main component (Ivanov 2008; Ávila Olías 2014); EHT1864 is a chemical compound that inhibits Rac function (Désiré et al. 2005; Shutes et al. 2007); and Cytochalasin D is an inhibitor of actin polymerisation similar to the Cytochalasin B previously used (Ivanov 2008; Ávila Olías 2014). As a positive control of the effect of the inhibitors I used FITC-Dextran70S again but at a higher concentration to increase the fluorescence yield (100 µg/mL). Endocytic markers were incubated separated this time to avoid any interference on the internalization route of each. For each of the incubation of the compounds and Ang1 I included 3 replicates to visualize the robustness of the results. Also, two of the repeats of Ang1 incubation with each drug treatment were stained for Tie2 receptor or phalloidin conjugated with TRITC to have a visual control of the effect of the drugs on the distribution of Tie2 receptor and on the actin filaments in cells respectively. The inhibitor of Rac1 EHT1864 and the TRITC-Phalloidin were kindly donated by Dr. Dan Humphreys and Dr. Mark Bass in the Biomedical Science Department. I used the HT ImageXpress microscope and the MetaXpress image analysis

software to automatically acquire and analyse several images for each condition and replicate. Images were analysed using the same segmentation protocol used for the siRNA screen in HUVEC, albeit some variations were introduced for detecting the FITC fluorescence of Dextran70S. Unfortunately, Filipin complex at 2 µg/ml was too toxic for HUVEC cells and I could only see remaining nuclei surrounded by traces of membranes. When observing the images it was clearly appreciable that the internalization of Dextran 70S was being inhibited by EIPA, EHT1864 and Cytochalasin D treatment. This was also reflected by the quantitation of the FITC fluorescence as the amount of FITC-containing vesicles per cell, although I did not have repeats to perform a statistical analysis of the differences between treatments (**Figure *61***). Strangely, EIPA appeared to inhibit the internalization of Tfn, what was unexpected as EIPA is not supposed to affect CME, I wonder if this may be an effect of the long incubation of Tfn within the cells or maybe only a reflection of the lack of replicates for Tfn incubation. Actually, Ang1 quantitation of the three plate replicates incubated with EIPA and Ang1 shown a high variation of results. In the case of Ang1, internalization of Ang1 only appeared to be affected by Cytochalasin D, which seemed to change the size and distribution of the intracellular structures containing Ang1 and overall the amount of internalized Ang1, still, this could not be reflected by the automatic quantitation (**Figure *61***). Since the quantitation is based on the amount of vesicles per cell only, changes in the size or intensity of Ang1-containing vesicles might not be reflected by this parameter. These changes were consistent with previous results in HeLa T-REx Tie2^{FLAG} cells, where it appeared that cells exposed to Cytochalasin B internalized Ang1 into numerous small and dimmer Ang1-conaining vesicles yet according to the results the amount of Ang1-containing vesicles/cell was not affected by Cytochalasin B (**Figure *59*** and **Figure *60***). Again, the control of the internalization of FITC-Dextran under exposure to Cytochalasin D was clearly indicating that the drug at the concentrations used was effective for this marker. Furthermore, the actin filaments of cells were clearly being disrupted by Cytochalasin D and also the distribution of the Tie2 receptor appeared to be disturbed by the inhibitor. On the other hand, Tfn internalization did not appear to be disrupted under exposure to Cytochalasin D: although the staining pattern of internalized Tfn was changed the Tfn-

containing vesicles did not appear dimer in the images and the Tfn vesicle count was not decreased compared to the DMSO control (**Figure *61***). This was expected as the formation of CCVs in cells in culture is generally not dependent on actin polymerisation (Boulant et al. 2011; Engqvist-Goldstein & Drubin 2003). Therefore, the fact that the total amount of Ang-1 containing vesicles did not change under exposition to Cytochalasin D as neither did Tfn could indicate that Tie2 internalization is internalized via actin-independent mechanisms in these conditions. Still, Tfn-containing vesicles did not appear to be dimmer nor smaller under exposition to Cytochalasin D as did Ang1-containing vesicles so a role of actin cytoskeleton during the internalization of Ang1 could not be discarded. Hence, further experimentation would be necessary to determine whether actin cytoskeleton influences the internalization mechanism of Tie2.

That Tie2 internalisation was not obviously inhibited by either EIPA or Rac1 inhibitor EHT1864 was intriguing as Rac1 and its effector Pak1 had been found a robust hit throughout the siRNA screening. Still, it is true that in this case I had to work with a high confluency of cells and in most of the images cells were rather confluent, since RAC1 siRNA did not have any significant effect on the Ang1 internalization when HeLa T-REx $Tie2^{FLAG}$ were plated in confluent conditions I wondered whether this may be suggesting whether Rac1 could only have a role in the internalization of Tie2 when cells are in sparse cultures. Nonetheless, I believe that further corroboration of the role of Rac1 in the internalization of Tie2 should be determined by other means, such as using constitutively active or inactive mutants of Rac1 and its regulators.

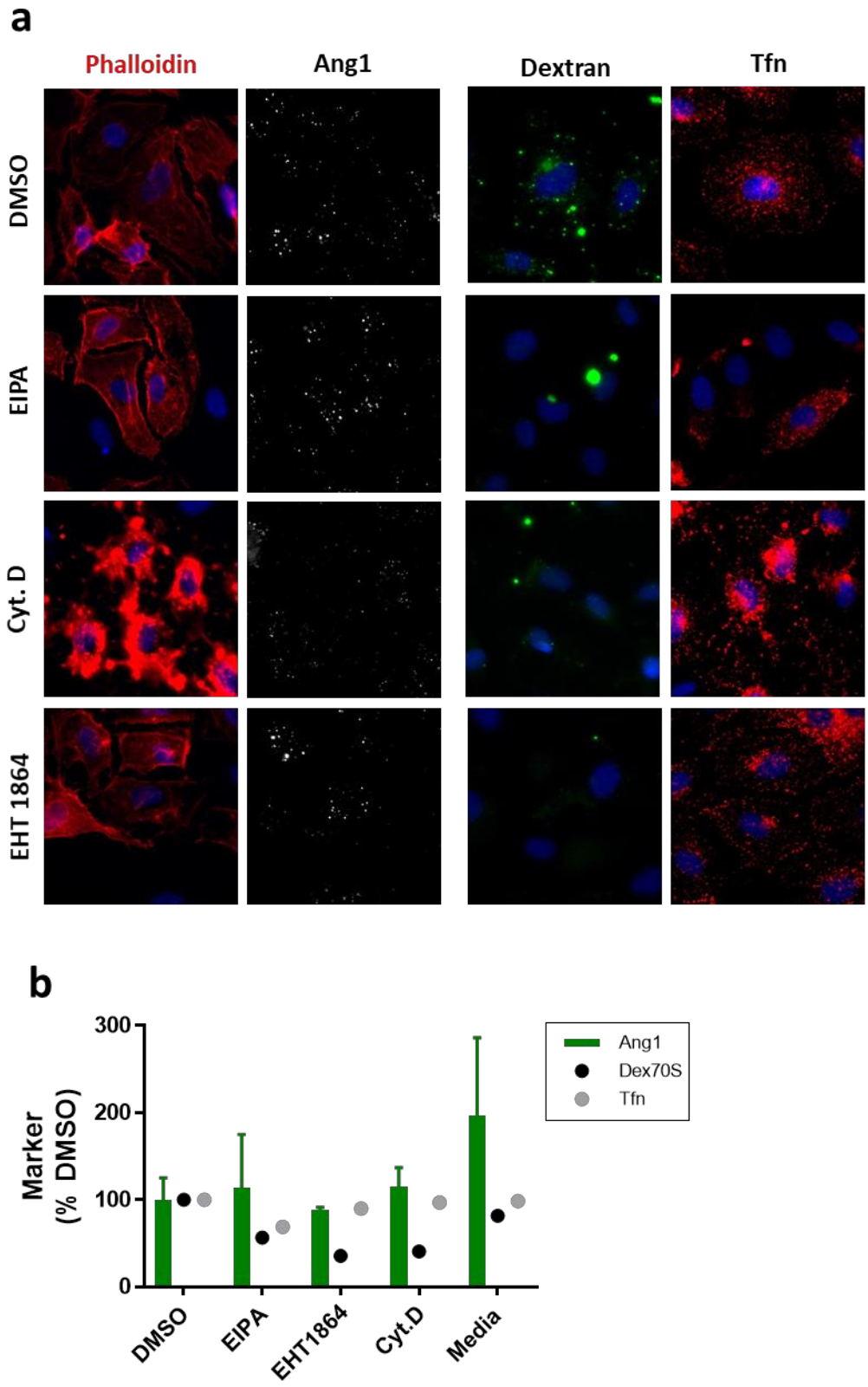

Figure 61. The effect of different chemical inhibitors of internalization on the internalization of Tie2 was evaluated using the high throughput format internalisation assay. HUVECs grown in a 96-well plate were

pre-incubated for 30 min with DMSO (2%), EIPA (834 nM), EHT1864 (10 µM), Cytochalasin D (20 µM) or left untreated before incubation for 45 min with hrAng1^{His} (300 ng/mL), FITC-Dextran 70S (100 µg/mL) or Alexa Fluor 568-conjugated transferrin (10 µg/mL). Membrane trafficking was stop by washing wells in ice-cold PBS. Remaining cell surface ligands were removed using 3 series of 5 min washes with Acid Wash Buffer. After fixation, cells incubated with hrAng1^{His} were immunostained for the hrAng1^{His} and Tie2 or stained with TRITC-phalloidin. Nuclei of all conditions were stained with DAPI. **(a)** Images were automatically acquired with the ImageXpress Microscope and **(b)** the internalization of each endocytic marker was quantified using variations of the CME1 algorithm in MetaXpress Image analysis software. Internalization of each marker is represented as the percentage of vesicles per cell to the DMSO control. Several images for each well/condition were automatically acquired. Only 1 replicate for FITC-Dextran and TF^{568} were included and are represented by a dot. Bars represent the average and SD of 3 replicates for hrAng1^{His} incubation (n=1 independent experiment) No statistically significant differences were found between the different conditions on the internalization of Ang1. Dunnett's multiple comparisions test for one-way ANOVA, α =0.05.

Overall, although I was not able to obtain any robust conclusions from these two experiments due to the lack of repeats and statistical strength, I believe that it was reasonable to think that actin cytoskeleton could somehow be involved in the regulation of Tie2 internalization. I reason so as despite that the amount of vesicles per cell was not affected by Cytochalasin B nor D, the size and intensity of Ang1-containing vesicles appeared to be reduced in both HeLa and HUVECs respectively. I think it could be interesting to test the effect of other inhibitors of actin polymerisation to see how the internalization of Tie2 in HUVECs is affected, as well as optimizing an image analysis algorithm to measure the size and intensity of the vesicles. Also, the fact that Tie2 internalization was not inhibited by EIPA nor EHT1864 while Dextran70S was would argue against an internalization of Tie2 via macropinocytosis, although it would be interesting to see if this effect would stand when treating cells in sparse conditions; when I found the transfection of RAC1 and PAK1 siRNA to affect Ang1 internalization and also when Rac1 is mediating the Ang1 induced migratory response of endothelial cells (Cascone et al. 2003). Also, in case that Tie2 was internalized via compensatory endocytic pathways it would be recommendable to improve inhibitory assays by determining the rate of internalization of Tie2 or by also studying whether co-localization of the receptor with key endocytic markers is altered after exposure to inhibitory compounds. For instance, it could be interesting to see whether co-localization with CME markers is increased under exposure to inhibitors of actin polymerisation. However, due to the multiple effects that pharmacological inhibitors

can have in cells and due to the lack of specificity for particular internalization pathways I decided to prioritize other lines of investigation about the endocytic pathway of Tie2.

Localization of activated Tie2 on Triton resistant membranes

In order to determine whether $Tie2^{FLAG}$ in HeLa T-REx $Tie2^{FLAG}$ cells was being internalized in a cholesterol dependent manner I also decided to investigate whether $Tie2^{FLAG}$ receptor would localize in cholesterol-enriched domains of the plasma membrane. Cholesterol is a modified steroid found in cell membranes, where it plays an important structural role by regulating membrane fluidity (Mayor & Pagano 2007). Although cholesterol can be found in all membranes, many lines of evidence suggest that it can be enriched in particular membrane domains which can have different physiological roles (Mayor & Rao 2004; Mayor & Pagano 2007). Indeed, some endocytic mechanisms are described to be dependent on cholesterol, such as macropinocytosis or caveolin-dependent endocytosis. Due to the increased rigidity and lipid organization conferred by cholesterol, the cholesterol enriched domains are characterized by being insoluble to the detergents normally used to lyse cells. Actually, I found that Ang1-activated Tie2 in HUVECs had been reported to localize in membrane domains that are not solubilized by Triton-based lysis buffers, which the authors identify as lipid rafts (Katoh et al. 2009). Furthermore, it was shown that the Tie2/Akt/FOXO1 pathway was dependent on the presence of cholesterol as the Ang1-dependent phosphorylation of Akt in HUVECs was inhibited by the cholesterol-sequestering compound mβCD (Katoh et al. 2009). Although treatment of HeLa $Tie2^{FLAG}$ cells with Filipin did not affect the internalization of Ang1, in the same experiment I had observed a fraction of internalized Ang1 co-localizing with $CTxB^{555}$, which can be internalized in a cholesterol-dependent manner (Shogomori & Futerman 2001; Torgersen et al. 2001; Blagojević & Mahmutefendić 2008). Hence, I decided to test whether Ang1-activated $Tie2^{FLAG}$ in HeLa T-REx $Tie2^{FLAG}$ cells was also localized in an insoluble fraction of their plasma membranes.

To do so, I incubated serum starved HeLa $Tie2^{FLAG}$ cells with or without $hrAng1^{His}$ for 30 min to then solubilize cells in basic cell lysis buffer (Methods) containing only 1 % Triton X-100. After spinning of the sample the pellet obtained was re-suspended in a Radio ImmunoPrecipitation Assay buffer (RIPA) similar to the one used by Katoh et al. (2009) (10 mM Tris–HCl pH 7.4, 1 % NP- 40, 0.5 % sodium deoxycholate, 0.1 % sodium dodecyl sulfate (SDS), 150 mM NaCl, 1 mM EDTA-2Na, PIC and 1 mM APMSF), although I could

not completely solubilise the pellet and hence a second supernatant fraction and a final pellet were obtained. In parallel, I used RIPA to directly solubilise Ang1 treated or untreated serum starved cells to see if this could be a better lysis buffer to be used in future experiments. All samples were run in an SDS-PAGE gel and analysed by Western Blotting for Tie2, p(Y992)Tie2 and tubulin. As expected, tubulin was only present in the supernatant fractions of the cell lysates (**Figure *62*** lanes 1, 2, 7 and 8). Tie2 was also mainly found in the same supernatant fractions as tubulin, albeit a small portion of Tie2 appeared to be present in the pellet from the RIPA cell lysate if cells had been incubated with hrAng1^{His} (**Figure *62***, lane 10). Remarkably, it was clear that a small portion of p(Y992)Tie2 was present in the insoluble fractions of cell lysates only in the presence of hrAng1^{His} (**Figure *62***, lanes 6 and 10).

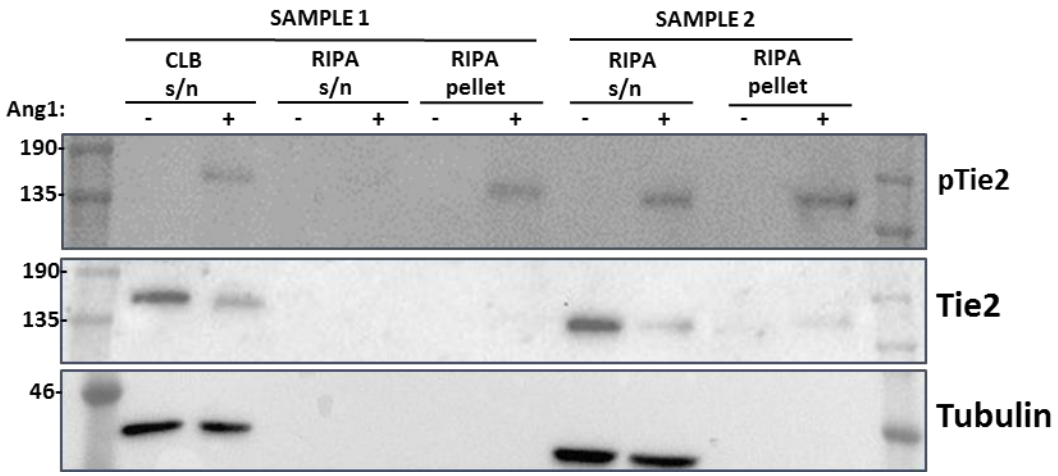

Figure 62. A portion of the activated Tie2 in HeLa T-REx Tie2^{FLAG} cells was left in the insoluble pellet of cell lysates. Serum starved HeLa T-REx Tie2^{FLAG} cells were incubated with hrAng1^{His} for a total of 30 min or left untreated (**+** and **-** lanes respectively). Cells were then solubilised with normal Cell Lysis Buffer (CLB, Sample 1) or RIPA buffer (Sample 2) (10 mM Tris–HCl pH 7.4, 1 % NP- 40, 0.5 % sodium deoxycholate, 0.1 % sodium dodecyl sulfate (SDS), 150 mM NaCl, 1 mM EDTA-2Na, PIC and 1 mM APMSF) and spun down at 10000g for 15 min to obtain a supernatant fraction (s/n) and an insoluble pellet. The pellet from sample 1 was resuspended in RIPA buffer and spun at 10000g for 15 min to obtain a second supernatant fraction and a final pellet. Pellets were solubilized by directly boiling them in sample buffer for the SDS-PAGE gel. Samples were run in a SDS-PAGE gel and transferred to a nitrocellulose membrane. Bands were obtained after immunostaining for the total Tie2, phospho-Tie2 (Y992) and tubulin. N=1 independent experiment.

To further confirm that activated Tie2^{FLAG} was localized in detergent resistant domains of the plasma membrane of HeLa T-REx Tie2^{FLAG} I applied a protocol based on cell immunofluorescence that consists of stripping detergent sensitive lipid membranes of

cells by applying a short wash with Triton X-100 before fixation of cells. The Triton wash-out strips most of the transferrin bound or internalized to cells, while it does not strip CtxB bound to cell surface of cells nor the human polyomavirus JC after 30 min of internalization in SVG-A cells (Querbes et al. 2006; Blagojević & Mahmutefendić 2008). Actually, it was described that after incubation with Ang1 a Tie2-GFP construct expressed in HUVECs was not stripped from the basal membrane by a Triton wash (Fukuhara et al. 2008). Therefore, I incubated serum starved HeLa T-REx $Tie2^{FLAG}$ cells with Ang1 (200 ng/mL) and transferrin conjugated to Alexa Fluor 488 (5 µg/mL) for 30 min on ice and then cells were applied a 1 min wash with Triton X-100 (0.5% in PBS) before or after fixation with 4 % PFA, cells were then immunostained for Ang1 to indirectly detect any remaining Tie2 receptor. I co-incubated Ang1 with transferrin as a measure to validate that the Triton wash had been effective. I also used fluorescently labelled CtxB as a negative control for the stripping of detergent sensitive membranes, but the distribution of CtxB in HeLa cells was not homogenous and was therefore difficult to determine how much of CtxB had been removed from each cell. After attempting several repeats of the experiment I found that it was technically difficult to reproduce the same exact result between repeats or even replicates, as the effectiveness of the Triton wash and the effect on cell survival could be very variable and in occasions not even the positive control Tfn would be stripped away from the membranes. Nonetheless, as seen in **Figure *63***, I observed that in those successful attempts where most of the Tfn would be washed away, much of the Ang1 remained on cells after the Triton stripping. Consistent with previous work, Ang1 presented little co-localization with Tfn.

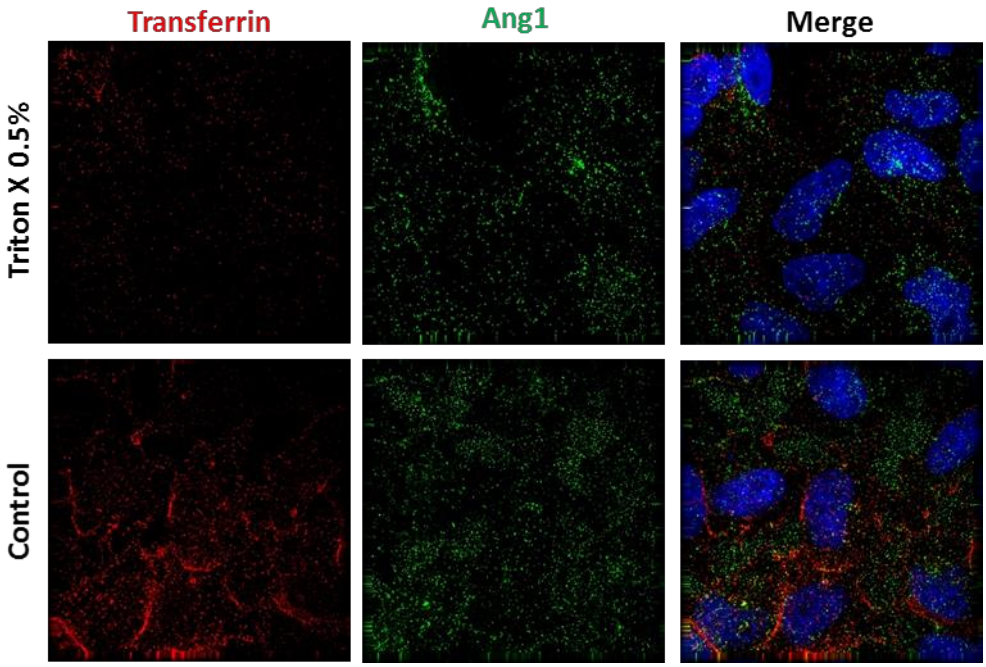

Figure 63. Some of the hrAng1^{His} on HeLa T-REx Tie2^{FLAG} cells was associated with Triton resistant domains of the HeLa T-REx Tie2^{FLAG} cells. Serum starved HeLa T-REx Tie2 FLAG cells were incubated with serum-free media containing 5 µg/mL transferrin AF488 and 200 ng/mL oligomerised hrAng1^{His} for a total of 30 min on ice. Cells were then treated with 0.5% Triton for 1 min before (Triton X 0.5%) or after (Control) fixation with 4 % PFA. The amount of Tie2^{FLAG} remaining in cells was assessed by immunofluorescence staining of hrAng1^{His}. Images representative of 2 independent experiments where Transferrin was effectively washed away (n=2).

Therefore, I believe that these results indicate that, as CtxB, Tie2^{FLAG} can also located to particular membrane domains in the plasma membrane of HeLa T-REx Tie2^{FLAG} cells after incubation with Ang1, the resistance to Triton X-100 of these membrane domains suggests that those are most probably cholesterol-enriched domains of the plasma membrane. Indeed, the localization of Tie2 in detergent resistant domains of HUVECs had been documented before (Katoh et al. 2009; Saharinen et al. 2008). However, whether this localization could be relevant for the internalization of the receptor should be determined with further experimentation as data is not conclusive in that sense; for instance, exposition to Filipin did not appear to have a clear effect on the amount of internalized hrAng1^{His} in HeLa Tie2^{FLAG} cells.

Interestingly, I have identified up to 6 cholesterol recognition amino-acid consensus sequences (CRAC) (L/V- X_{1-5} -Y- X_{1-5} -R) within the cytoplasmic tail of Tie2. CRAC can be

found in many of the membrane proteins that are known to localize in cholesterol-enriched membrane domains, such as caveolin-1, and is believed to be responsible for targeting proteins into these domains (Li et al. 2001; Epand et al. 2005; Singh et al. 2012). Further experimentation would be necessary to determine if this sequences are truly CRAC motifs and whether those could have an effect on Ang1-induced Tie2 signalling or localization.

Analysing the clathrin independent component of the Tie2 receptor by cell immunofluorescece

It has been suggested that Tie2 could be internalized via clathrin mediated endocytosis, however, the data were not conclusive. Furthermore, work from a former lab member showed that Ang1 was not internalized into the same endocytic structures as transferrin (Ferreira and Maxwell, Data not shown), a classical marker of clathrin mediated endocytosis. I wanted to investigate whether Tie2 would co-localize with a different endocytic marker such as Cholera Toxin B subunit. Hence, I incubated serum starved HeLa T-REx Tie2^{FLAG} cells with both Ang1 and fluorescently labelled CtxB for different amounts of time, cells were later co-stained for Tie2 and Ang1. In this case the ligands were pre-incubated with cells for 30 min on ice before being transferred to a warm waterbath in order to adapt the usual protocol to the addition of CtxB. As shown in **Figure *64***a, CtxB labelled the plasma membrane of HeLa T-REx Tie2^{FLAG} cells after the pre-binding of ligands on ice, but it was already internalized into intracellular endosomal-like structures by 15 min independently of the presence of Ang1. Although the localization of Tie2 on the cells was changed after 15 of incubation with Ang1, the receptor did not co-localise with CtxB in perinuclear endosomes (**Figure *64***b).

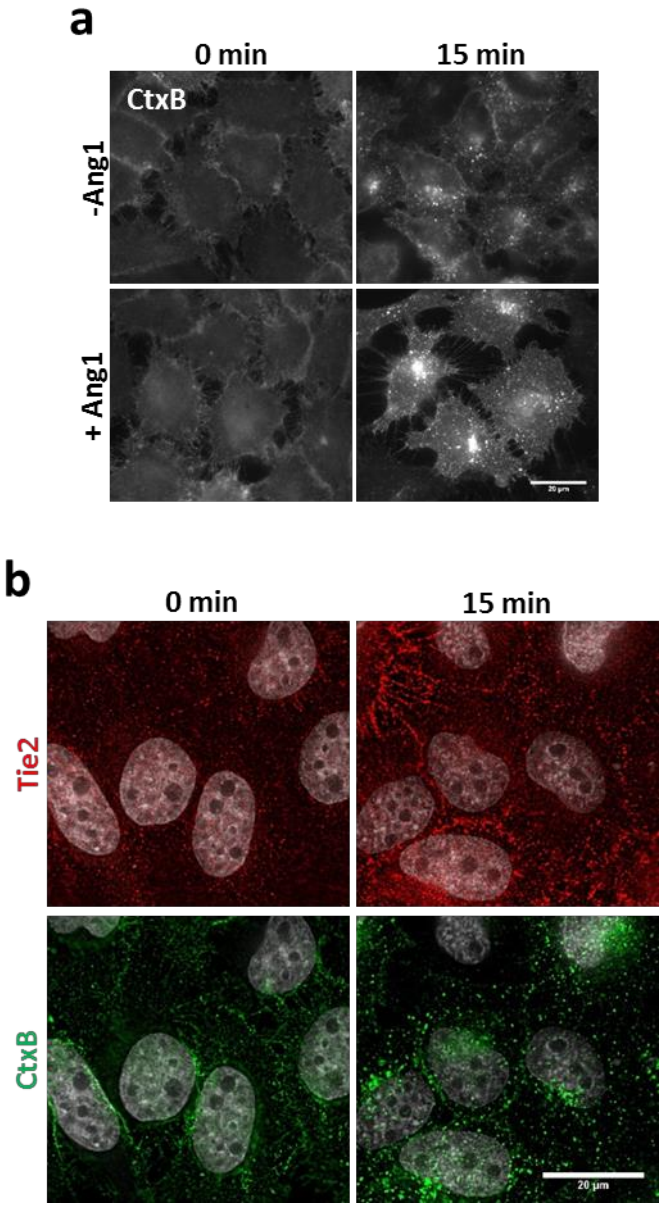

Figure 64. CtxB is internalized in HeLa T-REx Tie2^{FLAG} cells before Tie2^{FLAG} and independently of the presence of hrAng1^{His}. (a) Serum starved cells were pre-incubated in ice for 30 min with serum-free media containing 5 µg/mL Alexa Fluor 555-CtxB alone or with 200 ng/mL hrAng1^{His} as indicated (**-Ang1** or **+Ang1**). Then cells were transferred to a 37˚C waterbath for 15 min or fixed directly. Nuclei were stained with DAPI. Images were acquired with a Nikon dual camera microscope system and deconvolved using the Nikon software. Images show a basal Z-section of representative cells. CtxB was seen to be internalized regardless of the presence of hrAng1^{His}. **(b)** As in (a) but cells were co-incubated with both hrAng1^{His} and CtxB^{AF555}. Fixed cells were immunostained for Tie2^{FLAG} and hrAng1^{His} (not shown) and images were acquired and deconvolved with the Deltavision microscope and software. Images show a basal Z-section from cells. At 15 min, Tie2^{FLAG} receptor did not appear to be internalized into endosomal-like compartments as was CtxB. Scale Bar equals 20 µm. Representative images from a single experiment are shown (n=1).

Interestingly, Tie2 co-localized with CtxB on the plasma membrane of cells after the pre-binding on ice. This co-localization was particularly prominent on the apical membrane of the cells, where Tie2 and CtxB could be seen forming patches of similar shapes. This co-localization was not dependent on the activation of Tie2, since it was observed whether there was Ang1 present in the media or not (**Figure *65***). However, this co-localization was lost after 15 min of incubation at 37°C, when CtxB had already been internalized (**Figure *66***).

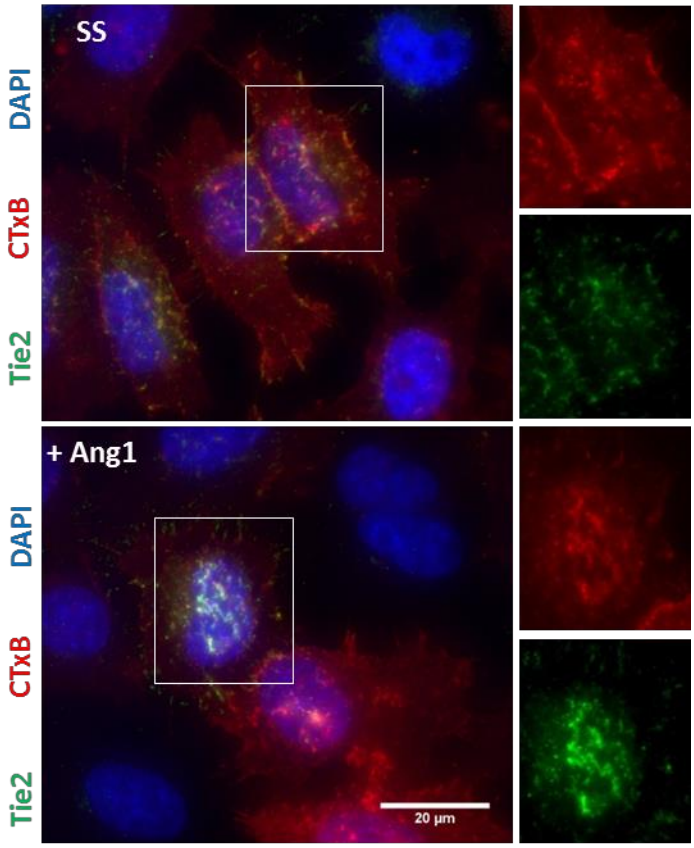

Figure 65. Tie2^{FLAG} receptor co-localized with CtxB on the cell surface of HeLa T-REx Tie2^{FLAG} regardless of the presence of hrAng1^{His}. Serum starved HeLa T-REx cells expressing Tie2^{FLAG} receptor were incubated 30 min on ice with serum-free media containing 5 µg/mL CtxB^{AF555} alone (**SS**) or with 200 ng/mL hrAng1^{His} (**+ Ang1)** and then fixed for immunostaining of Tie2^{FLAG} receptor and hrAng1^{His} (not showing). Cells nuclei were stained with DAPI. Images were acquired with the Nikon dual camera microscope system and deconvolved with the Nikon software. A compilation of several Z-sections are shown. Scale bar equals 20 µm. Representative images from a single experiment are shown (n=1).

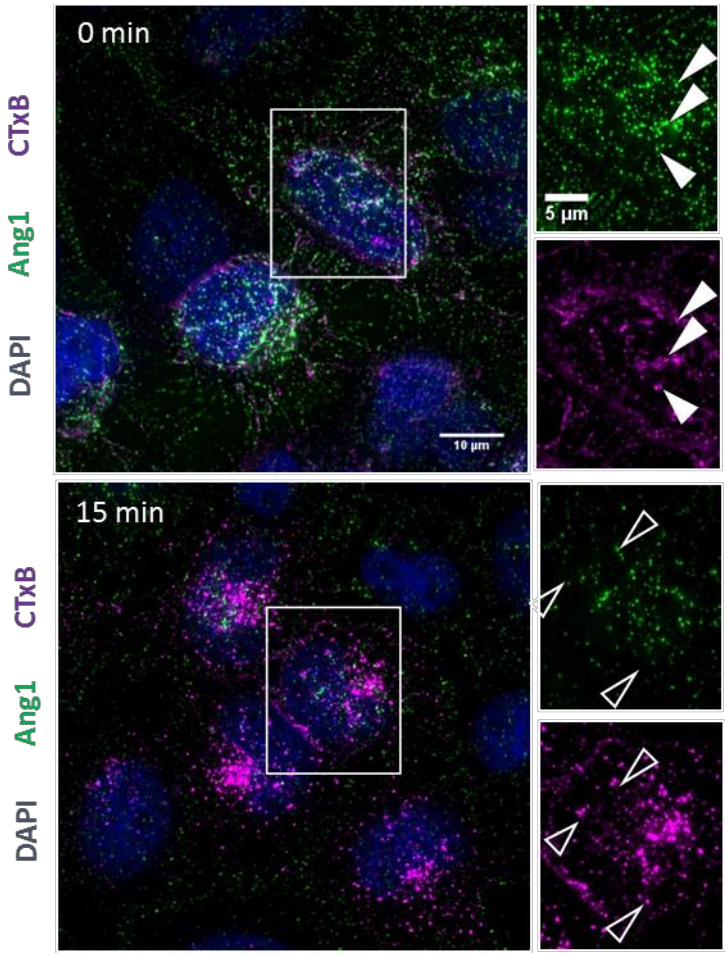

Figure 66. Co-localization between CtxB^{AF555} and hrAng1^{His}/ Tie2^{FLAG} complex was lost after the internalization of CtxB^{AF555}. Serum starved HeLa T-REx cells expressing Tie2^{FLAG} receptor were incubated on ice with CtxB^{AF555} with hrAng1^{His} and then moved to a 37˚C waterbath for **15 min** or left on ice until fixation (**0 min**). Cells were fixed for immunostaining of Tie2^{FLAG} (not showing) and hrAng1^{His}. Nuclei were stained with DAPI. Images were acquired with the Deltavision microscope and deconvolved with the Deltavision software. A compilation of several Z-sections are shown. Scale bar equals 20 µm. Representative images from a single experiment are shown (n=1).

Altogether these results indicated that Tie2^{FLAG} expressed in HeLa T-REx cells was localized into particular areas of the plasma membrane, marked by binding of CtxB, even in the absence of Ang1 and after a 2h serum starvation period. However, since Tie2 was not seen to co-localize with the internalized CtxB in endosomal structures our results appear to indicate that Tie2 and CtxB are not co-internalized within the same vesicles.

CtxB is mainly internalized via CIE and can be internalized via caveolae (Doherty & McMahon 2009). Since I found that Ang1 and Tie2 co-localized with CtxB at early time-points of incubation I decided to evaluate whether Tie2 could also be co-localizing with caveolin. Actually, Tie2 has been previously reported to co-localize with caveolin on the plasma membrane of HUVECs, and the absence of caveolin and cholesterol on HUVECs modified the Tie2 downstream signalling driven by the activation of Ang1 (Yoon et al. 2003). However, the implication of caveolin in Tie2 internalization had not been approached. I first decided to start investigating whether internalized Ang1 co-localized with caveolin by staining HUVECs. As reported before, I was able to observe some degree of co-localization between Tie2 and caveolin on the cell edges. Furthermore, I also observed a considerable number of Ang1-containing endosomes stained with Tie2 and Caveolin (**Figure *67***).

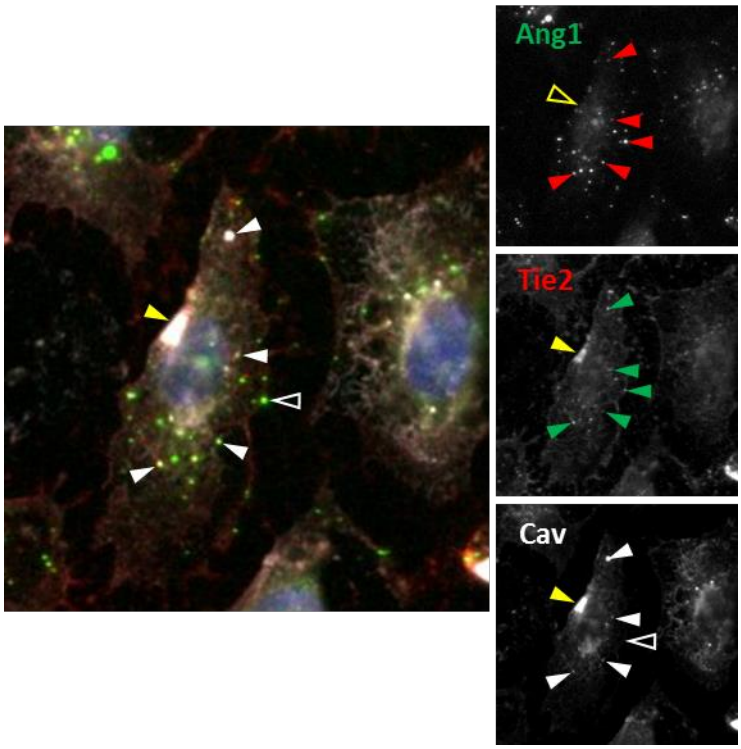

Figure 67. Endogenous Tie2 receptor and hrAng1^{His} were found to co-localize with caveolin1 in HUVECs. HUVECs incubated with 300 ng/mL hrAng1^{His} for 45 min were immunostained for hrAng1^{His}, Tie2 and Caveolin-1. Nuclei were stained with DAPI. Images were acquired using the ImageXpress microscope. Representative images from a single experiment are shown (n=1).

To investigate further, I decided to see if the localization of caveolin in HUVECs would change due to the presence of Ang1. Hence, serum starved HUVECs were incubated with Ang1 for different amounts of time and then co-stained for Tie2 and caveolin. As seen in **Figure *68***, caveolin appeared to localize on both the plasma membrane and in peri-nuclear structures of HUVECs. Furthermore, caveolin seemed to be enriched in the retracting edge of those HUVECs presenting a migratory parameter (**Figure *68***b). As seen before, Tie2 was found in some of the peri-nuclear structures staining for caveolin, although the degree of co-localization with caveolin in this structures seemed independent of the incubation with Ang1. Again, I observed the co-localization of Tie2 and caveolin on the cell surface as reported before (Yoon et al. 2003). However, I noticed that the localization of Tie2 with caveolin on the plasma membrane was usually more remarkable in the retracting edge of cells presenting a migratory parameter (**Figure *68***b). In fact, in the absence of Ang1 the co-localization between Tie2 and caveolin was higher in the migratory cells compared to the non-migratory cells (**Figure *68***b and c). Furthermore, despite the fact that the co-localization between Tie2 and Caveolin did not appear to change in non-migratory cells during the incubation with Ang1, it appear to be decreased in an Ang1 dependent way on those cells presenting a migratory parameter (**Figure *68***b and c). At 30 min of incubation the level of co-localization between migratory and non-migratory cells was indistinguishable (**Figure *68***b). Although I find these results interesting, I believe that more repeats would be needed to confirm such effect of Ang1 on the localization of caveolin-1.

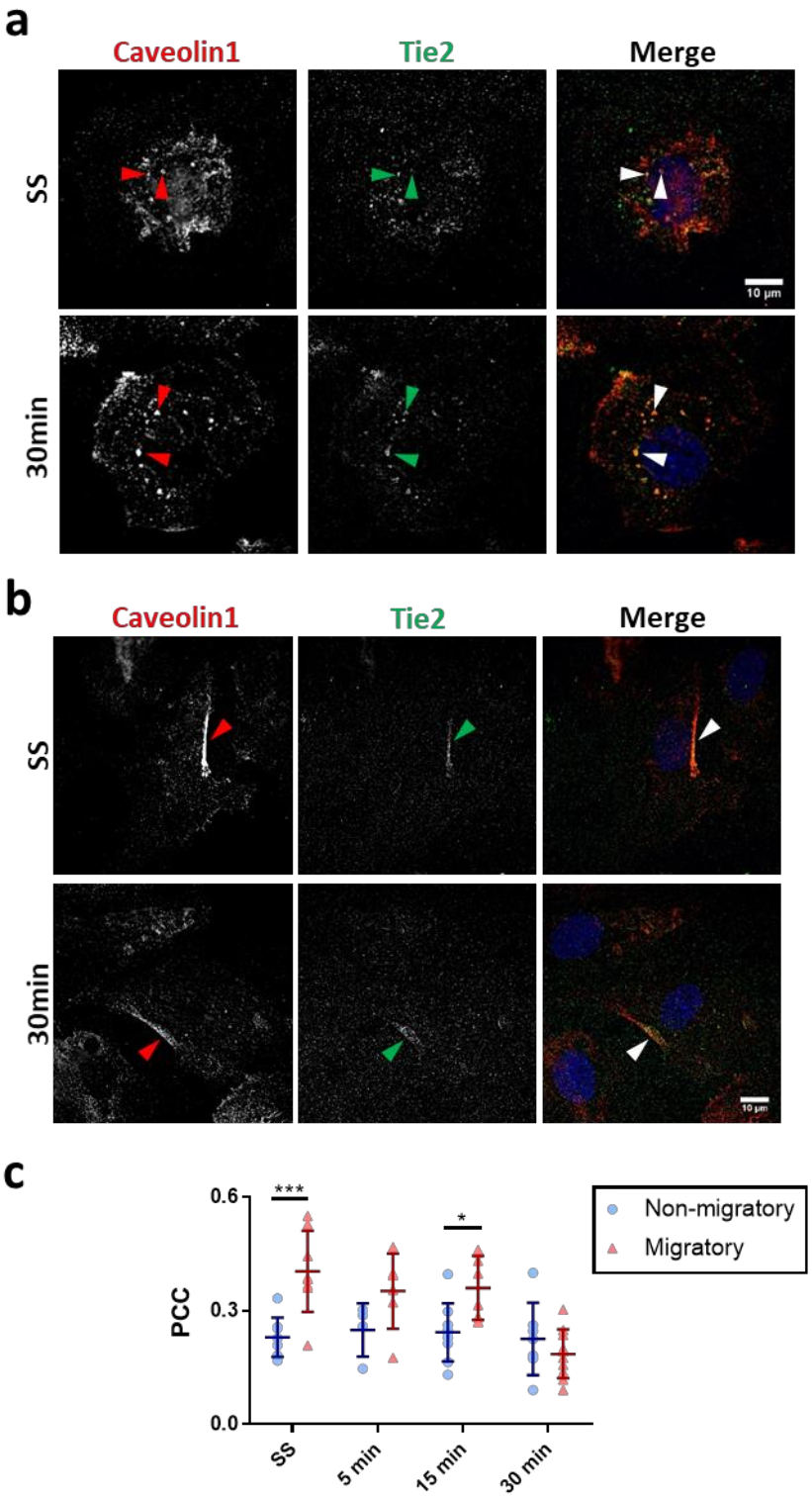

Figure 68. The ectodomain of endogenous Tie2 was found to co-localize with caveolin1 in HUVECs before and after incubation with hrAng1^{His}. Serum starved HUVECs were incubated with hrAng^{His} for 5, 15 or 30 min at 37˚C or left untreated (SS). Fixed cells were then immunostained for Tie2 and Caveolin 1 and stained with DAPI. The Goat anti-Tie2 antibody targeting the ectodomain of Tie2 was used for this experiment. Images were acquired and deconvolved with the Deltavision microscope. **(a)** Middle cell z-

sections showed Tie2 localization in peri-nuclear compartments containing caveolin. **(b)** Representative basal cell z-sections. Tie2 was found to co-localize with caveolin in the retracting edge of migratory cells. **(c)** The co-localization between Tie2 and caveolin1 in cells with a migratory parameter and a non-migratory parameter was quantitated using Volocity. Dots represent measurements of individual cells and bars show Mean ± SD of at least 4 measured cells for each condition from a single experiment (n=1). Statistics were used to infer whether differences observed in the images of this experiment were statistically significant. Dunnett's multiple comparisons test for *two-way* ANOVA, $\alpha = 0.05$ (* if $p < 0.05$, ***$p < 0.001$).

CHAPTER 7

Discussion and conclusion

In order to set the ground for investigating the role of endocytosis in the modulation of the Ang1/Tie2 signalling pathway and cellular behaviour, I have attempted to unveil the molecular pathways implicated in the internalization of Ang1-activated Tie2 tyrosine kinase receptor. Although I have not been able to conclusively determine the main endocytic pathway of the Ang1/Tie2 complex, this results expand the knowledge in the internalization of Tie2 and appear to indicate that the internalization of Tie2 may be a process dependent on different internalization pathways.

Validation of technical approaches

HeLa Flp-In T-REx Tie2 clones

In order to facilitate the study of Tie2 internalization I created HeLa cell clones that express the receptor upon induction by doxycycline. Since HeLa cells do not have endogenous expression of Tie2 I was able to work in a null background and did not have to further manipulate the clones in order to knock-down the expression of the receptor. Moreover, the Flp-In T-REx system allows for an inducible expression of the protein of interest hence avoiding any effects on the clone cells due to the long-term exposure to doxycycline or expression of Tie2. Lastly, due to being able to control for those clone cells expressing low levels of the receptor I was able to avoid any secondary effects of an overexpression of the receptor such as spontaneous phosphorylation of the receptor.

On the other hand, since HeLa cells do not usually express Tie2 it could be possible that Tie2 function is altered due to the expression in a different cell environment. Nonetheless, different validation assays corroborated that the $Tie2^{FLAG}$ expressed by the HeLa T-REx cells behaved similarly to the endogenous Tie2 in HUVECs. As previously reported for Tie2 in HUVECs, I found that $Tie2^{FLAG}$ receptor localized to the plasma membrane of HeLa T-REx $Tie2^{FLAG}$ cells (Dumont et al. 1992). The $Tie2^{FLAG}$ stably transfected in HeLa T-REx cells was expressed at similar levels to endogenous Tie2 in HUVECs and did not present spontaneous phosphorylation due to overexpression. Furthermore, $Tie2^{FLAG}$ receptor was also auto-phosphorylated and localized to cell-cell contacts after incubation with the oligomerised agonistic $hrAng1^{His}$ ligand, as described for endogenous Tie2 in HUVECs (Fukuhara et al. 2008; Saharinen et al. 2008). Also, activated $Tie2^{FLAG}$ in HeLa T-REx cells localized into Triton-resistant domains of the membranes as reported in HUVECs (Fukuhara et al. 2008; Katoh et al. 2009). As previously described for endothelial cells, $Tie2^{FLAG}$ receptor in HeLa T-REx clones was internalized after incubation with $hrAng1^{His}$ and the internalization was dependent on the catalytic activity of the kinase domain, since the kinase-dead mutant $Tie2^{K855R/FLAG}$ was not internalized (Bogdanovic et al. 2006; Bogdanovic et al. 2009; Wehrle et al. 2009).

Lastly, my experiments using immunofluorescence to localize Ang1 with endocytic markers in HeLa T-REx Tie2^{FLAG} were similar to results obtained previously with HUVEC by former members of our lab (Ferreira and Maxwell, unpublished).

Quantitation of the internalized Tie2

To quantitate the internalization of Tie2 I took advantage of the fact that Ang1 was clearly being internalized with the receptor to early endosomal compartments, as directly measuring the internalized receptor would require more complex and time-demanding protocols. Nonetheless, this strongly contrasted with previous work that reported that Ang1 and Ang2 were mostly being released after activation of Tie2 (Bogdanovic et al. 2006). This effect was not exclusive to the Tie2^{FLAG} receptor expressed in HeLa T-REx cells as it was also observed for endogenous Tie2 expressed in HUVECs in experiments run for this project and by former members of our lab (data not shown).

I think that a possible cause of such contrasting conclusions could be differences in the approaches applied to determine the presence of intracellular Ang1. While I was able to directly visualize endosomal Ang1 co-localizing with Tie2 using fixed cell-immunofluorescence, Bogdanovic et al (2006) determined that Ang1 and Ang2 were being released after activation of Tie2 by measuring the radioactivity from iodinated ligands present in the media or lysates of HUVECs after incubation. They reached the conclusion that none of the ligands were being internalised after they observed that the background radioactivity associated with pellets of surface-stripped cells did not significantly increase from 15 min to 2 h of incubation. Still, the background radioactivity that they reported in the pellets of surface-stripped cells accounted for a 10% and 12% of the total ^{125}I-Ang1 and ^{125}I-Ang2 associated to cells yet it was not contrasted with a non-internalization control, such as cells incubated for the same time with the ligand on ice. Also, although they determined that Ang1 and Ang2 stimulation induced the degradation of Tie2 in the long term, whether a proportion of activated Tie2 could be quickly recycled back was not addressed. Since they mentioned that the released ligands were still structurally intact and functional (Bogdanovic 2009), it could be that a pool of re-internalized ligands was also maintained in cells and hence why the levels of associated ligands to the pellets of surface-stripped cells was maintained along different

incubation times. Therefore, in light of our contrasting results, it could be possible that the remaining iodinated ligands associated with the pellets of surface-stripped cells were representing a pool of constantly internalized and recycled Ang1 (Bogdanovic et al. 2006). Actually, our results show that only a small portion of the Ang1 associated to cells was being internalized and this would be consistent with their reported residual radioactivity in pellets of surface stripped cells.

It is true, though, that results about internalization of Tie2 have brought to light slight discrepancies within reports. For instance, two different groups reported that in confluent cultures of HUVECs Tie2 was retained at cell-cell contacts by Ang1 and not being internalized (Fukuhara et al. 2008; Saharinen et al. 2008), while ourselves and Bogdanovic (2009) have both detected internalization of Ang1 or Tie2 in confluent cultures of cells as well (Appendix I in Bogdanovic 2009). Giving the complex regulation of Tie2 and the multiple factors that affect its activity and determine the activation of different signalling cascades, it is also feasible that differences in experimental conditions were ultimately generating slightly different endocytic patterns. For instance, a very clear difference between reports is the use of different recombinant ligands and at different concentrations, as well as using different ratios of hrAng1^{His} and the His antibody, which ultimately influence the oligomerisation state of the ligands. The association of Ang1 and Ang2 in different orders of clustering was seen to be crucial for the binding to the receptor and determined the level of activation of the receptor (Kim et al. 2005). Furthermore, in a later work it was shown that different oligomerization states of the ligands determined the mobilisation of Tie2 to different areas of cells (Pietilä et al. 2012). Indeed, multiple publications indicate that ligand clustering and size by itself can determine the endocytic trafficking of cargoes (Mellman & Plutner 1984; Tabas et al. 1991; Marsh et al. 1995; Jiang et al. 2008). Hence it could be that although using the same ligand, different levels of ligand clustering between reports were the cause behind some of the variation in results from different groups.

As explained, taking advantage of the fact that hrAng1^{His} was being internalized with the receptor I aimed to develop a protocol to determine the internalization rate of the

receptor by indirectly measuring the intra-cellular ligand. A usual approach to reveal the endocytic mechanisms involved in the internalization of plasma membrane receptors is to compare the internalization rates of different mutants or after disruption of known endocytic mediators. In order to do so with Tie2 receptor I designed and optimized a sandwich ELISA to quantitate internalized Ang1. However, although the assay was sensitive to hrAng^{His} diluted in blocking buffer as standard, I found that a component of the cell lysates was significantly decreasing the signal generated by the assay. The inhibitory effect of cell lysates was present even when I clarified the lysates by centrifugation, indicating that the interferent was a soluble component of cell lysates (data not shown). In consequence, I could not quantitate any internalized Ang1 either in HUVECs or in HeLa T-REx Tie2^{FLAG}. The commercially available Quantikine ELISA kit is not specified to be used for the detection of Ang-1 in cell lysates but only in plasma, serum, cell culture supernatants or body secretions. Nonetheless, I found that other groups had managed to quantitate Ang1 in tissue homogenates (Shim et al. 2008; Boucherat et al. 2010). Therefore, I think that in the future I could attempt again to quantitate Ang1 by solubilising cells with T-Per tissue protein extraction reagent or RIPA buffer as used in these publications.

As an alternative to the quantitation of Ang1 by ELISA, I optimised an internalization assay based in cell immunofluorescence in a high throughput format as I had been successful in detecting internalized Ang1 using this methodology. Furthermore, as an alternative to analysing the internalization of Tie2 mutants, I adapted the internalization assay to a high throughput format in order to screen the effect of selected siRNAs to the internalization of Tie2. Screening of siRNA libraries had been published before to reveal the role of target proteins on different aspects of endocytosis of cargoes such as vesicles size, vesicle location or vesicle shape (Pelkmans et al. 2005; Collinet et al. 2010). In contrast, I opted for a more simplified analysis of the internalization by measuring a single parameter: number of Ang1-containing vesicles per cell. Our ligand based internalization assay was proven to be sensitive to the internalization levels of Tfn, CtxB and Ang1 thanks to the addition of a cold-acid stripping wash which ensured that only internalized ligand was being quantitated. Nonetheless, even if detection of positive

controls without internalization detection was clear, negative controls of internalization generated a high variability of vesicle/cell values. I believe that besides heterogeneity within cells, also technical limitations that impeded to acquire images of the totality of cells were also influencing this variability in the negative control: since the internalization of ligand was quantitated from a single Z-stack, small differences in plate depth, cell confluence or shape between wells could hamper the quality and reproducibility of the measurements. In order to compensate for this variability I attempted to repeat each screen at least 3 times although due to different problems it was not always possible. Therefore, I had to assume that this potentially increased the number of false positive from the screens.

In order to obtain as reliable results as possible from the high-throughput siRNA immunofluorescence assay I applied different measures to reduce the occurrence of "off-target" effects and to obtain as much information as possible from the screens. To reduce the occurrence of the non-specific "off-target" effects I combined a pool of 4 targeting siRNAs while maintaining a low final concentration of siRNA and transfectant; likewise I used ON-Target*plus* siRNAs for the primary screen, which have been designed to ensure the knock-down of target proteins while reducing the incidence of off-target effects (GE healthcare Dharmacon Inc 2016). Also, I included in the assays scrambled non-targeting siRNAs to normalize the results of each repeat, as using the mean of a small group of pre-selected siRNA could bias the normalized values and generate false negative results. Besides ensuring a low incidence of off-target effects, I also used different assay parameters in order to aid in the selection of hits. For instance, I screened for the internalization of transferrin to corroborate the reliability of some of the knock-downs and to aid in the selection of hits. Also, being impractical to determine the total expression of Tie2 after all of the knock-downs, I also measured the immunofluorescence staining of Tie2. In the primary screen the effect on Tie2 staining of the different siRNA transfected was assessed in a separate plate, yet in the secondary and HUVEC pilot screen Tie2 staining was performed in parallel to Ang1 staining. Indeed, in the secondary screen with HeLa T-REx Tie2^{FLAG} and the pilot screen with HUVECs I was able to calculate an Ang1/Tie2 ratio to highlight disproportionate changes between the

internalization and localization of the receptor. I believe that although the measurement of Tie2 staining may not always be representative of the total expression of Tie2 in cells, the analysis of the Ang1/Tie2 ratio together with the subsequent interpretation with the Ang1 and Tie2 detection individually can be used to approach the effect of the transfections into the pathway.

Nonetheless, I are aware that the siRNA screening on the internalization of Tie2 is only an approach to set a path for further experiments on candidate regulators of the endocytosis of the receptor. For instance, it would be necessary to validate the efficacy of the knock-downs by analysing protein levels by western blot or cell immunofluorescence. As well as quantitating the total levels of Tie2 by western blot to discard that the effects on internalized Ang1 were due to a change in the expression of the receptor. Although the only way of determining whether a siRNA generates non-specific effects on a cell would be by performing a transcriptomic analysis of transfected cells, this is not a protocol usually followed due to its impracticality. Alternatively, rescue experiments with siRNA resistant constructs can be used to determine if the parameter generated by a siRNA is specific to the targeted protein. Likewise, another way of investigating whether the effects of a knock-down are specific is by validating the results using alternative techniques such as overexpression of dominant negative mutants of the hits or its regulators and effectors. Nevertheless, the analysis of the interrelation between the targeted hits is an approach to increase the confidence on the validity of results and used for the selection of hits to validate. With this in mind, I evaluated the resulting hits from the screens to determine potential candidates involved in the Ang1-induced trafficking of Tie2. Furthermore, while the screenings were in progress I undertook some parallel characterisation experiments to corroborate the feasibility of some of our conclusions.

Characterisation of the mechanisms regulating the internalization of Tie2

Determinants of Tie2 internalization

Defining the molecular determinants that are required for the internalization of endocytic cargos is an important part of the characterisation of endocytic pathways, as it is then possible to investigate the specific interaction with endocytic mediators. Also, by creating internalization deficient mutants it is possible to specifically inhibit the internalization of a cargo to study the effect of endocytosis on cell signalling. For this reason, I aimed to purify ubiquitinated Tie2 in order to identify the particular lysines being ubiquitinated after the phosphorylation of the receptor by Ang1. Nonetheless, although it had been published that ubiquitination of Tie2 by the ubiquitin ligase c-Cbl after activation of the receptor by Ang1 was required for the internalization and degradation of the receptor (Wehrle et al. 2009), I did not detect an increase of the ubiquitination levels of Tie2 after incubation with Ang1, either in HUVECs or in HeLa T-REx Tie2^{FLAG} cells. This is consistent with the results of former members of our group, who, although they were able to isolate Cbl after an immunoprecipitation of Tie2 from lysates of HUVECs incubated with Ang1, they were not able to isolate ubiquitinated Tie2 from HUVECs either (data not shown, Marron and Smythe). Interestingly, transfection of CBL siRNA (targeting c-Cbl) had a significant effect on the internalization of Tie2^{FLAG} in HeLa Flp-In T-REx cells, supporting both previous data from our lab and from Wehrle et al (2009). Still, I cannot be certain why I was not able to reproduce the Ang1-dependent increase of Tie2 ubiquitination. I suspect that experimental differences could be again the cause behind the discrepancies. As before, both groups happen to use different concentrations of hrAng1^{His} ligand and clustered with a different ratio of ligand to His antibody (1:12.5 in Prof. Dumont's group to 1:25 ourselves). Also, although ubiquitination of Tie2 in an Ang1 dependent manner was detected in HUVECs, the rest of Wehrle's work was done with embryonic A293F cells stably transfected with Tie2 and the endothelial hybrid EA.hy926, both of which appeared to overexpress Tie2. Although it doesn't invalidate the results, the overexpression of Tie2 in the cell lines used might had facilitated achieving them, as it seemed that only a small proportion of the total phosphorylated Tie2 was being ubiquitylated. Furthermore, in light of the more recent findings that activated Tie2 can be localized in the pellet of clarified lysates, it is also possible that I had been discarding any ubiquitylated Tie2 with the pellets (Katoh et al.

2009). Another option is that c-Cbl was required for the ubiquitination of protein in complex with activated Tie2, as was the case for Eritropoietin Receptor, the internalization of which was dependent on the ubiquitination of p85 by Cbl (Bulut et al. 2013). On the other hand, despite CBL siRNA caused a significant decrease in the internalization of Tie2 in the Primary screen, it was not the case for the secondary and the screen in HUVECs. Curiously, in those, CBL siRNA caused a significant decrease in the detection of Tie2. This could mean that c-Cbl was required for the cell surface localization of Tie2 and I believe that it would be interesting to validate this result and investigate further.

Our results with HeLa Flp-In T-Rex expressing the kinase dead Tie2^{K855R} are in agreement with previous reports that showed that transfected Tie2$^{K855R/GFP}$ was not being internalized (Saharinen et al. 2008) and further confirm that phosphorylation of oligomerized Tie2 is required to trigger the ligand-mediated internalization of the receptor. Interestingly, it appeared that even though Tie2^{K855R} was able to bind hrAng1^{His}, the association was lost after a relatively long incubation with the ligand (30 min). Even though this results should be further confirmed by specifically designed experimentation this could mean that somehow the phosphorylation of the receptor could be stabilizing the interaction with the ligand.

Due to time restrictions I finally were not able to address whether any of the potential AP-2 recognition motifs or the potential CRAC sequences present in the C-terminus of Tie2 could be involved in the regulation of the membrane localization or the internalization of Tie2. I believe that it will be important in the future to investigate this and determine if the internalization rate or endocytic mechanism of Tie2 is changed due to mutation of any of these motifs.

Intracellular trafficking of internalized Tie2

Because I found that most of the hrAng1^{His} co-localized with Tie2 receptor and that the ligand was being internalized with the receptor I was able to use hrAng1^{his} to indirectly track the internalization of Tie2 receptor by cell immunofluorescence. For example, I was able to indirectly determine by fixed cell immunofluorescence that internalized Tie2

was delivered to early endosomes marked by the Rab5 effectors EEA1 and APPL1, although I did not attempt to determine whether the compartments were part of the same sub-populations of early endosomes or not (Kalaidzidis et al. 2015). The localization of internalized Tie2 to early endosomes, characterised by the presence of Rab5 and its effectors, had not been confirmed in the past due to technical difficulties with electron microscopy staining (Bogdanovic 2009). The presence of the Ang1-activated Tie2 in early endosomes is not indicative of any particular endocytic pathway as cargos internalized via both CME and CIE have been reported to be delivered into EEA1 or APPL1 labelled endosomes (Mayor & Pagano 2007). Still, localization of the ligand within endosomes labelled by Rab5 effectors were in accordance with results from former members of our lab; as mentioned before, overexpression of HA-hRme-6 in HUVECs caused the inhibition of the Akt activation after Ang1 incubation (Maxwell and Smythe, unpublished).

Characterization of the internalization of Tie2

I believe that it was clear from the siRNA screening and posterior experiments that internalization of Tie2 could dependent in some extent to the remodelling of actin cytoskeleton. Several siRNA targeting regulators of actin cytoskeleton where highlighted from the primary screen and the Arp2/3 component Arpc2 was validated from the sequential screenings. Furthermore, even though treatment of cells with drugs known to disrupt actin filaments appeared to affect the Tie2 internalization by reducing its apparent localization in internalized vesicles the quantitated amount of Ang1-containing vesicles was not affected by exposition to actin cytoskeleton disruptors. Actin filaments and cytoskeleton remodelling are involved in a variety of cellular process as well as endocytic pathways so actin polymerisation implication in Tie2 trafficking could be not be directly implicated to the receptor internalization.

On the other hand, the fact that multiple mediators of clathrin-mediated endocytosis were found significant in the primary screen increases the confidence in the results and indicates that is highly probable that Tie2 could be internalized via clathrin-mediated internalization. In support of this, most of the mediators of CME found to be involved in the internalization of Tie2 were also found to significantly affect the internalization of

transferrin, which is a canonical marker of CME (Collinet et al. 2010; Mayle et al. 2012). Additionally, I also showed that Ang1 co-localized with endogenous CHC and transfected CLC-mCherry and çAP-2-eGFP in HeLa T-REx Tie2^{FLAG} cells, which a former member of our lab also corroborated in HUVECs (Ferreira, unpublished). Likewise, previous work from Dumont's lab reported the co-localization of Tie2 with CCPs on the cell surface and in CCVs, as assessed by electronic microscopy with HUVECs (Bogdanovic et al. 2009). Exposition of both HeLa T-REx Tie2^{FLAG} and HUVECs to inhibitors of actin polymerisation revealed that Tie2 was only partially affected by those in comparison to Dextran70S. At the same time, internalization rates of Tie2 measured by a former member of our lab was consistent with a clathrin-mediated internalization of the receptor (Marron and Smythe, unpublished). However, it is intriguing that the co-localization with CME components is not visualized until later time-points and that it is not very frequent: even though the formation and internalization of CCPs is a quick and transitory process I would expect more of the internalized ligand to co-localize with markers of CME. Hence, this suggests that CME might not be the main internalization pathway of Tie2 and that the receptor could be internalized via an alternative mechanism.

Indeed, other evidence seems to point that Tie2 internalization could be also occurring in a clathrin-independent fashion. For instance, Bogdanovic et al. (2009) did not succeed in inhibiting the internalization of Tie2 after knock-down of either clathrin or dynamin 2 in HUVECs (Bogdanovic et al. 2009), suggesting that compensatory or alternative endocytic mechanisms were taking place. An alternate endocytic mechanism would also explain the intriguing fact that the co-localization between Tie2 and clathrin was not observed until 15 min and that it peaked at 30 min of incubation with Ang1, as it could be that this alternative route was preferred by Tie2 in front of CME. It might also be that this alternate route is stronger in HUVECs than in HeLa T-REx Tie2^{FLAG} and hence the reason why the knock-downs of CME components were not effective in HUVECs, together with the fact that the knock-downs were not very effective. Given published and present results candidate endocytic mechanisms could be caveolae-mediated endocytosis or macropinocytosis (Mayor & Pagano 2007; Doherty & McMahon 2009). In further support of a potential CIE mechanism there is the localization of activated Tie2

in cholesterol enriched membranes. Although not completely specific in all situations, cholesterol-dependence has been used as a criteria to characterise CIE including macropinocytosis and caveolae formation (Rodal et al. 1999; Doherty & McMahon 2009). In that sense, I consider it would be interesting to determine whether any of the potential Tie2 CRAC sequences are involved in the subcellular localization of the receptor or its function as well as endocytosis. The exhistence of different endocytic pathways for a single cargo have been described before and also for other RTKs. Since the characterisation of transferrin receptor as a canonical marker of CME, multiple membrane components have been shown to have lesser specificity for a single pathway and rather be able to follow internalization via different endocytic mechanisms: For instance, CtxB can be internalized via CME or caveolae-mediated internalization depending on the cell type (Blagojević & Mahmutefendić 2008), EGFR has been shown to be either internalized via CME and a CIE recently identified as FEME in HeLa cells (Sigismund et al. 2005; Boucrot et al. 2015) and VEGFR-2 was shown to be constitutively internalized via CME yet to be internalized via Cdc42-dependent macropinocytosis upon stimulation with VEGF-2 (Basagiannis et al. 2016).

Various results regarding the internalization of Tie2 could suggest an internalization of the receptor through macropinocytosis. Firstly, as observed in the micrographs from HUVECs incubated with Ang1, the activation of the receptor by Ang1 induced strong ruffling of the plasma membrane and in occasions Tie2 was spotted at the base of microvilli extending from the cell surface (Bogdanovic 2009). It would be interesting to determine whether incubation with hrAng1^{His} also induces membrane ruffling in HeLa T-REx Tie2^{FLAG}. Furthermore, although not abundant, I did observe some co-localization between Tie2 and Dextran 70S. Since the co-localization was only analysed at incubation time-points where I found Ang1 already co-localizing with EEA1 and APPL1 it would be interesting to see whether co-localization between Tie2 and Dextran 70S was stronger at earlier time-points. Lastly, I found that knock-down of Rac1 and Pak1, which were reported to mediate re-modelling of actin cytoskeleton during macropinocytosis (Dharmawardhane et al. 2000), differently affected the internalization of Ang1 and Tfn in the primary screen. Although not completely specific for macropinocytosis, Rac1 has

been shown before to be necessary for the formation of the membrane ruffles characteristic of this endocytic mechanism, while other Rho GTPases such as RhoA and Cdc42, not highlighted by the screen of the Ang1 parameter, have been preferentially related to other CIE pathways and the formation of other cellular structures (Mayor & Pagano 2007; Doherty & McMahon 2009). Furthermore, Rac1 and Pak1 were accompanied by other relevant hits; for instance, Wave2 in particular has been reported to be more active nucleating actin in response to Rac1 than other Rho GTPases such as RhoA or Cdc42 (Miki et al. 1998). Also, activated Pak1 was reported to phosphorylate the Arpc1b subunit of the Arp2/3 complex in the course of cell migration initiation and I found Arpc1b to have a similar effect on the internalized Ang1 than Pak1 in the primary screen (Vadlamudi et al. 2004). Although Rac1 can be also involved in intracellular trafficking of clathrin-coated vesicles, the co-occurrence of Pak1 and components of the Wave and Arp2/3 complexes instead of synaptojanin 2, which mediates un-coating of clathrin coated pits and it is inhibited by activated Rac1 (Malecz et al. 2000), suggests a potential implication of membrane ruffling in the internalization of Tie2. On the other hand, Arf6, which has been related to Rac1 membrane trafficking and was reported to be necessary for the generation of Rac1-induced membrane ruffling (Di Cesare et al. 2000), was not found to significantly affect none of the parameters. Furthermore, either EIPA or the Rac1 inhibitor EHT1864 had any evident effect on the internalization of hrAng1^{His} in HeLa T-REx Tie2^{FLAG} or HUVECs, while Dextran70S was clearly affected. Therefore, due to conflicting results, further experimentation should aim at addressing whether Ang1/Tie2 complex could be internalized within micropinosomes.

Likewise, several results could be pointing at the existence of a caveolae-mediated internalization of Tie2 in cells. Caveolae can account for up to a 20 % of endothelial cell surface and have been shown to be playing an important role in multiple physiological functions of vessels so it could be feasible that caveolae played also a role in the internalization and regulation of the Ang1/Tie2 pathway (Parton & Simons 2007). Indeed, previous reports and ourselves have showed that Tie2 colocalizes with caveolin-1, a classical marker of caveolae, at the cell surface and at the rear of endothelial cells (Yoon et al. 2003; Saharinen et al. 2008). Furthermore, I was also able to visualize Tie2

and internalized Ang1 co-localizing with caveolin-1 in intracellular compartments of cells with both migratory and static parameters. Bogdanovic stated in her thesis that they did not observe any co-localization with caveolin-1 by electron microscopy of HUVECs in the apical and basolateral membrane of cells, yet it was not mentioned whether migratory cells were specifically analysed (Bogdanovic 2009). In our siRNA screen CAV1 siRNA had different effects on the quantitation of Ang1 and Tie2 in the first and third screen, yet did not appear to induce any change in the internalization of Tfn in any of the screens. I also found that Syntaxin 6 (STX6) siRNA and VCP siRNA also affected the quantitation of Ang1 and the expression of Tie2 in opposite directions, furthermore, VCP siRNA did not have an effect on Tfn internalization, as neither did CAV1 siRNA. The SNARE protein syntaxin-6 has been involved in the delivery of membrane components required for caveolae formation and caveolin-1 as well (Choudhury et al. 2006), while Vcp ubiquitinates and targets caveolin-1 for degradation (Kirchner et al. 2013; Burana et al. 2016). Intriguingly, the knock-down of caveolin-1 in the primary screen increased the detected Ang1 in cells albeit decreasing the detection of Tie2. A similar result was obtained in HUVECs, where Tie2 detection was increased and the overall Ang1/Tie2 ratio was decreased. While unexpected, if Tie2 could be internalized by different mechanisms including via caveolae, it could be that inhibition of caveolae-mediated endocytosis increased the internalization of the receptor through a compensatory and faster pathway hence increasing the amount of Ang1 detected. The decrease on the detection of Tie2 could then also be explained by a decrease of the amount of Tie2 detected at the basal Z-stack imaged towards a central Z-stack containing endosomes not included in the analysis.

Even though I did not obtain the same results in the secondary screen, when transfecting siGENOME siRNAs in HeLa T-REx Tie2^{FLAG}, the functional relevance of caveolin-1 in endothelial cells and the fact that it has been functionally related to Tie2 dissuaded us from discarding caveolin-1 as a hit. Polarization of caveolin-1 in the rear end of migratory cells was reported to be essential for acquiring the migratory parameter of endothelial and fibroblasts and to start directional movement (Beardsley et al. 2005; Grande-García et al. 2007; Saharinen et al. 2008). Furthermore, localization of caveolin-1 at the rear of

migratory cells was shown to be dependent on Tie2 as caveolin-1 polarization upon Ang1 stimulation was not observed in endothelial cells from conditional Tie2$^{-/-}$ mice so it would seem that Tie2 directs the polarization of caveolin-1 that is required for cell migration (Saharinen et al. 2008). Also, as mentioned before some results suggest that caveolae can act as signalling platforms of Tie2 (Yoon et al. 2003). Therefore, I believe there are enough reasons to further investigate the role of caveolin 1 in Tie2 endocytosis or trafficking.

Regulation of Tie2 internalization by molecular mechanisms involved in cell migration

As well as caveolin-1, Rac1 and Pak1 have also been reported to be key regulators of endothelial cell migration response to growth factors and Ang1 in particular. Indeed, Rac1 is considered a strong target candidate for developing anti-angiogenic therapies (Sawada et al. 2010; Bid et al. 2013). Rac1 is an important regulator of multiple cell signalling events in endothelial cells and it has been described to regulate multiple cell responses to extracellular stimulus. Amongst other roles, Rac1 and its effector Pak1 are being investigated due to their role in actin cytoskeleton rearrangement during the formation of lamellipodia leading to endothelial cell migration (Bid et al. 2013). Furthermore, induction of endothelial cell motility after activation of Tie2 by Ang1 in endothelial cells is mediated through Rac1 and Pak1, which can also cause the phosphorylation of Tie1 during regulation of angiogenesis (Cascone et al. 2003; Reinardy et al. 2015). Interestingly, based in work by Cascone et al (2003) it appears that a negative feedback loop between Rac1 at the leading edge and RhoA at the rear of migrating cells directs endothelial cell migration in response to Ang1 (Cascone et al. 2003), yet I only found RAC1 siRNA to significantly affect the internalization or localization of Tie2. To add on, early works on Tie2 determined that the Ang1-induced migration of endothelial cells is mediated by the adaptor protein Dok-R, which is recruited by activated Tie2 and subsequently phosphorylated (Jones et al. 2003). Phosphorylated Dok-R, which mediates the activation of signalling cascades leading to actin re-organisation such as the Nck/Pak pathway, was seen to co-localize with Tie2 at

the rear of migrating cells (Jones et al. 2003; Saharinen et al. 2008). In non-motile cells, RhoA and Rac1 appear to both be regulating endothelial barrier function although they could response to different stimulus; RhoA specifically but not Rac1 was found to reduce endothelial cell barrier after induced activation by the bioactive lipid sphingosine-1-phosphatase (Zhang et al. 2016), yet Rac1 reduced endothelium permeability downstream of the Ang1/Tie2 pathway by inducing the endocytosis of VE-PTP in association with Tie2 (Winderlich et al. 2009). Since I had performed most of our experiments with non-confluent cells, it is reasonable to think that Rac1 was involved in migration of cells during stimulation of HUVECs and possibly HeLa T-REx Tie2^{FLAG} cells as well. Noteworthy, in the secondary screen Rac1 and Pak1 were only found to be significantly affecting the Ang1/Tie2 ratio in the plates with cells growing in sparse conditions but not when confluent.

Intriguingly, Rac1 and Caveolin-1 have been previously shown to interact in the regulation of cell motility of various cell types including endothelial cells. To start with, direct binding between rac1 and caveolin-1 had been reported in two different works (Zuluaga et al. 2007; Kanters et al. 2008). This led to the investigation of a potential functional link between caveolin-1 and Rac1 that showed that caveolin-1 interacted also with RhoA and RhoC, yet not with Cdc42, RhoG, Rac2 or RhoB, suggesting a specific functional interaction between the proteins (Nethe et al. 2010). Interestingly, in this last work by Nethe et al (2010) Rac1 and Caveolin-1 interaction was shown to be part of a molecular mechanism regulating cell migration: activation of Rac1 induced the mobilization of caveolin-1 from the rear of migrating cells to the leading edge, where active Rac1 is mostly localized. This migration was shown to be specifically induced by Rac1 activation as it was not promoted by either RhoA or Cdc42 activation. Finally, co-localization of caveolin-1 with Rac1 at cell migratory focal adhesions induced the ubiquitination of Rac1 and promoted its degradation as a negative-feedback loop (Nethe et al. 2010). Significantly, the work by Nethe *et al.* (2010) was mostly run using HeLa cells and some of the key concepts were tested using HUVECs. In accordance to this, previous work from a different group showed that internalization of integrins regulating cell-mediated adhesion of fibroblasts was modulated by caveolin-1 as part of a down-

regulatory mechanism of Erk, PI3K and Rac signalling pathways inducing adhesion and migration (del Pozo et al. 2004; Del Pozo et al. 2005).

Based on data from previous reports and ourselves, I believe that a functional link between caveolin-1 and Rac-1 regarding endothelial cell migration could be explaining part of the results obtained on the internalization of Tie2. Based in the co-localization of Tie2 with caveolin-1 at the rear of the cell and in the resulting parameters of CAV1 siRNAs, I think that it could be possible that caveolin-1 co-localizing with Tie2 could be sequestering the receptor and inhibiting its internalization. Endocytosis of Tie2 in a caveolae-mediated pathway could still be possible as due to the slow progression of this endocytic mechanism it could itself behave as an inhibitory mechanism of endocytosis, indeed, caveolin-1 has been described to have a negative role in the internalization of caveolae (Le et al. 2002; Bastiani & Parton 2010). In agreement with a previous report, I saw that caveolin-1 and Tie2 co-localized in the rear of migrating cells (Saharinen et al. 2008). Although this effect had been shown to be dependent of Ang1 I was able to see this polarization even in serum starved cells; this could be due to the short serum starvation that I apply to cells (2h) compared to other groups (overnight). Nonetheless, I did observe that the localization of caveolin-1 and Tie2 appeared to gradually fade during incubation with Ang1 and up to until 30 min. I believe that this effect could be caused by the reported recruitment of caveolin-1 to the leading edge of migrating cells by Rac1 (Nethe et al. 2010). As in this experiment I used an antibody specific for the ectodomain of Tie2 this effect could also be due to the cleavage of receptor so the loss of co-localization should be confirmed using an antibody targeting the endodomain of Tie2. Interestingly, although I was able to visualize Ang1 and Tie2 contained in intracellular caveolin-1-containing compartments of HUVECs, transfection of caveolin-1 siRNA induced an increase in the internalization of Ang1 rather than a decrease. Because this was accompanied by a decrease in the detection of Tie2 (observed as well in the pilot screen of HUVECs) it is not likely that the effect was due to a change of the total expression of the receptor. I believe that this results could also be explained if caveolin-1 was determining the timing of the internalization of Tie2 and retaining the receptor in the rear basolateral membrane of migrating cells; in that case a knock-down of caveolin-

1 would then cause a faster internalization of the ligand, generating a higher readout of the internalized Ang1 and a lower detection of the receptor due to its internalization and/or re-location away from the imaged basal Z-stack. Saharinen et al (2008) also showed that Tie2-GFP was retained at the rear of migrating cells until being internalized into highly mobile endosomal-like compartments. In agreement with this, transfection of VCP siRNA, which targets caveolin-1 for degradation, not only caused a decrease in the internalization of Ang1 yet also an increase in the detection of Tie2 in HeLa T-REx $Tie2^{FLAG}$ cells, what could be explained by a reduced internalization of Tie2 due to an accumulation of caveolin-1. Additionally, if I imagine that this mobilization of caveolin-1 to the leading edge is led by activated Rac1, in the absence of Rac1 caveolin-1 would not be mobilized from the rear of migrating cells and the internalization of Tie2 would then be delayed or inhibited. Indeed, in all of the screens where sparse cell cultures were used Rac1 siRNA caused an overall decrease in the internalization of Ang1 yet also causing an increase in the detection of Tie2 in the secondary screen with siGENOME and in the pilot screen with HUVECs.

Moreover, I believe that the functional interrelationship between Tie2 and the fibronectin-sensing integrin α5β1 could also expand the link between Tie2, caveolin-1 and Rac1 in migratory endothelial cells. Integrins are believed to have a pivotal role in angiogenesis and are also the target of potential anti-tumoral therapies (Avraamides et al. 2008). Indeed, the role of the Ang/Tie pathway regulating vascular functionality is believed to be tuned by interaction with integrins and the extracellular matrix (ECM). For instance, as mentioned before, Angiopoietin 2 binding and activation of β1 integrin in endothelial cells was shown to cause an increase in endothelium permeability to tumoral cells (Hakanpaa et al. 2015). Furthermore, Ang1 was reported to cause focal adhesion kinase (FAK) phosphorylation specifically via activation of the fibronectin sensing α5β1 integrin. At the same time, Tie2 was also reported to form stable complexes with α5β1 integrin in endothelial cells (Cascone et al. 2005). Integrin α5β1 mediates directional cell migration through sensing the extracellular matrix (ECM) component fibronectin, a process known as haptotaxis. Interaction of integrin α5β1 with fibronectin, which is usually exposed in developing basal membranes, leads to the

activation of focal adhesion proteins such as FAK and paxillin. Interestingly, downstream of activated FAK and paxillin, interaction of fibronectin with α5β1 lead to the recruitment of Rac1-GTP at the leading edge of migrating cells (Nethe et al. 2010). Continuous recycling of activated integrins is key to continuous migration of cells and it was reported that α5β1 integrin recycling was regulated by the Trans Golgi network t-SNARE syntaxin 6 (Tiwari et al. 2011). Tiwari et al. (2011) shown that a minority of syntaxin 6 also localized with α5β1 integrin in endosomes of endothelial cells and that knock-down of syntaxin 6 but not of syntaxin 16 caused accumulation of α5β1 integrin in intracellular compartments, while other integrins were little or not affected. Furthermore, they showed that Rac1 activation at the leading edge of migrating endothelial cells was also dependent on syntaxin 6 and that knockdown of syntaxin 6 lead to re-localization of Rac1 into perinuclear endosomes, as it was α5β1 integrin as well. Interestingly, in our case STX6 siRNA transfected in HeLa T-REx Tie2^{FLAG} cells led to an increase of the detection of Tie2^{FLAG} at the basal Z-stack of cells yet an increase in the amount of internalized Ang1 detected, similar to the effects of RAC1 siRNA and opposite to the transfected CAV1 siRNA. Despite I did not follow up with STX6 siGENOME in HeLa T-REx Tie2^{FLAG} cells, in the pilot screen on HUVECs STX6 siRNA caused a decrease in the Ang1/Tie2 ratio, suggesting an overall decrease of the internalization of Ang1 and/or an increase in the detection of Tie2 although the individual parameters did not show a significant difference from controls. This results would fit with the hypothetical model in which Tie2 internalization is triggered after mobilization of caveolin-1 from the rear of migrating cells towards the leading edge by Rac1, which is in its turned recruited by integrins, based on published results. I understand that the role of syntaxin 6 could be controversial, as it has also been involved to other cellular functions and pathways. For instance, syntaxin 6 was reported to be necessary for the anterograde transport of caveolin 1 and other components required for the formation of caveolae in human skin fibrobasts (Choudhury et al. 2006). Also, syntaxin 6 has been reported to be involved in the anterograde transport of VEGFR-2 upon ligand stimulation (Manickam et al. 2011). Still, our results regarding STX6 siRNA transfection would not fit considering only a supposedly caveolin 1 internalization of Tie2, since I would then expect STX6 siRNA and

CAV1 siRNA to yield similar effects; and neither with an involvement in the recycling of Tie2 as I would then expect STX6 knock-down to yield an accumulation of intracellular Ang1 and Tie2.

This model where the internalization of Tie2 is only triggered after mobilization of caveolin-1 to the leading edge of the cell could also explain the coexistence of at least two endocytic mechanisms. For instance, Tie2 “sequestered” by caveolin-1 could be internalized via caveolae-mediated internalization, once caveolin-1 was recruited to the leading edge of migrating cells Tie2 would then be internalized by a different endocytic mechanism such as CME, hence explaining the duality in the results. Nonetheless, as explained before our results are not complete enough to define a particular endocytic mechanism responsible for the internalization of Tie2.

Conclusions and future perspectives

Overall, I have provided a validated in vitro model for the study of the endocytosis of Tie2 and I have also developed an immunofluorescence-based assay to study the internalization of Tie2 in an automated high throughput format, which I used to screen a library of siRNA targeting components of different endocytic pathways and membrane trafficking. Also, together with immunofluorescence analysis of the internalized ligand I provide evidence in support of a CME of the receptor as previously published. Nonetheless, the circumstances of this CME should be investigated further, as based on our results and others' I cannot discard an alternative CIE of Tie2 such as macropinocytosis or caveolae-mediated internalization. However, based on numerous published results and some of our data I suggest a hypothetical yet very interesting model where the timing and pathway of Tie2 internalization would be determined by molecular mechanisms regulating endothelial cell migration.

Based in our results and conclusions, I believe that the knock-downs of Rac1, Pak1, dynamin 2, arpc2, chc and caveolin 1 should be validated in HeLa TREx $Tie2^{FLAG}$ cells by western blot analysis of the total expression of Tie2 and the targeted proteins. Furthermore, after implementation of the siRNA transfection in HUVECs, knock-down experiments and siRNA rescue validations should be carried out in HUVECs to evaluate the significance of these hits in endothelial cells. I think it would be important to study the effect of the knock-downs on the localization of Tie2 within endothelial cells before and after incubation with Ang1, as well as determining whether interference with the mentioned targets modify the internalization rate of the receptor. On that account, I think it is key to either improve the Ang1 quantitative ELISA or design a new method to measure the internalization of Tie2 in response to incubation with Ang1. Importantly, due to the role in cell migration of multiple of the hits I believe that it would be important to maintain a consistency with cell confluency used in future experiments.

Regarding the internalization pathway of Tie2, it would be important to analyse the co-localization of the ligand and the receptor with significant endocytic markers in order to clarify which endocytic mechanisms are involved. Due to the potential co-existence of different endocytic mechanisms, I think it would be important to do so without

interfering with the system to avoid compensatory mechanisms. Also it would be interesting to monitor the internalization of Tie2 by live cell imaging if possible.

Lastly, I believe that the HT internalization assay that I have developed could be further used to study the internalization of Tie2 by for instance investigating the effect on the internalization of Ang1 of different Tie2 mutations. In that sense, I would be interested in determining which of the motifs within the intracellular domain of Tie2 mediate the interaction with AP-2 adaptor. Also, in the event that caveolin 1 is validated as a regulator of Tie2 internalization, it would be interesting to determine whether any of the CRAC motifs that I have identified are involved in regulating the internalization of Tie2.

Annex A

Sup. Table 1. Coding sequence of the Tie2^{FLAG}. Coding region for the wild-type K855 is shown in bold format and coloured green. Coding nucleotides for the FLAG tag are underlined. Silent mutations are highlighted in yellow.

Tie2^{FLAG} 3399 bp

ATGGACTCTTTAGCCAGCTTAGTTCTCTGTGGAGTCAGCTTGCTCCTTTCTGGAACTGTGGAAGGTGCCATGGACTTGATCTTGA
TCAATTCCCTACCTCTTGTATCTGATGCTGAAACATCTCTCACCTGCATTGCCTCTGGGTGGCGCCCCCATGAGCCCATCACCATA
GGAAGGGACTTTGAAGCCTTAATGAACCAGCACCAGGATCCGCTGGAAGTTACTCAAGATGTGACCAGAGAATGGGCTAAAA
AAGTTGTTTGGAAGAGAGAAAAGGCTAGTAAGATCAATGGTGCTTATTTCTGTGAAGGGCGAGTTCGAGGAGAGGCAATCAG
GATACGAACCATGAAGATGCGTCAACAAGCTTCCTTCCTACCAGCTACTTTAACTATGACTGTGGACAAGGGAGATAACGTGAA
CATATCTTTCAAAAAGGTATTGATTAAAGAAGAAGATGCAGTGATTTACAAAAATGGTTCCTTCATCCATTCAGTGCCCCGGCAT
GAAGTACCTGATATTCTAGAAGTACACCTGCCTCATGCTCAGCCCCAGGATGCTGGAGTGTACTCGGCCAGGTATATAGGAGG
AAACCTCTTCACCTCGGCCTTCACCAGGCTGATAGTCCGGAGATGTGAAGCCCAGAAGTGGGGACCTGAATGCAACCATCTCTG
TACTGCTTGTATGAACAATGGTGTCTGCCATGAAGATACTGGAGAATGCATTTGCCCTCCTGGGTTTATGGGAAGGACGTGTGA
GAAGGCTTGTGAACTGCACACGTTTGGCAGAACTTGTAAAGAAAGGTGCAGTGGACAAGAGGGATGCAAGTCTTATGTGTTCT
GTCTCCCTGACCCCTATGGGTGTTCCTGTGCCACAGGCTGGAAGGGTCTGCAGTGCAATGAAGCATGCCACCCTGGTTTTTACG
GGCCAGATTGTAAGCTTAGGTGCAGCTGCAACAATGGGGAGATGTGTGATCGCTTCCAAGGATGTCTCTGCTCTCCAGGATGG
CAGGGGCTCCAGTGTGAGAGAGAAGGCATACCGAGGATGACCCCAAAGATAGTGGATTTGCCAGATCATATAGAAGTAAACA
GTGGTAAATTTAATCCCATTTGCAAAGCTTCTGGCTGGCCGCTACCTACTAATGAAGAAATGACCCTGGTGAAGCCGGATGGGA
CAGTGCTCCATCCAAAAGACTTTAACCATACGGATCATTTCTCAGTAGCCATATTCACCATCCACCGGATCCTCCCCCCTGACTCA
GGAGTTTGGGTCTGCAGTGTGAACACAGTGGCTGGGATGGTGGAAAAGCCCTTCAACATTTCTGTTAAAGTTCTTCCAAAGCCC
CTGAATGCCCCAAACGTGATTGACACTGGACATAACTTTGCTGTCATCAACATCAGCTCTGAGCCTTACTTTGGGGATGGACCA
ATCAAATCCAAGAAGCTTCTATACAAACCCGTTAATCACTATGAGGCTTGGCAACATATTCAAGTGACAAATGAGATTGTTACAC
TCAACTATTTGGAACCTCGGACAGAATATGAACTCTGTGTGCAACTGGTCCGTCGTGGAGAGGGTGGGGAAGGGCATCCTGGA
CCTGTGAGACGCTTCACAACAGCTTCTATCGGACTCCCTCCTCCAAGAGGTCTAAATCTCCTGCCTAAAAGTCAGACCACTCTAA
ATTTGACCTGGCAACCAATATTTCCAAGCTCGGAAGATGACTTTTATGTTGAAGTGGAGAGAAGGTCTGTGCAAAAAAGTGATC
AGCAGAATATTAAAGTTCCAGGCAACTTGACTTCGGTGCTACTTAACAACTTACATCCCAGGGAGCAGTACGTGGTCCGAGCTA
GAGTCAACACCAAGGCCCAGGGGGAATGGAGTGAAGATCTCACTGCTTGGACCCTTAGTGACATTCTTCCTCCTCAACCAGAAA
ACATCAAGATTTCCAACATTACACACTCCTCGGCTGTGATTTCTTGGACAATATTGGATGGCTATTCTATTTCTTCTATTACTATCC
GTTACAAGGTTCAAGGCAAGAATGAAGACCAGCACGTTGATGTGAAGATAAAGAATGCCACCATCACTCAGTATCAGCTCAAG
GGCCTAGAGCCTGAAACAGCATACCAGGTGGACATTTTTGCAGAGAACAACATAGGGTCAAGCAACCCAGCCTTTTCTCATGA
ACTGGTGACCCTCCCAGAATCTCAAGCACCAGCGGACCTCGGAGGGGGGGAAGATGCTGCTTATAGCCATCCTTGGCTCTGCTG
GAATGACCTGCCTGACTGTGCTGTTGGCCTTTCTGATCATATTGCAATTGAAGAGAGCAAATGTGCAAAGGAGAATGGCCCAA
GCCTTCCAAAACGTGAGGGAAGAACCAGCTGTGCAGTTCAACTCAGGGACTCTGGCCCTAAACAGGAAGGTCAAAAACAACCC
AGATCCTACAATTTATCCAGTGCTTGACTGGAATGACATCAAATTTCAAGATGTGATTGGGGAGGGCAATTTTGGCCAAGTTCT
TAAGGCGCGCATCAAGAAGGATGGGTTACGGATGGATGCTGCCATCAAAAGAATGAAAGAATATGCCTCCAAAGATGATCAC
AGGGACTTTGCAGGAGAACTGGAAGTTCTTTGTAAACTTGGACACCATCCAAACATCATCAATCTCTTAGGAGCATGTGAACAT
CGAGGCTACTTGTACCTGGCCATTGAGTACGCGCCCCATGGAAACCTTCTGGACTTCCTTCGCAAGAGCCGTGTGCTGGAGACG
GACCCAGCATTTGCCATTGCCAATAGCACCGCGTCCACACTGTCCTCCCAGCAGCTCCTTCACTTCGCTGCCGACGTGGCCCGGG
GCATGGACTACTTGAGCCAAAAACAGTTTATCCACAGGGATCTGGCTGCCAGAAACATTTTAGTTGGTGAAAACTATGTGGCAA
AAATAGCAGATTTTGGATTGTCCCGAGGTCAAGAGGTGTATGTGAAAAAGACAATGGGAAGGCTCCCAGTGCGCTGGATGGC
CATCGAGTCACTGAATTACAGTGTGTACACAACCAACAGTGATGTATGGTCCTATGGTGTGTTACTATGGGAGATTGTTAGCTT
AGGAGGCACACCCTACTGCGGGATGACTTGTGCAGAACTCTACGAGAAGCTGCCCCAGGGCTACAGACTGGAGAAGCCCCTG
AACTGTGATGATGAGGTGTATGATCTAATGAGACAATGCTGGCGGGAGAAGCCTTATGAGAGGCCATCATTTGCCCAGATATT
GGTGTCCTTAAACAGAATGTTAGAGGAGCGAAAGACCTACGTGAATACCACGCTTTATGAGAAGTTTACTTATGCAGGAATTG
ACTGTTCTGCTGAAGAAGCGGCCGATTACAAGGATGACGACGATAAGTAG

Sup. Table 2. Coding sequence of the Tie2$^{K855R/FLAG}$. Coding region for the mutated R855 is shown in bold format and coloured red. Coding nucleotides for the FLAG tag are underlined. Silent mutations are highlighted in yellow.

Tie2$^{K855R/FLAG}$ 3399 bp

ATGGACTCTTTAGCCAGCTTAGTTCTCTGTGGAGTCAGCTTGCTCCTTTCTGGAACTGTGGAAGGTGCCATGGACTTGATCTTGA
TCAATTCCCTACCTCTTGTATCTGATGCTGAAACATCTCTCACCTGCATTGCCTCTGGGTGGCGCCCCCATGAGCCCATCACCATA
GGAAGGGACTTTGAAGCCTTAATGAACCAGCACCAGGATCCGCTGGAAGTTACTCAAGATGTGACCAGAGAATGGGCTAAAA
AAGTTGTTTGGAAGAGAGAAAAGGCTAGTAAGATCAATGGTGCTTATTTCTGTGAAGGGCGAGTTCGAGGAGAGGCAATCAG
GATACGAACCATGAAGATGCGTCAACAAGCTTCCTTCCTACCAGCTACTTTAACTATGACTGTGGACAAGGGAGATAACGTGAA
CATATCTTTCAAAAAGGTATTGATTAAAGAAGAAGATGCAGTGATTTACAAAAATGGTTCCTTCATCCATTCAGTGCCCCGGCAT
GAAGTACCTGATATTCTAGAAGTACACCTGCCTCATGCTCAGCCCCAGGATGCTGGAGTGTACTCGGCCAGGTATATAGGAGG
AAACCTCTTCACCTCGGCCTTCACCAGGCTGATAGTCCGGAGATGTGAAGCCCAGAAGTGGGGACCTGAATGCAACCATCTCTG
TACTGCTTGTATGAACAATGGTGTCTGCCATGAAGATACTGGAGAATGCATTTGCCCTCCTGGGTTTATGGGAAGGACGTGTGA
GAAGGCTTGTGAACTGCACACGTTTGGCAGAACTTGTAAAGAAAGGTGCAGTGGACAAGAGGGATGCAAGTCTTATGTGTTCT
GTCTCCCTGACCCCTATGGGTGTTCCTGTGCCACAGGCTGGAAGGGTCTGCAGTGCAATGAAGCATGCCACCCTGGTTTTTACG
GGCCAGATTGTAAGCTTAGGTGCAGCTGCAACAATGGGGAGATGTGTGATCGCTTCCAAGGATGTCTCTGCTCTCCAGGATGG
CAGGGGCTCCAGTGTGAGAGAGAAGGCATACCGAGGATGACCCCAAAGATAGTGGATTTGCCAGATCATATAGAAGTAAACA
GTGGTAAATTTAATCCCATTTGCAAAGCTTCTGGCTGGCCGCTACCTACTAATGAAGAAATGACCCTGGTGAAGCCGGATGGGA
CAGTGCTCCATCCAAAAGACTTTAACCATACGGATCATTTCTCAGTAGCCATATTCACCATCCACCGGATCCTCCCCCCTGACTCA
GGAGTTTGGGTCTGCAGTGTGAACACAGTGGCTGGGATGGTGGAAAAGCCCTTCAACATTTCTGTTAAAGTTCTTCCAAAGCCC
CTGAATGCCCCAAACGTGATTGACACTGGACATAACTTTGCTGTCATCAACATCAGCTCTGAGCCTTACTTTGGGGATGGACCA
ATCAAATCCAAGAAGCTTCTATACAAACCCGTTAATCACTATGAGGCTTGGCAACATATTCAAGTGACAAATGAGATTGTTACAC
TCAACTATTTGGAACCTCGGACAGAATATGAACTCTGTGTGCAACTGGTCCGTCGTGGAGAGGGTGGGGAAGGGCATCCTGGA
CCTGTGAGACGCTTCACAACAGCTTCTATCGGACTCCCTCCTCCAAGAGGTCTAAATCTCCTGCCTAAAAGTCAGACCACTCTAA
ATTTGACCTGGCAACCAATATTTCCAAGCTCGGAAGATGACTTTTATGTTGAAGTGGAGAGAAGGTCTGTGCAAAAAAGTGATC
AGCAGAATATTAAAGTTCCAGGCAACTTGACTTCGGTGCTACTTAACAACTTACATCCCAGGGAGCAGTACGTGGTCCGAGCTA
GAGTCAACACCAAGGCCCAGGGGGAATGGAGTGAAGATCTCACTGCTTGGACCCTTAGTGACATTCTTCCTCCTCAACCAGAAA
ACATCAAGATTTCCAACATTACACACTCCTCGGCTGTGATTTCTTGGACAATATTGGATGGCTATTCTATTTCTTCTATTACTATCC
GTTACAAGGTTCAAGGCAAGAATGAAGACCAGCACGTTGATGTGAAGATAAAGAATGCCACCATCACTCAGTATCAGCTCAAG
GGCCTAGAGCCTGAAACAGCATACCAGGTGGACATTTTTGCAGAGAACAACATAGGGTCAAGCAACCCAGCCTTTTCTCATGA
ACTGGTGACCCTCCCAGAATCTCAAGCACCAGCGGACCTCGGAGGGGGGAAGATGCTGCTTATAGCCATCCTTGGCTCTGCTG
GAATGACCTGCCTGACTGTGCTGTTGGCCTTTCTGATCATATTGCAATTGAAGAGAGCAAATGTGCAAAGGAGAATGGCCCAA
GCCTTCCAAAACGTGAGGGAAGAACCAGCTGTGCAGTTCAACTCAGGGACTCTGGCCCTAAACAGGAAGGTCAAAAACAACCC
AGATCCTACAATTTATCCAGTGCTTGACTGGAATGACATCAAATTTCAAGATGTGATTGGGGAGGGCAATTTTGGCCAAGTTCT
TAAGGCGCGCATCAAGAAGGATGGGTTACGGATGGATGCTGCCATC**CGG**AGAATGAAAGAATATGCCTCCAAAGATGATCAC
AGGGACTTTGCAGGAGAACTGGAAGTTCTTTGTAAACTTGGACACCATCCAAACATCATCAATCTCTTAGGAGCATGTGAACAT
CGAGGCTACTTGTACCTGGCCATTGAGTACGCGCCCCATGGAAACCTTCTGGACTTCCTTCGCAAGAGCCGTGTGCTGGAGACG
GACCCAGCATTTGCCATTGCCAATAGCACCGCGTCCACACTGTCCTCCCAGCAGCTCCTTCACTTCGCTGCCGACGTGGCCCGGG
GCATGGACTACTTGAGCCAAAAACAGTTTATCCACAGGGATCTGGCTGCCAGAAACATTTTAGTTGGTGAAAACTATGTGGCAA
AAATAGCAGATTTTGGATTGTCCCGAGGTCAAGAGGTGTATGTGAAAAAGACAATGGGAAGGCTCCCAGTGCGCTGGATGGC
CATCGAGTCACTGAATTACAGTGTGTACACAACCAACAGTGATGTATGGTCCTATGGTGTGTTACTATGGGAGATTGTTAGCTT
AGGAGGCACACCCTACTGCGGGATGACTTGTGCAGAACTCTACGAGAAGCTGCCCCAGGGCTACAGACTGGAGAAGCCCCTG
AACTGTGATGATGAGGTGTATGATCTAATGAGACAATGCTGGCGGGAGAAGCCTTATGAGAGGCCATCATTTGCCCAGATATT
GGTGTCCTTAAACAGAATGTTAGAGGAGCGAAAGACCTACGTGAATACCACGCTTTATGAGAAGTTTACTTATGCAGGAATTG
ACTGTTCTGCTGAAGAAGCGGCC<u>GATTACAAGGATGACGACGATAAG</u>TAG

Annex B

Sup. Table 3. Sequences of the ON-TARGET*plus* siRNAs included in the TraffickOme library. The library, obtained from Dharmacon was used as a mix of 4 targeting siRNA for each target (SMARTpool) in the primary screen.

Gene Symbol	GENE ID	Gene Accession	GI Number	Sequence
ALS2	57679	NM_020919	40316934	GAAUGUGUCCUUCGACUAA
ALS2	57679	NM_020919	40316934	GAAUUUAGGCUCUGAGGUA
ALS2	57679	NM_020919	40316934	CGAGUUAGCUACUACAGAA
ALS2	57679	NM_020919	40316934	GAUUCCAGCUUCUUGCUAA
ANKFY1	51479	NM_020740	31317251	GGUGUUAUGUCUCUAGUGA
ANKFY1	51479	NM_020740	31317251	GUGCAAACAACUAGAUUUA
ANKFY1	51479	NM_020740	31317251	CAGAGUACCCGCUACAUAA
ANKFY1	51479	NM_020740	31317251	CAAAUCGGUUUCAGCUACA
APPL1	26060	NM_012096	6912241	GAAACUAUGCGCCAAAUCU
APPL1	26060	NM_012096	6912241	CAAAGUCGGUUGAUAGCUG
APPL1	26060	NM_012096	6912241	GGAAAUGGACAGUGAUAUA
APPL1	26060	NM_012096	6912241	GAUCUGAGUCUACAAAUUU
APPL2	55198	NM_018171	82617617	CUAGUAGAGAUGCGCGAUA
APPL2	55198	NM_018171	82617617	CGAACAUAGAGGCGCAGAA
APPL2	55198	NM_018171	82617617	GCGGAAAAGAUGCGGGUGU
APPL2	55198	NM_018171	82617617	AGAUCUACCUGACCGACAA
ARHGAP26	23092	NM_015071	32189359	GCACUACUGUACAUAUCAA
ARHGAP26	23092	NM_015071	32189359	CAAGGGCUGUAUCGAAUUG
ARHGAP26	23092	NM_015071	32189359	GAACGGAUACGGAUGAUUG
ARHGAP26	23092	NM_015071	32189359	GGAGAAACGUCACUUUGGA
ARHGDIA	396	NM_004309	34147601	GGUGUGGAGUACCGGAUAA
ARHGDIA	396	NM_004309	34147601	CAGCAUACGUACAGGAAAG
ARHGDIA	396	NM_004309	34147601	CCGGGUUAACCGAGAGAUA
ARHGDIA	396	NM_004309	34147601	GGGCCGAGGAGUACGAGUU
BET1	10282	NM_005868	83779007	GGAACUAUGGCUAUGCUAA
BET1	10282	NM_005868	83779007	GAAACUUAGUGGGAGAGUA
BET1	10282	NM_005868	83779007	AAAUAGGCCAUGAAGUUAA
BET1	10282	NM_005868	83779007	CCUAAUAACCUGUCAGUUU
BET1L	51272	NM_016526	34365798	UCCCUUAGGACUCGGAUUU
BET1L	51272	NM_016526	34365798	GCGGGUGGGUGGUCAAAUC
BET1L	51272	NM_016526	34365798	AGUGUGAGAGCCAGGGUUA
BET1L	51272	NM_016526	34365798	CCUUCUAGCUUGCUGGUAA
BNIP1	662	NM_013978	153946402	GGUCCUCUAUAUUGUGAAA
BNIP1	662	NM_013978	153946402	ACAGUUGCGUCACAGAAUA
BNIP1	662	NM_013978	153946402	GGAUAUCCGUGAUUGUUCA
BNIP1	662	NM_013978	153946402	UCUCAUCUUCCUUGCGCUA
EHD1	10938	NM_006795	30240931	CCGCAAGCUCAACGCGUUU
EHD1	10938	NM_006795	30240931	GGCAGUACAGCACGGGCAA
EHD1	10938	NM_006795	30240931	ACCAGAAGAUUGAGCGCGA
EHD1	10938	NM_006795	30240931	UGAUGGUGAUGGUGCGGCA
EXOC6	54536	NM_001013848	62243651	GAUAAUUGCUGUCCUUAGA
EXOC6	54536	NM_001013848	62243651	GAAGUUUGGUGAAUGGUAU
EXOC6	54536	NM_001013848	62243651	GAUAGAGACAGUCGUGAAA
EXOC6	54536	NM_001013848	62243651	AGUCAGUGCCUCAUAUUUA
EXOC7	23265	NM_015219	62241043	CUAAGCACCUAUAUCUGUA
EXOC7	23265	NM_015219	62241043	GACCUUCGACUCCCUGAUA
EXOC7	23265	NM_015219	62241043	GAGAUGACAUGCUGGACGU
EXOC7	23265	NM_015219	62241043	GGAAGGCCAUUGUGCGACA
FLOT1	10211	NM_005803	6552331	GCAGAGAAGUCCCAACUAA
FLOT1	10211	NM_005803	6552331	GUGGUUAGCUACACUCUGA
FLOT1	10211	NM_005803	6552331	GAUCAGUGGUCCCUUGACU

FLOT1	10211	NM_005803	6552331	GAAGACGGAGGCUGAGAUU
GAPVD1	26130	NM_015635	51093831	AAGAAGUGGCCAAUCGAUA
GAPVD1	26130	NM_015635	51093831	UUAGAAUAGUGGUGCGUUA
GAPVD1	26130	NM_015635	51093831	AGAAUGUGCUCUACGAUUA
GAPVD1	26130	NM_015635	51093831	ACGCAAAGAUAGCGAUGAU
GOPC	57120	NM_001017408	62868212	GGCCUUGGCAUUUCAAUUA
GOPC	57120	NM_001017408	62868212	UGACGGUGCUUCAAAAUUA
GOPC	57120	NM_001017408	62868212	GGACAUCGUUACCGUUUGU
GOPC	57120	NM_001017408	62868212	AAGCGGACAUCACUUAUGA
GOSR1	9527	NM_001007025	55770857	CAGAAGAACUGAGCUAUUU
GOSR1	9527	NM_001007025	55770857	GAAGUCAAUUCACAGCAAA
GOSR1	9527	NM_001007025	55770857	GGGAGAAUCUUAUGGGAUC
GOSR1	9527	NM_001007025	55770857	GAGACAUAUUGCAGGAUUA
GOSR2	9570	NM_054022	60499002	ACGAAUCACUGCAGUUUAA
GOSR2	9570	NM_054022	60499002	CGAAAUCCAAGCAAGCAUA
GOSR2	9570	NM_054022	60499002	GAUCCAGUCUUGCAUGGGA
GOSR2	9570	NM_054022	60499002	UUAGAUGGGCACAAUAUUU
MICAL1	64780	NM_022765	20127615	UGGAGAACAUUGUGUACUA
MICAL1	64780	NM_022765	20127615	CCUCAGGCACCAUGAAUAA
MICAL1	64780	NM_022765	20127615	GAGUCCACGUCUCCGAUUU
MICAL1	64780	NM_022765	20127615	GUACGAGACCUGUAUGAUG
OCRL	4952	NM_001587	21396492	GAACGAAGGUACCGGAAAG
OCRL	4952	NM_001587	21396492	CGAAGAAGACUAAGGCUUU
OCRL	4952	NM_001587	21396492	GCGGGAGGGUCUCAUCAAA
OCRL	4952	NM_001587	21396492	GAAAGGAUCAGUGUCGAUA
PICALM	8301	NM_001008660	56788367	CAACAGGCAUGAUAGGAUA
PICALM	8301	NM_001008660	56788367	GUUCAAAGAUGCCAUUAGA
PICALM	8301	NM_001008660	56788367	GUAAUGGCCUAUCCUGCUA
PICALM	8301	NM_001008660	56788367	CAUUACAACUCAUCAUUUG
RAB21	23011	NM_014999	7661921	GAUAACUGUUCACGCCUAA
RAB21	23011	NM_014999	7661921	GGAAAAUGUUGGGAAAUGA
RAB21	23011	NM_014999	7661921	GAGAACAAGUUUAACGACA
RAB21	23011	NM_014999	7661921	GAACAAAGGAAUUGAGGAA
RAB22A	57403	NM_020673	34577103	GGACUACGCCGACUCUAUU
RAB22A	57403	NM_020673	34577103	GAAGAAUUCCAUCCACUGA
RAB22A	57403	NM_020673	34577103	GAAACAACCUCUGCGAAUU
RAB22A	57403	NM_020673	34577103	GCAGUUUGAUUAUCCGAUU
RAB31	11031	NM_006868	33589860	UGAAGGAUGCUAAGGAAUA
RAB31	11031	NM_006868	33589860	GAUAUUACCAAGCAGGAUU
RAB31	11031	NM_006868	33589860	GGCCAUCGCUGGAAACAAG
RAB31	11031	NM_006868	33589860	CAACAUCAGCCCUACUAUU
RABEP1	9135	NM_004703	49574500	UGAGAGACAUGCAGCGAAU
RABEP1	9135	NM_004703	49574500	GUAGUAUGCUGUAUGAAUA
RABEP1	9135	NM_004703	49574500	CCAAGUGGGUUUAUGUUAA
RABEP1	9135	NM_004703	49574500	CGGACAAUGACAUGUUUAA
RABGEF1	27342	NM_014504	7657495	AAAUUAAGCCUCCGAAUCA
RABGEF1	27342	NM_014504	7657495	GAAUUCAUGUGGAUCAAUC
RABGEF1	27342	NM_014504	7657495	GAAAGGAUGCAAACUCGUG
RABGEF1	27342	NM_014504	7657495	GAAAGUGCCUCCAGAAAGA
RAPH1	65059	NM_025252	47132517	GGAAACAGUAAGCGUCAAA
RAPH1	65059	NM_025252	47132517	GAACAGGCCUCUUUGAGUA
RAPH1	65059	NM_025252	47132517	GGAAGCAGCUCUAUAUGAA
RAPH1	65059	NM_025252	47132517	CCACUGCGGUUAUAGUUUA
RBSN	64145	NM_022340	70980546	CGUGAAGCUCUACGAGAAA
RBSN	64145	NM_022340	70980546	CGGGAGUUGGAACGAGAAA
RBSN	64145	NM_022340	70980546	UCGAUAACAUCAAGGCAUA
RBSN	64145	NM_022340	70980546	GGGUCUAUUAUGUGCAAGA
RIN1	9610	NM_004292	68989255	AGAAGCUGCUGUCGCCUAA

RIN1	9610	NM_004292	68989255	CCGAGUAGCCUAUCAGGAU
RIN1	9610	NM_004292	68989255	CCACGCAGCCACUCACAAA
RIN1	9610	NM_004292	68989255	CCAGAAGCCUCGAUUGCCA
RIN2	54453	NM_018993	35493905	GGUCUGGACAAGCGAGGAA
RIN2	54453	NM_018993	35493905	AAGAUGUAUUCGCCGGAAA
RIN2	54453	NM_018993	35493905	UAACAAACAUGGGAACGUA
RIN2	54453	NM_018993	35493905	ACGCAAGGUAGCUGAGGUU
RIN3	79890	NM_024832	40353728	UCAGAUUGAUUGCGUUCUA
RIN3	79890	NM_024832	40353728	GCAGCAUGUUCCACGCUUU
RIN3	79890	NM_024832	40353728	ACCUCAGGGUGUCGGUUAA
RIN3	79890	NM_024832	40353728	GAAGAUGGCAUGCGGCUUU
SCFD1	23256	NM_182835	33469977	AAGCAUUGGUGCACGAUGU
SCFD1	23256	NM_182835	33469977	GACAAGAAACUUCGAGAAA
SCFD1	23256	NM_182835	33469977	GUGCCAGGAUCUUCGAAAU
SCFD1	23256	NM_182835	33469977	GAUAUCACAGACACGGAAA
SEC22A	26984	NM_012430	14591918	GGGCAAGGCUCCCGAUUAU
SEC22A	26984	NM_012430	14591918	AGGACCAAGCAGCGAUAUA
SEC22A	26984	NM_012430	14591918	GAACAUCACAAGUAUCGAA
SEC22A	26984	NM_012430	14591918	CAAAUUUCCAUGUGCGAAC
SEC22B	9554	NM_004892	34335289	AAUAGUGUAUGUCCGAUUC
SEC22B	9554	NM_004892	34335289	GCUAAGCAACUCUUUCGAA
SEC22B	9554	NM_004892	34335289	CCUAGAAGAUUUGCACUCA
SEC22B	9554	NM_004892	34335289	GAAGCACUCUCAGCAUUGG
SEC22C	9117	NM_032970	21536309	CCUCCAGGCCAUACGCUUU
SEC22C	9117	NM_032970	21536309	CCGAAUGGAACCAGUGACA
SEC22C	9117	NM_032970	21536309	GGUUGUGACUUUAGUAUAC
SEC22C	9117	NM_032970	21536309	GUAUCCAGGUCGAGGUUCU
SH3GL2	6456	NM_003026	4506930	CAACCUAAACCACGAAUGA
SH3GL2	6456	NM_003026	4506930	ACAAAGAUCUUAGGGAAAU
SH3GL2	6456	NM_003026	4506930	GAUAUCAUCACACUCACUA
SH3GL2	6456	NM_003026	4506930	UAAAGAAGUUGGAGGGUCG
SNAP23	8773	NM_130798	18765730	UAACAGAACUCAACAAAUG
SNAP23	8773	NM_130798	18765730	CAACUAAACCGCAUAGAAG
SNAP23	8773	NM_130798	18765730	GAAACUCAUUGACAGCUAA
SNAP23	8773	NM_130798	18765730	ACAGAGAUCGUAUUGAUAU
SNAP25	6616	NM_130811	18765734	CUGGAAAGCACCCGUCGUA
SNAP25	6616	NM_130811	18765734	CAGAAUCGCCAGAUCGACA
SNAP25	6616	NM_130811	18765734	GUGUAGUGGACGAACGGGA
SNAP25	6616	NM_130811	18765734	ACAAAUGAUGCCCGAGAAA
SNAP29	9342	NM_004782	18765736	GAAGCUAUAAGUACAAGUA
SNAP29	9342	NM_004782	18765736	GACAAGAUGGACCAAGAUU
SNAP29	9342	NM_004782	18765736	CAACCAAAGUGGACAAGUU
SNAP29	9342	NM_004782	18765736	UUAGAAAGCUGGAUGAUAC
SNAP47	116841	NM_053052	26024192	CCACUCACCUUACGAAAUU
SNAP47	116841	NM_053052	26024192	CAGACAUGGCCUAUCGUUU
SNAP47	116841	NM_053052	26024192	GAACAGAGUCUCACGUUAA
SNAP47	116841	NM_053052	26024192	CAACCUUGACCAUCGACAA
SNX9	51429	NM_016224	23111056	GUAACCGGAUCUAUGAUUA
SNX9	51429	NM_016224	23111056	GGACAGAACGGGCCUUGAA
SNX9	51429	NM_016224	23111056	GAGUCAGCAUCAUGUCUUA
SNX9	51429	NM_016224	23111056	CGAGGAAACAGUCGUGCUA
STX10	8677	NM_003765	4507284	GGAAGAGACCAUCGGUAUA
STX10	8677	NM_003765	4507284	CGACCAAUGAGCUGCGGAA
STX10	8677	NM_003765	4507284	AGGUGUUCGUGGAGCGGAU
STX10	8677	NM_003765	4507284	AGGAAGUUGGCCAAAGUAU
STX11	8676	NM_003764	33667037	AGCACUGAAUAUCGAACAA
STX11	8676	NM_003764	33667037	GGGUAAGUGGGACGUGUUU
STX11	8676	NM_003764	33667037	GCAAGGAAGUCUCGGGCGA

STX11	8676	NM_003764	33667037	GGAAGGCCGUGCAGUACGA
STX12	23673	NM_177424	28933464	CCACAAAUCAGCUCGCCAA
STX12	23673	NM_177424	28933464	GAGGAUCAGUAUAUCGGUA
STX12	23673	NM_177424	28933464	ACACUACAGUCUCGUAAUA
STX12	23673	NM_177424	28933464	GCUCAGAGGUGCACGUCGA
STX16	8675	NM_001001434	47778944	GUAUGAUGUUGGCCGGAUU
STX16	8675	NM_001001434	47778944	AAAUAUUCCACCAGCGAUU
STX16	8675	NM_001001434	47778944	GCUAAUUGAGAGAGCGUUA
STX16	8675	NM_001001434	47778944	AGUAGGACUUCAUCGUUUA
STX17	55014	NM_017919	8923603	CGAUCCAAUAUCCGAGAAA
STX17	55014	NM_017919	8923603	UAUCAAUGCAGGACGUACA
STX17	55014	NM_017919	8923603	CCUUAGAAGCGGACUUAAU
STX17	55014	NM_017919	8923603	GACUGUUGGUGGAGCAUUU
STX18	53407	NM_016930	39725935	CUGUCUGAGUCAACGAAUA
STX18	53407	NM_016930	39725935	CAGAGAGCCAUCCGAGUUA
STX18	53407	NM_016930	39725935	GUUCAGACAGACAGACGUA
STX18	53407	NM_016930	39725935	CAAGAGAUAUUCACGGAAA
STX19	415117	NM_001001850	49258195	GAGAAGGUUUAGUCUACUU
STX19	415117	NM_001001850	49258195	UGUCCAUGCUGUAGCUCAA
STX19	415117	NM_001001850	49258195	GAACUUGUUAAUUUGGAGA
STX19	415117	NM_001001850	49258195	GAGAAGUGCAAGACAUUUA
STX1A	6804	NM_004603	4759181	GGAACACGCGGUAGACUAU
STX1A	6804	NM_004603	4759181	AAACAAAGUUCGUUCCAAG
STX1A	6804	NM_004603	4759181	GGAGGAGAUUCGAGGCUUC
STX1A	6804	NM_004603	4759181	GAGGUGAAGCGGAAGCACA
STX2	2054	NM_001980	37577286	UAGACAAGCUCUCAAUGAA
STX2	2054	NM_001980	37577286	CUUGUGAUCCUUGGAAUUA
STX2	2054	NM_001980	37577286	UAGCAACCAUAUCCCAAGA
STX2	2054	NM_001980	37577286	GUUAAAGGCUAUUGAACAA
STX3	6809	NM_004177	34147491	GAUCAUUGACUCACAGAUU
STX3	6809	NM_004177	34147491	AAGAAACUCUACAGUAUCA
STX3	6809	NM_004177	34147491	AGGGUGAGAUGUUAGAUAA
STX3	6809	NM_004177	34147491	AAACUCGGCUUAACAUUGA
STX4	6810	NM_004604	34147603	GGACAAUUCGGCAGACUAU
STX4	6810	NM_004604	34147603	GCGUCACAGUGGUUGGAUA
STX4	6810	NM_004604	34147603	GCGAGGUGUUUGUGUCCAA
STX4	6810	NM_004604	34147603	CGUCAACACAAGAAUGAGA
STX5	6811	NM_003164	94400931	CAGAACAUUGAGUCGACAA
STX5	6811	NM_003164	94400931	CAAUCUUGGCAAAGCGCAA
STX5	6811	NM_003164	94400931	GCUCCAGGAUUUCGUGAGA
STX5	6811	NM_003164	94400931	GAGCCCAGCUGGACGUUGA
STX6	10228	NM_005819	58294156	GCAGUUAUGUUGGAAGAUU
STX6	10228	NM_005819	58294156	CAGCAUAGUUGAAGCAAAU
STX6	10228	NM_005819	58294156	GCCCAGGGAUUGUUUCAGA
STX6	10228	NM_005819	58294156	UAUCUCAUAUGACCAGUGA
STX7	8417	NM_003569	4507294	GAGUUUGUUGCUCGAGUAA
STX7	8417	NM_003569	4507294	CAGCAGAUUAUCAGCGCAA
STX7	8417	NM_003569	4507294	UGUCAUUGGAGUUGCGAUU
STX7	8417	NM_003569	4507294	GGAGCACACUGUCGCACUA
STX8	9482	NM_004853	4759187	AAUGAAACCAGGCGGGUAA
STX8	9482	NM_004853	4759187	GAAUGAGGGUGCCGAACCA
STX8	9482	NM_004853	4759187	GAUCUUGUAACUCGAGAGA
STX8	9482	NM_004853	4759187	GAGUGAAGAGGCUAAGCGA
STXBP1	6812	NM_001032221	73760414	GGACCUUGUUUGUCGAAGA
STXBP1	6812	NM_001032221	73760414	UGACCCAGGCCAACGGAAA
STXBP1	6812	NM_001032221	73760414	GGAAGGAACGCAUCAGCGA
STXBP1	6812	NM_001032221	73760414	CCUCAAAGCUGUUGUCGGA
STXBP2	6813	NM_006949	5902127	GAGCGGAGUUAUUCGGAGU

STXBP2	6813	NM_006949	5902127	CCACAUGCAUAUCGCAGAU
STXBP2	6813	NM_006949	5902127	CGUUCCAGGCCAUGGCGUA
STXBP2	6813	NM_006949	5902127	CCACGGACAAGGCGAACAU
STXBP3	6814	NM_007269	6005885	AGAGUGACAUGAUUCGUAA
STXBP3	6814	NM_007269	6005885	UCAACAAGGCAAACCGUUA
STXBP3	6814	NM_007269	6005885	GUAAAUCGGAGAACAAGUA
STXBP3	6814	NM_007269	6005885	GAAGAUGACCUCUGGGUUA
STXBP5L	9515	XM_938898	88970941	AGACACGGCCAGUGCGAAU
STXBP5L	9515	XM_938898	88970941	GAUUAAUGCAACCGCCAUA
STXBP5L	9515	XM_938898	88970941	GUUGUACAUUUAAGCGAUA
STXBP5L	9515	XM_938898	88970941	GUUCAUAACAUCACGGAGA
STXBP6	29091	NM_014178	46048194	GGUUAAUGGUAUCGAUCCU
STXBP6	29091	NM_014178	46048194	GAAUGAGCGUGGAGAGCGA
STXBP6	29091	NM_014178	46048194	AACUGGAGGUCAAGGCGAA
STXBP6	29091	NM_014178	46048194	CGGCAGAGUUUGAUUUGUU
USE1	55850	NM_018467	49574516	UGAAGGUCCACGCGAGCAA
USE1	55850	NM_018467	49574516	GAGCCUGAGAUGGACGUAA
USE1	55850	NM_018467	49574516	AGCUAAACCUGGUGCGGCU
USE1	55850	NM_018467	49574516	CGAAUCAUGCCUAAACUCA
VAMP1	6843	NM_016830	40549443	UAACAUGACCAGUAACAGA
VAMP1	6843	NM_016830	40549443	GGCAGGAGCAUCACAAUUU
VAMP1	6843	NM_016830	40549443	CCAUCAUCGUGGUAGUUAU
VAMP1	6843	NM_016830	40549443	GUGGACAUCAUACGUGUGA
VAMP2	6844	NM_014232	7657674	GCGCAAAUACUGGUGGAAA
VAMP2	6844	NM_014232	7657674	CAUCAUAGUUUACUUCAGC
VAMP2	6844	NM_014232	7657674	GGGAGUGAUUUGCGCCAUC
VAMP2	6844	NM_014232	7657674	UCAUGAGGGUGAACGUGGA
VAMP3	9341	NM_004781	42544205	GGAUUACUGUUCUGGUUAU
VAMP3	9341	NM_004781	42544205	GAGUUAACGUGGACAAGGU
VAMP3	9341	NM_004781	42544205	GGCAGGCGCUUCUCAAUUU
VAMP3	9341	NM_004781	42544205	UCAAGUAGAUGAGGUGGUG
VAMP4	8674	NM_003762	42544206	CAACUUCGAAGGCAAAUGU
VAMP4	8674	NM_003762	42544206	GGACAAAUCAGAAAGCUUA
VAMP4	8674	NM_003762	42544206	GGGACCAUCUGGACCAAGA
VAMP4	8674	NM_003762	42544206	GGAUGAAGUUAUUGAUGUC
VAMP5	10791	NM_006634	31543930	UGACGGAAAUUAUGCGUAA
VAMP5	10791	NM_006634	31543930	GAUAUGAGCUCAACCUUCA
VAMP5	10791	NM_006634	31543930	GAAUAGAGUUGGAGCGGUG
VAMP5	10791	NM_006634	31543930	GCAGCAGCGUUCAGACCAA
VAMP7	6845	NM_005638	27545446	GUACUCACAUGGCAAUUAU
VAMP7	6845	NM_005638	27545446	GAACGUUCCCGAGCCUUUA
VAMP7	6845	NM_005638	27545446	CGAGUUCUCAAGUGUCUUA
VAMP7	6845	NM_005638	27545446	GCCAAGACAGGAUUGUAUA
VAMP8	8673	NM_003761	14043025	CCACUGGUGCCUUCUCUUA
VAMP8	8673	NM_003761	14043025	GUCCUUAUCUGCGUGAUUG
VAMP8	8673	NM_003761	14043025	GAAAUGAUCGUGUGCGGAA
VAMP8	8673	NM_003761	14043025	GGGAAAACUUGGAACAUCU
VPS33A	65082	NM_022916	91206458	GGGCGUAACCUUCGCUGAA
VPS33A	65082	NM_022916	91206458	GAAGAAACGUCAACCGGGA
VPS33A	65082	NM_022916	91206458	AGGAGAAUGCGCUCGGCAA
VPS33A	65082	NM_022916	91206458	UUACCCAACUAUACGGAAA
VPS33B	26276	NM_018668	18105057	CCAGUAUGAUCGCCGGAGA
VPS33B	26276	NM_018668	18105057	ACAAACAGCGCUCGCCUUA
VPS33B	26276	NM_018668	18105057	ACGUGUGGACGGCGAGUAU
VPS33B	26276	NM_018668	18105057	CCUGAAGCAACACGAAGUA
VPS45	11311	NM_007259	91822913	GCAUAAACAACAAUCGGAU
VPS45	11311	NM_007259	91822913	GGCCAUGGUCCACGAACUA
VPS45	11311	NM_007259	91822913	AGACUUGCAGAGUGCGUUA

VPS45	11311	NM_007259	91822913	UAGCAGACAUGAAGGCGUU
VTI1A	143187	NM_145206	21624647	CGUGAAAGACUUCGGGAAA
VTI1A	143187	NM_145206	21624647	GGGCACAUCUGCUCGAUAA
VTI1A	143187	NM_145206	21624647	UGACAGGGAUGUUGCGAAG
VTI1A	143187	NM_145206	21624647	GAGAAAAGAUACAGCGAGC
VTI1B	10490	NM_006370	5454165	CCAAAGUAUUGAACGUUCU
VTI1B	10490	NM_006370	5454165	GAGCAUAUGAAUCGGCUAC
VTI1B	10490	NM_006370	5454165	UGGAGGAGGAGCUACGUUA
VTI1B	10490	NM_006370	5454165	UUGCUAAACUCCAUCGGGA
YKT6	10652	NM_006555	34304384	GCUCAAAGCCGCAUACGAU
YKT6	10652	NM_006555	34304384	CUAUAAAACUGCCCGGAAA
YKT6	10652	NM_006555	34304384	AUACCAGAACCCACGAGAA
YKT6	10652	NM_006555	34304384	CUAAAGUGCAGGCCGAACU

Annex C

Sup. Table 4. Sequences of the siGENOME library from Dharmacon provided by the Sheffield siRNA Screening Facility. SMART*pool*s of 4 targeting siRNAs were used in the secondary screen.

Gene Symbol	Sequence
ACTR2	GAAGUUAACUACCCUAUGG
ACTR2	GCAAGUGAAUUACGAUCAA
ACTR2	GAAACGGUUCGCAUGAUUA
ACTR2	UGGUGUGACUGUUCGAUAA
AP1M2	GGAGAGAAACGUCGUGAUU
AP1M2	CCACUGAUCUGGAUUGAGU
AP1M2	AGAACGAGGUCUUCAUUGA
AP1M2	CCGAGGGUAUCAAGUAUAA
ARPC2	GCAUCAAGCUGGCAUGUUG
ARPC2	GUACGGGAGUUUCUUGGUA
ARPC2	GGAGAGAACAGGGCAGUUA
ARPC2	CCAUGUAUGUUGAGUCUAA
CAV1	CUAAACACCUCAACGAUGA
CAV1	GCAGUUGUACCAUGCAUUA
CAV1	AUUAAGAGCUUCCUGAUUG
CAV1	GCAAAUACGUAGACUCGGA
CBL	UCAAGUGGAUGAUCAAGAA
CBL	CGAAGAUCCUGGCAAGUUU
CBL	UCACAGACAUCUCAGACUU
CBL	GCUACGAGCCCAUGACAAU
CLTB	GCGCCAGAGUGAACAAGUA
CLTB	GAAGGUGGCCCAGCUAUGU
CLTB	GGAACCAGCGCCAGAGUGA
CLTB	GAGCGAGAUUGCAGGCAUA
DAB2	GCAAAGAUAUCCUGUUAGU
DAB2	GAACCAGCCUUCACCCUUU
DAB2	CAAAGGAUCUGGGUCAACA
DAB2	GAUCUAAACUCUGAAAUCG
DNM2	CCGAAUCAAUCGCAUCUUC
DNM2	GACAUGAUCCUGCAGUUCA
DNM2	CCUCCGAGCUGGCGUCUAC
DNM2	AGUCCUACAUCAACACGAA
EHD1	GGAGAGAUCUACCAGAAGA
EHD1	CAUCAGCUCCCUCAAGAAA
EHD1	UGGCAACGCUUUCCUCAAC
EHD1	AUAAAGACUGAGCGGAUGU
EPN3	GCGAGAACCUCUACACCAU
EPN3	UAACAUUGCUGGACUACCU
EPN3	UCGCUGACCUGACCUUCAA
EPN3	UGCCAAACCUCCAGAAUCC
HIP1	GGAAGUGGCUGUAAAGGAA
HIP1	GAACCAAGAUGGAGUACCA
HIP1	GCAAAUCACAGAUCGAAGA
HIP1	CUAAUGGUGUGUUCUCAUG

Gene Symbol	Sequence
RAB1A	GGAAACCAGUGCUAAGAAU
RAB1A	CAGCAUGAAUCCCGAAUAU
RAB31	GGAACGGUUUCAUUCAUUG
RAB31	CAGCUGUUAUCGUGUAUGA
RAB31	CAACAUCAGCCCUACUAUU
RAB31	GAGAAUGGGCUCCGAUGAA
RAB3B	GCCAUGGGCUUCAUUCUGA
RAB3B	CUACUCAGAUCAAGACCUA
RAB3B	AAGGAGAACAUCAGUGUAA
RAB3B	CUGAUUCGCUGGACACAGA
RAB4B	GCACUAUCCUCAACAAGAU
RAB4B	AGAAUGAGCUGAUGUUCCU
RAB4B	GGUGAUUGGCAGUGCAGGA
RAB4B	UCAGUGACGCGGAGUUAUU
RAB8A	GAAUUAAACUGCAGAUAUG
RAB8A	GAACAAGUGUGAUGUGAAU
RAB8A	GAACUGGAUUCGCAACAUU
RAB8A	GAAGACCUGUGUCCUGUUC
RAC1	UAAGGAGAUUGGUGCUGUA
RAC1	UAAAGACACGAUCGAGAAA
RAC1	CGGCACCACUGUCCCAACA
RAC1	AUGAAAGUGUCACGGGUAA
ROCK1	GGACACAGCUGUAAGAUUG
ROCK1	GAAGAAACAUUCCCUAUUC
ROCK1	GAGAUGAGCAAGUCAAUUA
ROCK1	GCCAAUGACUUACUUAGGA
ROCK2	GUAGAAACCUUCCCAAUUC
ROCK2	GCAACUGGCUCGUUCAAUU
ROCK2	GCAAAUCUGUUAAUACUCG
ROCK2	GCAGCAAUGGUAAGCGUAA
SH3GLB1	AGAAUUGGAUGCUCACUUA
SH3GLB1	GCACAGUGUUACCAGUAUA
SH3GLB1	GAAGUGUUAUUGCAGCCAA
SH3GLB1	GGUGCCAAUUACCUACUUA
STX16	GAACAUGCCAUUGAGAUAA
STX16	AACCGACGCUUUCUUGUUG
STX16	GGUGUCAGGCAUCAGCUUA
STX16	GUAUGAUGUUGGCCGGAUU
STX2	GUUAAAGGCUAUUGAACAA
STX2	GAAAUCGAGUCACGUCACA
STX2	GAGGAGAUUAGAAACAGUA
STX2	CACCAAACCCGGAAGGAAA
STX4	CGACAGGCCUUAAAUGAGA
STX4	GGACAAUUCGGCAGACUAU

MAPK8IP1	GAAUAAAUGUAGCCACUUU
MAPK8IP1	GUACGAGGCCUACAACAUG
MAPK8IP1	CCAAGAAAUUCCUGAACGU
MAPK8IP1	GAGCAUUCCAGCAGUUCUA
MAPK8IP3	GAACUAUGCCGAUCAGAUU
MAPK8IP3	GUUUGAAGAUGCUCUGGAA
MAPK8IP3	GAACAAAGCUUUCGGCAUC
MAPK8IP3	CCACCAUCGCCAACGGGAA
PAK1	CAUCAAAUAUCACUAAGUC
PAK1	CAACAAAGAACAAUCACUA
PAK1	AGAAAUACCAGCACUAUGA
PAK1	GUGAAAUGCUCUCGGCUAU
RAB11B	CGAGUACGACUACCUAUUC
RAB11B	GACAGAAGCCCAACAAGCU
RAB11B	GGAUUCCACUAACGUAGAG
RAB11B	UAACGUAGAGGAAGCAUUC
RAB1A	GAACAAUCACCUCCAGUUA
RAB1A	CAAUCAAGCUUCAAAUAUG

STX4	GCGAGGUGUUUGUGUCCAA
STX4	CGUCAACACAAGAAUGAGA
STX8	CGAAAUCAAUAUGAACGAA
STX8	CACCAAAGCUUACCGUGAC
STX8	UCUUGUAACUCGAGAGAGA
STX8	GAAUGAGGGUGCCGAACCA
TEK	GAAAGAAUAUGCCUCCAAA
TEK	UGAAGUACCUGAUAUUCUA
TEK	CGAAAGACCUACGUGAAUA
TEK	GUGCAGAACUCUACGAGAA
VPS4A	GCUGAAGGAUUAUUUACGA
VPS4A	UCAAAGAGAACCAGAGUGA
VPS4A	GAAUAACAAUGAUGGGACU
VPS4A	GAGCCAAGUGCGUGCAGUA
VTI1B	GAAACCCCAUGAUGUCUAA
VTI1B	CGAGACCAGUUAGAACGUA
VTI1B	GCUUUCCAUUAUCAUCUUA
VTI1B	GAAGAAAUUGAUCAGGGAU

Annex D

Sup. Table 5. List of Robust Z-scores obtained for each siRNA screened in the primary siRNA screen in HeLa T-REx Tie2^{FLAG}.

Gene ID	Gene	Ang1	TF	Tie2
10097	ACTR2	-1.54	0.00	-0.64
10096	ACTR3	-0.88	-1.94	0.19
102	ADAM10	0.39	-1.27	-1.32
57679	ALS2	-0.31	-0.20	3.25
273	AMPH	-0.21	-1.34	0.15
51479	ANKFY1	0.19	-1.39	2.03
162	AP1B1	-1.34	-3.46	-1.76
8907	AP1M1	-1.44	-2.97	1.23
10053	AP1M2	1.40	0.42	0.03
160	AP2A1	-2.17	-4.79	-1.50
161	AP2A2	-0.19	-1.03	-1.01
163	AP2B1	-0.85	-1.56	-1.25
1173	AP2M1	-2.08	-5.03	-0.04
8943	AP3D1	0.84	-1.76	-1.55
23431	AP4E1	0.40	-0.46	-1.16
26060	APPL1	0.41	-0.98	0.55
55198	APPL2	0.93	2.55	-2.43
375	ARF1	-0.46	0.25	-0.77
382	ARF6	0.99	0.17	0.32
23647	ARFIP2	0.43	0.92	0.65
23092	ARHGAP26	1.23	1.60	-0.74
396	ARHGDIA	0.25	-3.74	0.35
10095	ARPC1B	1.39	3.19	0.68
10109	ARPC2	-1.52	0.10	-0.33
10094	ARPC3	0.13	-0.29	0.00
10093	ARPC4	-0.93	-0.90	-0.10
10092	ARPC5	1.39	2.53	0.33
408	ARRB1	-0.09	0.13	-2.29
409	ARRB2	-1.96	-2.15	-2.32
9140	ATG12	0.51	-0.84	-1.04
472	ATM	0.18	0.45	-2.03
535	ATP6V0A1	0.77	0.31	-1.49
8678	BECN1	0.15	0.19	0.24
10282	BET1	-0.88	0.22	-1.81
51272	BET1L	-0.03	-2.39	-1.70
274	BIN1	-0.86	-0.90	-0.38
662	BNIP1	1.05	-2.74	1.21
51028	C13ORF9	-0.57	2.52	-0.08
8536	CAMK1	0.59	-3.77	-0.56
857	CAV1	1.21	-0.05	-1.04
858	CAV2	0.03	0.90	-1.04
859	CAV3	-0.26	-0.61	-0.56
867	CBL	-1.04	0.84	-0.50
868	CBLB	0.22	0.05	-0.55
23624	CBLC	1.19	2.90	0.08
998	CDC42	-0.81	0.34	0.08
1072	CFL1	0.15	0.25	-1.25
10519	CIB1	0.76	0.79	0.37
10518	CIB2	-0.63	0.21	0.20
117286	CIB3	-0.19	-2.93	3.32
1211	CLTA	-0.08	0.62	-0.41
1212	CLTB	1.16	-0.54	-0.41
1213	CLTC	-1.65	-5.38	-0.50
8218	CLTCL1	0.23	-0.63	-0.25
	Control#1	-0.36	-0.13	0.86
	Control#5	-1.07	-1.16	-0.43
1314	COPA	-2.18	-5.30	-0.62
1601	DAB2	-1.53	-0.01	-0.12
8853	DDEF2	-0.89	-0.63	2.23
1729	DIAPH1	-0.10	-1.17	0.11
1759	DNM1	0.19	2.15	-0.22
1785	DNM2	-2.31	-0.26	0.81
26052	DNM3	-0.44	0.24	0.51
8411	EEA1	-1.23	-2.26	0.77
10278	EFS	-0.32	-0.68	0.27
10938	EHD1	3.20	0.81	-0.40
23085	ELKS	0.76	0.77	2.27
9685	ENTH	0.39	1.82	-1.18
29924	EPN1	-1.42	-1.65	-0.53
22905	EPN2	-0.46	1.64	1.03
55040	EPN3	1.05	-0.52	0.36
2060	EPS15	-0.57	0.08	-1.59
58513	EPS15L1	-0.65	-3.06	1.51
54536	EXOC6	-0.07	2.58	1.72
23265	EXOC7	-1.04	2.13	1.33
10211	FLOT1	0.48	-3.14	0.06
2534	FYN	-0.35	-1.40	-1.28
26056	GAF1	0.53	-2.72	2.24
26130	GAPVD1	-0.84	-2.57	0.40
28964	GIT1	1.70	1.76	3.75
57120	GOPC	1.96	1.84	1.99
64689	GORASP1	-0.33	-1.96	1.84
9527	GOSR1	-0.75	0.51	-0.72
9570	GOSR2	0.08	-0.31	-0.37
2885	GRB2	-0.77	-0.08	-0.38
9146	HGS	-0.63	-0.80	-0.68
3092	HIP1	-1.08	-0.50	-1.26
9026	HIP1R	-0.59	-0.60	-1.18
117283	IHPK3	-1.65	-4.12	3.52
6453	ITSN1	-0.44	-0.60	-0.21
50618	ITSN2	-0.84	0.97	-0.53
3984	LIMK1	-0.22	1.75	-0.53

Continue Sup. Table 1

Gene ID	Gene	Ang1	TF	Tie2
84557	MAP1LC3A	-0.11	-0.59	0.45
5871	MAP4K2	0.25	0.32	-0.30
9479	MAPK8IP1	1.37	-0.12	1.65
23542	MAPK8IP2	0.00	0.73	-0.53
23162	MAPK8IP3	2.56	0.97	-1.56
64780	MICAL1	2.39	3.41	2.53
4734	NEDD4	-0.86	0.19	-0.64
23327	NEDD4L	-0.19	-0.26	-1.10
4905	NSF	-0.26	-0.59	0.28
4952	OCRL	-0.34	0.67	2.46
29993	PACSIN1	-0.90	-0.58	-0.81
29763	PACSIN3	0.72	-0.30	-1.05
5058	PAK1	2.64	-1.09	1.80
10015	PDCD6IP	1.05	1.25	-0.21
8301	PICALM	-0.27	1.48	2.14
8301	PIK3C2G	-0.98	-2.72	1.81
5288	PIK3CG	-0.39	0.92	-1.43
5294	PIK4CA	-0.19	-1.36	-0.14
5297	PIP5K1A	-0.07	0.79	2.09
8394	PSCD3	-0.85	-1.45	0.09
9265	RAB11A	-0.47	-0.15	-1.08
8766	RAB11B	1.43	0.62	-0.54
9230	RAB1A	-1.80	-0.29	-0.82
5861	RAB2	-1.40	2.76	-1.18
5862	RAB21	0.14	-2.70	1.56
23011	RAB22A	0.08	-2.50	2.81
57403	RAB31	1.63	0.35	-0.54
11031	RAB3A	0.14	1.01	-1.07
5864	RAB3B	-1.79	2.61	-0.83
5865	RAB3C	-0.08	-1.71	1.46
115827	RAB3D	0.18	0.72	-2.00
9545	RAB4A	-1.80	-2.92	-0.66
5867	RAB4B	1.57	-1.58	1.56
53916	RAB5A	-0.76	-2.08	0.33
5868	RAB5B	-0.12	-2.64	0.52
5869	RAB5C	-1.01	-3.04	-0.02
5878	RAB6A	0.62	1.00	-0.17
5870	RAB6B	0.49	0.03	0.70
51560	RAB7B	0.60	0.30	1.72
338382	RAB7L1	-1.88	-1.63	3.64
8934	RAB8A	-1.17	-0.84	-0.51
4218	RAB8B	-0.48	-0.68	0.01
51762	RABEP1	-0.88	0.83	-1.28
9135	RABGEF1	-0.98	0.45	-0.22
27342	RAC1	-1.51	0.17	-0.21
5879	RAPH1	0.17	0.25	3.38

Gene ID	Gene	Ang1	TF	Tie2
65059	RBSN	-0.13	0.96	0.81
64145	RHOA	-0.65	-2.23	0.57
387	RIN1	-1.00	-1.66	1.62
9610	RIN2	-0.80	-0.67	0.96
54453	RIN3	-0.70	-2.49	2.46
79890	ROCK1	-1.40	0.74	-0.49
6093	ROCK2	1.28	-0.85	0.11
9475	SARA1	0.17	-0.17	-0.16
56681	SCFD1	-0.95	-2.13	0.12
23256	SEC13L1	1.97	-3.69	2.58
6396	SEC22A	0.01	1.50	-2.32
26984	SEC22B	2.13	4.37	3.46
9554	SEC22C	0.31	1.53	6.60
9117	SH3GL1			
6456	SH3GL2	-1.00	-2.48	4.22
51100	SH3GLB1	-1.71	0.35	-0.77
56904	SH3GLB2	-0.68	-2.22	2.88
867	siGenome_CBL	-1.71		
1785	siGenome_DNM2	-2.28	-4.46	
8773	SNAP23	0.87	2.34	-2.15
6616	SNAP25	0.38	1.15	-0.48
9342	SNAP29	0.55	-3.30	-0.47
116841	SNAP47	-0.68	-0.39	0.07
9892	SNAP91	0.82	1.69	-0.43
6642	SNX1	-0.92	-1.44	1.49
6643	SNX2	-0.32	-0.60	1.75
51429	SNX9	-0.56	0.24	-0.66
6780	STAU	-0.88	-1.97	6.57
8677	STX10	-0.71	-1.42	1.77
8676	STX11	1.16	0.13	3.40
23673	STX12	0.10	-0.48	-1.14
8675	STX16	1.35	0.56	-1.52
55014	STX17	-0.56	-0.81	-1.66
53407	STX18	0.47	1.11	-0.87
415117	STX19	-0.88	1.74	-0.69
6804	STX1A	0.54	-0.40	-1.86
2054	STX2	1.02	-1.29	-0.81
6809	STX3	-0.23	-0.12	-0.88
6810	STX4	2.08	-2.28	-0.95
6811	STX5	-0.16	-2.61	-0.95
10228	STX6	-2.07	-1.95	2.70
8417	STX7	-0.36	0.46	-0.24
9482	STX8	1.98	-1.29	1.36
6812	STXBP1	-0.52	-3.98	1.07
6813	STXBP2	1.09	-2.16	2.78
6814	STXBP3	0.45	0.21	0.04

Continue Sup. Table 1

Gene ID	Gene	Ang1	TF	Tie2
9515	STXBP5L	0.82	0.54	2.00
29091	STXBP6	0.98	0.83	2.53
8867	SYNJ1	0.54	-0.35	0.94
8871	SYNJ2	0.03	-0.32	0.96
6857	SYT1	1.13	1.27	0.00
127833	SYT2	0.62	-0.63	1.78
	TEK			-3.28
23043	TNIK	-0.17	1.49	1.00
7251	TSG101	0.40	1.66	1.24
55850	USE1	-0.28	-2.96	0.12
6843	VAMP1	0.53	-0.48	0.60
6844	VAMP2	0.41	-0.13	-1.05
9341	VAMP3	0.48	0.44	-0.72
8674	VAMP4	-0.14	0.07	-0.35
10791	VAMP5	0.88	0.37	-0.54
6845	VAMP7	0.01	0.44	0.05
8673	VAMP8	0.46	1.68	1.56
9218	VAPA	0.95	-0.84	-0.14
9217	VAPB	0.07	-0.95	-0.15
7410	VAV2	0.84	1.05	0.10
7415	VCP	-1.13	0.48	3.08
7430	VIL2	-0.17	2.25	0.93
65082	VPS33A	0.91	0.44	0.04
26276	VPS33B	-0.23	1.70	1.19
11311	VPS45	-0.82	1.16	2.85
27183	VPS4A	1.71	-0.90	2.75
143187	VTI1A	-0.89	0.88	-0.18
10490	VTI1B	-1.77	0.95	-0.01
7454	WAS	-0.45	2.57	1.39
8936	WASF1	-0.54	-0.01	-1.03
10163	WASF2	-1.40	-1.35	-1.16
10810	WASF3	-0.90	0.50	0.51
	water	1.12	0.43	0.36
10652	YKT6	0.84	1.93	0.53

Annex E

Sup. Table 6. Robusts % to Control#1 of the siRNA screened in the secondary assay

Gene ID	Gene symbol	Sparse				Confluent			
		Ang1	Tie2	Ang1/Tie2	TF	Ang1	Tie2	Ang1/Tie2	TF
10097	ACTR2	44.2	47.2		65.6	57.9		63.4	64.9
10053	Ap1M2								
10109	ARPC2	46.6		47.8	34.5	49.0		37.5	63.8
857	CAV1					130.2	117.8		
867	CBL	63.7			50.7				67.1
1212	CLTB	69.0				186.3			
	Control#3			87.2		140.6	143.3		136.4
	Control#4					149.2	140.5		120.4
	Control#5			80.5		126.3	122.6		
1601	DAB2	61.3	64.8			153.2	120.8		
1785	DNM2	63.9		52.6	26.5		137.6	72.6	41.9
10938	EHD1	58.4		61.2			171.2	60.0	130.6
55040	EPN3								
3092	HIP1		80.5			133.2	133.8		
9479	MAPK8IP1	83.2	69.5				128.2		
23162	MAPK8IP3			78.0		123.8	150.3	79.3	128.5
5058	PAK1		49.1	143.1					
9230	RAB11B								
5861	RAB1A	72.2			36.5				
11031	RAB31					118.1			
5865	RAB3B	69.4		80.1	49.0		123.8		
53916	RAB4B		133.5	69.9					
4218	RAB8A				66.1	171.1	150.7		
5879	RAC1	61.3	210.4	38.0	45.5		137.6		64.1
6093	ROCK1	80.5					73.1	124.7	
9475	ROCK2			71.8					
51100	SH3GLB1	79.5		84.5	52.1	147.8	164.5		
8675	STX16	73.2		68.6	36.6	148.0		128.1	
2054	STX2		74.7		68.5	156.8			
6810	STX4	70.8	59.6	116.4	54.0		77.0	141.8	72.6
9482	STX8						128.3		
7010	TEK	25.6	22.0			4.6	2.0	257.8	
27183	VPS4A			63.9		139.1	131.7		
10490	VTI1B		80.1	114.2		67.2			
	NT			119.1	78.9				

Annex F

Sup. Table 7. The genes targeted in the siRNA screen on HUVECs are listed together with their Gene ID and the result obtained for each parameter. The average normalized value for each parameter analysed is shown for the non-targeting controls and for the siRNAs found to significantly affect the parameters. Since I only had two successful independent experiments the targeting siRNAs were considered statistically significant only if the values of both repeats were above or below the significant limits. The values for RAB4A. SHC1. STX8. DNM2. SH3GLB1 and TEK in the first repeat are the % to the non-targeting siRNA C#1 in the same row. The rest of values are presented as % of the non-targeting siRNA #1. 2. 3 or 4 depending on the parameter as explained elsewhere. Blue highlight notes the values positively affecting the parameters and green highlight notes the values negatively affecting the parameters. The siRNAs whose values of Tie2 expression and Ang1/Tie2 ratio are based in a single repeat are indicated with *.

Gene ID	Name	Ang1	Tie2	Ang1/Tie2
10097	ACTR2	116.4		73.7
160	AP2A1*		10.7	138.1
10053	AP2M1*		28.0	
23092	ARHGAP26			
10109	ARPC2*	77.5	36.8	139.0
857	CAV1		42.5	147.2
858	CAV2	73.8	26.7	
867	CBL*		69.9	90.7
1212	CLTB			79.0
1213	CLTC		64.7	
1785	DNM2	76.5	54.5	149.3
8411	EEA1	71.6	45.6	
1785	EHD1		52.8	
29924	EPN1		51.2	
26056	GAF1		49.3	140.4
5058	PAK1		122.3	72.1
10015	PDCD6IP		70.5	
9230	RAB11B			
11031	RAB31			
5865	RAB3B			114.3
5867	RAB4A			
53916	RAB4B	138.9		
5879	RAC1	127.5	183.7	67.5
6093	ROCK2			
6455	SH3GL1			
6456	SH3GL2			
51100	SH3GLB1		65.2	
6464	SHC1			
8675	STX16			
6810	STX4			
10228	STX6			76.3
9482	STX8*		41.8	204.5
7010	TEK	123.1		84.4
27183	VPS4A	121.2		119.7
	Control#1	103.1	97.2	100.7
	Control#2	103.5	100.0	100.1
	Control#3	119.3	102.8	99.2
	Control#4	96.5	60.6	118.9
	siGLO			
	NT*		115.9	63.5

References

Adams, R.H. & Alitalo, K., 2007. Molecular regulation of angiogenesis and lymphangiogenesis. *Nat Rev Mol Cell Biol*, 8(6), pp.464–478.

Aghamohammadzadeh, S. & Ayscough, K.R., 2009. Differential requirements for actin during yeast and mammalian endocytosis. *Nature Cell Biology*, 11(8), pp.1039–1042.

Ahmed, Z. et al., 2013. Grb2 controls phosphorylation of FGFR2 by inhibiting receptor kinase and Shp2 phosphatase activity. *The Journal of cell biology*, 200(4), pp.493–504.

Aigner, A., 2007. Applications of RNA interference: Current state and prospects for siRNA-based strategies in vivo. *Applied Microbiology and Biotechnology*, 76(1), pp.9–21.

Aman, J. et al., 2016. Using cultured endothelial cells to study endothelial barrier dysfunction: Challenges and opportunities. *American Journal of Physiology - Lung Cellular and Molecular Physiology*, 311(2).

Aronin, N., 2006. Target selectivity in mRNA silencing. *Gene Therapy*, 13, pp.509–516.

Audero, E. et al., 2004. Adaptor ShcA Protein Binds Tyrosine Kinase Tie2 Receptor and Regulates Migration and Sprouting but Not Survival of Endothelial Cells. *Journal of Biological Chemistry*, 279(13), pp.13224–13233.

Augustin, H.G. et al., 2009. Control of vascular morphogenesis and homeostasis through the angiopoietin-Tie system. *Nature reviews. Molecular cell biology*, 10(3), pp.165–77.

Ávila Olías, M.M., 2014. *Cellular uptake of PMPC-PDPA polymersomes in mammalian cells. - The University of Sheffield*. University of Sheffield.

Avraamides, C.J., Garmy-Susini, B. & Varner, J.A., 2008. Integrins in angiogenesis and lymphangiogenesis. *Nature Reviews Cancer*, 8(8), pp.604–617.

Barton, W. a et al., 2006. Crystal structures of the Tie2 receptor ectodomain and the angiopoietin-2–Tie2 complex. *Nature Structural & Molecular Biology*, 13(6), pp.524–532.

Basagiannis, D. et al., 2016. VEGF induces signalling and angiogenesis by directing VEGFR2 internalisation through macropinocytosis. *Journal of Cell Science*, 129(21), pp.4091–4104.

Bastiani, M. & Parton, R.G., 2010. Caveolae at a glance. *Journal of Cell Science*, 123(22).

Bazzoni, G. & Dejana, E., 2004. Endothelial cell-to-cell junctions: molecular organization and role in vascular homeostasis. *Physiol Rev.*, 84(0031–9333 (Print)), pp.869–901.

Beardsley, A. et al., 2005. Loss of Caveolin-1 Polarity Impedes Endothelial Cell Polarization and Directional Movement*. *The Journal of Biological Chemistry*, 5(February 4), pp.3541–3547.

Bid, H.K. et al., 2013. RAC1: An Emerging Therapeutic Option for Targeting Cancer Angiogenesis and Metastasis. *Molecular Cancer Therapeutics*, 12(10).

Bierings, R. et al., 2012. The interplay between the Rab27A effectors Slp4-a and MyRIP controls hormone-evoked Weibel-Palade body exocytosis. *Blood*, 120, pp.2757–2767.

Birmingham, A. et al., 2009. Statistical methods for analysis of high-throughput RNA interference screens: Supplementary material. *Nature methods*, 6(8), pp.569–75.

Blagojević, G. & Mahmutefendić, H., 2008. Endocytic Trafficking of cholera toxin in Balb 3T3 cells. *Croatica Chemica …*, 81(1), pp.8–10.

Bogdanovic, E., 2009. *Regulation of Tie2 by angiopoietin-1 and angiopoietin-2 in endothelial cells*. University of Toronto.

Bogdanovic, E., Coombs, N. & Dumont, D.J., 2009. Oligomerized Tie2 localizes to clathrin-coated pits in response to angiopoietin-1. *Histochemistry and Cell Biology*, 132(2), pp.225–237.

Bogdanovic, E., Nguyen, V.P.K.H. & Dumont, D.J., 2006. Activation of Tie2 by angiopoietin-1 and angiopoietin-2 results in their release and receptor internalization. *Journal of cell science*, 119(Pt 17), pp.3551–60.

Boll, W. et al., 1996. Sequence requirements for the recognition of tyrosine-based endocytic signals by clathrin AP-2 complexes. *The EMBO journal*, 15(21), pp.5789–95.

Boon, L.M. & Vikkula, M., 1993. *Multiple Cutaneous and Mucosal Venous Malformations*,

Boucherat, O. et al., 2010. Defective angiogenesis in hypoplastic human fetal lungs correlates with nitric oxide synthase deficiency that occurs despite enhanced angiopoietin-2 and VEGF. *American Journal of Physiology - Lung Cellular and Molecular Physiology*, 298(6).

Boucrot, E. et al., 2015. Endophilin marks and controls a clathrin-independent endocytic pathway. *Nature*, 517(7535), pp.460–5.

Boulant, S. et al., 2011. Actin dynamics counteract membrane tension during clathrin-mediated endocytosis. *Nature Cell Biology*, 13, pp.1124–1132.

Bulut, G.B. et al., 2013. Cbl ubiquitination of p85 is essential for Epo-induced EpoR endocytosis. *Blood*, 122(24), pp.3964–72.

Burana, D. et al., 2016. The Ankrd13 Family of Ubiquitin-interacting Motif-bearing Proteins Regulates Valosin-containing Protein/p97 Protein-mediated Lysosomal Trafficking of Caveolin 1. *The Journal of biological chemistry*, 291(12), pp.6218–31.

Caì, Y. et al., 2015. Simian hemorrhagic fever virus cell entry is dependent on CD163 and uses a clathrin-mediated endocytosis-like pathway. *Journal of virology*, 89(1), pp.844–56.

Carlson, T.R. et al., 2001. Direct cell adhesion to the angiopoietins mediated by integrins. *The Journal of biological chemistry*, 276(28), pp.26516–25.

Cascone, I. et al., 2005. Stable interaction between α5β1 integrin and Tie2 tyrosine kinase receptor regulates endothelial cell response to Ang-1. *Journal of Cell Biology*, 170(6), pp.993–1004.

Cascone, I. et al., 2003. Tie-2–dependent activation of RhoA and Rac1 participates in endothelial cell motility triggered by angiopoietin-1. *Blood*, 102(7), pp.2482–2490.

Di Cesare, A. et al., 2000. p95-APP1 links membrane transport to Rac-mediated reorganization of actin. *NATURE CELL BIOLOGYnature.com*, 2.

Cheng, J.P.X. & Nichols, B.J., 2016. Caveolae: One Function or Many? *Trends in Cell Biology*, 26(March 2016).

Chiu, J.W. et al., 2016. A phase I trial of ANG1/2-Tie2 inhibitor trebaninib (AMG386) and temsirolimus in advanced solid tumors (PJC008/NCI♯9041). *Investigational New Drugs*, 34(1), pp.104–111.

Choudhury, A. et al., 2006. Regulation of caveolar endocytosis by syntaxin 6-dependent delivery of membrane components to the cell surface. *Nature cell biology*, 8(4), pp.317–328.

Cole, L. et al., 1990. Internalisation of fluorescein isothiocyanate and fluorescein isothiocyanate- dextran by suspension-cultured plant cells. *Journal of Cell Science*, 96(1985), pp.721–730.

Collinet, C. et al., 2010. Systems survey of endocytosis by multiparametric image analysis. *Nature*, 464, pp.243–250.

Conner, S.D. & Schmid, S.L., 2003. Regulated portals of entry into the cell. *Nature*, 422(6927), pp.37–44.

Davis, S. et al., 2003. Angiopoietins have distinct modular domains essential for receptor binding, dimerization and superclustering. *Nature Structural Biology*, 10(1), pp.38–44.

Davis, S. et al., 1996. Isolation of angiopoietin-1, a ligand for the TIE2 receptor, by secretion-trap expression cloning. *Cell*, 87(7), pp.1161–1169.

Désiré, L. et al., 2005. RAC1 inhibition targets amyloid precursor protein processing by gamma-secretase and decreases Abeta production in vitro and in vivo. *The Journal of biological chemistry*, 280(45), pp.37516–25.

Dharmawardhane, S. et al., 2000. Regulation of macropinocytosis by p21-activated kinase-1. *Molecular biology of the cell*, 11(10), pp.3341–52.

Doherty, G.J. & Lundmark, R., 2009. GRAF1-dependent endocytosis: Figure 1. *Biochemical Society Transactions*, 37(5), pp.1061–1065.

Doherty, G.J. & McMahon, H.T., 2009. Mechanisms of Endocytosis. *Annual review of biochemistry78*, 78, pp.857–902.

Dumont, D.J. et al., 1994. Dominant-negative and targeted null mutations in the endothelial receptor tyrosine kinase, tek, reveal a critical role in vasculogenesis of the embryo. *Genes & development*, 8(16), pp.1897–909.

Dumont, D.J. et al., 1992. tek, a novel tyrosine kinase gene located on mouse chromosome 4, is expressed in endothelial cells and their presumptive precursors. *Oncogene*, 7(8), pp.1471–80.

Dumont, D.J. et al., 1993. The endothelial-specific receptor tyrosine kinase, tek, is a member of a new subfamily of receptors. *Oncogene*, 8(5), pp.1293–301.

Edwards, D.C. et al., 1999. Activation of LIM-kinase by Pak1 couples Rac/Cdc42 GTPase signalling to actin cytoskeletal dynamics. *NATURE CELL BIOLOGY cellbio.nature.com*, 1.

Eklund, L., Kangas, J. & Saharinen, P., 2016. Angiopoietin–Tie signalling in the cardiovascular and lymphatic systems. *Clinical Science*, 131, pp.87–103.

Eklund, L. & Olsen, B.R., 2006. Tie receptors and their angiopoietin ligands are context-dependent regulators of vascular remodeling. *Experimental Cell Research*, 312(5), pp.630–641.

Eklund, L. & Saharinen, P., 2013. Angiopoietin signaling in the vasculature. *Experimental Cell Research*, 319(9), pp.1271–1280.

Elbashir, S.M. et al., 2001. Duplexes of 21-nucleotide RNAs mediate RNA interference in cultured mammalian cells. *Nature*, 411(6836), pp.494–498.

Engqvist-Goldstein, Å.E.Y. & Drubin, D.G., 2003. Actin Assembly and Endocytosis: From Yeast to Mammals. *Annual Review of Cell and Developmental Biology*, 19(1), pp.287–332.

Epand, R.M., Sayer, B.G. & Epand, R.F., 2005. Caveolin Scaffolding Region and Cholesterol-rich Domains in Membranes. *Journal of Molecular Biology*, 345, pp.339–350.

Ferguson, S. et al., 2009. Coordinated Actions of Actin and BAR Proteins Upstream of Dynamin at Endocytic Clathrin-Coated Pits. *Developmental Cell*, 17, pp.811–822.

Ferrara, N., 2004. Vascular Endothelial Growth Factor: Basic Science and Clinical Progress. *Endocrine Reviews*, 25(4), pp.581–611.

Ferrara, N. & Kerbel, R.S., 2005. Angiogenesis as a therapeutic target. *Nature*, 438(7070), pp.967–974.

Di Fiore, P.P. & De Camilli, P., 2001. Endocytosis and signaling: An inseparable partnership. *Cell*, 106(1), pp.1–4.

Friend, D.S. & Farquhar, M.G., 1967. Functions of coated vesicles during protein absorption in the rat vas deferens. *The Journal of Cell Biology*, 35, pp.357–376.

Fujita, H. et al., 2002. A dominant negative form of the AAA ATPase SKD1/VPS4 impairs membrane trafficking out of endosomal/lysosomal compartments: class E vps phenotype in mammalian cells. *Journal of Cell Science*, 116(2).

Fukuhara, S. et al., 2008. Differential function of Tie2 at cell–cell contacts and cell–substratum contacts regulated by angiopoietin-1. *Nature Cell Biology*, 10(5), pp.513–526.

Gampel, A. et al., 2006. VEGF regulates the mobilization of VEGFR2/KDR from an intracellular endothelial storage compartment. *Blood*, 108(8), pp.2624–2631.

Gauthier, N.C., Masters, T.A. & Sheetz, M.P., 2012. Mechanical feedback between membrane tension and dynamics. *Trends in Cell Biology*, 22, pp.527–535.

Gavard, J. & Gutkind, J.S., 2006. VEGF controls endothelial-cell permeability by promoting the β-arrestin-dependent endocytosis of VE-cadherin. *Nature Cell Biology*, 8(11), pp.1223–1234.

Gavard, J., Patel, V. & Gutkind, J.S., 2008. Angiopoietin-1 Prevents VEGF-Induced Endothelial Permeability by Sequestering Src through mDia. *Developmental Cell*, 14(1), pp.25–36.

GE healthcare Dharmacon Inc, 2016. Product Information and Gene Search | GE Dharmacon. Available at: http://dharmacon.gelifesciences.com/rnai-and-custom-rna-synthesis/sirna/on-targetplus-sirna/search-gene/#data [Accessed April 25, 2017].

Goh, L.K. et al., 2010. Multiple mechanisms collectively regulate clathrin-mediated endocytosis of the epidermal growth factor receptor. *Journal of Cell Biology*, 189(5), pp.871–883.

Goley, E.D. & Welch, M.D., 2006. The ARP2/3 complex: an actin nucleator comes of age. *Nature Reviews Molecular Cell Biology*, 7(10), pp.713–726.

Grande-García, A. et al., 2007. Caveolin-1 regulates cell polarization and directional migration through Src kinase and Rho GTPases. *The Journal of Cell Biology*, 177(4).

Hakanpaa, L. et al., 2015. Endothelial destabilization by angiopoietin-2 via integrin β1 activation. *Nature communications*, 6, p.5962.

Hansen, T.M. et al., 2010. Effects of angiopoietins-1 and -2 on the receptor tyrosine kinase Tie2 are differentially regulated at the endothelial cell surface. *Cellular Signalling*, 22(3), pp.527–532.

Hong, W., 2005. SNAREs and traffic. *Biochimica et Biophysica Acta (BBA)*, 1744(April 21), pp.120–144.

Huang, L. et al., 1995. GRB2 and SH-PTP2: potentially important endothelial signaling molecules downstream of the TEK/TIE2 receptor tyrosine kinase. *Oncogene*, 11(10), pp.2097–103.

Hughes, D.P., Marron, M.B. & Brindle, N.P.J., 2003. The Antiinflammatory Endothelial Tyrosine Kinase

Tie2 Interacts With a Novel Nuclear Factor-κB Inhibitor ABIN-2. *Circulation Research*, 92(6).

Huth, U.S., Schubert, R. & Peschka-Süss, R., 2006. Investigating the uptake and intracellular fate of pH-sensitive liposomes by flow cytometry and spectral bio-imaging. *Journal of Controlled Release*, 110(3), pp.490–504.

Huyer, G. et al., 1997. Mechanism of Inhibition of Protein-tyrosine Phosphatases by vanadate and pervanadate. *The Journal of biological chemistry*, 272(January 10), pp.843–851.

Ivanov, A.I. ed., 2008. *Exocytosis and Endocytosis*, Totowa, NJ: Humana Press.

Jae-Bong Park, 2003. Phagocytosis induces superoxide formation and apoptosis in macrophages. *EXPERIMENTAL and MOLECULAR MEDICINE*, 35(5), pp.325–335.

Jeltsch, M. et al., 2013. Receptor tyrosine kinase-mediated angiogenesis. *Cold Spring Harbor perspectives in biology*, 5(9), p.a009183.

Jiang, W. et al., 2008. Nanoparticle-mediated cellular response is size-dependent. *Nature nanotechnology*, 3(March).

Jones, M.C. et al., 2009. VEGFR1 (Flt1) Regulates Rab4 Recycling to Control Fibronectin Polymerization and Endothelial Vessel Branching. *Traffic*, 10(6), pp.754–766.

Jones, N. et al., 2003. A unique autophosphorylation site on Tie2/Tek mediates Dok-R phosphotyrosine binding domain binding and function. *Molecular and cellular biology*, 23(8), pp.2658–68.

Jones, N. et al., 1999. Identification of Tek/Tie2 Binding Partners. Binding to multifunctional docking site mediates cell survival and migration. *The Journal of biological chemistry*, 274(43), pp.30896–30905.

Jones, N. & Dumont, D.J., 1998. The Tek/Tie2 receptor signals through a novel Dok-related docking protein, Dok-R. *Oncogene*, 17(9), pp.1097–1108.

Jordens, I. et al., 2001. The Rab7 effector protein RILP controls lysosomal transport by inducing the recruitment of dynein-dynactin motors. *Current Biology*, 11(21), pp.1680–1685.

Kaksonen, M., Toret, C.P. & Drubin, D.G., 2006. Harnessing actin dynamics for clathrin-mediated endocytosis. *Nature Reviews Molecular Cell Biology*, 7(6), pp.404–414.

Kalaidzidis, I. et al., 2015. APPL endosomes are not obligatory endocytic intermediates but act as stable cargo-sorting compartments. *The Journal of Cell Biology*, 211(1), pp.123–144.

Kanters, E. et al., 2008. Filamin B mediates ICAM-1-driven leukocyte transendothelial migration. *The Journal of biological chemistry*, 283(46), pp.31830–9.

Katoh, S.Y. et al., 2009. Lipid rafts serve as signaling platforms for Tie2 receptor tyrosine kinase in vascular endothelial cells. *Experimental Cell Research*, 315(16), pp.2818–2823.

Keating, M.T. & Williams, L.T., 1987. Processing of the platelet-derived growth factor receptor. Biosynthetic and degradation studies using anti-receptor antibodies. *Journal of Biological Chemistry*, 262(16), pp.7932–7937.

Kim, I., Kim, H.G., Moon, S.-O., et al., 2000. Angiopoietin-1 Induces Endothelial Cell Sprouting Through the Activation of Focal Adhesion Kinase and Plasmin Secretion. *Circulation Research*, 86(9).

Kim, I., Kim, H.G., So, J.-N., et al., 2000. Angiopoietin-1 Regulates Endothelial Cell Survival Through the Phosphatidylinositol 3'-Kinase/Akt Signal Transduction Pathway. *Circulation Research*, 86(1).

Kim, K.T. et al., 2005. Oligomerization and multimerization are critical for angiopoietin-1 to bind and phosphorylate Tie2. *Journal of Biological Chemistry*, 280(20), pp.20126–20131.

Kirchhausen, T., 2000. Clathrin. *Annual Review of Biochemistry*, 69, pp.699–727.

Kirchner, P., Bug, M. & Meyer, H., 2013. Ubiquitination of the N-terminal region of caveolin-1 regulates endosomal sorting by the VCP/p97 AAA-ATPase. *The Journal of biological chemistry*, 288(10), pp.7363–72.

Ko, S.H. & Bandyk, D.F., 2014. Therapeutic angiogenesis for critical limb ischemia. *Seminars in Vascular Surgery*, 27(1), pp.23–31.

Kobayashi, S. et al., 2004. The c-Cbl/CD2AP complex regulates VEGF-induced endocytosis and degradation of Flt-1 (VEGFR-1). *The FASEB Journal*, (March 4).

Koivusalo, M. et al., 2010. Amiloride inhibits macropinocytosis by lowering submembranous pH and preventing Rac1 and Cdc42 signaling. *The Journal of Cell Biology*, 188(4), p.547.

Kontos, C.D. et al., 1998. Tyrosine 1101 of Tie2 is the major site of association of p85 and is required for activation of phosphatidylinositol 3-kinase and Akt. *Molecular and cellular biology*, 18(7), pp.4131–4140.

Kumar, R. & Vadlamudi, R.K., 2002. Emerging functions of p21-activated kinases in human cancer cells. *Journal of Cellular Physiology*, 193(2), pp.133–144.

Le, P.U. et al., 2002. Caveolin-1 is a negative regulator of caveolae-mediated endocytosis to the endoplasmic reticulum. *The Journal of biological chemistry*, 277(5), pp.3371–9.

de Leeuw, H.P.J.C. et al., 2001. Small GTP-Binding Protein Ral Modulates Regulated Exocytosis of von Willebrand Factor by Endothelial Cells. *Arteriosclerosis, Thrombosis, and Vascular Biology*, 21(6).

Lemmon, M. a & Schlessinger, J., 2010. Cell signaling by receptor-tyrosine kinases. *Cell*, 141(7), pp.1117–1134.

Li, H. et al., 2001. Cholesterol binding at the cholesterol recognition/ interaction amino acid consensus (CRAC) of the peripheral-type benzodiazepine receptor and inhibition of steroidogenesis by an HIV TAT-CRAC peptide. *Proceedings of the National Academy of Sciences*, 98(3), pp.1267–1272.

Li, L. et al., 2015. The effect of the size of fluorescent dextran on its endocytic pathway. *Cell Biology International*, 39(5), pp.531–539.

Lin, P. et al., 1997. Inhibition of tumor angiogenesis using a soluble receptor establishes a role for Tie2 in pathologic vascular growth. *Journal of Clinical Investigation*, 100(8), pp.2072–2078.

Lin, X. et al., 2005. siRNA-mediated off-target gene silencing triggered by a 7 nt complementation. *Nucleic Acids Research*, 33(14), pp.4527–4535.

Liu, Z. et al., 2017. APPLs: More than just adiponectin receptor binding proteins. *Cellular Signalling*, 32, pp.76–84.

Maisonpierre, P.C. et al., 1997. Angiopoietin-2, a Natural Antagonist for Tie2 That Disrupts in vivo Angiogenesis. *Science*, 277(5322), pp.55–60.

Malecz, N. et al., 2000. Synaptojanin 2, a novel Rac1 effector that regulates clathrin-mediated endocytosis. *Current biology : CB*, 10(21), pp.1383–6.

Mallard, F. et al., 2002. Early/recycling endosomes-to-TGN transport involves two SNARE complexes and a Rab6 isoform. *The Journal of Cell Biology*, 156(4).

Manickam, V. et al., 2011. Regulation of vascular endothelial growth factor receptor 2 trafficking and angiogenesis by Golgi localized t-SNARE syntaxin 6. *Blood*, 117(4), pp.1425–1435.

Marieb, E.N. & Hoehn, K., 2013. *Human Anatomy & Physiology: Pearson New International Edition* 9th ed. Pearson education Limited, ed., Essex, England: Pearson.

Marin, V. et al., 2001. Endothelial cell culture: protocol to obtain and cultivate human umbilical endothelial cells. *Journal of Immunological Methods*, 254, pp.183–190.

Marron, M.B. et al., 2000. Evidence for heterotypic interaction between the receptor tyrosine kinases Tie-1 and Tie-2. *Journal of Biological Chemistry*, 275(50), pp.39741–39746.

Marron, M.B. et al., 2007. Regulated proteolytic processing of Tie1 modulates ligand responsiveness of the receptor-tyrosine kinase Tie2. *Journal of Biological Chemistry*, 282(42), pp.30509–30517.

Marsh, E.W. et al., 1995. Oligomerized transferrin receptors are selectively retained by a lumenal sorting signal in a long-lived endocytic recycling compartment. *The Journal of Cell Biology*, 129(6).

Master, Z. et al., 2001. Dok-R plays a pivotal role in angiopoietin-1-dependent cell migration through recruitment and activation of Pak. *The EMBO Journal*, 20(21), pp.5919–5928.

Mayle, K.M., Le, A.M. & Kamei, D.T., 2012. The intracellular trafficking pathway of transferrin ☆. *BBA - General Subjects*, 1820, pp.264–281.

Mayor, S. & Pagano, R.E., 2007. Pathways of clathrin-independent endocytosis. *Nature Reviews Molecular Cell Biology*, 8(August), p.603.

Mayor, S. & Rao, M., 2004. Rafts: Scale-Dependent, Active Lipid Organization at the Cell Surface. *Traffic*, 5(4), pp.231–240.

McCarron, J.G., Lee, M.D. & Wilson, C., 2017. The Endothelium Solves Problems That Endothelial Cells Do Not Know Exist. *Trends in Pharmacological Sciences*, 38(April 2017), pp.322–338.

Mellman, I. & Plutner, H., 1984. Internalization and degradation of macrophage Fc receptors bound to polyvalent immune complexes. *The Journal of Cell Biology*, 98(4).

Miaczynska, M., Pelkmans, L. & Zerial, M., 2004. Not just a sink: Endosomes in control of signal transduction. *Current Opinion in Cell Biology*, 16(4), pp.400–406.

Miki, H., Suetsugu, S. & Takenawa, T., 1998. WAVE, a novel WASP-family protein involved in actin reorganization induced by Rac. *The EMBO Journal*, 17(23), pp.6932–6941.

Moore, K.N. et al., 2015. A phase II trial of trebananib (AMG 386; IND#111071), a selective angiopoietin 1/2 neutralizing peptibody, in patients with persistent/recurrent carcinoma of the endometrium: An NRG/Gynecologic Oncology Group trial. *Gynecologic Oncology*, 138(3), pp.513–518.

Mundell, S.J. et al., 2006. Distinct Clathrin-Coated Pits Sort Different G Protein-Coupled Receptor Cargo. *Traffic*, 7(10), pp.1420–1431.

Muro, S. et al., 2003. A novel endocytic pathway induced by clustering endothelial ICAM-1 or PECAM-1. *Journal of Cell Science*, 116(8).

Murray, B.W. et al., 2001. Mechanistic effects of autophosphorylation on receptor tyrosine kinase catalysis: Enzymatic characterization of Tie2 and phospho-Tie2. *Biochemistry*, 40(34), pp.10243–10253.

Nabi, I.R. & Le, P.U., 2003. Mini-Review Caveolae/raft-dependent endocytosis. *The Journal of Cell Biology JCB □ The The Journal of Cell Biology*, 56735(4), pp.21–9525.

Neel, B.G. & Frangioni, J. V., 1993. Solubilization and purification of enzymatically active Glutathione S-Transferase (pGEX) Fusion Proteins. *Analytical Biochemistry*, 210(1), pp.179–187.

Nethe, M. et al., 2010. Focal-adhesion targeting links caveolin-1 to a Rac1-degradation pathway. *Journal of Cell Science*, 123(11), pp.1948–1958.

O'Gorman, S., Fox, D. & Wahl, G., 1991. Recombinase-mediated gene activation and site-specific integration in mammalian cells. *Science*, 251(4999), pp.1351–1355.

Oksvold, M.P. et al., 2000. Immunocytochemical Localization of Shc and Activated EGF Receptor in Early Endosomes After EGF Stimulation of HeLa Cells. *Journal of Histochemistry & Cytochemistry*, 48(1), pp.21–33.

Partanen, J. et al., 1992. A novel endothelial cell surface receptor tyrosine kinase with extracellular epidermal growth factor homology domains. *Mol Cell Biol*, 12(4), pp.1698–1707.

Parton, R.G. & Simons, K., 2007. The multiple faces of caveolae. *Nature reviews*, 8.

Pauwels, A.-M. et al., 2017. Patterns, Receptors, and Signals: Regulation of Phagosome Maturation.

Pelicci, G. et al., 1992. A Novel Transforming Protein (SHC) with an SH2 Domain Is Implicated in Mitogenic Signal Transduction. *Cell*, 70, pp.93–104.

Pelkmans, L. et al., 2005. Genome-wide analysis of human kinases in clathrin-and caveolae/raft-mediated endocytosis. *Nature*, 436(7).

Pietilä, R. et al., 2012. Ligand oligomerization state controls Tie2 receptor trafficking and angiopoietin-2-specific responses. *Journal of cell science*, 125(Pt 9), pp.2212–23.

del Pozo, M.A. et al., 2004. Integrins Regulate Rac Targeting by Internalization of Membrane Domains. *Science*, 303(5659).

Del Pozo, M.A. et al., 2005. Phospho-caveolin-1 mediates integrin-regulated membrane domain internalization. , 7(9), pp.901–908.

Procopio, W.N. et al., 1999. Angiopoietin-1 and -2 coiled coil domains mediate distinct homo-oligomerization patterns, but fibrinogen-like domains mediate ligand activity. *Journal of Biological Chemistry*, 274(42), pp.30196–30201.

Puthenveedu, M.A. & von Zastrow, M., 2006. Cargo Regulates Clathrin-Coated Pit Dynamics. *Cell*, 127(1), pp.113–124.

Querbes, W. et al., 2006. Invasion of host cells by JC virus identifies a novel role for caveolae in endosomal sorting of noncaveolar ligands. *Journal of virology*, 80(19), pp.9402–9413.

R&D systems, 2016. *Quantikine ELISA. Human Angiopoietin-1 Immunoassay*,

R&D Systems, 2017. *ELISA Reference Guide & Catalog. Systems Tools for Cell Biology Research™* R&D Systems, ed.,

Radeva, M.Y. & Waschke, J., 2017. Mind the gap: mechanisms regulating the endothelial barrier. *Acta Physiologica*.

Raghu, H. et al., 2009. Kaposi's sarcoma-associated herpesvirus utilizes an actin polymerization-dependent macropinocytic pathway to enter human dermal microvascular endothelial and human umbilical vein endothelial cells. *Journal of virology*, 83(10), pp.4895–911.

Ravichandran, K.S., 2001. Signaling via Shc family adapter proteins. *Oncogene*, 20, pp.6322–6330.

Reinardy, J.L. et al., 2015. Phosphorylation of Threonine 794 on Tie1 by Rac1/PAK1 Reveals a Novel Angiogenesis Regulatory Pathway. *PloS one*, 10(10), p.e0139614.

Renard, H.-F. et al., 2014. Endophilin-A2 functions in membrane scission in clathrin-independent endocytosis. *Nature*, 517.

Rodal, S.K. et al., 1999. Extraction of cholesterol with methyl-beta-cyclodextrin perturbs formation of clathrin-coated endocytic vesicles. *Molecular biology of the cell*, 10(4), pp.961–74.

Saharinen, P. et al., 2008. Angiopoietins assemble distinct Tie2 signalling complexes in endothelial cell-cell and cell-matrix contacts. *Nature cell biology*, 10(5), pp.527–537.

Saharinen, P. et al., 2005. Multiple angiopoietin recombinant proteins activate the Tie1 receptor tyrosine kinase and promote its interaction with Tie2. *Journal of Cell Biology*, 169(2), pp.239–243.

Sato, M. et al., 2005. Caenorhabditis elegans RME-6 is a novel regulator of RAB-5 at the clathrin-coated pit. *Nature Cell Biology*, 7(6), pp.559–569.

Sato, T.N. et al., 1995. Distinct roles of the receptor tyrosine kinases Tie-1 and Tie-2 in blood vessel formation. *Nature*, 376(6535), pp.70–74.

Sawada, N., Li, Y. & Liao, J.K., 2010. Novel aspects of the roles of Rac1 GTPase in the cardiovascular system. *Current Opinion in Pharmacology*, 10, pp.116–121.

Schenck, A. et al., 2008. The Endosomal Protein Appl1 Mediates Akt Substrate Specificity and Cell Survival in Vertebrate Development. *Cell*, 133(3), pp.486–497.

Scherr, M. & Eder, M., 2007. Gene Silencing by Small Regulatory RNAs in Mammalian Cells. *Cell Cycle*, 6(4), pp.444–449.

Schnürch, H. & Risau, W., 1993. Expression of tie-2, a member of a novel family of receptor tyrosine kinases, in the endothelial cell lineage. *Development*, 119(3), pp.957–968.

Seegar, T.C.M. et al., 2010. Tie1-Tie2 Interactions Mediate Functional Differences between Angiopoietin Ligands. *Molecular Cell*, 37(5), pp.643–655.

Semerdjieva, S. et al., 2008. Coordinated regulation of AP2 uncoating from clathrin-coated vesicles by rab5 and hRME-6. *Journal of Cell Biology*, 183(3), pp.499–511.

Shewchuk, L.M. et al., 2000. Structure of the Tie2 RTK domain: self-inhibition by the nucleotide binding loop, activation loop, and C-terminal tail. *Structure*, 8(11), pp.1105–1113.

Shim, W.S.N. et al., 2008. Structural stability of neoangiogenic intramyocardial microvessels supports functional recovery in chronic ischemic myocardium. *Journal of Molecular and Cellular Cardiology*, 45(1), pp.70–80.

Shogomori, H. & Futerman, A.H., 2001. Cholesterol depletion by methyl-β-cyclodextrin blocks cholera toxin transport from endosomes to the Golgi apparatus in hippocampal neurons. *Journal of Neurochemistry*, 78(5), pp.991–999.

Shrestha, R. et al., 2015. Mitotic Control of Planar Cell Polarity by Polo-like Kinase 1. *Developmental Cell*, 33(5), pp.522–534.

Shutes, A. et al., 2007. Specificity and mechanism of action of EHT 1864, a novel small molecule inhibitor of Rac family small GTPases. *The Journal of biological chemistry*, 282(49), pp.35666–78.

Shvets, E. et al., 2014. News from the caves: update on the structure and function of caveolae. *Current Opinion in Cell Biology*, 29, pp.99–106.

Sigismund, S. et al., 2005. Clathrin-independent endocytosis of ubiquitinated cargos. *Proceedings of the National Academy of Sciences of the United States of America*, 102(8), pp.2760–5.

Singh, A.K. et al., 2012. Multiple cholesterol recognition/interaction amino acid consensus (CRAC) motifs in cytosolic C tail of Slo1 subunit determine cholesterol sensitivity of Ca2+- and voltage-gated K+ (BK) channels. *The Journal of biological chemistry*, 287(24), pp.20509–21.

Sledz, C.A. et al., 2003. Activation of the interferon system by short-interfering RNAs. *Nature Cell Biology*, 5(9), pp.834–839.

Song, S.H. et al., 2012. Tie1 regulates the Tie2 agonistic role of angiopoietin-2 in human lymphatic endothelial cells. *Biochemical and Biophysical Research Communications*, 419(2), pp.281–286.

Sönnichsen, B. et al., 2000. Distinct Membrane Domains on Endosomes in the Recycling Pathway Visualized by Multicolor Imaging of Rab4, Rab5, and Rab11. *The Journal of Cell Biology*, 149(4).

Sorkin, A. & Von Zastrow, M., 2009. Endocytosis and signalling: intertwining molecular networks. *Nat Rev Mol Cell Biol*, 10(9), pp.609–622.

Stenmark, H., 2009. Rab GTPases as coordinators of vesicle traffic. *Nature reviews. Molecular cell biology*, 10(8), pp.513–25.

Sturk, C. et al., 2010. A negative regulatory role for Y1111 on the Tie-2 RTK. *Cellular signalling*, 22(4), pp.676–83.

Sturk, C. & Dumont, D.J., 2010. Tyrosine phosphorylation of Grb14 by Tie2. *Cell communication and signaling : CCS*, 8(1), p.30.

Su, A.I. et al., 2004. A gene atlas of the mouse and human protein-encoding transcriptomes. *Proceedings of the National Academy of Sciences of the United States of America*, 101(16), pp.6062–7.

Sundborger, A. et al., 2010. An endophilin–dynamin complex promotes budding of clathrin-coated vesicles during synaptic vesicle recycling. *Journal of Cell Science*, 124(1).

Suri, C. et al., 1996. Requisite Role of Angiopoietin-1, a Ligand for the TIE2 Receptor, during Embryonic Angiogenesis. *Cell*, 87, pp.1171–1180.

Sverdlov, M., Shajahan, A.N. & Minshall, R.D., 2007. Tyrosine phosphorylation-dependence of caveolae-mediated endocytosis. *Journal of Cellular and Molecular Medicine*, 11(6), pp.1239–1250.

Tabas, I. et al., 1991. The influence of particle size and multiple apoprotein E-receptor interactions on the endocytic targeting of beta-VLDL in mouse peritoneal macrophages. *The Journal of Cell Biology*, 115(6).

Tadros, A. et al., 2003. ABIN-2 protects endothelial cells from death and has a role in the antiapoptotic effect of angiopoietin-1. *Blood*, 102(13).

Takayama, Y. et al., 2005. Low density lipoprotein receptor-related protein 1 (LRP1) controls endocytosis and c-CBL-mediated ubiquitination of the platelet-derived growth factor receptor beta (PDGFR beta). *The Journal of biological chemistry*, 280(18), pp.18504–10.

Tarallo, V. & De Falco, S., 2015. The vascular endothelial growth factors and receptors family: Up to now the only target for anti-angiogenesis therapy. *International Journal of Biochemistry and Cell Biology*, 64, pp.185–189.

Thomas, M. & Augustin, H.G., 2009. The role of the Angiopoietins in vascular morphogenesis. *Angiogenesis*, 12(2), pp.125–37.

Thurston, G., 2003. Role of Angiopoietins and Tie receptor tyrosine kinases in angiogenesis and lymphangiogenesis. *Cell and Tissue Research*, 314(1), pp.61–68.

Thurston, G. & Daly, C., 2012. The complex role of angiopoietin-2 in the angiopoietin-Tie signaling pathway. *Cold Spring Harbor Perspectives in Medicine*, 2(9), p.a006550.

Tiwari, A. et al., 2011. Endothelial Cell Migration on Fibronectin Is Regulated by Syntaxin 6-mediated α5β1 Integrin Recycling * □ S. *The journal of biological chemistry*, 286(42), pp.36749–36761.

Torgersen, M.L. et al., 2001. Internalization of cholera toxin by different endocytic mechanisms. *Journal of Cell Science*, 114(20), pp.3737–3747.

Traub, L.M., 2003. Sorting it out: AP-2 and alternate clathrin adaptors in endocytic cargo selection. *The Journal of cell biology*, 163(2), pp.203–8.

Tsao, P.I. & Von Zastrow, M., 2000. Type-specific sorting of G protein-coupled receptors after endocytosis. *Journal of Biological Chemistry*, 275(15), pp.11130–11140.

Vadlamudi, R.K. et al., 2004. p41-Arc subunit of human Arp2/3 complex is a p21-activated kinase-1-interacting substrate. *EMBO reports*, 5, pp.154–160.

Valenzuela, D.M. et al., 1999. Angiopoietins 3 and 4: diverging gene counterparts in mice and humans. *Proceedings of the National Academy of Sciences of the United States of America*, 96(5), pp.1904–9.

Vestweber, D., 2012. Relevance of endothelial junctions in leukocyte extravasation and vascular permeability. *Annals of the New York Academy of Sciences*, 1257(1), pp.184–192.

Wasmuth, E. V & Lima, C.D., 2016. UniProt: the universal protein knowledgebase. *Nucleic Acids Research*, 45(D1), pp.1–12.

Watanabe, S. & Boucrot, E., 2017. Fast and ultrafast endocytosis. *Current Opinion in Cell Biology*, 47, pp.64–71.

Weber, E. et al., 1994. Expression and Polarized Targeting of a Rab3 Isoform in Epithelial Cells. *Journal of Cell Biology*, 125(3), pp.583–594.

Wehrle, C., Van Slyke, P. & Dumont, D.J., 2009. Angiopoietin-1-induced ubiquitylation of Tie2 by c-Cbl is required for internalization and degradation. *The Biochemical journal*, 423(3), pp.375–80.

Wernick, N.L.B., Haucke, V. & Simister, N.E., 2005. Recognition of the tryptophan-based endocytosis signal in the neonatal Fc Receptor by the mu subunit of adaptor protein-2. *The Journal of biological chemistry*, 280(8), pp.7309–16.

Wilson, M.D. et al., 2012. MultiDsk: A Ubiquitin-Specific Affinity Resin. *PLoS ONE*, 7(10), p.e46398.

Winderlich, M. et al., 2009. VE-PTP controls blood vessel development by balancing Tie-2 activity. *Journal of Cell Biology*, 185(4), pp.657–671.

Wu, F.T.H. et al., 2015. Vasculotide reduces endothelial permeability and tumor cell extravasation in the absence of binding to or agonistic activation of Tie2. *EMBO molecular medicine*, 7(6), pp.770–87.

Yamamoto, Y. et al., 2003. Distinct roles of Rab3B and Rab13 in the polarized transport of apical, basolateral, and tight junctional membrane proteins to the plasma membrane. *Biochemical and Biophysical Research Communications*, 308, pp.270–275.

Yao, L.-H. et al., 2013. Actin Polymerization Does Not Provide Direct Mechanical Forces for Vesicle Fission during Clathrin-Mediated Endocytosis. *The Journal of Neuroscience*, 33(40), pp.15793–

15798.

Ye, W., 2016. The Complexity of Translating Anti-angiogenesis Therapy from Basic Science to the Clinic. *Developmental Cell*, 37(2), pp.114–125.

Yokouchi, M. et al., 1999. Ligand-induced ubiquitination of the epidermal growth factor receptor involves the interaction of the c-Cbl RING finger and UbcH7. *The Journal of biological chemistry*, 274(44), pp.31707–12.

Yoon, M.-J. et al., 2003. Localization of Tie2 and phospholipase D in endothelial caveolae is involved in angiopoietin-1-induced MEK/ERK phosphorylation and migration in endothelial cells. *Biochemical and Biophysical Research Communications*, 308(1), pp.101–105.

Yoshimori, T. et al., 2000. The mouse SKD1, a homologue of yeast Vps4p, is required for normal endosomal trafficking and morphology in mammalian cells. *Molecular biology of the cell*, 11(2), pp.747–63.

Yu, X. et al., 2013. Structural basis for angiopoietin-1-mediated signaling initiation. *Proceedings of the National Academy of Sciences of the United States of America*, 110(18), pp.7205–10.

Yuan, H.T. et al., 2007. Activation of the orphan endothelial receptor Tie1 modifies Tie2-mediated intracellular signaling and cell survival. *The FASEB Journal*, 21(12), pp.3171–3183.

Zhang, J. et al., 2011. Angiopoietin-1/Tie2 signal augments basal notch signal controlling vascular quiescence by inducing delta-like 4 expression through AKT-mediated activation of ??-catenin. *Journal of Biological Chemistry*, 286(10), pp.8055–8066.

Zhang, X.E. et al., 2016. Activation of RhoA, but Not Rac1, Mediates Early Stages of S1P-Induced Endothelial Barrier Enhancement B. Tharakan, ed. *PLOS ONE*, 11(5), p.e0155490.

Zhang, Z. & Henzel, W.J., 2004. Signal peptide prediction based on analysis of experimentally verified cleavage sites. *Protein science : a publication of the Protein Society*, 13(10), pp.2819–2824.

Zheng, Y. et al., 2013. Temporal regulation of EGF signalling networks by the scaffold protein Shc1. *Nature*, 499(7457), pp.166–171.

Zheng, Z.-Y. et al., 2012. CHMP6 and VPS4A mediate the recycling of Ras to the plasma membrane to promote growth factor signaling. *Oncogene*, 31(43), pp.4630–8.

Zografou, S. et al., 2012. A complete Rab screening reveals novel insights in Weibel–Palade body exocytosis. *Journal of Cell Science*, 125(20).

Zuluaga, S. et al., 2007. p38α MAPK can positively or negatively regulate Rac-1 activity depending on the presence of serum. *FEBS Letters*, 581(20), pp.3819–3825.